I. The Generalized Valence Bond Theory of Electronic Structure

II. An Orbital Interpretation of Superexchange in Antiferromagnetic Insulators

Thesis by

PHILIP JEFFREY HAY

In Partial Fulfillment of the Requirements

For the Degree of

Doctor of Philosophy

California Institute of Technology

Pasadena, California

1972

(Submitted October 21, 1971)

Acknowledgements

I should like to thank Professor William A. Goddard III for his advice and encouragement during my years at Caltech. Much of the stimulation in my graduate work has come from my many conversations with him and with the other members of his research group.

In particular, I thank William Hunt for collaborating on several aspects of the generalized valence bond investigations. I am also indebted to Robert C. Ladner, David L. Huestis, and Richard J. Blint for the use of their computer programs. Valuable assistance on the calculations of ozone was given by Dr. David C. Cartwright and Nick Fiamengo of Aerospace Corporation and by Dr. Thomas H. Dunning, Jr.

I thank Mrs. Adria Larson, Miss Sharon Vedrode, and Mrs. Edith Klinkerman for expert typing assistance and the National Science Foundation for financial support.

Finally, I wish to express my appreciation to my wife for her patience and understanding.

ABSTRACT

I. A discussion is given of the generalized valence bond (GVB) method--a multi-configuration approach to electronic structure that combines a valence bond interpretation with the self-consistent techniques of Hartree-Fock theory. Ab initio calculations on simple hydrocarbons give improved descriptions of bonding in terms of localized C-C and C-H bonds.

-- The nine lowest states of the ozone molecule are treated by GVB and configuration interaction techniques and an assignment of the spectrum of O_3 is made. A metastable excited singlet state with an equilateral geometry and an energy 1.5 eV above the ground state is discovered.

-- The calculated energy barrier of 60.5 kcal for the cis-trans isomerization of cyclopropane is in good agreement with the experimental value of 64.2 kcal. No barrier to ring closure is found in the trimethylene biradical in contrast to commonly accepted biradical mechanisms.

-- The $^1A_1$ state of CH_2 is calculated to be 0.50 eV (11.5 kcal) above the ground $^3B_1$ state. The $^1B_1 \leftarrow {}^1A_1$ transition--calculated to be 1.40 eV--agrees with the lowest observed $^1B_1 \leftarrow {}^1A_1$ band and suggests a reinterpretation of this as a 0-0 band. A new $^1A_1$ state at 3.2 eV is also discussed. Good values of the barrier to internal rotation in ethane and of the dissociation energy of O_2 are obtained.

II. An orbital interpretation of superexchange suggests that antiferromagnetism arises from increased metal-metal overlap due to the ligand orbitals. A theoretical value of the exchange parameter from ab initio calculations on the Ni^{++}-F^{-}-Ni^{++} "molecule" is 10% of the experimental value in $KNiF_3$.

I. THE GENERALIZED VALENCE BOND THEORY OF ELECTRONIC STRUCTURE

A. The GVB Description of Hydrocarbons

TABLE OF CONTENTS

Generalized Valence Bond Description of Simple Alkanes, Ethylene and Acetylene.

P. Jeffrey Hay, William J. Hunt, and William A. Goddard III.

Contribution from the Arthur Amos Noyes Laboratory of Chemical Physics, California Institute of Technology, Pasadena, California 91109

Received

I. Introduction

Considerable progress in the understanding of bonding and molecular structure was made through the use of valence bond wavefunctions.[1] In recent years accurate calculations have been carried out using the Hartree-Fock method, which yields a qualitatively different interpretation of electronic structure. Recently the ab initio generalized valence bond (GVB) method has been developed[2] which takes the wavefunction to have the form of a VB function but which allows all orbitals to be solved for self-consistently (as in Hartree-Fock). Thus in GVB no special hybridization is imposed on the orbitals and, in addition, the orbitals are permitted to delocalize onto other centers. It is the hope of these investigators that GVB orbitals will lead to the formation of useful conceptual ideas concerning similarities and differences in bonding in various molecules. We consider here the results of GVB calculations on a number of related hydrocarbons (CH, CH_2, CH_3, CH_4, C_2, C_2H_2, C_2H_4, C_2H_6, and C_3H_6).

In the GVB approach we replace the doubly occupied molecular orbitals ϕ_i of the many-electron Hartree-Fock wavefunction by two-electron valence bond functions ϕ_{ia} and ϕ_{ib}:

$$\phi_i(1)\phi_i(1)\alpha(1)\beta(2) \rightarrow [\phi_{ia}(1)\phi_{1b}(2) + \phi_{ib}(1)\phi_{1a}(2)]\,\alpha(1)\beta(2)$$

We solve for the optimum orbitals, ϕ_{ia} and ϕ_{ib}, of each pair subject only to the restriction that they be orthogonal to the orbitals in other pairs. In addition to yielding a lower energy than the Hartree-Fock

energy, this method offers two major conceptual advantages:

(1) The orbitals of each pair turn out to be localized hybrid atomic-like orbitals in close correspondence to chemists' "intuitive" ideas of bonds and lone pairs in molecules.

(2) The process of breaking chemical bonds is correctly described since the GVB orbitals change smoothly into the atomic orbitals of the products.

For example, for ethylene, we find two types of GVB sigma bonding pairs as shown in Fig. 1. One pair (Fig. 1a) is localized mainly in the C-C region and can be considered a CCσ-bonding pair. One also obtains four other equivalent pairs (Fig. 1b) each localized in a different CH region. These CH bonding pairs are each described by two orbitals: a hybrid orbital (74 percent p character) mainly on the C but oriented towards the H (ϕ_{2a} in Fig. 1b), and by an essentially hydrogen atomic orbital (ϕ_{2b}).

The C-C bond is described by a symmetrically related pair (ϕ_{1a} and ϕ_{1b}) of hydrid orbitals (each with 68 percent p character), but much more delocalized onto the other center than the orbitals of the Ch bonds. Also shown is a plot (in a perpendicular plane) of the π-orbitals, (ϕ_{3a} and ϕ_{3b}) each of which is nearly a pure $2p_z$ orbital or the respective carbon atoms. Allowing the π orbitals to split in this way leads to a bond energy 30 kcal greater than the conventional doubly occupied π-orbital. Another conclusion is that the σ, π representation of the bond gives a lower energy) than a bent-bond description, whereas in localized MO theory both descriptions would be equivalent in energy.

II. Calculational Details

Hurley, Lennard-Jones and Pople[3] pointed out that wavefunctions of the GVB form

$$\phi_{1a}\phi_{1b} + \phi_{ib}\phi_{ia} \qquad (1)$$

may be transformed to an equivalent natural orbital (NO) representation

$$C_{1i}\phi_{1i}\phi_{1i} + C_{2i}\phi_{2i}\phi_{2i} \qquad (2)$$

where

$$\langle\phi_{1i}|\phi_{2i}\rangle = 0$$

[Coulson and Fischer[4] had previously pointed out that two electron, two basis function CI wavefunction can be written in the form (1)]. When the many-electron wavefunction in written in this form, one can see that ψ_{GVB} is a special case of a multiconfiguration wavefunction where all orbitals ϕ_i and configuration interaction (CI) coefficients C_i are optimized. Setting $C_1 = 1$ and $C_2 = 0$ for each pair would result in the Hartree-Fock wavefunction, except that in HF the orbitals would lose their localized nature and would revert back to become symmetry functions. The relation of GVB to other approaches is discussed more fully in Ref. 2.

As shown in Ref. 1 the GVB natural orbitals are obtained by solving a set of equations

$$H_i\phi_i = E_i\phi_i \qquad (3)$$

and iterating until self-consistency is achieved, analogous to the procedure used in Hartree-Fock calculations. However, we will always analyze the wavefunction in terms of the GVB orbitals (1).

There will usually be a separate hamiltonian H_i for each orbital, except for the doubly-occupied orbitals which can all be taken to be eigenfunctions of a single closed-shell hamiltonian. In addition such wavefunctions as open-shell doublets or singlets can easily be handled in this approach. The procedure of handling orthogonality constraints in the GVB equations has been discussed in Ref. 2.

As for Hartree-Fock calculations the GVB self-consistent variational equations (3) are solved by expanding each orbital in terms of a large basis set and solving for the expansion coefficients.

Three basis sets were used in the present calculations:

(a) MBS--the minimum basis set (STO-4G) of contracted gaussians developed by Pople.[5]

(b) DZ--the $(9s_C 5p_C/4s_H)$ basis of gaussians contracted to "double zeta" [4s2p/2s] size.

(c) POL--the DZ basis plus 3d polarization functions with exponent 0.532.

A CH distance of 2.1 a.u. was assumed for CH and CH_2, and HCH angles in the range of 90° to 180° were used for CH_2. For CH_3, R(C-H) was 2.039 (from CD_3)[7] while the geometries for other hydrocarbons were taken from experiment.[8]

Configuration interaction (CI) calculations were also performed for CH CH_2 and C_2H_4 by using all configurations constructed from the orthogonal GVB natural orbitals. For excited states the configurations were constructed from the self-consistent orbitals for those states rather than using ground state orbitals.

III. The GVB Description of the CH_n Series

First we will consider the CH_n series of molecules.

C and CH. In the usual HF description of the ground ^3P state of the C atom, the configuration is $(1s)^2(2s)^2 2p_x \alpha 2p_y \alpha$ (we will neglect the 1s orbitals in the rest of this discussion). The GVB orbitals of C polarize in opposite directions along the z axis

$$\phi_{sz} = \phi_{2s} + \lambda \phi_{2p_z}$$

$$\phi_{sz} = \phi_{2s} - \lambda \phi_{2p_z}$$

to form directed sp lobes sz and $\overline{sz}$ which will be schematically represented as

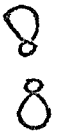

The wavefunction then becomes

$$\psi_{GVB} = A(sz\ s\bar{z} + s\bar{z}\ sz)\ x\ y\ \alpha\beta\alpha\beta$$

which is represented in Fig. 2a. The sp lobes are shown as before along with two perpendicular

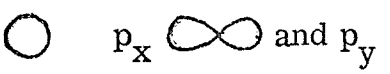

orbitals, where the arrows denote unpaired electron. In the diagrams at the right of Fig. 2, orbitals in the same row are singlet coupled while the x and y orbitals in the same column have maximum (triplet) multiplicity.

If we now bond a H atom to the p_x carbon orbital we obtain the $^2\Pi$ state of CH (Fig. 2b). (The solid line denotes a bond). The self-consistent GVB lone pair orbitals [sz, $s\bar{z}$] bend back from the CH bond at an angle of 128° while the x orbital incorporates some s character as the bond is formed (see Fig. 3). At large internuclear distance the x and y orbitals are triplet coupled, corresponding to $C(^3P) + H(^2S)$. At this point the GVB coupling is no longer appropriate and one should permit recoupling of the orbitals to attain proper dissociation. Spin-coupling changes, best treated within the SOGI[9] approach, are discussed for CH by Bobrowicz and Goddard.[10]

Bonding H to the sz lobe of C would yield the $^4\Sigma^-$ state of CH (Fig. 2c) which we find to be only 0.46 eV above the ground $^2\Pi$ state. The self-consistent sz, $\overline{sz}$ and H orbitals are shown in Fig. 3. The difference in bonding is dramatically reflected by the p character in the bonding orbital of the $^2\Pi$ (82 percent) and $^4\Sigma^-$ (35 percent) states [see Table I].

One can recouple the $s\bar{z}$, x, and y orbitals of the $^4\Sigma^-$ state to form the $^2\Delta$ $^2\Sigma^-$ and $^2\Sigma^-$ and $^2\Sigma^+$ states of CH. The self-consistent excitation and CI energies are compared with the experimentally observed transitions in Table II.

CH_2. Forming a CH bond with the unpaired p_y orbital of $CH(^2\Pi)$ results in the $^1A_1$ state of CH_2; where the sz and $s\bar{z}$ lobes point above and below the HCH plane respectively. Interaction of the orbitals of the new bond with those of the old would increase the HCH angle to a value greater than 90° (experimentally the angle

is 103.2°).[7]

Similarly bonding to one of the sp lobes would produce the $^3B_1$ state (in CH_2 the two CH bonds become equivalent), as well as the higher $^1B_1$ state (see Fig. 2e). Since the initial angle between the sp lobe and the CH bond is 128° the increase in bond angle due to formation of the second bond should be less than for the $^1A_1$ state (13°). An angle increase of 8° would lead to agreement with the experimental value of 136° ± 8° [11-13] and recent CI calculations.[14]

Again the hybridization indicates that CH bonds in the $^3B_1$ state (47 percent p) involve less p bonding than the $^1A_1$ state (78 percent). The bonding orbitals and lone pair orbitals for the two states are shown in Figs. 4 ($^1A_1$) and 5 ($^3B_1$). From Fig. 6, where the change in hybridization with angle is shown, it is seen that the $^1A_1$ state contains more p character in the CH bond even at the same HCH angles.

As we reported in an earlier communication,[1] the $^3B_1$ state remains the lowest state for $\theta > 100°$, but below 100° its curve is crossed by the $^1A_1$ state (see Fig. 7). The $^1A_1 \leftarrow {}^3B_1$ energy separation (experimentally estimated [15] to occur at < (eV) is found to be 0.50 eV. The $^1B_1 \leftarrow {}^1A_1$ energy separation (1.40 eV) does not agree with the experimentally extrapolated value (0.88 eV); however, it does agree with the lowest observed transition[22] (1.34 eV). This indicates that these transitions may be mis-assigned and that the lowest observed transition is the O–O band.

CH_3 and CH_4. One of the 3 equivalent bonding pairs in planar CH_3, obtained from bonding a H to the σ unpaired orbital of CH_2 ($^3B_1$), is shown in Fig. 8. These results differ somewhat from the usual notion of hybridized atomic orbitals, since the C bonding orbitals in the MBS basis have $sp^{1.5}$ and $sp^{2.1}$ hybridization, respectively, as compared with the usual sp^2 and sp^3 bonding assumed in VB description of methyl and methane. The orbitals can now delocalize onto the hydrogen and hence the orthogonality conditions no longer uniquely fix the hybridization.

IV. C_2H_2, C_2H_4, C_2H_6, and the C_2 Molecule

In the earlier discussion of ethylene, we showed that the GVB orbitals have the form of four equivalent pairs of C—H bonding orbitals, a pair of C—C σ-bonding orbitals, and two nearly atomic-like π-bonding orbitals. For single bonds, one can construct only a σ and σ* orbital from localized orbitals on each center. By explicitly including the $\sigma^2 \rightarrow \sigma^{*2}$ excitation in the GVB form of the wavefunction as in (2), GVB recovers essentially all the additional binding energy left out of a Hartree-Fock MO calculation. In multiple bonds, such as C_2H_4, even though GVB obtains an energy 0.054 hartree (34 kcal) lower than HF, only a restricted number of excitations are included in GVB because of the "perfect pairing" and "strong orthogonality" assumptions. We can test these assumptions by using the four orbitals in the C=C double bond of ethylene in a CI calculation. For a MBS basis, this results in an increase of 0.018 hartree (11 kcal) in the binding energy (see Table III), due mainly to the $\sigma\pi \rightarrow \sigma^*\pi^*$ excitation which is needed to dissociate C_2H_4 into two ground state $CH_2(^3B_1)$ fragments.

A similar description is obtained for acetylene (Fig. 9). The C≡C triple bond is described by a σ-bonding pair and two equivalent π_y bonding pairs. If the bond were described as originating from equivalent tetrahedral lobes on each C, one would have obtained three equivalent bent "banana" bonds. Indeed certain schemes of localizing HF molecular orbitals[16] suggest

that this arrangement minimizes electronic repulsion (although the total HF energy remains the same whether the MO's are localized or not). [Klessinger's[17] group function calculations on C_2H_4 and C_2H_2 found that the $\sigma\pi$ description is lower by about .013 and .016 a.u., respectively.] The bent bond solution of the GVB equations is higher than the $\sigma\pi$ solution and only the lower state ($\sigma\pi$) could be solved for self-consistently.

Removal of the two H's in C_2H_2 results in the $\cdot C{\equiv}C \cdot$ biradical, whose ground state is found experimentally to be $^1\Sigma_g^+$. We would expect a poor description of the two unpaired electrons by requiring all orbitals to be doubly occupied (the HF configuration would be $1\sigma_g^2\, 1\sigma_u^2\, 2\sigma_g^2\, 1\pi_u^2\, 2\sigma_u^2$). In fact Pople[18] found the heat of reaction for $C_2 \rightarrow 2C$ to be -22.1 kcal as compared with the experimental value of +144 kcal. For a MBS calculation, we obtain +72.7 kcal. The two biradical orbitals have an overlap of only 0.331 (one of which is shown in Fig. 10) outside of the CC bond region and are localized on the respective carbons.

In ethane, the main property of interest is the barrier to internal rotation. Since Hartree-Fock correctly predicts the difference between the eclipsed and staggered forms to be 3.3 kcal (in our MBS basis) in good agreement with the value of +2.9 kcal obtained from microwave spectra,[19] one would hope that the GVB description would not reduce the agreement between the theory and experiment. Although both the staggered and eclipsed forms are lowered from HF, the relative difference is essentially the

same (+3.1 kcal). This contrasts with the group function calculations[17b] on ethane which predicted the eclipsed form was lower by 5.1 kcal. In Fig. 11 we show one of the 6 equivalent CH bonding pairs and the CC bonding pair.

V. Cyclopropane and the Trimethylene Biradical

We have reported previously[20, 21] the results of GVB calculations on cyclopropane and the broken-bond trimethylene intermediate involved in the geometrical and optical isomerizations of C_3H_6. In Fig. 12a we note that the orbitals of the C—C bond have essentially sp^4(82% p character)and are bent outside the ring in agreement with Coulson and Moffitt's earlier calculations.[22] As the central CCC angle is increased the orbitals charge continuously into p orbitals for planar end groups. We found essentially no barrier to ring closure (< 1 kcal) for trimethylene and an activation energy of 60.6 kcal in good agreement with the experimental value (64.2 kcal).

VI. General Characteristics of GVB Orbitals

In Table 4 we summarize the results of the GVB calculations of hydrocarbons. In addition to the HF and GVB energies, for each GVB pair we report the overlap $\langle \phi_{ia} | \phi_{ib} \rangle$ and the pair splitting energy $\Delta\epsilon_i$ (i.e., the energy charge due to adding the second natural orbital to the pair). To a very good approximation, ($\sim$ 0.001 h) the total improvement in energy in GVB over HF is given by the sum of the pair splitting energies. In Table V we note that improved agreement with experimental heats of reaction is obtained using GVB functions.

Typically for reactions involving breaking of single bonds, GVB accounts for an improvement of 10 - 12 kcal in ΔH of the reaction which is normally 10 - 15 percent of the total bond strength. For multiple bonds, although the pair lowerings are much larger than for single bonds, these are partially offset by pair lowerings in the molecular fragments with the result that total improvements in heats of reaction are 14 - 40 kcal.

Table I. Hybridization of GVB Orbitals

	Pair	Percent MBS[a]	p character DZ[b]
$C(^3P)$	lone (2)	13.2	13.2
$CH(^2\Pi)$	bond	92.8	81.5
	lone (σ)	21.3	25.7
$CH(^4\Sigma^-)$	bond	37.6	34.8
	lone (σ)	37.9	42.0
$CH_2(^1A_1)$	bond	86.1	78.5
	lone (sp)	36.1	43.2
$CH_2(^3B_1)$	bond	51.9	51.5
	lone (a_1)	70.9	72.4
$CH_2(^1B_1)$	bond	46.5	47.2
	lone (a_1)	82.8	83.8
CH_3	bond	59.8	60.8
CH_4	bond	67.9	70.3
C_2H_2	CH bond	53.2	--
	CC bond	42.9	52.2
C_2H_4	CH bond	74.4	--
	CC bond	68.0	--
C_2H_6	CH bond	68.5	--
	CC bond	66.3	72.0
C_3H_6	CC bond	81.7	--

[a]Minimum basis set.

[b]Double zeta basis set.

Table II. Excitation Energies (eV). All Results were Obtained in the POL Basis.

State	CH Molecule HF	GVB	GVB-CI	Exp[a]
$^2\Pi$	--	--	--	--
$^4\Sigma^-$	-0.28	0.46	0.36	--
$^2\Delta$	+2.73	3.52	3.43	2.87
$^2\Sigma^-$	3.36	4.22	3.81	3.22
$^2\Sigma^+$	4.18	4.97	4.46	3.94

State	HF	GVB (pair)	GVB-CI	Exp
$^1A_1 \leftarrow {}^3B_1$	1.03	0.45	0.50	(< 1.0)[b]
$^1B_1 \leftarrow {}^1A_1$	0.75	1.34	1.40	0.88[c] (1.34)[d]
$^1B_1 \leftarrow {}^1A_1$ (vert)	1.32	1.91	1.88	1.98[e]

[a] Ref. 19.

[b] Estimated upper limit (Ref. 15).

[c] Extrapolated value.

[d] Lowest observed transition.

[e] Obtained from median excitation energy of $^1B_1 \leftarrow {}^1A_1$ band.

Table III. Sigma-pi Correlation in Ethylene

	E (a.u.)	$\Delta H[C_2H_4 \rightarrow 2(H_2(^3B_1)]$
HF	-77.6246	126
GVB (2-pair)	-77.6797	168
GVB (CI)	-77.6978	179
EXP		171[a]

[a]Quoted from Ref. 18.

Table IV. Generalized Valence Bond Results for Hydrocarbons

Molecule	Basis	Energy E_{HF}(a.u.)[a]	Energy E_{GVB}(a.u.)	Pair Information: Pair	Overlap	$\Delta\epsilon_i$(a.u.)
$C(^3P)$	MBS	-37.4897	-37.5086	lone	0.732	-.0189
	DZ	-37.6845	-37.7033	lone	0.732	-.0193
$C(^1D)$	MBS	-37.4401	-37.4590	lone		-.0189
	DZ	-37.6268	-37.6463	lone	0.733	-.0195
$CH(^2\Pi)$	MBS	-38.0455	-38.0832	bond	0.812	-.0173
				lone	0.717	-.0204
	DZ	-38.2582	-38.2941	bond	0.810	-.0181
				lone	0.733	-.0178
	POL	-38.2703	-38.3085	bond	0.826	-.0165
				lone	0.704	-.0217
$CH(^4\Sigma)$	MBS	-38.0581	-38.0685	bond	0.863	-.0104
	DZ	-38.2649	-38.2757	bond	0.863	-.0108
	POL	-38.2805	-38.2914	bond	0.864	-.0109
$CH_2(^1A_1)$	MBS	-38.6491	-38.7015	bond(2)	0.816	-.0168
				lone	0.699	-.0188
	DZ	-38.8614	-38.9113	bond(2)	0.816	-.0173
				lone	0.734	-.0153
	POL	-38.8822	-38.9362	bond(2)	0.826	-.0163
				lone	0.683	-.0214
$CH_2(^3B_1)$	MBS	-38.7065	-38.7337	bond(2)	0.840	-.0136
	DZ	-38.9119	-38.9391	bond(2)	0.840	-.0136
	POL	-38.9202	-38.9483	bond(2)	0.843	-.0140
$CH_2(^1B_1)$	MBS	-38.6244	-38.6375	bond(2)	0.843	-.0131
	DZ	-38.8546	-38.8685	bond(2)	0.842	-.0139
	POL	-38.8681	-38.8818	bond(2)	0.845	-.0137
CH_3	MBS	-39.3529	-39.3959	bond(3)	0.837	-.0143
	DZ	-39.5492	-39.5935	bond(3)	0.839	-.0147
	POL	-39.5598	-39.6038	bond(3)	0.841	-.0147
CH_4	MBS	-40.0071	-40.0691	bond(4)	0.828	-.0155
	DZ	-40.1849	-40.2467	bond(4)	0.832	-.0154
	POL	-40.1982	-40.2596	bond(4)	0.834	-.0153
$C_2(^1\Sigma_g^+)$	MBS	-74.8567	-75.1318	σ	0.940	-.0030
				π(2)	0.648	-.0354
				lone	0.331	-.1013
C_2H_2	MBS	-76.4037	-76.5016	CH(2)	0.841	-.0138
				CC-σ	0.929	-.0045
				CC-π(2)	0.664	-.0329
	DZ	-76.7991	-76.8573	CC-σ	0.908	-.0070
				CC-π(2)	0.691	-.0260

Table V. Heats of Reaction (kcal/mole)

Reaction	Basis	HF	GVB	EXP
$CH \rightarrow C + H$	MBS	23.1	35.0	81
	DZ		68.8	
	POL	54.0	65.8	
$CH_2 \rightarrow CH + H$	MBS	101.1	94.4	103
	DZ	96.5	91.0	
	POL	94.1	87.8	
$CH_3 \rightarrow CH_2 + H$	MBS	91.9	101.8	111
	DZ	86.2	96.9	
	POL	87.6	97.6	
$CH_4 \rightarrow CH_3 + H$	MBS	96.8	108.7	103
	DZ	85.2	96.2	
	POL	86.9	97.8	
$C_2 \rightarrow 2C$	MBS	-22.1	72.7	144
$C_2H_2 \rightarrow 2CH$	MBS	198	210	231
	DZ	178	192	
$C_2H_4 \rightarrow 2CH_2$	MBS	126.4	168.4	171
	DZ	117	140	
$C_2H_6 \rightarrow 2CH_3$	MBS	95.5	106.8	87
	DZ	66.5	76.2	
$C(^3P) \rightarrow C(^1D)$	MBS	31.1	31.1	29.1[b]
	DZ	36.1	36.0	
	POL	36.1	36.0	
$C(^3P) \rightarrow C(^5S)$	MBS	49.1	60.9	61.7[b]
	DZ	56.1	68.2	
	POL	56.1	68.2	
$CH(^2\Pi) \rightarrow CH(^4\Sigma^-)$	MBS	-7.9	+9.2	
	DZ	-4.2	+11.5	
	POL	-6.4	+10.7	
$CH(^2\Pi) \rightarrow CH(^2\Delta)$	MBS	75.5	93.8	66.6[c]
	DZ	58.7	75.4	
	POL	63.0	81.2	
$CH_2(^3B_1) \rightarrow CH_2(^1A_1)$	MBS	36.0	20.2	(<23)[d]
	DZ	31.7	17.5	
	POL	23.9	7.6	

Table V (Continued)

C_2H_4	MBS	-77.6246	-77.7353	CH(4)	0.839	-.0142
				CC-σ	0.893	-.0078
				CC-π	0.578	-.0462
	DZ	-78.0100	-78.0519	CC-σ	0.875	-.0102
				CC-π	0.631	-.0317
C_2H_6 (staggered)	MBS	-78.8608	-78.9691	CH(6)	0.826	-.0157
				CC	0.835	-.0139
	DZ	-79.2044	-79.2198	CC	0.822	-.0154
C_2H_6 (eclipsed)	MBS	-78.8555	-78.9641	CH(6)	0.826	-.0158
				CC	0.836	-.0139
C_3H_6	MBS	-116.4961	-116.5143	CC(1)	0.790	-.0183

[a]The "HF" energy is the energy of the principal natural orbital wavefunction obtained by adding the pair lowering energies to E_{GVB}. All experimental references are quoted from Ref. 18 except as noted.

[b]C. E. Moore, Atomic Energy Levels (National Bureau of Standards Circular 467, 1949).

[c]Ref. 19.

[d]Ref. 22.

References

(1) L. Pauling, "The Nature of the Chemical Bond," Cornell, Ithaca, N. Y., 1960.

(2) P. J. Hay, W. J. Hunt, and W. A. Goddard III, Chem. Phys. Lett., to be published.

(3) A. C. Hurley, J. E. Lennard-Jones, and J. A. Pople, Proc. Roy. Soc. (London), A220, 446 (1953).

(4) C. A. Coulson and I. Fischer, Phil. Mag., 40, 386 (1949).

(5) W. J. Hehre, R. F. Stewart, and J. A. Pople, J. Chem. Phys., 51, 2657 (1969).

(6) (a) S. Huzinaga, J. Chem. Phys., 42, 1293 (1965); (b) T. H. Dunning, Jr., J. Chem. Phys. 53, 2823 (1970).

(7) G. Herzberg, "Molecular Spectra and Molecular Structure," Van Nostrand, Princeton, N. J., 1945, 1967, Vol. II and III.

(8) (a) C_2H_6: G. E. Hansen and D. M. Dennison, J. Chem. Phys. 20, 313 (1952); (b) C_3H_6: O. Bastiansen, Acta Crystallogr., 17, 538 (1964).

(9) R.C. Ladner and W. A. Goddard III, J. Chem. Phys., 51, 1073 (1969).

(10) F. Bobrowicz and W. A. Goddard III, to be published.

(11) R. A. Bernheim, H. W. Bernard, P. S. Wang, L. S. Wood, and P. S. Skell, J. Chem. Phys., 53, 1280 (1970).

(12) E. Wassermann, W. A. Yager, and V. Kuck, J. Amer. Chem. Soc., 92, 7491 (1970).

(13) G. Herzberg and J.W.C. Johns, J. Chem. Phys. 54, 2276 (1971).

(14) S. V. O'Neil, H. T. Schaeffer III, and C. F. Bender, J. Chem. Phys., 55, 162 (1971).

(15) G. Herzberg and J. W. C. Johns, Proc. Roy. Soc. (London), A295, 107 (1966).

(16) M.D. Newton, E. Switkes, and W. N. Lipscomb, J. Chem. Phys. 53, 2645 (1970).

(17) (a) M. Klessinger, Int. J. Quant. Chem., 4, 191 (1970); (b) J. Chem. Phys., 53, 225 (1970).

(18) W. A. Lathan, W. J. Hehre, and J. A. Pople, J. Amer. Chem. Soc., 93, 808 (1971).

(19) S. Weiss and G. Leroi, J. Chem. Phys., 48, 962 (1968).

(20) P. J. Hay, W. J. Hunt, and W. A. Goddard III, J. Amer. Chem. Soc., to be published.

(21) P. J. Hay, W. J. Hunt, and W. A. Goddard III, Chem. Commun., to be published.

(22) C. A. Coulson and W. E. Moffitt, Phil. Mag., 40, 1 (1949).

Figure Captions

Fig. 1. Orbitals of ethylene.

Fig. 2. Schematic diagram of bonding in C, CH, and CH_2.

Fig. 3. Orbitals of CH ($^2\Pi$ and $^4\Sigma^-$ states).

Fig. 4. Orbitals of CH_2 ($^1A_1$).

Fig. 5. Orbitals of CH_2 ($^3B_1$).

Fig. 6. Change in hybridization of the orbitals of CH_2 with bond angle.

Fig. 7. Potential curves of the states of CH_2.

Fig. 8. Orbitals of CH_3 and CH_4.

Fig. 9. Orbitals of C_2H_2.

Fig. 10. The C_2 molecule ($^1\Sigma_g^+$).

Fig. 11. Orbitals of C_2H_6.

Fig. 12. C-C bond orbitals in (a) cyclopropane, (b) trimethylene [planar CH_2 groups] and (c) [canted CH_2 groups].

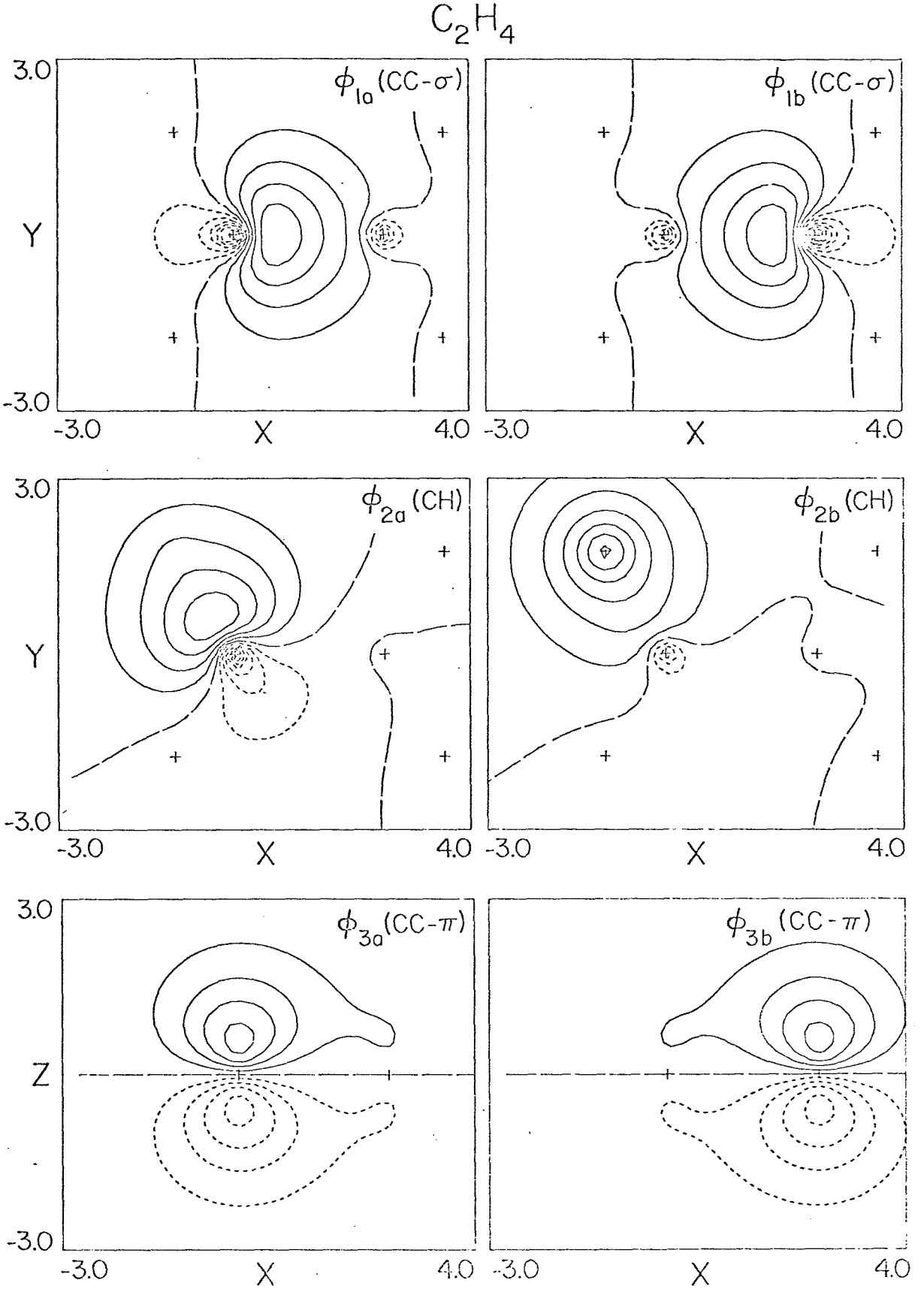
C_2H_4
ϕ_{1a}(CC-σ)
ϕ_{1b}(CC-σ)
ϕ_{2a}(CH)
ϕ_{2b}(CH)
ϕ_{3a}(CC-π)
ϕ_{3b}(CC-π)
3.0
-3.0
Y
Z
X
4.0

FIG. 1

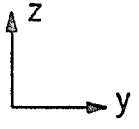

C (^{3}P)

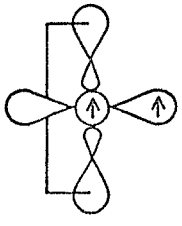

sz	$s\bar{z}$
x	
y	

CH ($^2\Pi$)

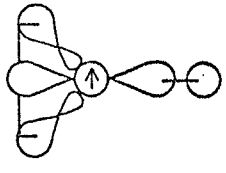

sz	$s\bar{z}$
y	h
x	

CH ($^4\Sigma^-$)

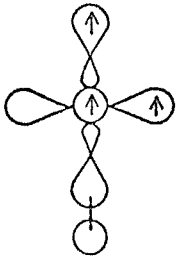

$s\bar{z}$	h
sz	
x	
y	

CH_2 ($^1A_1$)

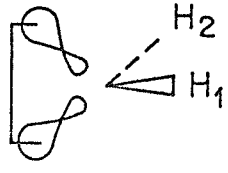

sz	$s\bar{z}$
y	h_1
x	h_2

CH_2 ($^3B_1$)

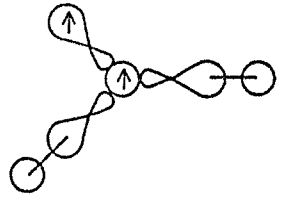

σ_1	h_1
σ_2	h_2
sz	
x	

FIG. 2

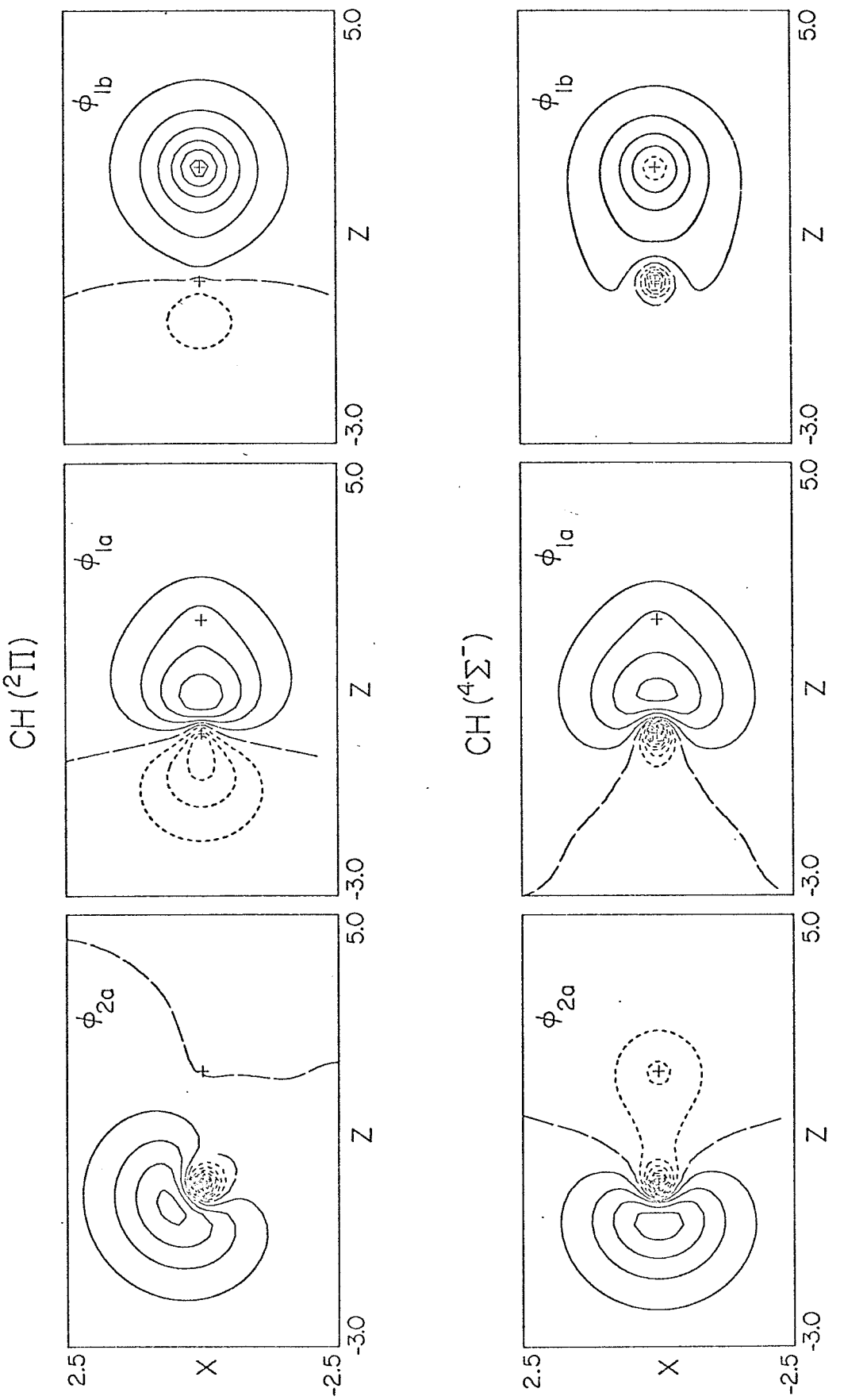

FIG. 3

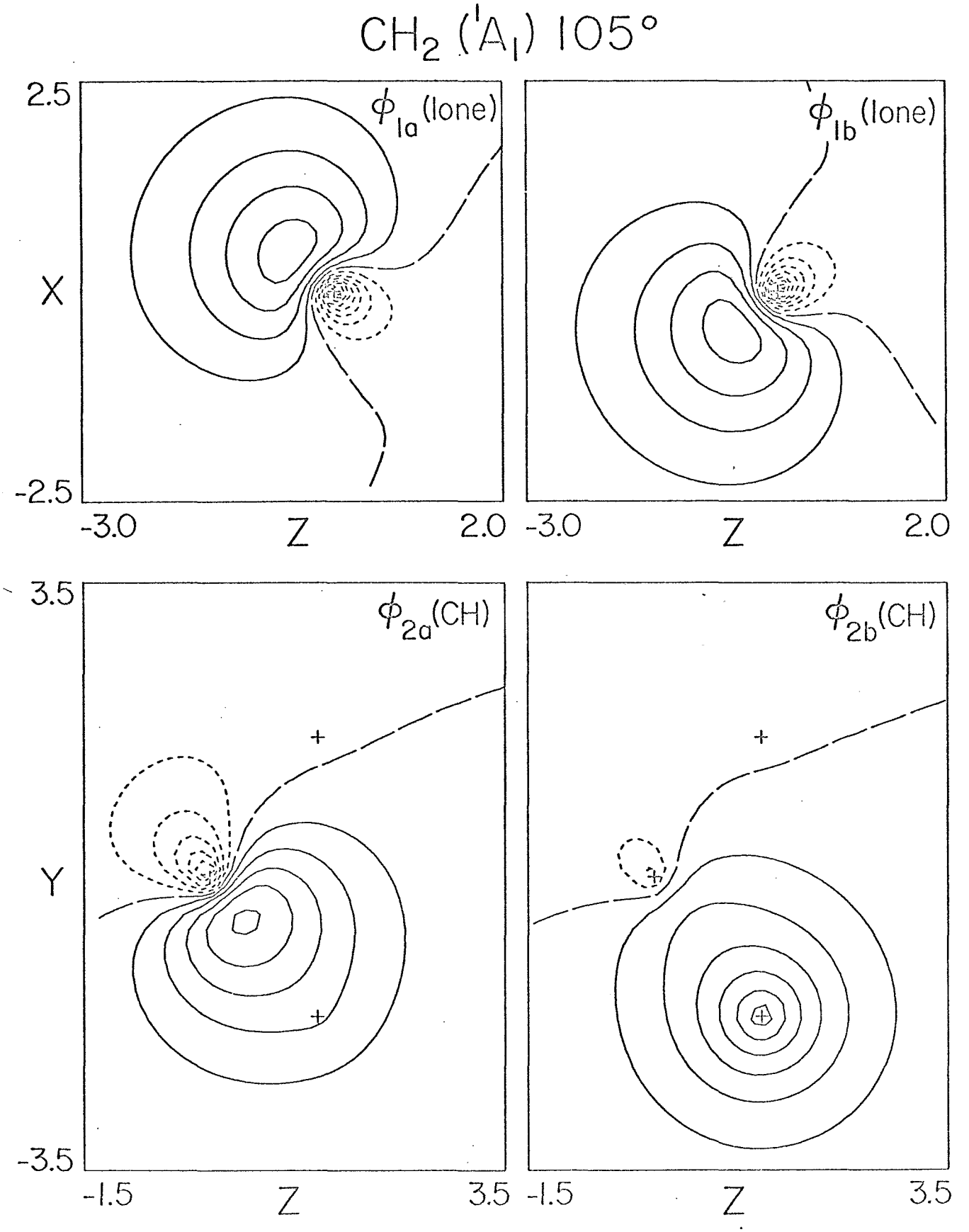
CH2 (1A1) 105°
φ1a(lone)
φ1b(lone)
φ2a(CH)
φ2b(CH)
2.5
X
-2.5
-3.0
Z
2.0
3.5
Y
-3.5
-1.5
3.5

FIG. 4

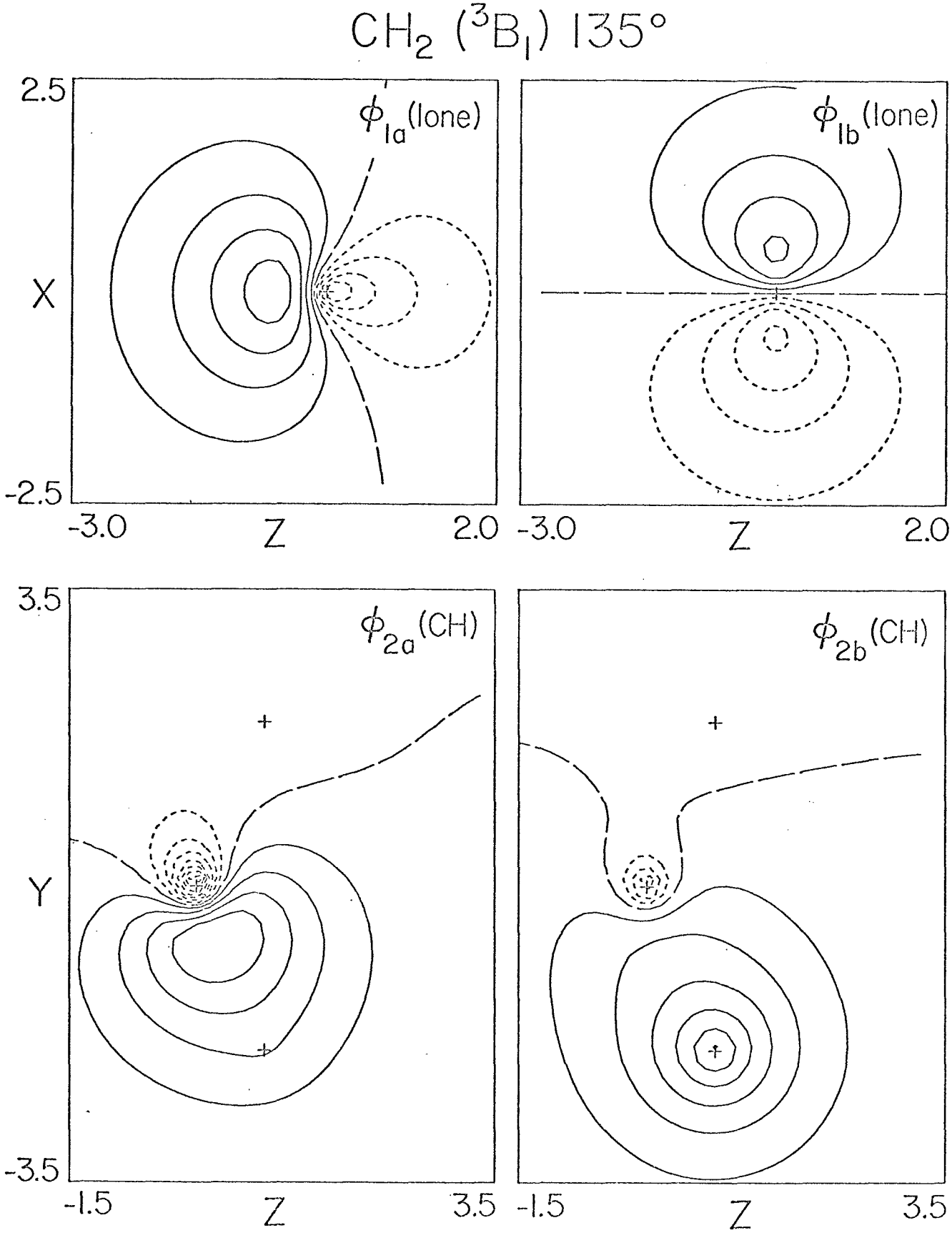
CH2 (3B1) 135°
2.5
X
-2.5
-3.0
Z
2.0
φ1a(lone)
φ1b(lone)
3.5
Y
-3.5
-1.5
3.5
φ2a(CH)
φ2b(CH)

FIG. 5

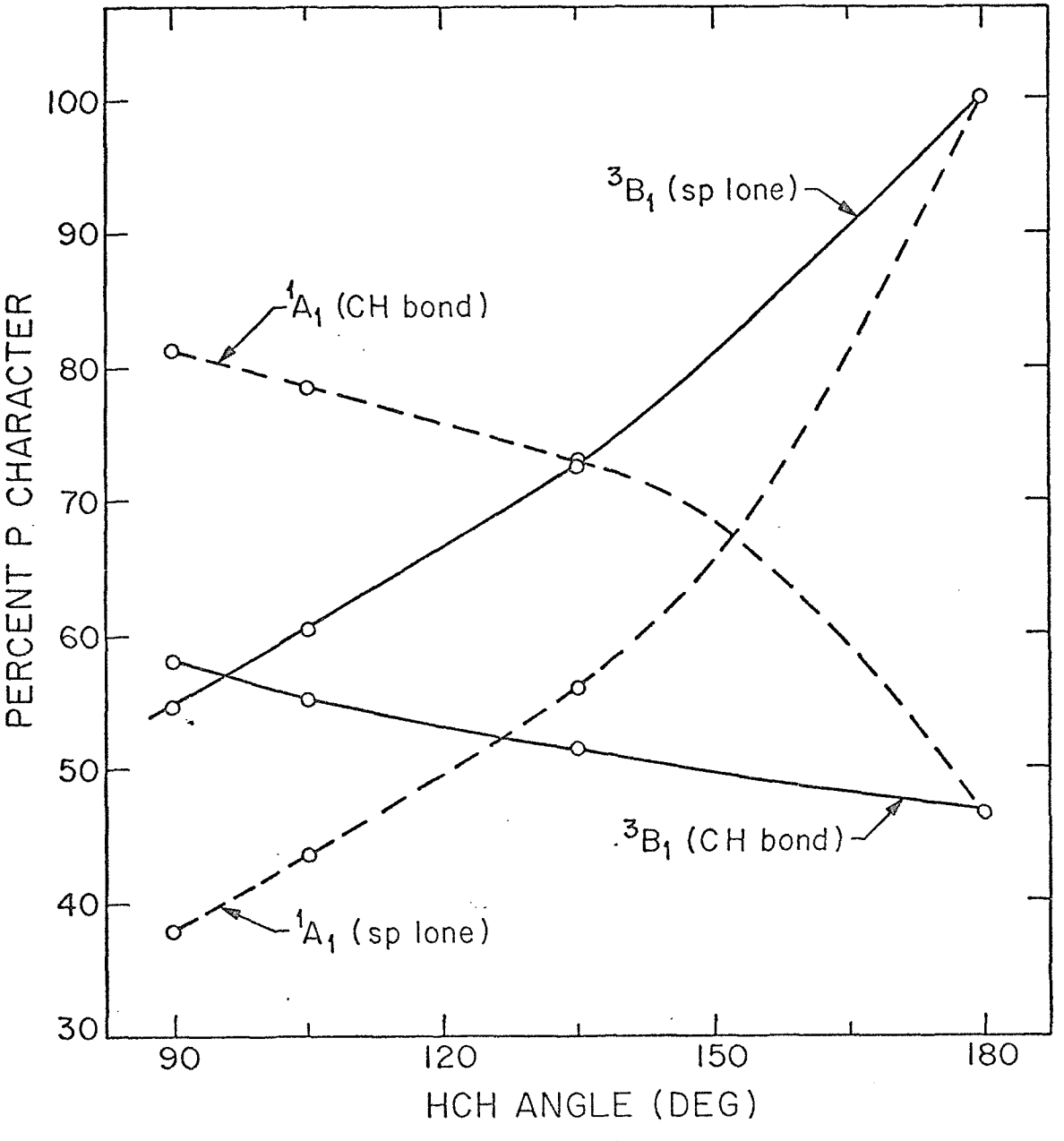
PERCENT P CHARACTER
100
90
80
70
60
50
40
30
90
120
150
180
HCH ANGLE (DEG)
$^3B_1$ (sp lone)
$^1A_1$ (CH bond)
$^3B_1$ (CH bond)
$^1A_1$ (sp lone)

FIG. 6

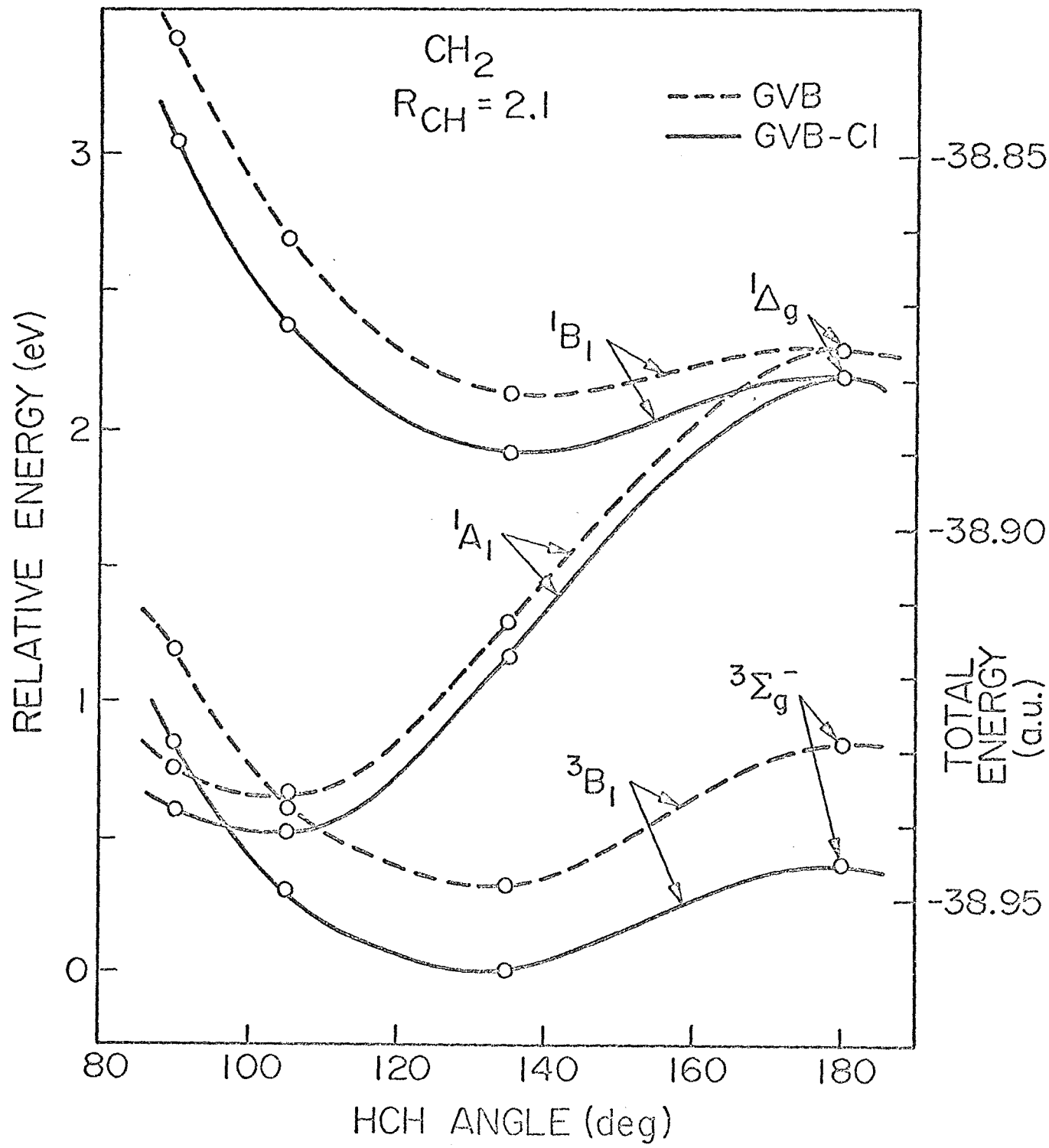
CH2
RCH = 2.1
GVB
GVB-CI
1B1
1Δg
1A1
3Σg−
3B1
RELATIVE ENERGY (eV)
TOTAL ENERGY (a.u.)
-38.85
-38.90
-38.95
0
1
2
3
80
100
120
140
160
180
HCH ANGLE (deg)

FIG. 7

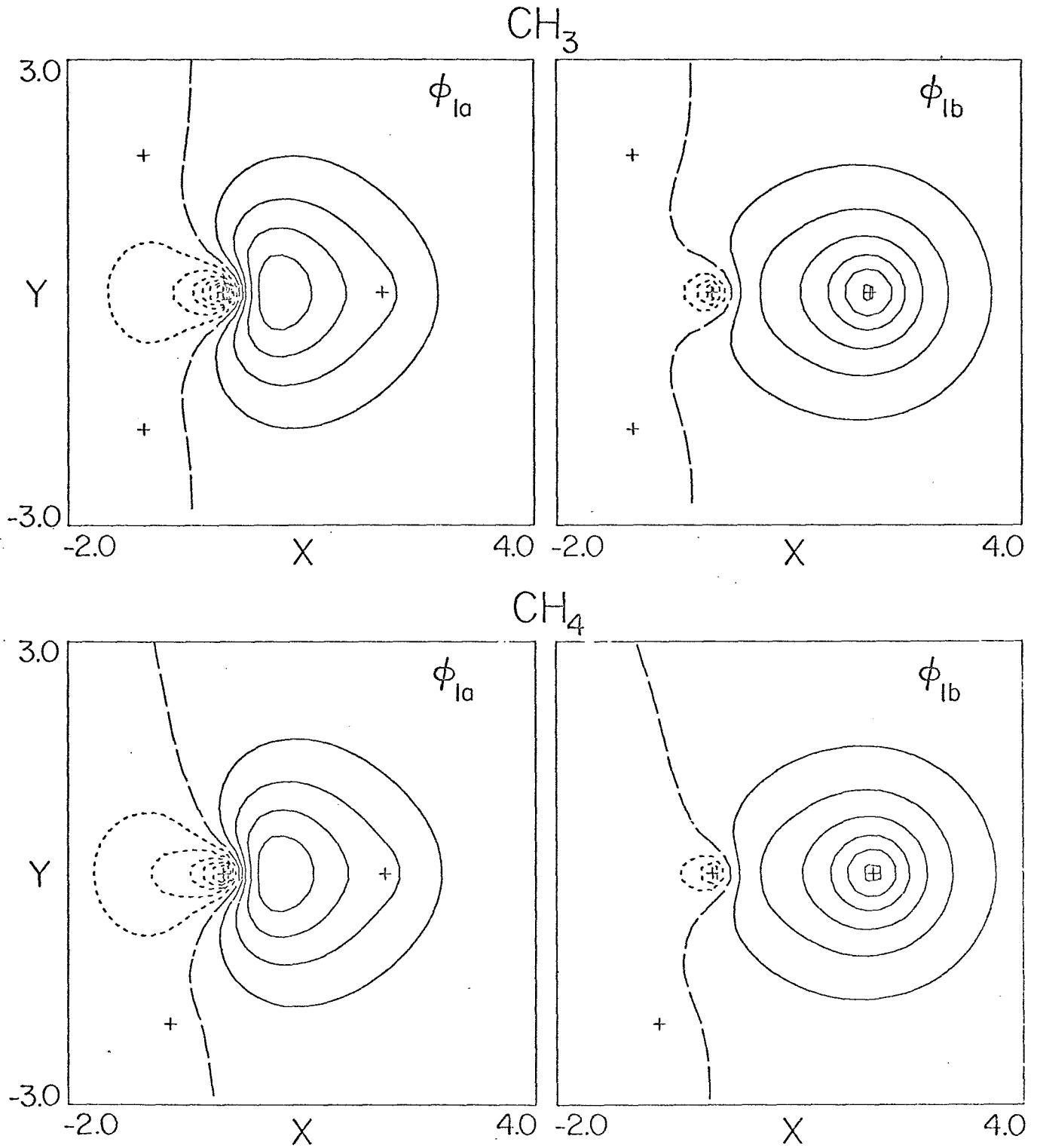

FIG. 8

C_2H_2

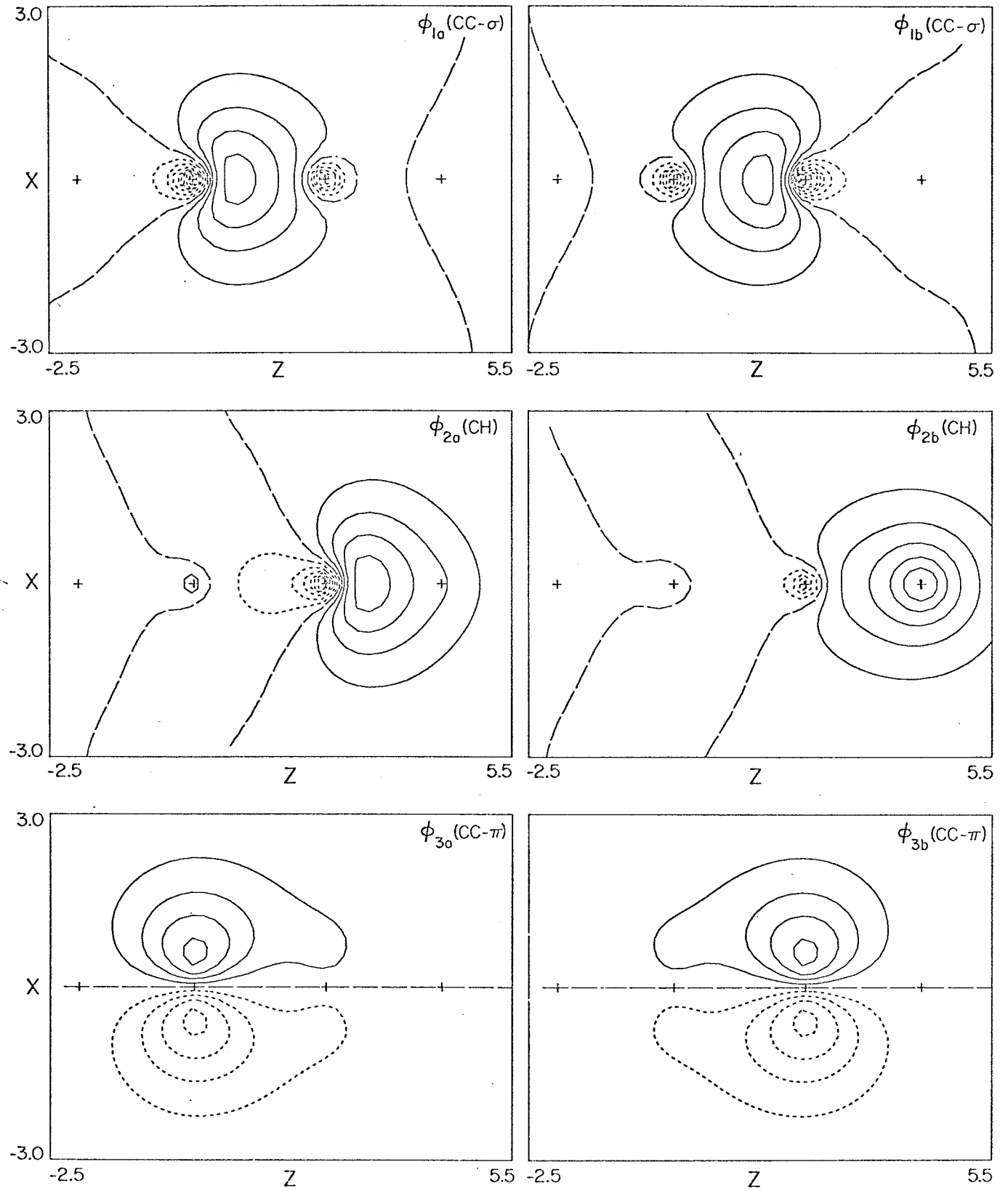
3.0
X
-3.0
-2.5
Z
5.5
ϕ_{1a}(CC-σ)
ϕ_{1b}(CC-σ)
ϕ_{2a}(CH)
ϕ_{2b}(CH)
ϕ_{3a}(CC-π)
ϕ_{3b}(CC-π)

FIG. 9

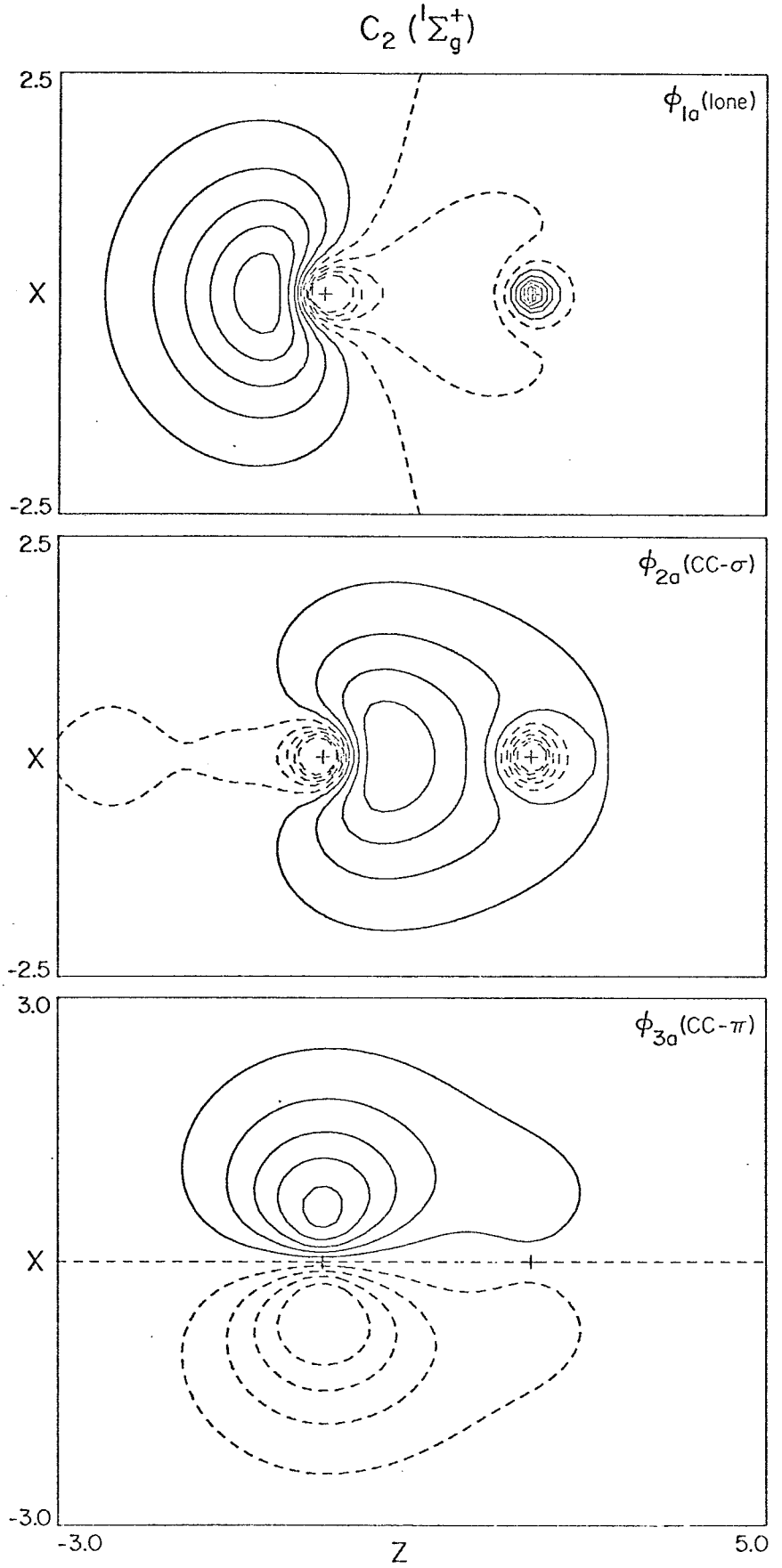
C_2 ($^1\Sigma_g^+$)
2.5
X
-2.5
ϕ_{1a}(lone)
2.5
X
-2.5
ϕ_{2a}(CC-σ)
3.0
X
-3.0
ϕ_{3a}(CC-π)
-3.0
Z
5.0

FIG. 10

ETHANE (STAGGERED)

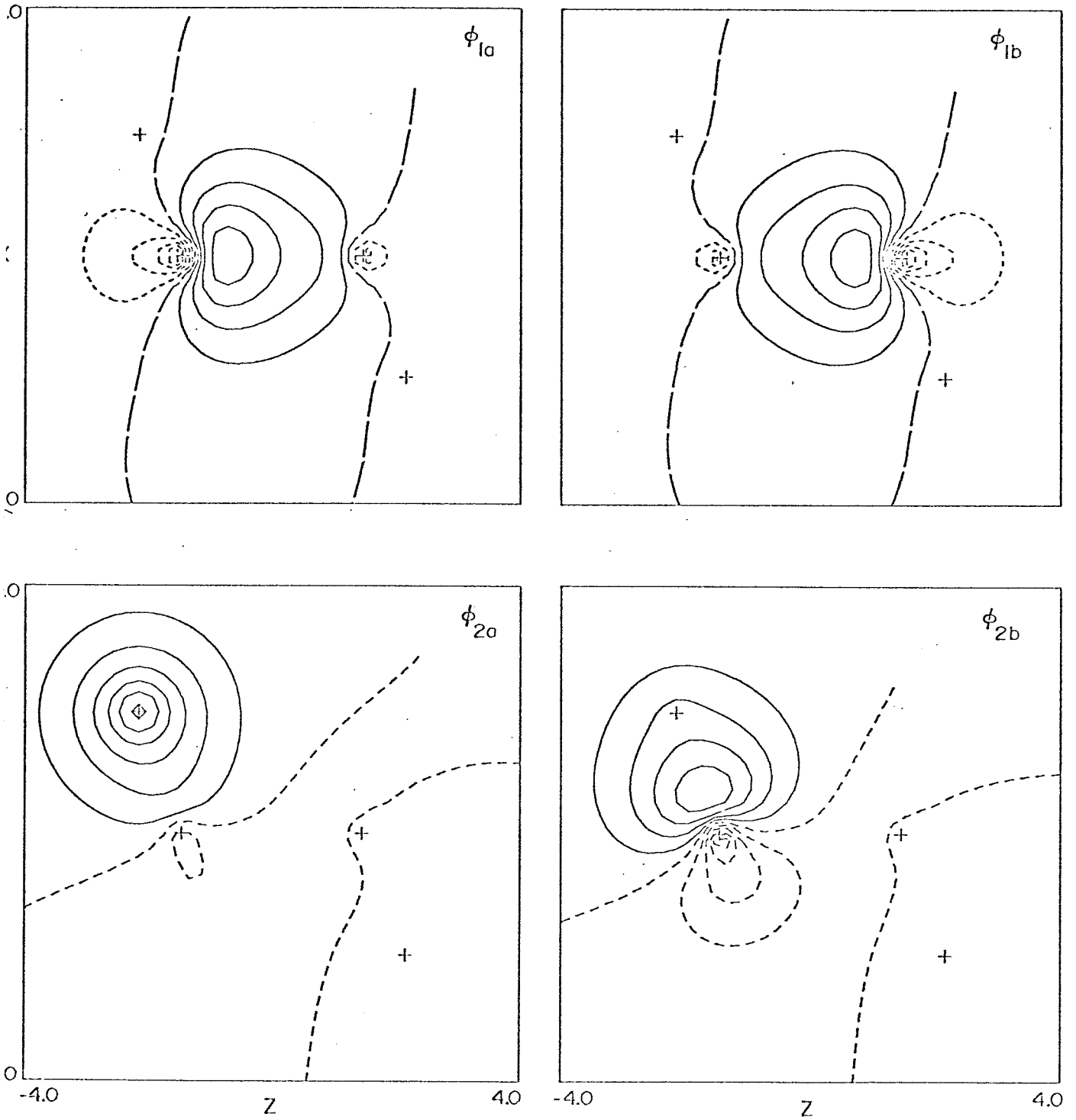

FIG. 11

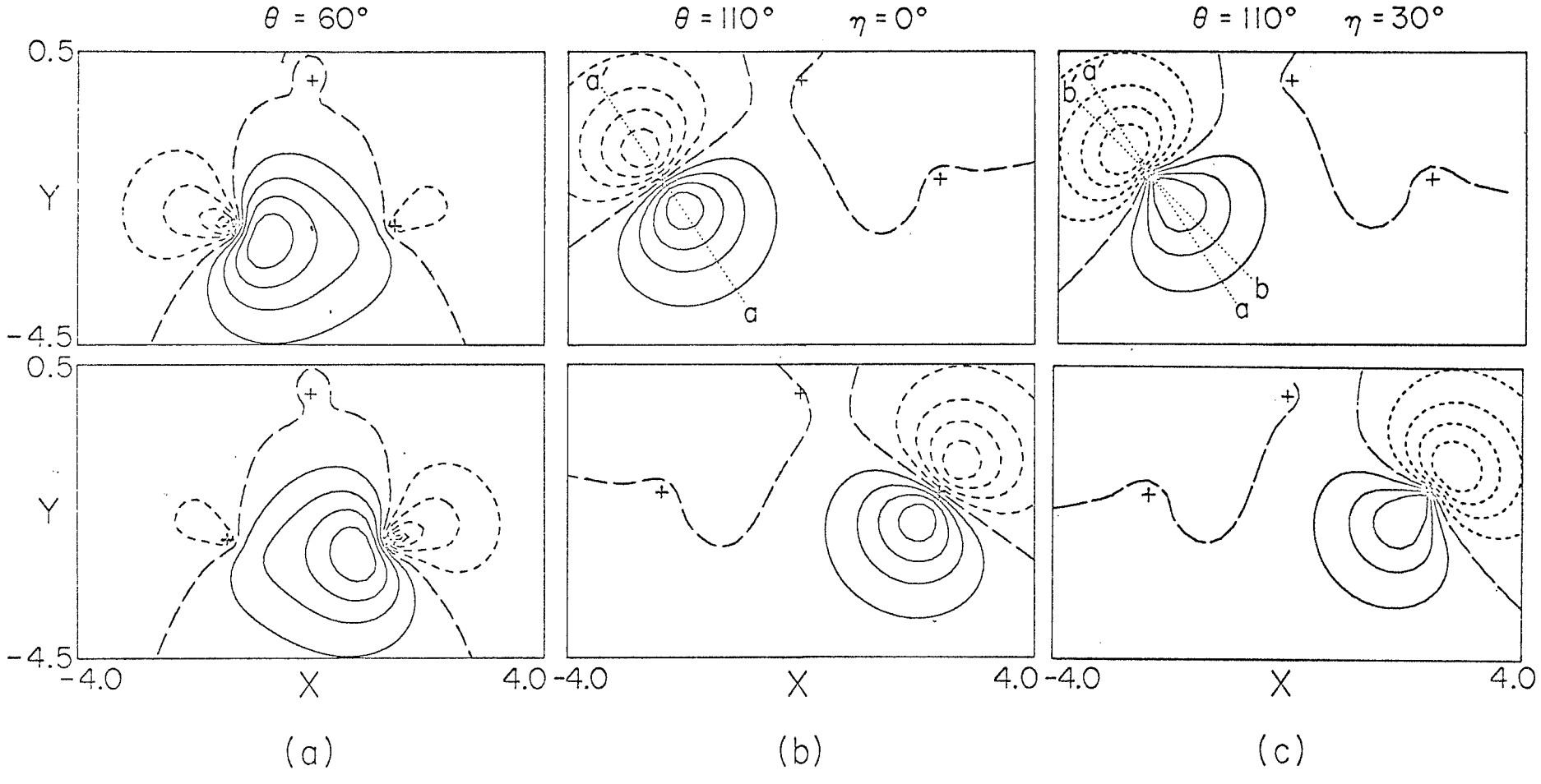

FIG. 12

B. The Electronic Structure of Ozone

The Electronic Structure of Ozone

P. Jeffrey Hay and William A. Goddard III

Contribution No. from the Arthur Amos Noyes Laboratory of Chemical Physics, California Institute of Technology, Pasadena, California 91109

Recent interest has centered on the properties,[1] reactions,[2-4] photolysis,[5-14] and excited states[15] of ozone. Although the first ozonolysis reaction was carried out in 1855,[16] the mechanism of ozonolysis is still being unraveled.[2-4] The study of the electronic bonds of O_3 dates from the work of Chappuis[17] in 1880 and Huggins[18] in 1890, but as yet there is little understanding of the nature of the excited states involved. Since ozone is the primary absorber of atmospheric solar uv radiation in the wavelength region 2000-3500Å, it is one of the principal sources of electronically excited atoms and molecules in the atmosphere.[5] Residents of the greater Los Angeles area are quite familiar with the effects of the chemistry of ozone in the lower atmosphere.

Although Mulliken[19] has discussed possible interpretations of the excited electronic states of O_3, little quantitative information is available from theoretical calculations. Aside from a few semi-empirical calculations,[20-22] the only ab initio study has been made by Peyerimhoff and Buenker,[23] who investigated the dependence of single-configuration $^1A_1$ states upon geometry. As will be discussed, six of the nine lowest states of O_3 are actually described by at

least two MO configurations. In such situations we have found the generalized valence bond (GVB) approach[24] to be quite useful for obtaining quantitative energy differences as well as for retaining a convenient orbital interpretation.

GVB Descriptions of the States of Ozone

A. Computational Details. The GVB method has been discussed previously.[24] In the calculations reported here three basis sets were used: (a) the STO-4G minimum basis of contracted Gaussian (MBS);[25] (b) a 7s3p primitive Gaussian basis contracted to 3s2p (32);[26] and (c) a 9s5p Gaussian basis contracted to 4s2p (DZ).[27] The experimental geometry was taken from the microwave studies of Hughes[28a] and Kaplan, et al.,[28b] who found a central angle θ of 116.8° and an O-O distance R of 1.278 Å (= 2.415 bohr). Other geometries used in the calculations included internuclear distances R (= R_{12} = R_{13}) of 2.601 and 2.787 bohr (the O-O distance in H_2O_2) at 60° and 116° and angles of 60°, 80°, 100°, 120° and 150° for R = 2.415. All results refer to one-pair self-consistent GVB calculations for ground and excited states. Triplet states were obtained in the usual open-shell Hartree-Fock scheme.

Minimum basis set configuration interaction calculations were also performed by using a self-consistent, three-pair GVB function for the ground state as a starting point; i.e., the π-pair and the OO sigma bonds were described by GVB functions with all other orbitals doubly occupied. This procedure effectively allows the valence sigma orbitals to localize into bond orbitals, 2s orbitals, and lone pair orbitals. Appropriate reference configurations

of given symmetry were constructed and all single and double excitations from these configurations were included in the CI calculation (except that excitations from 1s and 2s orbitals were excluded).

B. Orbital Descriptions of O_3 States. Although ozone has a ground $^1A_1$ state suggestive of a closed shell system, the molecule is essentially a biradical, as has been discussed by Gould and Linnett[21] and by Hayes.[29] In the ab initio generalized valence bond (GVB) method, we describe electron pairs in molecules by singlet-coupled orbital products

$$[\phi_{ia}(1)\phi_{ib}(2) + \phi_{ib}(2)\phi_{ia}(1)]\alpha(1)\beta(2) \tag{1}$$

instead of requiring the orbitals to be doubly occupied as in Hartree-Fock (HF) molecular orbitals. All orbitals are solved for

$$\phi_1(1)\phi_1(2)\alpha(1)\beta(2) \tag{2}$$

self-consistently as in SCF-MO theory subject to the restriction that the two orbitals of pair i be orthogonal to all other pairs.

The ground state of ozone can be described by a one-pair GVB function of the form

$$^1A_1\text{: } \mathcal{A}[\cdots(4b_2)^2(6a_1)^2(\phi_a\bar{\phi}_b + \phi_b\bar{\phi}_a)] \tag{4}$$

where $\mathcal{A}$ is the antisymmetrizer and where ϕ and $\bar{\phi}$ denote spin-orbitals with α and β spin, respectively. Equivalently, the GVB function can be written as

$$^1A_1:\ \mathcal{A}[\cdots(4b_2)^2(5a_1)^2\{C_1(1a_2)^2 + C_2(2b_1)^2\}] \qquad (5)$$

which has the form of a two-configuration MO wavefunction. As we shall show, the GVB method is particularly appropriate for describing the states of ozone, since very few states are adequately described by a single MO configuration.

In Figure 1 is shown a schematic representation of the GVB function in (4). The π orbitals can be regarded as consisting of (a) a doubly occupied orbital on the central oxygen delocalized onto the other atoms and (b) two singly occupied $p\pi$ orbitals--ϕ_a and ϕ_b--on each end of the molecule. Also shown in the figure are the two nonbonding $p\sigma$ orbitals on the terminal oxygens. In the MBS basis the one-pair GVB function gives a molecular energy 0.1335 hartree = 3.63 eV = 84 kcal lower than the single configuration MO function--indicating the substantial biradical nature of ozone. The GVB orbitals ϕ_a and ϕ_b in (4) have an overlap of 0.229.

Alternatively one can construct a low-lying triplet state of $^3B_2$ symmetry by taking the antisymmetric combination of the GVB orbitals in (4):

$$^3B_2:\ \mathcal{A}[\cdots(4b_2)^2(6a_1)^2(\phi_a\bar{\phi}_b - \phi_b\bar{\phi}_a)] \qquad (6)$$

where ϕ_a and ϕ_b may be taken to be b_1 and a_2 symmetry functions without restriction. From these b_1 and a_2 orbitals arises another singlet state ($^1B_2$), which we shall discuss later.

The oxygen atom with configuration $(p_z)^2p_xp_y$ can be pictured as

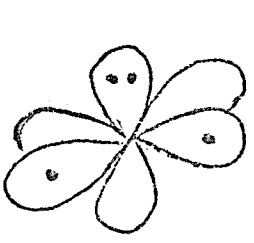

where the doubly occupied orbital will be taken to lie along the z (π) axis (and the singly occupied orbitals lie in the xy plane). Bonding the p-lobes of two other oxygen atoms to it produces the preceding 4π $^1A_1$ and $^3B_2$ states if the remaining unpaired p orbitals on each end are oriented perpendicular to the plane of the molecule (Figure 1a). ($n\pi$ refers to the number of π electrons.) The unpaired p lobes on each end can also be oriented so that one lies in the molecular plane and the other perpendicular to it (Figure 1b). These 5π structures with a single occupied π orbital on one end and a singly occupied σ orbital on the other do not have the correct symmetry with respect to σ_v reflection. Taking both possible structures, however, one can construct the many electron $^1A_2$, $^1B_1$, $^3A_2$ and $^3B_1$ states all of which should have comparable energies.

Finally, one can consider 6π states with two singly occupied σ orbitals (Figure 1c) with total $^1A_1$ and $^3B_2$ symmetries. While the 4π states were stabilized by three-electron pi-bonds in each O-O region, the 5π and 6π states should have increasingly higher energies because of the π-pair repulsions. The valence states of ozone are listed in Table I along with the dominant MO configurations appearing in each state.

C. Results. In Tables II and III the results of self-consistent GVB calculations are summarized for the nine lowest states of O_3. In the MBS basis (the results in the 32 basis do not differ appreciably) the 4π $^3B_2$ lies 0.51 eV above the ground state in GVB while the CI calculation placed it at 1.11 eV above the $^1A_1$ state. As noted earlier, the GVB calculations do not distinguish between the A_2 and B_2 5π states, since the lowest 5π solution has the form of one of the two equivalent "resonance structures."

When all orbitals are required to be symmetry functions, the many-electron functions have the correct total symmetry but also have unrealistically high energies (e.g., 3.3 eV higher for the $^3B_1$ state). Since CI gave an $A_2 - B_1$ splitting of only 0.23 eV for the 5π triplets and 0.28 eV for the singlets (A_2 lower in both instances), the "asymmetric" resonance structure in Figure 1b is seen to be a quite adequate description of the 5π states. The 5π triplet state lies below the singlet, since the two singly occupied orbitals are orthogonal. Similarly we find $^3A_2 < {}^1A_2$, $^3B_1 < {}^1B_1$ from the CI results.

The 6π $^3B_2$ and $^1A_1$ were found (from CI) to be 3.2 and 3.5 eV, respectively, above the ground state (2.09 and 2.26 in GVB). Still higher (8.05 eV in GVB) lay the 4π $^1B_2$ which can be represented

$$4\pi\ {}^1B_2\text{: } \mathcal{A}[\cdots(4b_2)^2(6a_1)^2(1b_1)^2(1a_2\overline{2b_1} + 2b_1\overline{1a_2})] \qquad (6)$$

Since the $2b_1$ orbital is unoccupied in the MO description of the ground state, this resembles a $\pi \rightarrow \pi^*$ ($1a_2 \rightarrow 2b_1$) excitation. The

representation in (6) is somewhat misleading, for the $1b_1$ doubly-occupied orbital, which was localized mostly on the central atom in the ground state, becomes localized on the terminal atoms in the $^1B_2$ state, giving them large O^- character. This state can be described by a difference of two ionic resonance structures as shown in Figure 1d. In the larger 32 basis, which has more freedom to describe ionic states, the $^1A_1$-$^1B_2$ splitting is lowered 0.83 eV; in the MBS-CI the calculated $^1B_2 \leftarrow {}^1A_1$ excitation is 6.70 eV.

D. Influence of Changes in Geometry. In Tables II and III we also show the effect of varying the internuclear distance ($R = R_{12} = R_{13}$) at the fixed equilibrium bond angle (116°) of the ground state. Although the STO-4G set may not be reliable for predicting absolute geometries in the states which have appreciable ionic character, we can still hope to obtain some understanding of the relative geometries. The ground state is found to have a calculated bond length 0.13 bohr longer than the experimental, while Newton, et al.,[30] found good agreement with the experimental geometry from Hartree-Fock calculations. The 4π $^3B_2$ and the 5π states have longer (0.05-0.07 bohr) bond lengths and have energies 0.29 to 0.42 eV below the calculated vertical excitation energies. The 6π states and the $^1B_2$ state have even longer calculated bond lengths and more drastic changes in the "adiabatic" excitation energy as compared to the "vertical" excitation energies for R = 2.415 (see Tables II and III).

With the exception of the $6\pi\ ^1A_1$ state variation of θ indicated that all states had equilibrium bond angles within 10 degrees of the ground state for R = 2.415 (see Figure 2). The $6\pi\ ^1A_1$ state crossed the $4\pi\ ^1A_1$ state near $\theta = 90°$ and became the ground state for smaller angles. It was found to have an equilibrium bond angle of 60° with equal O-O bond distances similar to the peroxide (R = 2.787 bohr) O-O single bond distance (Figure 1e). As shown in Table IV, the MBS basis indicated that "equilateral" ozone was nearly comparable in energy to the $4\pi\ ^1A_1$ ground state, but more accurate calculations in the DZ basis indicate equilateral ozone lies about 1.50 eV above the ground state. Since the estimated vertical excitation energy to this state at $\theta = 116°$ and R = 2.415 ($6\pi\ ^1A_1 \leftarrow 4\pi\ ^1A_1$) is 3.5 eV, even allowing for a lowering of 0.9 eV upon bond lengthening indicates that the potential curve for this state would be quite flat with a minimum at 60°. There is a barrier of about 0.7 eV for the transition from the minimum of the 6π state to the crossing point for the 4π state at 90°. In addition the mixing between them is quite small (since they differ by a two-electron transition) and as a result these states should act as essentially two different states, $1\ ^1A_1$ dissociating to $O_2(^3\Sigma_g^-) + O(^3P)$ and $2\ ^1A_1$ probably dissociating to $O_2(^1\Delta_g) + O(^1D)$.

Discussion

A. The Spectrum of Ozone. Experimental knowledge about the spectrum of ozone can be summarized as follows:[15, 31]

(1) The Hartley band--a broad peak extending from 2200-3000 Å with a maximum near 2537 Å (4.9 eV) with absorption coefficient f = 133 cm^{-1}.

(2) The Huggins band--a set of weak bands extending on the low energy side of the Hartley band and possibly due to the same transition from 3000-3400 Å (3.6-4.1 eV) with f = 3.32 cm^{-1} at 3021 Å and f = 0.067 cm^{-1} at 3341 Å .

(3) The Chappuis band--a weak band from 5500-6100 Å (2.04-2.26 eV) with peaks at 6020 and 5770Å (f = 0.052 cm^{-1}).

(4) The Wulf band--an extremely weak progression of bands from 6000-10000Å with rotational structure resolved in the band at 10000Å (1.2 eV).[32]

Transitions from the ground state to excited singlet states with other than 4π electrons would be expected to be quite weak since they correspond roughly to atomic $p_x \rightarrow p_y$ transitions (such as in the $n \rightarrow \pi^*$ transition of H_2CO). On this basis the only strong transition should be $^1B_2 \leftarrow {}^1A_1$ which we associate with the Hartley band. Although our best estimate for the vertical transition is 6.70 eV (see Table I), a longer bond length in the $^1B_2$ state resulted in a lowering of 1.4 eV relative to the ground state. This change in bond length accounts for the broad feature of this band and also improves the agreement with the observed energies (4.1-5.6 eV) in the Hartley band.

This change in geometry would also be consistent with the Huggins band being part of the $^1B_2 \leftarrow {}^1A_1$ transition with wavelengths too long (> 3100Å) to dissociate O_3 into $O_2(^1\Delta_g) + O(^1D)$.

The $6\pi\ ^1A_1 \leftarrow 4\pi\ ^1A_1$ transition could also be responsible for the Huggins band (the calculated energy is 3.5 eV) but would be expected to be quite weak since it corresponds to a two-electron transition. It would be allowed primarily by the small components of 4π character in the excited wavefunction.

We identify the Chappuis band with the dipole-allowed $^1B_1 \leftarrow {}^1A_1$ transition, essentially a $n \rightarrow \pi^*$ in nature. Good agreement is found between the calculated (2.24) and observed (2.07 and 2.16) energies. The $^1A_2 \leftarrow {}^1A_1$ transition, although dipole-forbidden, would become allowed by asymmetric stretching (b_2) modes and thus is probably responsible for the Wulf band.

Of the triplet states the $^3B_2 \leftarrow {}^1A_1$ transition should be strongest since they are both 4π systems and have comparable geometries. The vertical transition at 1.11 eV corresponds quite closely to the 1.2 eV transition often attributed to the O-O transition of the Wulf bands. However the 1.2 eV transition is much weaker than the other vibrational components of the Wulf band and is different in character in that rotational levels are resolved. We assign this 1.2 eV transition as $^3B_2 \leftarrow {}^1A_1$. The analysis of the rotational lines by Runyan and Robinson[32] has suggested an assignment of an upper triplet state.

Equilateral ozone, which is isoelectronic with cyclopropane, should be transparent in the visible and uv, since the first observed band in cyclopropane occurs at 8 eV.[33] Transitions to the $6\pi\ ^1A_1$ state could lead to appreciable population of the 60° form since it would have a barrier to ring-opening, but we find no

experimental evidence that would indicate the existence of such a metastable state of ozone.

B. Experimental Studies of O_3 Excited States. There appears to be no spectral evidence for triplet states other than the $^3B_2$ state already discussed, but there exists experimental evidence in the photochemistry of O_3. Recently Jones and Wayne[5] concluded that photolysis of ozone (λ = 3340Å) led to

$$O_3 + h\nu \rightarrow O_2(^1\Delta_g \text{ or } ^1\Sigma_g^+) + (^3P) \tag{7}$$

while irradiation at $\lambda \leq 3020$Å led to

$$O_3 + h\nu \rightarrow O_2(^1\Delta_g \text{ or } ^1\Sigma_g^+) + O(^1D) \tag{8}$$

Reaction (7) would involve one of the excited 5π or 6π O_3 triplet states. Recent controversy has centered on the nature of the products involved in the primary process of ozone photolysis for λ = 2537Å. Evidence now indicates[6, 8, 13, 14] that the reaction is

$$O_3 + h\nu \rightarrow O_2(^1\Delta_g) + O(^1D) \tag{9}$$

and that the $O(^1D)$ is rapidly quenched by the reaction[6, 8, 10-12]

$$O(^1D) + O_2(^3\Sigma_g^-) \rightarrow O(^3P) + O_2(^1\Sigma_g^+) \tag{10}$$

which could also involve excited triplet states. The reaction in (9) is due to the $^1B_2$ state of O_3, although it is uncertain whether the

$^1B_2$ state dissociates into $O_2(^1\Delta_g)$ + $O(^1D)$ or crosses over to the 6π $^1A_1$ state to give these dissociation products.

C. O_n Ring Structures for Triatomic Molecules. The existence of a metastable 60° state of O_3 only 1.5 eV above the ground (116°) state is not unexpected, since the isoelectronic systems cyclopropane and ethylene oxide have ring structures as their stable form. The ab initio calculations of Peyerimhoff and Buenker[23] also showed that an $^1A_1$ configuration became the ground state for small bond angles with a minimum inthe vicinity of 60°.

In NO_2, which has an equilibrium bond angle of 136°,[31] one of the excited $^2B_1$ states with configuration $(6a_1)^2(3b_2)^2(1b_1)^2(1a_2)^2(2b_1)^1$ would be expected to give a low-lying ring structure for small angles in (I). From the ab initio results of Fink[34] on the states of NO_2, the $^2B_1$ state appears to be the ground state for small ONO angles, although he did not consider angles less than 90°.

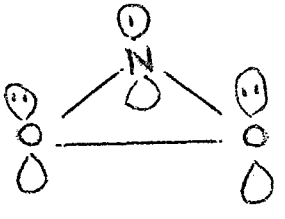

I

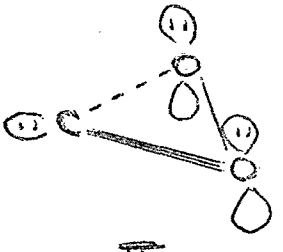

II

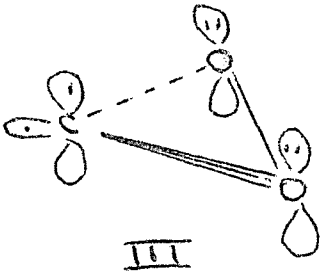

III

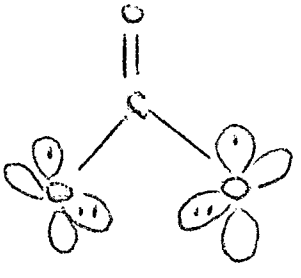

IV

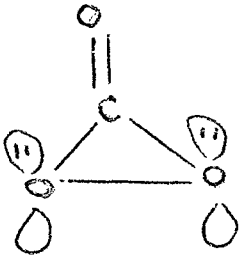

V

The CO_3 radical was found to have a Y-shaped structure (V) on the basis of semi-empirical calculations.[35, 36] This 6π state is quite analogous to the 6π $^1A_1$ state of ozone while the 4π open form (IV) of CO_3 corresponds to the 4π $^1A_1$, $^3B_2$ and $^1B_2$ states of O_3. In II and III are shown possible cyclic structures for CO_2 with respective $^1A_1$ and $^3B_1$ symmetries, similar to the $^1A_1$ and $^3B_1$ states of CF_2. Once found, these states, while higher in energy than the linear ground state, could have fairly long lifetimes if the barrier to ring opening were sufficiently large.

Conclusions

Eight valence states within an energy range of 3.5 eV were found for the ozone molecule with the generalized valence bond method. An ionic $^1B_2$ state, with quite different geometry from the ground state, has been determined to be responsible for the strong absorption in the Hartley band in the vicinity 4.1-5.6 eV. Both this $^1B_2$ state and an excited $^1A_1$ state are likely to lead to the O_2 ($^1\Delta_g$) + O(^{1}D) photolysis products observed at 2537Å. This excited $^1A_1$ state has an optimum geometry of an equilateral triangle with an energy 1.5 eV above the ground state and ring opening barrier of approximately 0.7 eV.

References

(1) S. Rothenberg and H. F. Schaefer III, Mol. Phys., 21, 317 (1971).

(2) R. W. Murray, Acc. Chem. Res., 1, 313 (1968).

(3) N. L. Bauld, J. A. Thompson, C. E. Hudson, and P. S. Bailey, J. Amer. Chem. Soc., 90, 1822 (1968).

(4) J. Renard and S. Fliszar, J. Amer. Chem. Soc., 92, 2628 (1970); S. Fliszar and M. Granger, ibid., 92, 3361 (1970).

(5) I. T. N. Jones and R. P. Wayne, Proc. Roy. Soc. A319, 273 (1970).

(6) R. Gilpin, H. I. Schiff, and K. H. Welge, J. Chem. Phys., 55, 1087 (1971).

(7) T. P. J. Izod and R. P. Wayne, Nature, 217, 947 (1968); Proc. Roy. Soc. (London), A308, 81 (1968).

(8) M. Gauthier and D. R. Snelling, J. Chem. Phys., 54, 4317 (1971).

(9) W. B. DeMore and O. F. Raper, J. Chem. Phys., 44, 1780

(10) S. V. Filseth, A. Zia, and K. H. Welge, J. Chem. Phys., 52, 4402 (1970).

(11) D. Biedenkapp and E. J. Bair, J. Chem. Phys., 52, 6119 (1970).

(12) J. F. Noxon, J. Chem. Phys., 52, 1852 (1970).

(13) E. Castellano and H. J. Schumacher, Z. Physik Chem., 44, 1780 (1966).

(14) I. T. N. Jones and R. P. Wayne, Proc. Roy. Soc. Lond., A321, 409 (1971).

(15) M. Griggs, J. Chem. Phys, 49, 857 (1968).

(16) C. F. Schönbein, J. Prakt. Chem., 66, 282 (1855).

(17) J. Chappuis, C. R. Acad. Sci. (Paris), 91, 985 (1880).

(18) W. Huggins, Proc. Roy. Soc., 48, 216 (1890).

(19) R. J. Mulliken, Can. J. Chem., 36, 10 (1958).

(20) I. Fischer-Hjalmars, Ark. Fys., 11, 529 (1956).

(21) R. D. Gould and J. W. Linnett, Trans. Faraday Soc., 59, 1001 (1963).

(22) H. J. Maria, D. Larson, M. E. McCarville, and S. P. McGlynn, Accts. Chem. Res., 3, 368 (1970).

(23) S. D. Peyerimhoff and R. J. Buenker, J. Chem. Phys., 47, 1953 (1967).

(24) P. J. Hay, W. J. Hunt and W. A. Goddard III, Chem. Phys. Lett. (to be published); W. J. Hunt, P. J. Hay, and W. A. Goddard III, J. Chem. Phys. (to be published).

(25) W. J. Hehre, R. F. Stewart and J. A. Pople, J. Chem. Phys., 51, 2657 (1969).

(26) D. R. Whitman and C. J. Hornback, J. Chem. Phys., 51, 398 (1969).

(27) (a) S. Huzinaga, J. Chem. Phys., 42, 1293 (1965). (b) T. H. Dunning, J. Chem. Phys., 53, 2823 (1970).

(28) (a) R. H. Hughes, J. Chem. Phys., 24, 131 (1956). (b) L. D. Kaplan, et al., J. Chem. Phys., 24, 1183 (1956).

(29) E. F. Hayes, J. Amer. Chem. Soc., 93, 2090 (1971).

(30) M. D. Newton, W. A. Lathan, W. J. Hehre, and J. A. Pople, J. Chem. Phys., 52, 4064 (1970).

(31) G. Herzberg, Molecular Spectra and Molecular Structure, Vol. III (VanNostrand Co., Princeton, 1967).

(32) C. C. Runyan and G. W. Robinson, to be published.

(33) H. Basch, M. B. Robin, N. A. Kuebler, C. Baker, and D. W. Turner, J. Chem. Phys., 51, 52 (1969).

(34) W. H. Fink, J. Chem. Phys., 49, 5054 (1968).

(35) J. F. Olsen and L. Burnelle, J. Amer. Chem. Soc., 91, 7286 (1969).

(36) B. M. Gimarc and T. S. Chan, J. Chem. Phys., 49, 4043 (1968).

Table I. Dominant MO Configurations in the GVB Valence States of Ozone

State	Configurations
$^1A_1$ (4π)	$(6a_1)^2$ $(4b_2)^2$ $(1a_2)^2$ $(2b_1)^0$
	$(6a_1)^2$ $(4b_2)^2$ $(1a_2)^0$ $(2b_1)^2$
$^{1,3}B_2$ (4π)	$(6a_1)^2$ $(4b_2)^2$ $(1a_2)^1$ $(2b_1)^1$
$^{1,3}A_2$ (5π)	$(6a_1)^2$ $(4b_2)^1$ $(1a_2)^2$ $(2b_1)^1$
	$(6a_1)^1$ $(4b_2)^2$ $(1a_2)^1$ $(2b_1)^2$
$^{1,3}B_1$ (5π)	$(6a_1)^2$ $(4b_2)^1$ $(1a_2)^1$ $(2b_1)^2$
	$(6a_1)^1$ $(4b_2)^2$ $(1a_2)^2$ $(2b_1)^1$
$^1A_1$ (6π)	$(6a_1)^2$ $(4b_2)^0$ $(1a_2)^2$ $(2b_1)^2$
	$(6a_1)^0$ $(4b_2)^2$ $(1a_2)^2$ $(2b_1)^2$
$^{1,3}B_2$ (6π)	$(6a_1)^1$ $(4b_2)^1$ $(1a_2)^2$ $(2b_1)^2$

Table II. Energies of the States of Ozone[a] (θ = 116.8°)

State	GVB[b] R = 2.415	GVB[b] R_{min}	GVB[b] E_{min}	CI[b] R = 2.415	GVB[c] R = 2.415
$^1A_1$ (4π)	-223.0126	2.55	-223.0234	-223.1256	-223.8063
$^3B_2$ (4π)	-222.9940	2.60	-223.0153	-223.0848	-223.7803
$^3A_2$ (5π)	-222.9744	2.61	-222.9987	-223.0598	-223.7623
$^3B_1$ (5π)				-223.0513	
$^1A_2$ (5π)	-222.9703	2.62	-222.9964	-223.0535	-223.7574
$^1B_1$ (5π)				-223.0433	
$^3B_2$ (6π)	-222.9359	2.65	-222.9765	-223.0080	-223.7221
$^1A_1$ (6π)	-222.9295	2.66	-222.9724	-222.9968	-223.7149
$^1B_2$ (4π)	-222.7164	2.72	-222.7791	-222.8792	-223.5407

[a] All energies in hartrees. [b] MBS basis. [c] 32 basis.

Table III. Excitation Energies (eV) for the States of Ozone at θ = 116°. Bond Lengths are Given in Bohr Radii.

State	GVB[a] R = 2.415	GVB[a] R_{min}[c]	GVB[b] R = 2.415	CI[a] R = 2.415	Exp[d]
$^1A_1$	—	— (2.55)	—	—	—
$^3B_2$	0.51	0.22 (2.60)	0.69	1.11	1.2
$^3A_2$	1.04	0.67 (2.61)	1.20	1.79	
$^1A_2$	1.15	0.73 (2.62)	1.33	1.96	1.2-2.0
$^3B_1$	1.04	0.67 (2.61)	1.20	2.02	
$^1B_1$	1.15	0.73 (2.62)	1.33	2.24	2.04-2.26
$^3B_2$	2.09	1.28 (2.65)	2.29	3.20	
$^1A_1$	2.26	1.39 (2.66)	2.49	3.50	[3.59-4.13][e]
$^1B_2$	8.05	6.65 (2.72)	7.23	6.70	4.13-5.65

[a] MBS basis. [b] 32 basis. [c] R_{min} indicated in parentheses. [d] Refs. 15 and 31. [e] Possibly an extension of the $^1B_2$ band.

Table IV. Comparison of the Energies of Ground State Ozone (4π $^1A_1$, θ = 116°, R = 2.415) and Equilateral Ozone (6π $^1A_1$, θ = 60°, R = 2.787)

Method	Basis	Energy (hartree) $^1A_1$ (θ = 116°)	Energy (hartree) $^1A_1$ (θ = 60°)	ΔE (eV)[a]
HF[b]	MBS	-222.8791	-222.9435	-1.75
GVB-1 pair	MBS	-223.0126	-223.0038	+0.24
CI	MBS	-223.1256	-223.1270	-0.04
HF[b]	32	-223.7003	-223.7376	-1.01
GVB-1 pair	32	-223.8063	-223.7956	+0.29
HF[b]	DZ	-224.2070	-224.1937	+0.36
GVB-1 pair	DZ	-224.3117	-224.1567	+1.50

[a] ΔE = E (θ = 116°) - E (θ = 60°). [b] Single configuration wavefunction.

FIGURE CAPTIONS

Figure 1 Schematic diagram of the valence states of ozone.

Figure 2. Energies of the states of ozone as a function of bending angle ($R_{12} = R_{13} = 2.415$ bohr)

Figure 3 Relative ordering of the states of O_3 with the states of $O_2 + O$. The calculated O_3 energies have been shifted to agree with the known (1.0 eV) dissociation energy.[31]

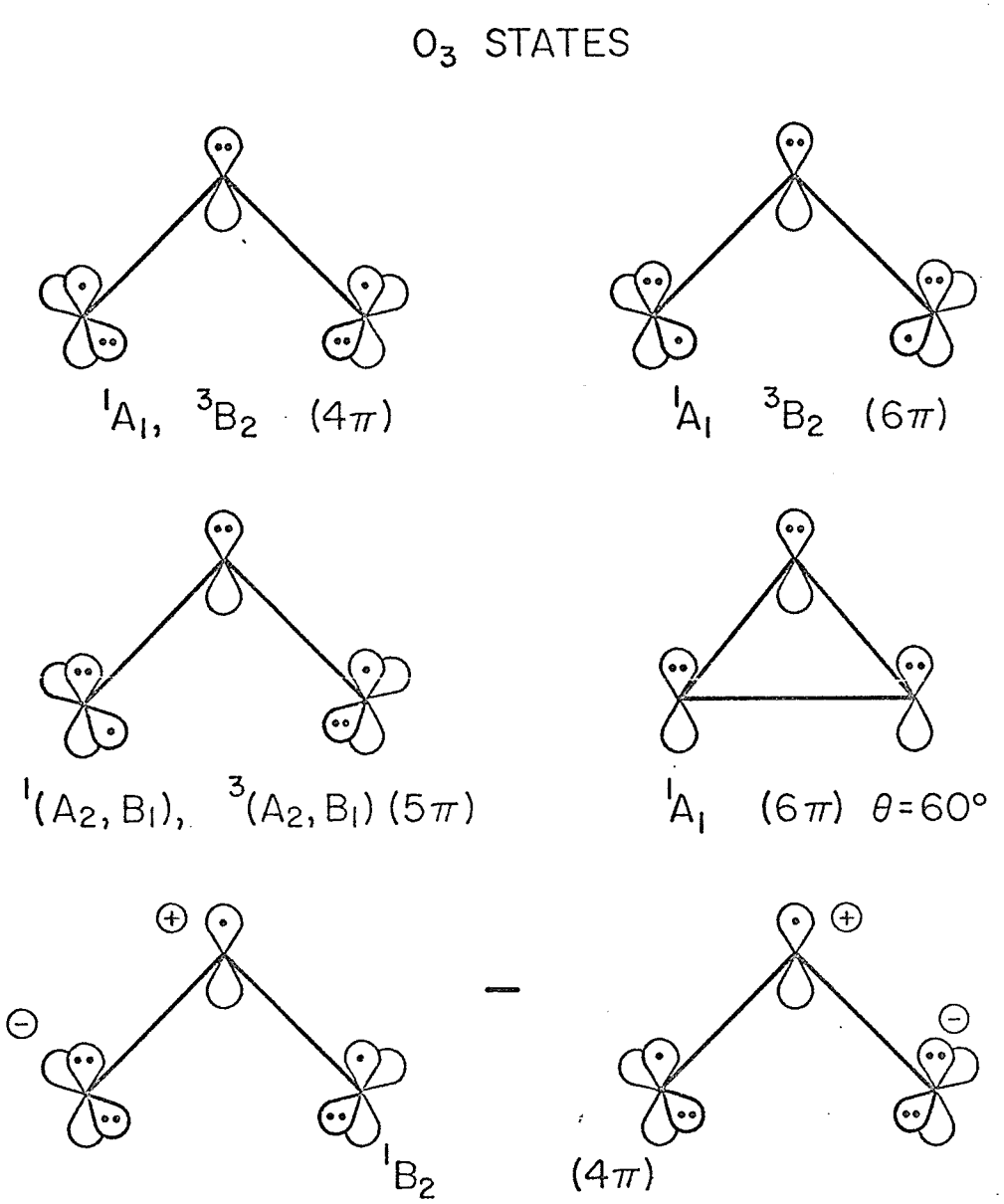
O_3 STATES
$^1A_1$, $^3B_2$ (4π)
$^1A_1$ $^3B_2$ (6π)
$^1(A_2, B_1)$, $^3(A_2, B_1)$ (5π)
$^1A_1$ (6π) $\theta = 60°$
$^1B_2$
(4π)

FIG. 1

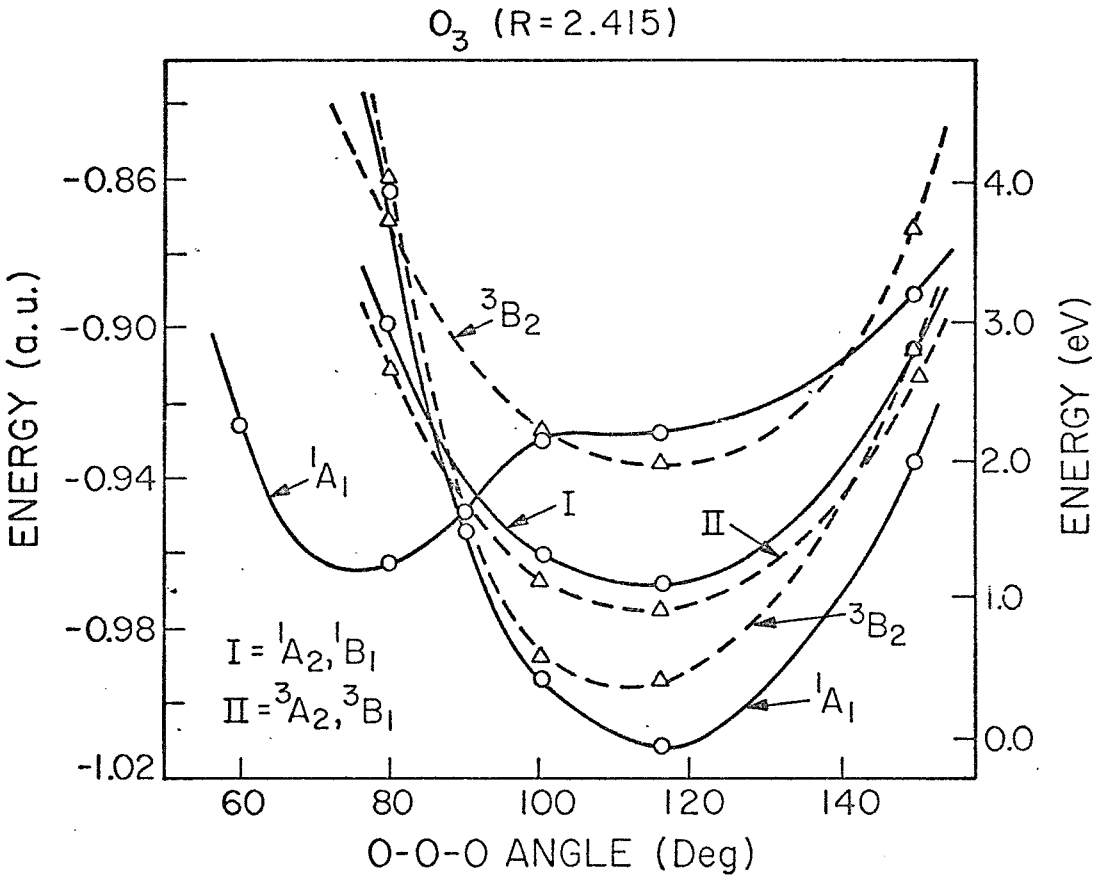
O_3 (R = 2.415)
ENERGY (a.u.)
-0.86
-0.90
-0.94
-0.98
-1.02
ENERGY (eV)
4.0
3.0
2.0
1.0
0.0
$^3B_2$
$^1A_1$
I
II
$^3B_2$
$^1A_1$
I = $^1A_2$, $^1B_1$
II = $^3A_2$, $^3B_1$
60
80
100
120
140
O-O-O ANGLE (Deg)

FIG. 2

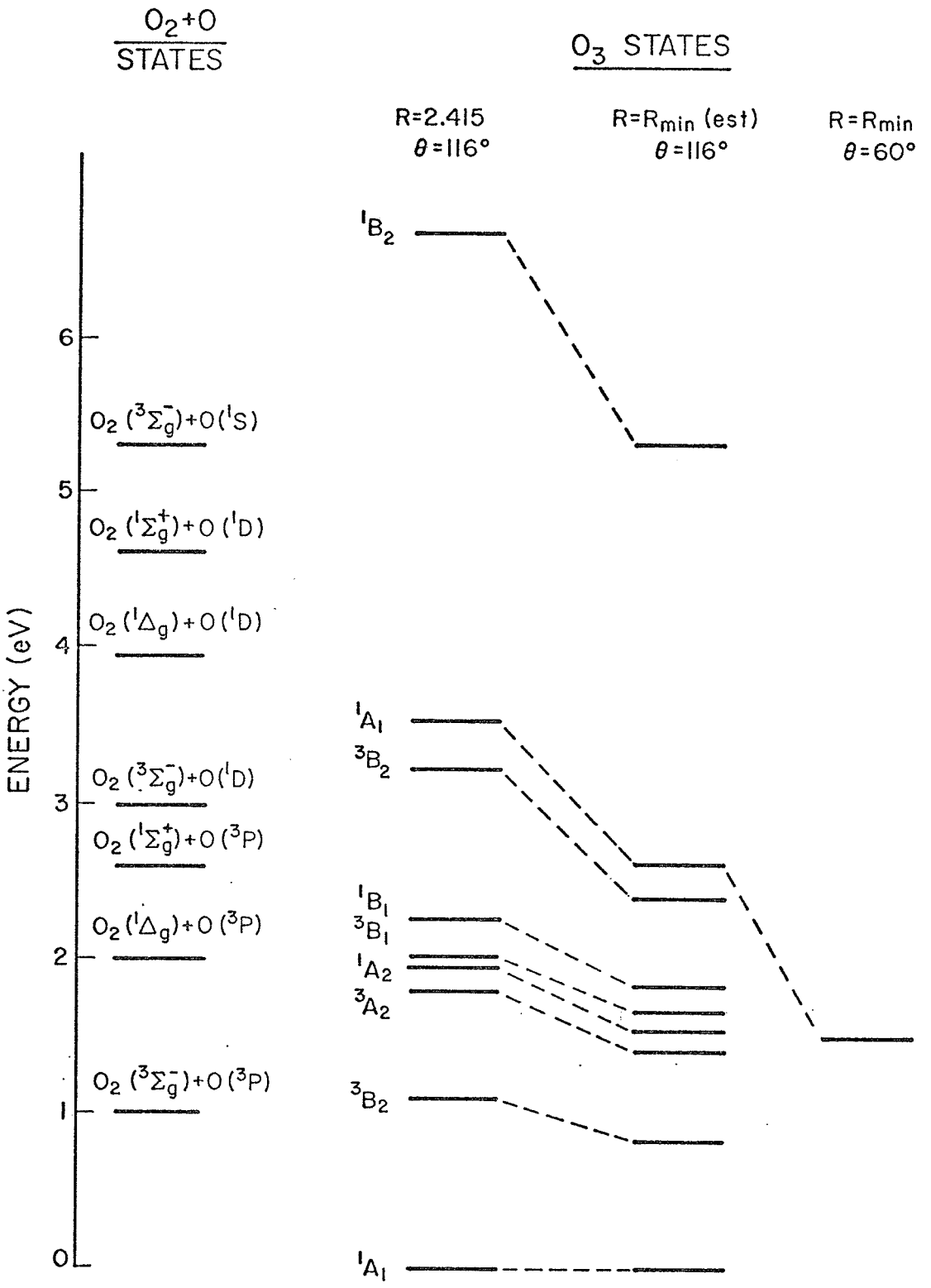
O_2+O
STATES
O_3 STATES
R=2.415
θ=116°
R=Rmin (est)
θ=116°
R=Rmin
θ=60°
ENERGY (eV)
0
1
2
3
4
5
6
$O_2(^3\Sigma_g^-)+O(^1S)$
$O_2(^1\Sigma_g^+)+O(^1D)$
$O_2(^1\Delta_g)+O(^1D)$
$O_2(^3\Sigma_g^-)+O(^1D)$
$O_2(^1\Sigma_g^+)+O(^3P)$
$O_2(^1\Delta_g)+O(^3P)$
$O_2(^3\Sigma_g^-)+O(^3P)$
$^1B_2$
$^1A_1$
$^3B_2$
$^1B_1$
$^3B_1$
$^1A_2$
$^3A_2$
$^3B_2$
$^1A_1$

FIG. 3

C. Cyclopropane and the Trimethylene Biradical

There is currently much interest in establishing the mechanisms and potential surfaces involved in both the geometric and structural isomerizations of small cyclic compounds such as cyclopropane. The experiments of Chambers and Kistiakowsky[1] had indicated that the isomerization of cyclopropane proceeded through a biradical I (trimethylene):

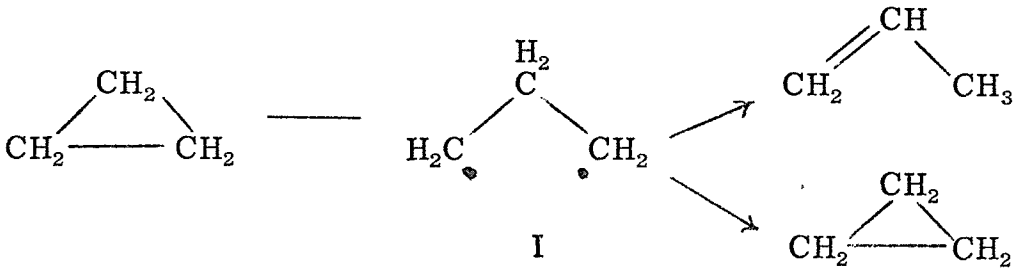

The studies of Setser and Rabinovitch[2] attempted to establish which isomers of substituted cyclopropane were formed in the reaction, but the experimental results were inconclusive. Recently, on the basis of semi-empirical calculations, Hoffmann[3] was led to explain the stereoselective pyrolysis of pyrazoline[4] on the basis of the existence of (0, 0) trimethylene (π-cyclopropane), which preferentially underwent conrotatory ring closure to form cyclopropane:

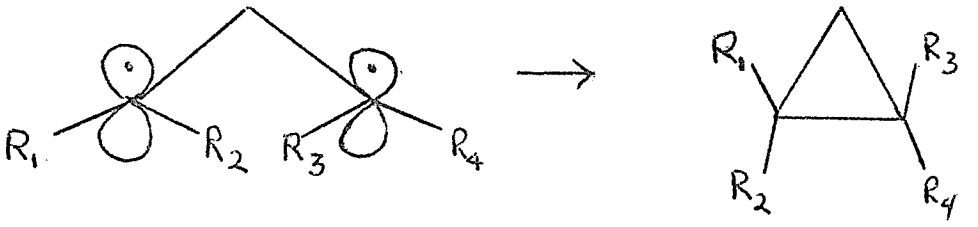

The subsequent studies of Carter and Bergman[5] on the isomerization of 1-methyl-2-ethyl-cyclopropane did not require the existence of such an intermediate.

Two ab initio calculations on trimethylene--one by Siu, St. John, and Hayes (SSH),[6] and one by Jean and Salem[7]--have used essentially modified Hartree-Fock models. The major reason for the lack of theoretical treatments of biradicals is the inadequacy of the molecular orbital (or Hartree-Fock) model in treating the breaking of a bond. In order to avoid this difficulty, we use the ab initio generalized valence bond (GVB) method in which a doubly-occupied pair $\phi_{ia}(1)\phi_{ib}(2) + \phi_{ib}(1)\phi_{ia}(2)$ and then all orbitals (for all 24 electrons) are solved for self-consistently, allowing each orbital to use all functions in the basis.

A. The Ring Opening of Cyclopropane

For equilateral cyclopropane ($\theta = 60°$) we carried out minimum basis set[8] GVB calculations allowing either one C-C pair or all three C-C pairs to be split. These calculations led to essentially equivalent descriptions of the C-C bonding pairs, one of which is shown in Figure 1a. We see that this bond is quite aptly described as a bent bond (the hybridization in each orbital is found to be 82% p-character), in good qualitative agreement with the VB results of Coulson and Moffitt.[9]

Similar calculations (with one pair split) were performed for several configurations of face-to-face trimethylene[10] (the terminal CH_2 groups perpendicular to the CCC plane, just as in cyclopropane). As shown in Figure 2a, the energy increases monotonically as θ (the CCC angle) is increased from 60° to 130°. As reported by Salem[7] for large θ, the terminal groups are not planar but are canted in such a way that the terminal CH bonds are staggered with respect to the bonds of the central C. The energy curves for the symmetrical canting of the

terminal groups are shown in Figure 2b. For $\theta = 110°$, the optimum angle (η) is about 30° for the singlet state and the energy drops 5.1 kcal over that for planar terminal groups (for the triplet state $\eta \sim 24°$ and the energy drop is about 1.2 kcal). For $\theta = 120°$, the energy drop is 4.0 kcal (1.1 kcal for the triplet state) and for $\theta = 130°$, the optimum η for the singlet state is about 25°. The nonbonded interactions normally favoring staggering of neighboring groups lead to 0.5 kcal energy lowering (with respect to a planar terminal group) in ethyl radical[11] and should lead to about 1 kcal energy lowering in trimethylene. This is about the energy lowering observed in the triplet state at $\theta = 110°$ and 120°; however, the singlet states drop several times as much.

The orbitals for the "broken bond" of trimethylene ($\theta = 110°$) are shown in Figure 1bc for the cases of $\eta = 0°$ and $\eta = 30°$. Here we see that the canting of terminal groups towards each other leads the orbitals to rehybridize such as to point away from each other (the hybridizations for the orbital pairs in Figure 1abc of these orbitals are 82%p, 100%p, and 91%p, respectively). As indicated by the dotted lines aa' and bb', the canting also leads to a rotation of the orbital axes towards each other (15° between aa' and bb'). For $\theta = 110°$ and $\eta = -15°$, 0°, 15°, 30°, and 45°, the orbital overlaps are 0.108, 0.140, 0.164, 0.178, and 0.192, respectively (the orbitals have an overlap of 0.790 at $\theta = 60°$ and an overlap of 0.073 for $\theta = 130°$ and $\eta = 30°$).

B. An Analysis of the Origin of the Crabbing in Face-to-Face Trimethylene

Recently Jean and Salem[7] found that face-to-face trimethylene biradical is significantly stabilized by a crabbing or canting of the terminal CH_2 groups toward each other. For a central CCC angle (θ) of 113°, they carried out Hartree-Fock-like calculations and found an energy lowering of 6.2 kcal for the singlet state and 1 kcal for the triplet state. We applied the ab initio generalized valence bond (GVB) method to trimethylene and also found that the crabbed or canted configuration possesses an extra large stability, 5.1 kcal for the singlet state at $\theta = 110°$ and 1.2 kcal for the triplet state. Here we will examine the GVB orbitals of trimethylene in order to determine the origin of the extra stability of the canted configuration of face-to-face trimethylene.

The canting of the terminal groups is such as to lead to staggering of the terminal CH bonds with respect to the bonds of the central C. However, for ethyl this staggering leads to an energy lowering of about 0.5 kcal[11] and the corresponding conformational effect in trimethylene would be expected to be about 1.0 to 1.5 kcal. This is consistent with the stability of the canted triplet state, but the singlet state has a stability four times as great.

In order to learn why the canted configuration is so stable, we will examine the orbitals, ϕ_{1a} and ϕ_{1b}, of the "broken" bond. We can expand these orbitals approximately as

$$\phi_{1a} = N(\phi_{1a}^{L} + \lambda\phi_{1a}^{R})$$
$$\phi_{1b} = N(\phi_{1b}^{R} + \lambda\phi_{1b}^{L}) \quad , \tag{1}$$

where L and R denote functions localized on the left and right terminal groups, respectively, and N is a normalization constant (for θ = 110°, λ = 0.15). At θ = 110° the total overlap $S = \langle \phi_{1a} | \phi_{1b} \rangle$ increases from 0.140 to 0.178 as η (the canting angle) increases from 0° to 30°, an increase consistent with the extra stability of the canted configuration.[12] The overlap S can be decomposed as $S = S_1 + S_2 + S_3$, where $S_1 = N^2\langle \phi_{1a}^{L} | \phi_{1b}^{R} \rangle$, $S_2 = N^2\lambda[\langle \phi_{1a}^{L} | \phi_{1b}^{L} \rangle + \langle \phi_{1a}^{R} | \phi_{1b}^{R} \rangle]$ and $S_3 = N^2\lambda^2\langle \phi_{1a}^{R} | \phi_{1b}^{L} \rangle$. As shown in Table I, S_1 decreases with canting as would be expected since the orbitals hybridize away from each other. S_3 is negligible and S_2 increases from 0.069 at η = 0° to 0.151 at η = 30°; hence it is S_2 that is responsible for the increase in S with canting. Since the increase in λ with canting is only 0.01, it is the change in $\langle \phi_{1a}^{R} | \phi_{1b}^{R} \rangle$ (and the equal quantity for the right group) that is responsible for the large increase in S_2. That is, the small component of ϕ_{1a} overlaps much more with the large component of ϕ_{1b} for the canted configuration.

In the GVB description of a normal two-electron bond (as in H_2 or cyclopropane) the bond orbitals ϕ_{1a} and ϕ_{1b} delocalize as in (1) where $\phi_{1bL} \approx \phi_{1aL}$ and $\phi_{1aR} \approx \phi_{1bR}$. In this case, the delocalization builds some ionic character into the two-electron wavefunction. This normal bonding effect will be referred to as the through-space effect. However, for a system with other bonds, the orbitals ϕ_{1a} and ϕ_{1b} must also adjust so as to become essentially orthogonal to

the other bonding pairs of orbitals (this results from restrictions in the form of the wavefunction due to Pauli's principle and, for example, is responsible for the conformational effects favoring staggered ethane over the eclipsed form). Modifications in the interactions between two orbitals due to these orthogonality conditions with these bonding pairs we will refer to as through-bond effects.[13]

From Fig. 1bc, we see that the small component of ϕ_{1a} is approximately in the plane of the right CH_2 terminal group rather than perpendicular to this group as would have been expected from through-space effects. Thus the shape of ϕ_{1aR} is primarily determined by the through-bond effects (orthogonality to the central CH bonds, the right CC bond, and the CH bonding pairs of the right C).

From Fig. 1bc, we see that this small component (ϕ_{1a}^{R}) is hybridized so as to point (approximately) from the terminal C toward the right of the central carbon and this hybridization does not change significantly with canting. Thus hybridizing the big component of ϕ_{1b} up and to the right of the right carbon would significantly increase S_2, as in fact is observed. Thus we may consider the extra large stability of the singlet canted configurations to be due to the special form of ϕ_{1a} near the right C, which in turn is due to the through-bond interactions due to the CC and CH bonding pairs.

As discussed by Hoffmann,[13] such through-bond effects are responsible for surprisingly large interactions between distant orbitals in several other systems. In addition, similar effects are also responsible for the enhanced antiferromagnetic coupling often known as "superexchange".

Salem[7] has suggested that the extra bonding for the canted configurations is due to increased ionic character in the wavefunction (i.e., resonance between two zwitterionic structures). However, we find little change in the ionic character in the wavefunction upon canting.

C. The Trimethylene Biradical

We will use the following notation in describing the trimethylene configurations: θ is the central CCC angle; (90, 90) indicates that the plane of each terminal CH_2 group is perpendicular to the CCC plane; (0, 0) indicates that both terminal CH_2 groups are in the CCC plane; (0, 90) is the obvious combination; a subscript c [e.g., $(0, 90_c)$] indicates that the terminal group is canted from planar to the nearest staggered configuration[14] (with respect to the bonds of the central carbon).

The geometric isomerization of cyclopropane involves breaking of one C-C bond [in the $(90_c, 90_c)$ configuration] followed by rotation of one (Path I) or both (Path II) terminal CH_2 groups. If the shape of each CH_2 group is kept fixed as one CH_2 group is rotated, there would occur three relative maxima in each of which both bonds of this group would eclipse the bonds of the central carbon; in between would be two points [both $(0_c, 90_c)$] at which the bonds would be staggered, leading to relative minima. However, the minimum energy path for rotating the CH_2 by 360° need not keep the shape of the CH_2 group fixed. By allowing the CH_2 group to wobble as it rotates, one can avoid eclipsing more than one bond, leading to a slightly lower (~0.5 kcal) barrier height. The saddle point for this path (I) is expected to be $(0, 90_c)$.

For path II the two groups can be rotated either in a conrotatory or a disrotatory sense and the saddle point is expected to be (0, 0). Some of these configurations are shown schematically in Fig. 3.

The calculated energy curves for the $(90_c, 90_c)$, $(0, 90_c)$, and (0, 0) configurations (Fig. 4a) indicate that for $\theta \leq 130°$ the unrotated $(90_c, 90_c)$ configuration remains below both possible saddle points and that the saddle points for paths I and II have comparable energies (60.9 and 60.5 kcal) and angles (112° and 114°).

Keeping the terminal groups planar and conrotating from (0, 0) to (90, 90) leads to no hump in the potential curve, as shown in Fig. 4b, and the similar rotation from (0, 90) to (90, 90) also should lead to no hump. We found that starting with trimethylene in the $(90_c, 90_c)$ configuration and closing the ring involved no energy barrier; hence there should be no energy barrier to ring closure from either saddle point.

If the terminal groups of trimethylene are taken as planar, we obtain the potential curves in Fig. 4c. The (0, 0) energy curve shows a minimum for $\theta = 114°$, which is essentially at the angle (115°) where the (90, 90) curve crosses the (0, 0) curve. On the other hand, the (0, 90) curve remains about 1 kcal above the (0, 0) curve in the $\theta = 110°$ to 120° region. These results are in qualitative agreement with the extended Hückel calculations of Hoffmann[3] who found the (90, 90) and (0, 0) curves to cross at $\theta \sim 117°$ with the (0, 90) curve somewhat higher. [He found the (0, 0) minimum to occur at $\theta = 125°$ with an energy 44 kcal above that of cyclopropane; considering an extensive set of geometries, he found a cycle-closing barrier of about 1 kcal.]

Our results are also in fair agreement with ab initio calculations on the (0, 0) and (90, 90) states by Siu, St. John, and Hayes[6] [they find the crossing to occur at $\theta = 109.5°$ and the minimum in the (0, 0) curve at 114.3° with an energy of 32 kcal above that of cyclopropane (leading to a cycle-closing barrier of about 1 kcal if the surface between (0, 0) and (90, 90) is assumed to be smooth)].

We also examined the energy changes for disrotatory and conrotatory motions of the planar terminal groups (see Fig. 4d). As suggested earlier by Hoffmann,[3] the conrotatory motion is favored, but only slightly.

Although for planar terminal groups the (0, 0) form is more stable than the (90, 90) for $\theta > 115°$, staggering of the terminal bonds relative to the central bonds lowers the energy (1.6 and 4.0 kcal, respectively, at 120°), with $(90_c, 90_c)$ remaining more stable than $(0_c, 0_c)$ for $\theta < 130°$ (Fig. 4a). There are both syn and anti forms of $(0_c, 0_c)$, but at $\theta = 120°$ these differ only by 0.1 kcal. The extra stability due to canting was first pointed out by Salem[7] who found energy lowerings of 1 kcal for $(0_c, 0_c)$ relative to (0, 0) and 6.2 kcal for $(90_c, 90_c)$ relative to (90, 90) (at $\theta = 113°$).

We have ignored the triplet states in most of this discussion since the singlet states are most relevant for these reactions. The $(0, 90_c)$ configuration leads to a triplet state about 1 kcal lower than (0, 0) and $(90_c, 90_c)$ and is compared with some singlet curves in Fig. 4c.

Summarizing we find that the barrier height for cis-trans isomerization of cyclopropane is essentially the same (calculated value, 60.5 kcal) whether one or both of the terminal CH_2 groups are rotated

after opening of the CC bond. In addition, we find no barrier to closing of the ring in trimethylene.

D. Some Implications of the Theoretical Potential Surface for Trimethylene Biradical

Recent theoretical calculations (using the ab initio GVB method) on the potential surface of trimethylene indicate that the reaction surface for the cis-trans isomerization of cyclopropane

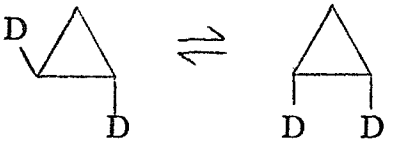

(1)

involves a reaction path of the shape in Fig. 5a, where regions A and C involve primarily opening of the CC bond and region B involves primarily rotation of the terminal group(s). The calculated barrier height is 60.5 kcal, which compares well with the experimental activation energy[15] of 64.2 kcal (Lin and Laidler[16] have used RRKM theory to estimate a barrier height of 0 °K of 61.1 kcal).

The reaction surface for such a reaction is usually viewed[17] as in Fig. 5b, with the biradical as a stable intermediate possessing a sizeable barrier for closing to reform the cyclic compound. (For trimethylene this cycle-closing barrier has been estimated to be 9.3 kcal.[17]) Despite the usual assumption of such large cycle-closing barriers, there is a lack of direct experimental evidence for them.[18] However, theoretical evidence against such large barriers is now available. Even the semi-empirical extended Hückel calculations of Hoffmann[3] give essentially the same sort of low-energy reaction paths

for (1) as in Fig. 1b (possessing a well of only 1 kcal/mole) and similar calculations by Hoffmann et al.[19] on the pyrolysis of cyclobutane to two ethylenes yield no indication of a tetramethylene well.

The best evidence in favor of Fig. 1b for (1) is from thermochemical considerations. Benson[17] obtains a cycle-closing barrier of 9.3 kcal by combining the known ΔH_f of cyclopropane (12.7 kcal), the experimental E_a for (1) (64.2 kcal) and Benson's estimate of the ΔH_f of trimethylene biradical (66.7 kcal). This latter ΔH_f is obtained by starting with propane (ΔH_f = -24.8 kcal) and forming trimethylene by breaking a C-H bond on each terminal group. Using 98 kcal for both bond energies, Benson[17] obtains ΔH_f = 66.7 kcal for trimethylene [including a 0.8 kcal increase in ΔH_f due to using the (90, 90) orientation]. But this ΔH_f is only 54 kcal above cyclopropane, leading to the supposition of a cycle-closing barrier of about 9.3 kcal as in Fig. 1b. Since the theoretical work establishes the shape of the reaction path to be more as in Fig. 1a (with at most a barrier of about 1 kcal), there would seem to be something wrong with the thermochemical procedure.[20] One difficulty with this procedure is that pulling off an H from each terminal group leads to a mixed spin state (neither singlet nor triplet) for trimethylene. The singlet state is strongly binding for configurations near (90, 90) and these configurations have an energy below that of the saddle point. [For the singlet state, the calculated barrier toward rotation of a terminal CH_2 group about the CC bond is 7.2 kcal for a central angle of 110° and 3.5 kcal for 120°; the triplet state at 110° leads to a barrier of less than 1 kcal.] Thus

the thermochemical procedure could well lead to too low an estimate of the saddle point energy.

Based on the results for trimethylene, we would question the existence of cycle-closing barriers from other biradical saddle points.[17] Hoffmann et al.[19] have suggested that such biradicals may generally have very flat potential surfaces and that such surfaces might lead to behavior similar to that expected from a potential curve of the form in Fig. 1b.

There has been some discussion of whether the cis-trans isomerization of cyclopropane involves a path passing through a (0, 90) transition state or a (0, 0) transition state.[2,5] We found that the barrier heights for these reaction paths are essentially identical (60.9 and 60.5 kcal, respectively). Thus both should contribute significantly to the geometric isomerization in cyclopropane. However, for substituted systems steric factors and the variation in the strengths of the various C-C bonds of the cycle could well be crucial in determining the dominant reaction path. Thus, for some substituted systems, the (0, 0) path might dominate and for others the (0, 90) path might dominate. In either case, however, the CCC bond should open to $> 110°$.[21]

The structural isomerization

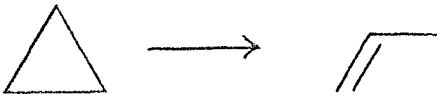

(2)

proceeds through a saddle point similar to that for the (0, 0) path of (1)[3] where only a small motion of one of the hydrogens on the central carbon should be required in order to reach the saddle point for (2).

Thus, a study of the rates of (1) and (2) should lead to information concerning the fraction of (1) proceeding via the (0, 90) path.[2, 5] Studies on geometric and optical isomerizations of 1-ethyl, 2-methyl-cyclopropane by Carter and Bergman[5] were fairly well fitted assuming only the (0, 90) paths. For this system the doubly-substituted ring bond should be weakest and hence we would expect (0, 90) to dominate for geometric isomerization and (0, 0) to dominate for optical isomerization (only the latter path should be involved in the structural isomerization).

The lowest energy triplet states are about 1 kcal below the energy of the singlet saddle point, however, the time spent by the system in the saddle point region is far too short for the triplet states to play any role in the isomerizations of cyclopropane.

The GVB calculations reaffirm Hoffmann's prediction that conrotatory twisting in the biradical is favored over disrotatory twisting, and hence also suggest a simple explanation for the stereoselectvity in the pyrolysis of substituted pyrazolines[4] and thietanes.[22] The only difference is that the GVB results do not support the existence of an actual π-bonded intermediate and instead suggest the possibility of a one-step process in which the conrotatory twisting occurs while the CN bonds are breaking.[4] It is of interest that without using the above results on trimethylene but assuming that the pyrolysis occurs as a one-step process, the recently developed orbital phase continuity principle[23] leads directly to the result that the conrotatory closing of the cyclopropane is favored. The generalized Woodward-Hoffmann rules[24] also predict a conrotatory closing for allowed processes.

References

1. T. S. Chambers and G. B. Kistiakowsky, J. Amer. Chem. Soc., 56, 399 (1934).
2. D. W. Setser and B. S. Rabinovitch, J. Amer. Chem. Soc., 86, 564 (1964).
3. R. Hoffmann, J. Amer. Chem. Soc., 90, 1475 (1968).
4. R. J. Crawford and A. Mishia, J. Amer. Chem. Soc., 88, 3963 (1966).
5. R. G. Bergman and W. L. Carter, J. Amer. Chem. Soc., 91, 7411 (1969).
6. A. K. Q. Siu, W. M. St. John III, and E. F. Hayes, J. Amer. Chem. Soc., 92, 7249 (1970).
7. (a) Y. Jean and L. Salem, Chem. Comm., 382 (1971). These calculations are open-shell Hartree-Fock using symmetry and equivalence restrictions and an adjusted coefficient for the exchange integral between the open-shell orbitals. For singlet states, such procedures lead to only approximate total energies; however, the relative energies may be adequate for comparing various geometries. (b) L. Salem, Bull. Soc. Chim. Fr., 3161 (1970).
8. The STO-4G basis [W. J. Hehre, R. F. Stewart, and J. A. Pople, J. Chem. Phys., 51, 2667 (1969)] was used.
9. (a) C. A. Coulson and W. E. Moffitt, Phil. Mag., 40, 1 (1949); (b) The usual MO description [A. D. Walsh, Trans. Faraday Soc., 45, 179 (1949)] is quite different, but these MO's can be

localized to lead to a description [M. D. Newton, E. Switkes, and W. N. Lipscomb, J. Chem. Phys., 53, 2645 (1970)] similar to the present one.

10. Standard C-C and C-H bond distances of 1.54 Å and 1.08 Å were used. For cyclopropane, the experimental geometry [O. Bastiansen, Acta Cryst., 17, 538 (1964)] was used.

11. W. A. Latham, W. J. Hehre, and J. A. Pople, J. Amer. Chem. Soc., 93 (1971).

12. The increase in overlap is not actually responsible for the increase in bonding but it is a byproduct of the changes leading to increased stability [see, for example, C. W. Wilson, Jr., and W. A. Goddard III, Chem. Phys. Lett., 5, 45 (1970)] and forms a useful approximate measure of these bonding effects.

13. R. Hoffmann, Accts. Chem. Res., 4, 1 (1971).

14. The rotation angle from planar to the canted configuration is taken as 30° in all cases. This is near the optimum value for those cases in which the angle was optimized.

15. B. S. Rabinovitch, E. W. Schlag, and K. B. Wiberg, J. Chem. Phys., 28, 504 (1958).

16. M. C. Lin and K. J. Laidler, Trans. Faraday Soc., 64, 927 (1968).

17. H. E. O'Neal and S. W. Benson, J. Phys. Chem., 72, 1866 (1968).

18. Since the potential surface of Fig. 1a becomes quite flat in the saddle point region, a reasonable definition of the entropy as a function of reaction coordinate might well, for high temperatures,

lead to a free energy of the shape in Fig. 1b.

19. R. Hoffmann, S. Swaminathan, B. G. O'Dell, and R. Gleiter, J. Amer. Chem. Soc., 91, 7091 (1970).

20. G. R. Freeman [Can. J. Chem., 44, 245 (1966)] obtains a cycle-closing barrier of 2 to 3 kcal/mole by using somewhat different values for various quantities.

21. The suggestion [F. T. Smith, J. Chem. Phys., 29, 235 (1958)] that the CH_2 group rotates without opening of the ring is clearly contradicted by the theoretical results, in agreement with earlier discussions by Benson [J. Chem. Phys., 34, 521 (1961)].

22. B. M. Trost, W. L. Shinski, F. Chen, and I. B. Mantz, J. Amer. Chem. Soc., 93, 676 (1971).

23. W. A. Goddard III, J. Amer. Chem. Soc., 92, 7520 (1970); ibid., 94, 0000 (1972).

24. R. B. Woodward and R. Hoffmann, Angew. Chem., 8, 781 (1969).

TABLE I. Comparison of the overlaps between ϕ_{1a} and ϕ_{1b} for the canted (η = 30°) and uncanted (η = 0°) configurations for θ = 110°.

η	S_1	S_2	S
0°	0.046	0.096	0.140
30°	0.029	0.151	0.178

Figure Captions

Figure 1. The GVB orbitals of (a) one C-C bonding pair of cyclopropane; (b) the pair of orbitals describing the broken bond of trimethylene for $\theta = 110°$ but planar terminal groups; (c) the same as (b) except that the terminal groups are canted inward by 30°. The location of each carbon nucleus is indicated by +. The nodal line is indicated by long dashes and the contour intervals are 0.1 (in atomic units).

Figure 2. (a) The energy curve for the ring opening of cyclopropane. (90, 90) indicates that the terminal groups are taken as planar ($\eta = 0°$) for $\theta \geq 100°$. (90_c, 90_c) indicates that the terminal groups have been canted ($\eta = 30°$) for $\theta \geq 100°$. (b) The energy curve for the symmetrical canting of the terminal groups in trimethylene.

Figure 3. Schematic representation of some of the trimethylene configurations. In (b)-(f) the molecule is shown twice, each part emphasizing one of the terminal groups.

Figure 4. (a) Energy curves for the (0, 0) and (0, 90_c) saddle points of trimethylene compared with (0_c, 0_c) and (90_c, 90_c) curves; (b), (d) Potential curves for rotation of planar terminal CH_2 groups at $\theta = 100°$ and 120°, respectively; (c) Energy curves for the case of planar terminal groups.

Figure 5. Schematic representations of the reaction surface for the cis-trans isomerization of cyclopropane. (a) Result of the theoretical calculations; (b) an often-assumed form for the surface.

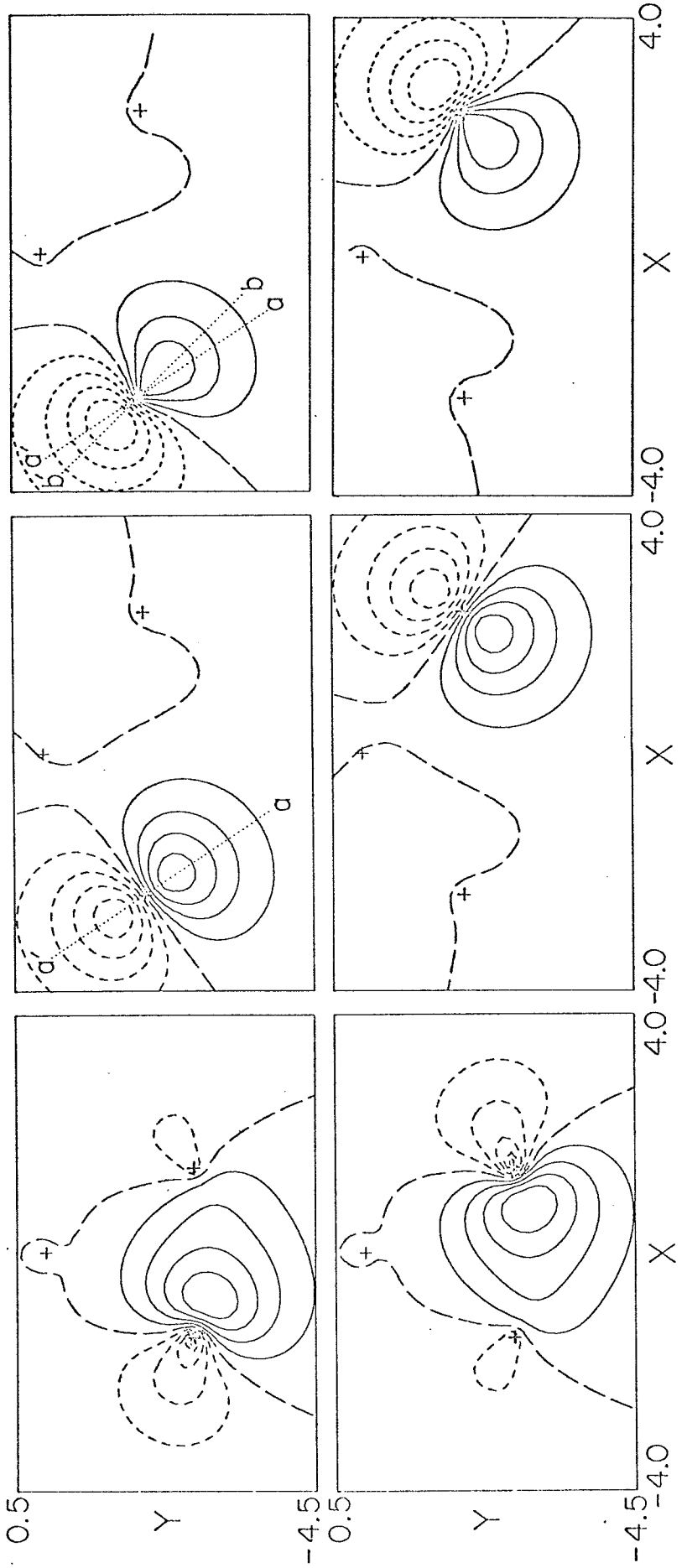

FIG. 1

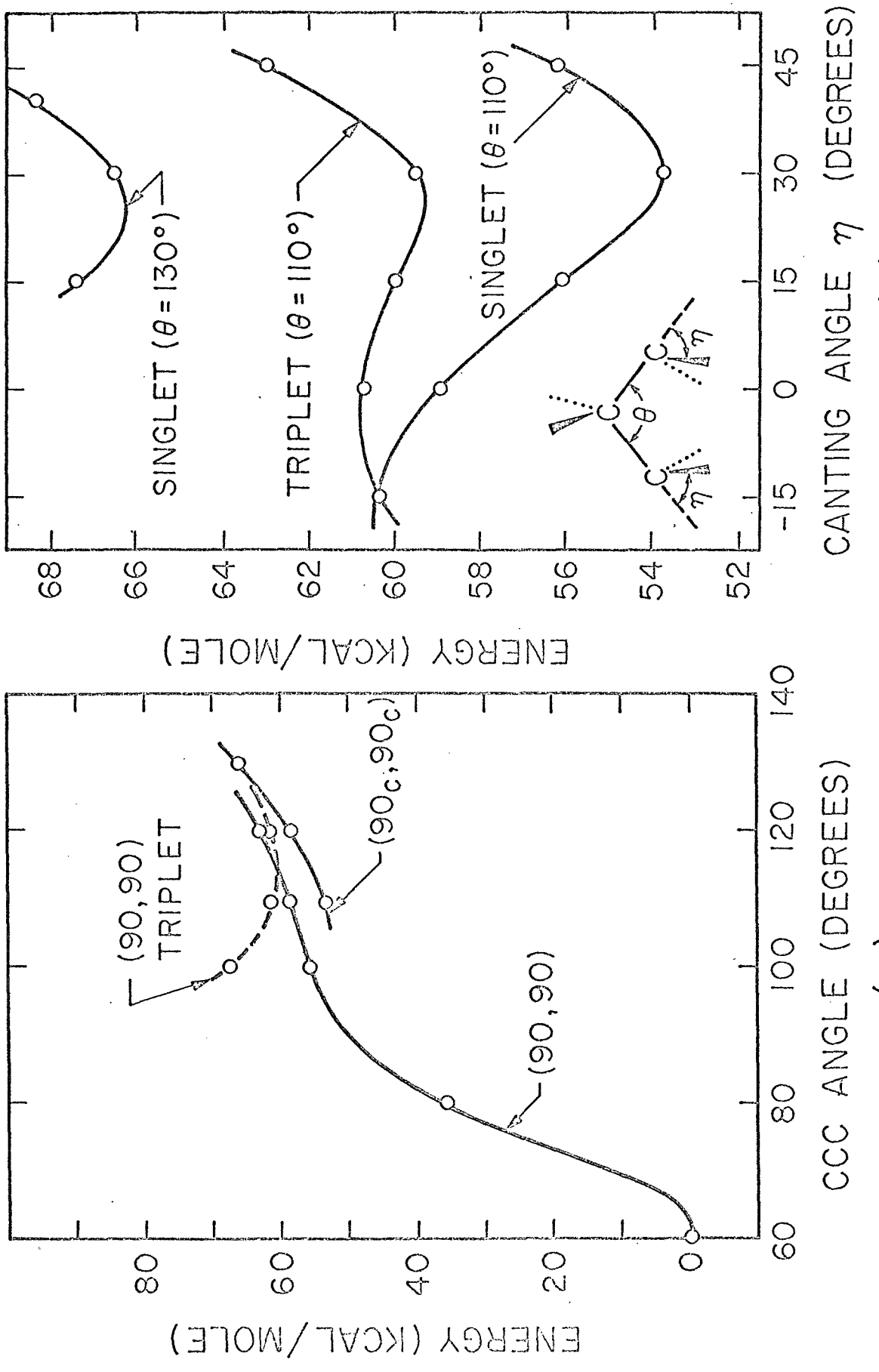
ENERGY (KCAL/MOLE)
68
66
64
62
60
58
56
54
52
SINGLET (θ=130°)
TRIPLET (θ=110°)
SINGLET (θ=110°)
θ
η
η
-15
0
15
30
45
CANTING ANGLE η (DEGREES)
(b)
ENERGY (KCAL/MOLE)
80
60
40
20
0
(90,90) TRIPLET
(90c;90c)
(90,90)
60
80
100
120
140
CCC ANGLE (DEGREES)
(a)

Fig. 2

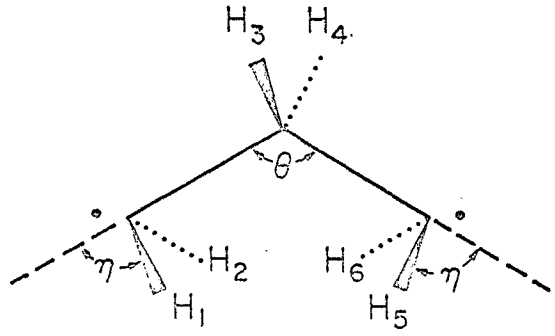

(a) $(90_c, 90_c)$

≡

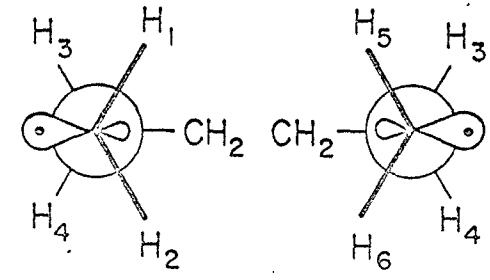

(b) $(90_c, 90_c)$

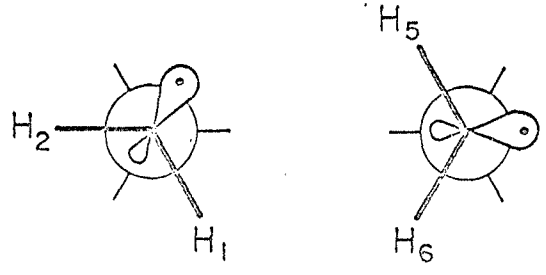

(c) $(0_c, 90_c)$

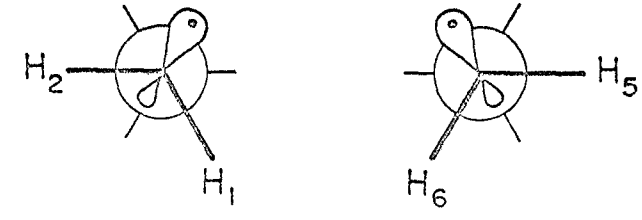

(e) $(0_c, 0_c)$-SYN

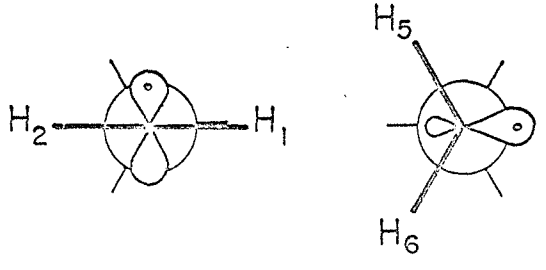

(d) $(0, 90_c)$

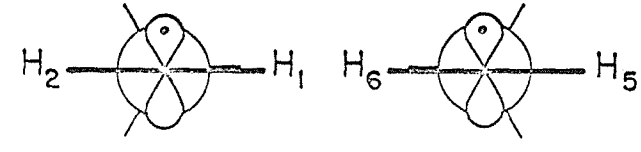

(f) $(0, 0)$

FIG. 3

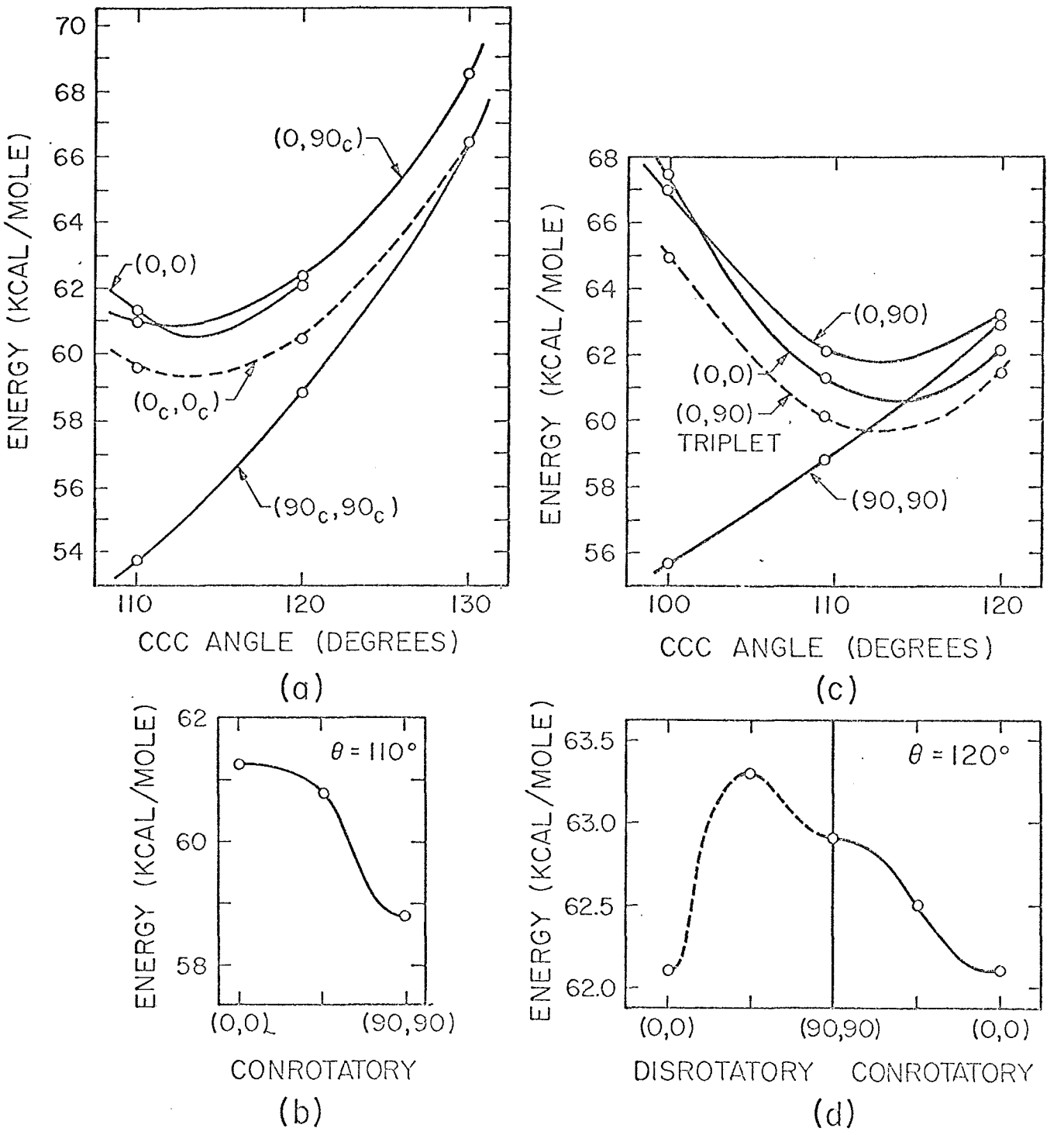
ENERGY (KCAL/MOLE)
70
68
66
64
62
60
58
56
54
(0,90c)
(0,0)
(0c,0c)
(90c,90c)
110
120
130
CCC ANGLE (DEGREES)
(a)
ENERGY (KCAL/MOLE)
68
66
64
62
60
58
56
(0,90)
(0,0)
(0,90)
TRIPLET
(90,90)
100
110
120
CCC ANGLE (DEGREES)
(c)
ENERGY (KCAL/MOLE)
62
60
58
θ = 110°
(0,0)
(90,90)
CONROTATORY
(b)
ENERGY (KCAL/MOLE)
63.5
63.0
62.5
62.0
θ = 120°
(0,0)
(90,90)
(0,0)
DISROTATORY
CONROTATORY
(d)

FIG. 4

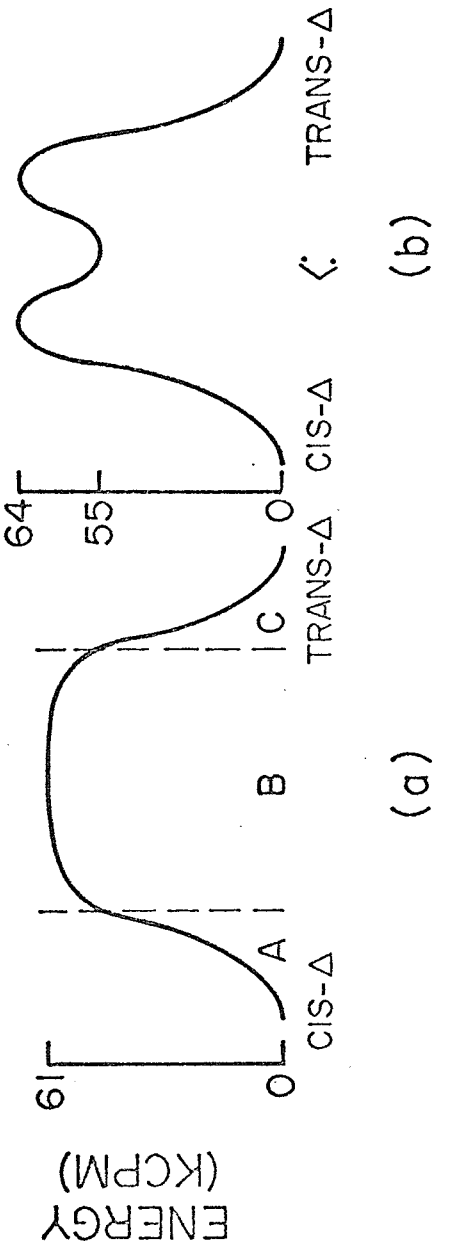

FIG. 5

D. The Valence States of CH_2

GENERALIZED VALENCE BOND CALCULATIONS ON THE LOW LYING STATES OF METHYLENE*

P. JEFFREY HAY,** WILLIAM J. HUNT,† and
W. A. GODDARD III

Arthur Amos Noyes Laboratory of Chemical Physics‡
California Institute of Technology
Pasadena, California 91109 U.S.A.

Generalized valence bond (GVB) calculations are reported for the $^3B_1$, $^1A_1$, and $^1B_1$ states of the CH_2 molecule. The GVB method is discussed and compared with other multi-configuration and separated pair methods. The lowest singlet state ($^1A_1$) is found to lie 0.50 eV about the lowest triplet state ($^3B_1$) and the $^1B_1$-$^1A_1$ separation is found to be 1.40 eV.

---

* Partially supported by a grant (GP-15423) from the National Science Foundation.

** NSF Predoctoral Fellow.

† National Defense Education Act.

‡ Contribution No.

We report here the results of both generalized valence bond (GVB) and GVB-CI calculations on the $^1A_1$, $^3B_1$, and $^1B_1$ states of the CH_2 molecule. In Section I we discuss the procedures involved in the GVB method, which is an extension of the valence bond and Hartree-Fock molecular orbital approaches. In Section II we present the results for CH_2.

I. METHOD

In the GVB approach [1] we replace the orbitals ϕ_i which are doubly occupied in the Hartree-Fock (HF) wavefunction:

$$\psi_{HF} = \mathcal{A}[\phi_1\alpha\phi_1\beta\phi_2\alpha\phi_2\beta\cdots\phi_n\alpha\phi_n\beta] \tag{1}$$

by singlet-coupled pairs of orbitals:

$$\psi_{GVB} = \mathcal{A}[(\phi_{1a}\phi_{1b} + \phi_{1b}\phi_{1a})(\phi_{2a}\phi_{2b} + \phi_{2b}\phi_{2a}) \tag{2}$$

$$\cdots(\phi_{na}\phi_{nb} + \phi_{nb}\phi_{na})\alpha\beta\alpha\beta\cdots\alpha\beta]$$

For a state of spin S the last 2S orbitals are usually taken as single occupied with up-spin α as in HF. Rather than using atomic orbitals in (2) as in the VB method,[2] we solve variationally for the optimum orbitals of (2). In addition to yielding lower energies than HF, the GVB approach also leads to proper treatment of the breaking of bonds and offers the conceptual advantage of leading to localized orbitals in close correspondence to the qualitative ideas of bonding and nonbonding pairs of molecules.

As was originally shown by Hurley, Lennard-Jones, and Pople,[3] each pair in (2) can be represented in terms of two natural orbitals (NO's),

$$\phi_{ia}(1)\phi_{ib}(2) + \phi_{ib}(1)\phi_{ia}(2) =$$

$$C_{1i}\phi_{1i}(1)\phi_{1i}(2) + C_{2i}\phi_{2i}(1)\phi_{2i}(2) \qquad (3)$$

[Coulson and Fischer[4] also discussed GVB-like descriptions for H_2.] In this representation GVB is seen to be a special case of the separated pair,[5-7] strongly orthogonal geminal,[8-10] self-consistent group,[11] and multi-configuration SCF[13-16] wavefunctions where, in general more than two NO's are used.[17]

In GVB, as in these other methods, the strong orthogonality constraint[18] is imposed, i.e., the NO's of pair i are taken to be orthogonal to each other as well as to the NO's of the other pairs. This means that the GVB orbitals satisfy the relations

$$\langle\phi_{ia}|\phi_{ib}\rangle \neq 0$$

$$\langle\phi_i|\phi_j\rangle = 0 \qquad \text{otherwise.} \qquad (4)$$

Without these orthogonality constraints the optimum wavefunction of (2) is the G1 wavefunction,[19] and hence GVB is a special case G1.

As has been shown by Kutzelnigg[7] and Silver, Mehler and Ruedenberg,[6] the total electronic energy of (2) has the form

$$E = \sum_k f_k h_k + \sum_{k,\ell} a_{k\ell} J_{k\ell} + b_{k\ell} K_{k\ell} \tag{5}$$

where h is the one-electron Hamiltonian (kinetic energy and nuclear attraction), $h_k = \langle k|h|k\rangle$, $J_{k\ell}$ and $K_{k\ell}$ are the usual Coulomb and exchange integrals, and f_k is the occupation number (f_k will be 2 for doubly-occupied orbitals, 1 for singly-occupied open-shell orbitals, and C_i^2 for GVB NO's.)

Applying the variational principle to (5) (to obtain the optimum orbital ϕ_k) leads to the variational equations

$$\begin{aligned} H_k \phi_k &= \epsilon_k \phi_k \qquad k = 1, 2, \cdots, M \\ H_k &= f_k \hat{h} + \sum_\ell a_{k\ell} \hat{J}_\ell + b_{k\ell} \hat{K}_\ell \end{aligned} \tag{6}$$

where M is the number of distinct orbitals and $\hat{J}_\ell$ and $\hat{K}_\ell$ are the Coulomb and exchange operators, respectively. To find the optimum orbitals of (5) the M equations (6) must be solved self consistently. (All doubly occupied orbitals may be taken to be eigenfunctions of the same Hamiltonian.) The restriction that the orbitals of each pair be orthogonal to the orbitals of all other pairs leads to Lagrange multipliers in the variational equations (6). Rather than replacing these Lagrange multipliers through use of coupling operators, we use the OCBSE method[20] in which each GVB pair is solved for in the space orthogonal to the other occupied orbitals.

To obtain full optimization of the orbitals, the mixing of all occupied orbitals amongst themselves is optimized each iteration as

discussed in Ref. 20c. In this way the partition of the basis set is continually changed until self-consistency is attained. With the exceptions of a few strongly orthogonal geminal calculations on small diatomic molecules[6] and several multi-configuration SCF calculations,[13-16] previous calculations[11, 21] have not fully optimized the orbitals since the total basis was partitioned into orthogonal sets to be used by the different orbitals and the partition was not iterated.

A good example of the importance of full optimization occurs in the case of ethane molecule. The Hartree-Fock wavefunction leads to a rotational barrier, 3.3 kcal, in good agreement with experiment (2.9 kcal). However, using the GVB form of wavefunction but not optimizing the orbitals fully, Klessinger[12] obtained a barrier of -5.1 kcal (eclipsed form lower rather than staggered). We carried out fully-optimized GVB calculations[1] on ethane and found a barrier of 3.1 kcal, showing the importance of full optimization. [In the STO-4G minimum basis set developed by Hehre, Stewart and Pople,[22] we obtained energies (in hartrees) of -78.8608 and -78.8555 for the respective staggered and eclipsed conformations in HF, compared with -78.9691 and -78.9641 in GVB.]

II. THE METHYLENE MOLECULE

Despite the great interest in the chemistry of methylene[23,27] only recently has the geometry of the ground state been firmly established and the separation of the lowest triplet and singlet states is not known.

There are three important low-lying states of CH_2, the $^3B_1$, $^1A_1$, and $^1B_1$ states. In the Hartree-Fock description each of these states involves a carbon 1s pair of orbitals ($1a_1$) and two pairs of orbitals ($2a_1$ and $1b_2$) primarily associated with the CH bonds. This leaves two low lying molecular orbitals, a nonbonding orbital in the molecular plane ($3a_1$) and a π orbital perpendicular to the plane ($1b_1$). The HF states are then described as

$$^3B_1: \quad (3a_1)^1(1b_1)^1$$

$$^1B_1: \quad (3a_1)^1(1b_1)^1$$

$$^1A_1: \quad (3a_1)^2$$

All ab initio calculations on CH_2 (dating back to the work by Foster and Boys[24] in 1960) have agreed in predicting the ground state to be a bent $^3B_1$ state.[25-27] The best published calculations are those of O'Neil, Schaefer and Bender[25] (OSB) which lead to a bond angle (θ) of 135°. The experimental observations on CH_2 by Herzberg[28] were interpreted to indicate that the $^3B_1$ state is linear (but also mentioned a possible second interpretation leading to θ = 140°). Recent experimental results[29-31] have confirmed the theoretical predictions of $\theta \sim 135°$.

Herzberg and Johns[31] reported an extensive study of the $^1B_1 - {}^1A_1$ spectra of CH_2. The lowest observed transition was at 1.34 eV; but they deduced that this was a (060) – (000) transition and extrapolated their results to obtain a 0-0 singlet – singlet transition energy of 0.88 eV. Although no phosphorescence from

$^1A_1$ to $^3B_1$ was observed, they estimated the (0, 0) triplet → singlet energy difference to be < 1.0 eV. The most complete theoretical calculations by OSB[25] lead to 0-0 transition energies‡ of 0.97 eV ($^1B_1 \leftarrow {}^1A_1$) and 0.96 eV ($^3A_1 \leftarrow {}^1B_1$).

The GVB wavefunctions for these states have the form

$$^3B_1: \mathcal{A}(1s_c)^2[1a, 1b][2a, 2b][3a, 3b]$$

$$^1B_1: \mathcal{A}(1s_c)^2[1a, 1b][2a, 2b][3a, 3b]$$

$$^1A_1: \mathcal{A}(1s_c)^2[1a, 1b][2a, 2b][3a, 3b]$$

where each pair [ia, ib] denotes a GVB singlet pair

$$(\phi_{ia}\phi_{ib} + \phi_{ib}\phi_{ia})\alpha\beta$$

as in (2) and where unpaired orbitals are taken to be triplet coupled. These orbitals are obtained in separate self-consistent calculations for each state, although the 1s orbital remains an essentially unchanged carbon atomic 1s orbital. In all three cases the ϕ_{1a} and ϕ_{1b} orbitals localize in the region of the left CH bond and ϕ_{2a} and ϕ_{2b} are symmetrically related to ϕ_{1a} and ϕ_{1b} and localized in the region of the right CH bond. The nonbonding orbitals ϕ_{3a} and ϕ_{3b} differ rather extensively between the $^3B_1$ and $^1A_1$ states as will be discussed below. In Figs. 1 and 2, respectively, we show the orbitals for the $^1A_1$ and $^3B_1$ states.

The calculations were performed at four HCH angles (90, 105, 135 and 180 degrees), each with a CH bond distance of 2.1 a_0. A bond angle of 105° is near the minimum of the $^1A_1$ potential

curve, and a bond angle of 135° is near the minimum for the $^3B_1$ and $^1B_1$ curves. The basis sets employed consisted of a double zeta (DZ) contracted gaussian basis[32, 33] and the same set augmented by a set of uncontracted d functions (with orbital exponent 0.532) on the carbon atom (POL).

For all three states each GVB bonding pair $[\phi_{1a}, \phi_{1b}]$ and $[\phi_{2a}, \phi_{2b}]$ consists of one orbital (ϕ_{1a}) concentrated mainly on the carbon but hybridized towards one of the hydrogens and an essentially hydrogenic orbital delocalized somewhat onto the carbon (see Figs. 1 and 2). For the B_1 states the ϕ_{3a} orbital lies in the molecular plane (a σ orbital) and the ϕ_{3b} orbital is antisymmetric with respect to the plane (a π orbital). For the $^1A_1$ state ϕ_{3a} and ϕ_{3b} have the form of sp hybridized lobe-type orbitals, hybridized to point above and below the molecular plane and bent back from the hydrogens. In the HF description $\phi_{3a} = \phi_{3b}$ is a σ orbital. Using (3) the GVB pair $[\phi_{3a}, \phi_{3b}]$ can be written as the sum of two doubly occupied natural orbitals $[C_1\sigma^2 - C_2\pi^2]$. This splitting of the HF nonbonding pair leads to a large drop in energy (0.0214 h = 0.48 eV = 13 kcal) as might be expected from the near degeneracy of the $3a_1$ and $1b_1$ orbitals.

In Table 1 we compare the energies of the GVB wavefunctions at the lowest calculated points for each state (in the GVB 1-pair calculation, the $^1B_1$ and $^3B_1$ states were treated as in open-shell Hartree-Fock theory and the $^1A_1$ was treated by splitting only the sp pair). We note that the 1-pair GVB description is a reasonably consistent description for all states in that each state

dropped approximately the same amount (0.0221, 0.0227, and 0.0274 h) in energy when the CH bonding pairs were split. The two configuration wavefunctions of OSB in the table is equivalent to the 1-pair GVB calculation although we used a larger basis set.

We also performed a configuration interaction calculation (denoted as GVB-CI) at each point using the six orthogonal GVB natural orbitals as a basis (keeping the 1s pair doubly occupied). This procedure provides a simple means of obtaining the optimum valence natural orbitals and thus forms an alternative to the iterative natural orbital method of Bender and Davidson.[16] As indicated in Table 1 the GVB-CI led to improvements in energy of 0.0115, 0.0052, and 0.0080 a.u. for the $^3B_1$, $^1A_1$, and $^1B_1$ states, respectively. OSB obtain a much larger improvement in energy in their CI calculations (see Table 1) as they also include excitations not involving valence orbitals (semi-external correlation). As shall be reported elsewhere in a more comprehensive study of hydrocarbons, the GVB spin coupling is expected to be appropriate for the $^1A_1$ state but not quite so appropriate for the $^3B_1$ and $^1B_1$ states. The use of GVB-CI removes this restriction in the spin-coupling and hence should increase the $^3B_1$-$^1A_1$ splitting (as observed). The GVB-CI calculation leads to a balanced consistent treatment of all three states and should lead to reliable values for these splittings.

As shown in Fig. 3 the $^3B_1$ state is the lowest state for $100° < \theta \leq 180°$, but the $^1A_1$ state is lower for $\theta < 100°$ (θ is the HCH angle). The $^3B_1$ and $^1B_1$ states exhibit shallow minima at approximately $\theta = 135°$ with energies 0.39 eV = 9.0 kcal and

0.28 eV = 6.5 kcal below that of the linear configurations ($^3\Sigma_g^-$ and $^1\Delta_g$). The observed zero point energy for the bending motion in the $^1A_1$ state is 676 cm^{-1} and hence the classically allowed range of bending for the $^1A_1$ state is approximately from 90° to 110°. Since the $^3B_1$-$^1A_1$ crossing occurs at 100, we would expect the intersystem crossing from the $^1A_1$ to the triplet manifold to be sufficiently rapid that phosphorescence from $^1A_1$ to $^3B_1$ would not be observed.

From the GVB-CI results we predict the $^1A_1$-$^3B_1$ splitting (see Table 2) to be 0.50 eV and the $^1B_1$-$^1A_1$ splitting to be 1.40 eV. This is in conflict with both the previously reported CI calculations and the experimental estimates for these quantities. However, the previous CI calculations did not include the 3d polarization functions which we find to be quite important for the $^1A_1$ state. We repeated the GVB-CI calculations with the polarization functions deleted and obtained 0.97 and 1.11 eV in good agreement with the values of 0.96 and 0.97 eV from the previous CI calculation. Recently Bender and Schaefer[34] have added d functions to their first order CI wavefunction and find that the $^1A_1$-$^3B_1$ separation decreases to 0.60 eV.

Correcting for the zero-point energies our calculations lead to 1.36 eV for the 0-0 singlet ← singlet transition, very close to the lowest transition (10823 cm^{-1} = 2.34 eV) observed by Johns and Herzberg.[31] They assigned this as (060) ← (000) based on an extrapolation of the isotope shifts for $^{12}CH_2$ and $^{13}CH_2$. However, we suspect that their first observed transition is in fact (000) ←

(000) and that the isotope shift extrapolation approach may break down for a transition to a state with a broad shallow double minimum such as $^1B_1$. With these suppositions, there is very good agreement between experiment and theory.

From the GVB-CI calculations we find a second $^1A_1$ state which has a minimum at 180° ($^1\Sigma_g^+$) with an energy 3.22 eV above the minimum of the first $^1A_1$ state. This excitation energy is in good agreement with the band observed at 27586-30035 cm^{-1} (3.42-3.72 eV)[30] which Herzberg and Johns tentatively assigned as a $^1A_1 - {}^1\Sigma^+$ transition. This upper $^1\Sigma_g^+$ state is just the one for which the nonbonding pair has the form $[(\pi x)^2 + (\pi y)^2]$ rather than $[(\pi x)^2 - (\pi y)^2]$ or $[\pi x \pi y + \pi y \pi x]$ as for the linear $^1A_1$ and $^1B_1$ states, respectively (both components of $^1\Delta_g$).

A conclusion from this work is that through the procedure of carrying out GVB calculations and then a CI calculation making use of the GVB orbitals, we can obtain useful interpretations of the wavefunction (in terms of the GVB orbitals) as well as high accuracy and a consistent treatment of different states. A reasonable approach to the CI would be to include single and double excitations within the space spanned by the GVB orbitals (the valence orbitals) and singlet excitations outside of this space (the virtual orbitals). This procedure would correspond closely to the first-order CI method of Schaefer[35] who uses an iterative natural orbital[16] approach to select the valence-like orbitals.

REFERENCES

[1] W. J. Hunt, P. J. Hay and W. A. Goddard III, to be published.

[2] L. Pauling, J. Amer. Chem. Soc. 53 (1931) 1367; J. C. Slater, Phys. Rev. 37 (1931) 481; 38 (1931) 1109.

[3] A. C. Hurley, J. E. Lennard-Jones and J. A. Pople, Proc. Roy. Soc. (London), A220 (1963) 446.

[4] C. A. Coulson and I. Fischer, Phil. Mag. 40 (1949) 386.

[5] J. M. Parks and R. G. Parr, J. Chem. Phys. 28 (1958) 335; 32 (1960) 1567.

[6] D. M. Silver, E. L. Mehler and K. Ruedenberg, J. Chem. Phys. 52 (1970) 1174, 1181, 1206.

[7] W. Kutzelnigg, J. Chem. Phys. 40 (1964) 3640; R. Ahrlichs and W. Kutzelnigg, J. Chem. Phys. 48 (1968) 1819.

[8] R. McWeeny and K. A. Ohno, Proc. Roy. Soc. (London), A255, (1960) 367.

[9] M. Klessinger and R. McWeeny, J. Chem. Phys. 42 (1965) 3343.

[10] M. Levy, W. J. Stevens, H. Shull and S. Hagstrom, J. Chem. Phys. 52 (1970) 5483.

[11] M. Klessinger, J. Chem. Phys. 43 (1965) 5117.

[12] M. Klessinger, J. Chem. Phys. 53 (1970) 225.

[13] A. C. Wahl and G. Das, Adv. Quant. Chem. 5 (1971) 261.

[14] E. Clementi and A. Veillard, J. Chem. Phys. 44 (1966) 3050.

[15] J. Hinze and C. C. J. Roothaan, Prog. Theor. Physics Supp. 40 (1967) 37.

[16] C. F. Bender and E. Davidson, J. Phys. Chem. 70 (1966) 2675.

[17] (a) P. O. Löwdin, Phys. Rev. 97 (1955) 1474. (b) P. O. Löwdin and H. Shull, Phys. Rev. 101 (1956) 1730.

[18] T. Arai, J. Chem. Phys. 33 (1960) 95; P. O. Löwdin, J. Chem. Phys. 35 (1961) 78.

[19] W. A. Goddard III, Phys. Rev. 157 (1967) 73, 81.

[20] (a) W. J. Hunt, T. H. Dunning, Jr., and W. A. Goddard III, Chem. Phys. Lett. 3 (1969) 606. (b) W. A. Goddard III, T. H. Dunning, Jr., and W. J. Hunt, Chem. Phys. Lett. 4 (1969) 231. (c) W. J. Hunt, W. A. Goddard III, and T. H. Dunning, Jr., Chem. Phys. Lett. 6 (1970) 147.

[21] P. F. Franchini and M. Zandomeneghi, Th. Chim. Acta 21 (1971) 90; P. F. Franchini, R. Moccia and M. Azndomeneghi, Int. J. Quantum Chem. 4 (1970) 487.

[22] W. J. Hehre, R. F. Stewart and J. A. Pople, J. Chem. Phys. 51 (1969) 2657.

[23] P. P. Gaspar and G. S. Hammond, Carbene Chemistry (Ed. W. Kirmse, Academic, New York, 1964); G. Class, Topics Stereochem. 3 (1968) 198; D. Bethell, Adv. Phys. Org. Chem. 7 (1969) 153.

[24] J. M. Foster and S. F. Boys, Rev. Mod. Phys. 32 (1960) 305.

[25] S. V. O'Neil, H. F. Schaefer III, and C. F. Bender, J. Chem. Phys. 55 (1971) 162.

[26] C. Salez and A. Veillard, Theoret. Chim. Acta 11 (1968) 441.

[27] J. F. Harrison and L. C. Allen, J. Amer. Chem. Soc. 91 (1969) 807.

[28] G. Herzberg, Proc. Roy. Soc. (London) A262 (1961) 291.

[29] R. A. Bernheim, H. W. Bernard, P. S. Wang, L. S. Wood, and P. S. Skell, J. Chem. Phys. 53 (1970) 1280.

[30] E. Wassermann, W. A. Yager and V. Kuck, J. Amer. Chem. Soc. 92 (1970) 7491.

[31] G. Herzberg and J. W. C. Johns, J. Chem. Phys. 54 (1971) 2276.

[32] S. Huzinaga, J. Chem. Phys. 42 (1965) 1293.

[33] T. H. Dunning, Jr., J. Chem. Phys. 53 (1970) 2823.

[34] C. F. Bender and H. F. Schaefer III, private communication.

[35] H. T. Schaefer III, R. A. Klemm, and F. E. Harris, Phys. Rev. 181 (1969) 137.

‡ All theoretical transition energies reported here (except vertical transition energies) refer to adiabatic differences calculated from the minima of the respective states without zero-point corrections.

Table 1

GVB energies for the states of CH_2[a]

Reference	Method	Energy (a.u.)		
		$^3B_1(135°)$	$^1A_1(105°)$	$^1B_1(135°)$
This work	HF	-38.9202	-38.8821	-38.8544
	GVB-1 pair		-38.9035	
	GVB-3 pair	-38.9483	-38.9362	-38.8818
	GVB-CI	-38.9598	-38.9414	-38.8898
O'Neil, Bender & Schaefer (Ref. 25)	HF	-38.9136	-38.8620	-38.8452
	1 pair		-38.8772	
	CI	-38.9826	-38.9472	-38.9114
Harrison and Allen (Ref. 27)	HF	-38.893	-38.843	-38.822
	VB-CI	-38.915	-38.864	-38.833
Foster and Boys (Ref. 24)	CI	-38.904	-38.865	-38.808

a) The energies reported from Refs. 24, 25, and 27 are the calculated minima for each state.

Table 2

CH_2 excitation energies (eV)*

References	Method	$^3A_1 \leftarrow {}^1B_1$	$^1B_1 \leftarrow {}^1A_1$	$^1B_1 \leftarrow {}^1A_1$ (vert)
This work	HF	1.03	0.75	1.32
	GVB-1 pair	0.45	1.34	1.91
	GVB-3 pair	0.32	1.49	2.06
	GVB-CI[a]	0.50 (0.97)[a]	1.40 (1.11)[a]	1.88 (1.69)[a]
O'Neill, Bender, Schaefer (Ref. 25)	CI	0.96	0.97	1.56
Harrison and Allen (Ref. 27)	VB-CI	1.39	0.84	1.52
Foster and Boys (Ref. 24)	CI	1.06	1.55	
Experimental (Ref. 32)		< 1.0[b]	0.88[c] 1.34[d]	1.98[e]

* Zero-point corrections have not been included.

a) The quantities in parentheses were obtained by using a DZ basis essentially identical to that used in Ref. 26.

b) Estimated upper limit.

c) Extrapolated

d) Lowest observed $^1B_1 \leftarrow {}^1A_1$ transition.

e) Assuming the vertical transition to correspond to the middle of the observed $^1B_1(0N0) \leftarrow {}^1A_1(000)$ spectrum and including the zero point energy of the $^1A_1$ state.

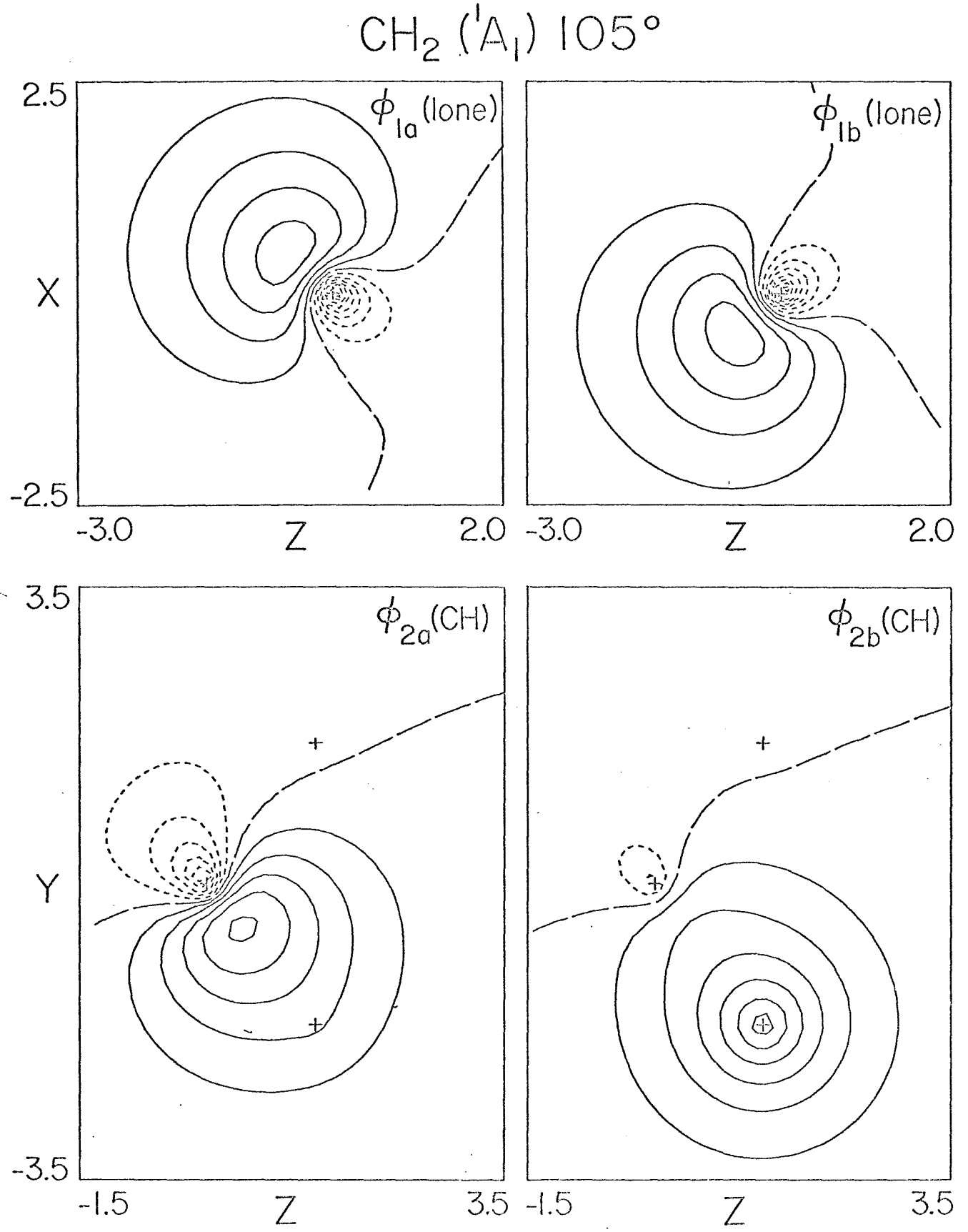
CH2 (1A1) 105°
2.5
X
-2.5
-3.0
Z
2.0
φ1a (lone)
φ1b (lone)
3.5
Y
-3.5
-1.5
3.5
φ2a (CH)
φ2b (CH)

FIG. 1

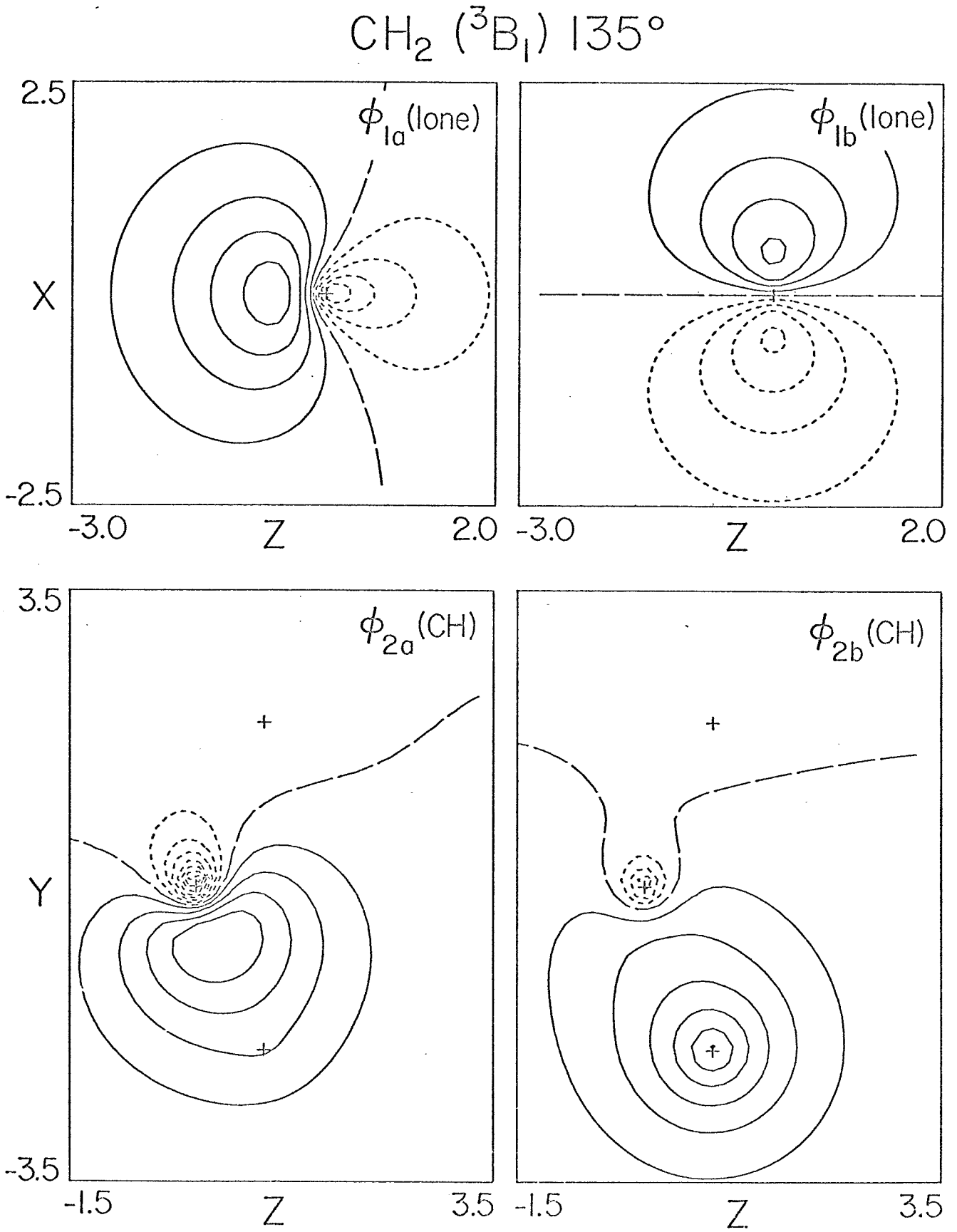
CH2 (3B1) 135°
2.5
X
-2.5
-3.0
Z
2.0
φ1a(lone)
φ1b(lone)
3.5
Y
-3.5
-1.5
3.5
φ2a(CH)
φ2b(CH)

FIG. 2

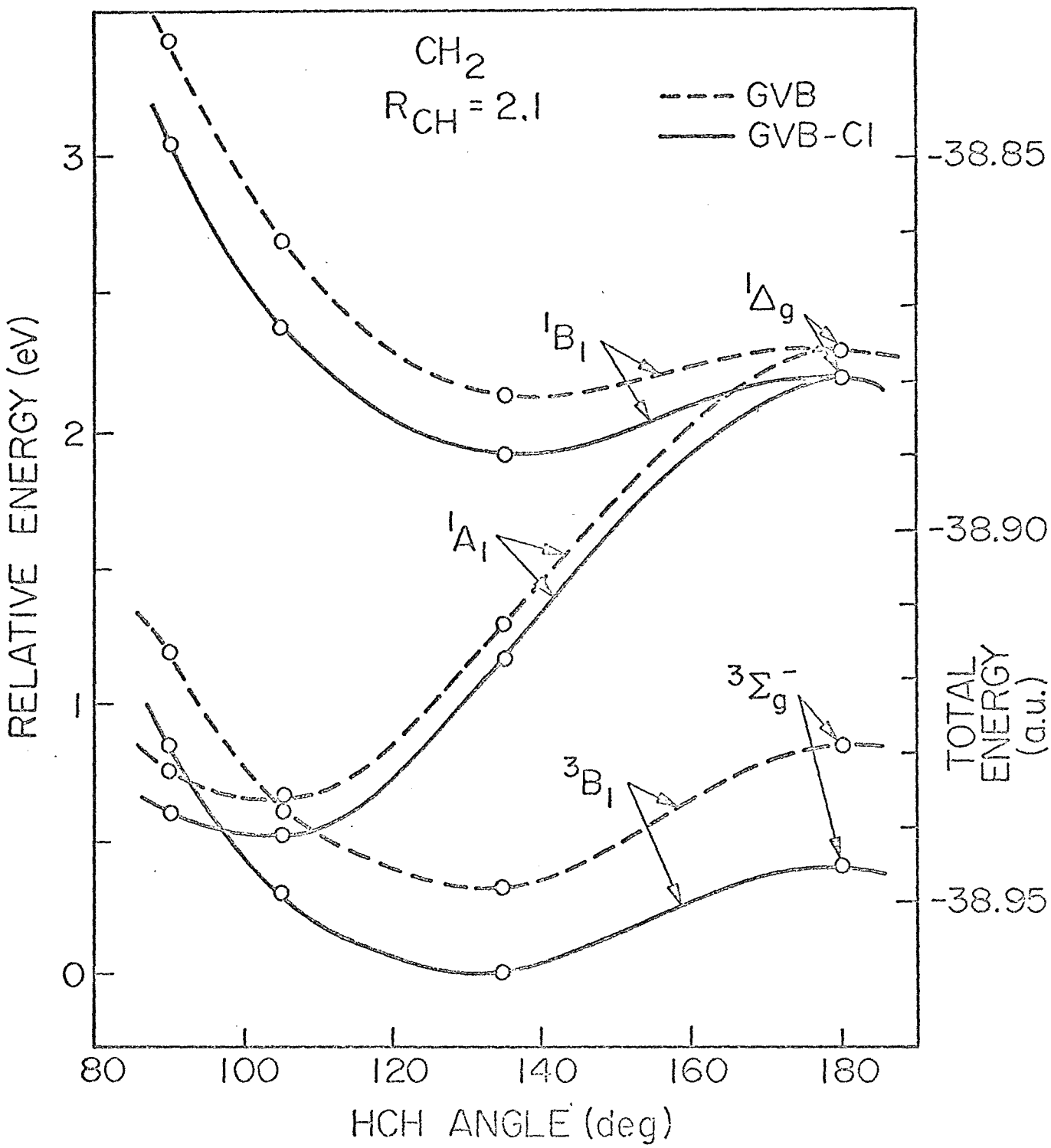
CH2
RCH = 2.1
GVB
GVB-CI
1B1
1Δg
1A1
3Σg−
3B1
RELATIVE ENERGY (eV)
TOTAL ENERGY (a.u.)
-38.85
-38.90
-38.95
0
1
2
3
80
100
120
140
160
180
HCH ANGLE (deg)

FIG. 3

E. Self-Consistent Procedures for GVB Wavefunctions--Applications to BH, H_3, H_2O, C_2H_6, and O_2

Self-Consistent Procedures for Generalized Valence Bond Wavefunctions and Applications H_3, BH, H_2O, C_2H_6 and O_2.**

W. J. HUNT,† P. J. HAY,‡ AND W. A. GODDARD III

Arthur Amos Noyes Laboratory of Chemical Physics*
California Institute of Technology
Pasadena, California 91109

Methods of efficiently optimizing the orbitals of Generalized Valence Bond (GVB) Wavefunctions are discussed, and applied to LiH, BH, H_3, H_2O, C_6H_6, and O_2. The strong orthogonality and perfect pairing restrictions are tested for the $X\ ^1\Sigma^+$ state of LiH, the $X\ ^1\Sigma^+$, a $^3\Pi$, and $A\ ^1\Pi$ states of BH, and the $H_2 + D \rightleftharpoons H + HD$ exchange reaction. The orbitals of H_2O and C_2H_6 naturally localize into OH, CH, and CC bonding pairs. The nonbonding orbitals of H_2O are approximately tetrahedral but this description is only 2 kcal lower than the optimum description in terms of symmetry functions. The calculated rotational barrier for C_2H_6 is 3.1 kcal, in good agreement with the experimental value.

---

* Contribution No.

** Partially supported by a grant (GP-15423) from the National Science Foundation.

† National Defense Education Act predoctoral fellow.

‡ National Science Foundation predoctoral fellow.

The description of the O_2 molecule in the GVB approach is presented and the results of carrying out CI calculations using the GVB orbitals is discussed. The GVB orbitals are found to be a good basis set for configuration interaction calculations. The general features of GVB orbitals in other molecules are summarized.

I. INTRODUCTION

The electronic structure of molecules is usually described in terms of either the molecular orbital (MO) or valence bond (VB) models. In particular, the single-configuration MO (or Hartree-Fock) wavefunction has proved extremely useful in computing properties of ground and excited state molecules. Configuration interaction studies have shown that for typical molecules near the equilibrium geometry the Hartree-Fock wavefunction is by far the most important configuration in the "exact" wavefunction. Conceptually, such advances as Walsh diagrams[1] for predicting molecular geometries and the Woodward Hoffmann rules[2] for predicting chemical reactions have their origins in molecular orbital theory.

There are, however, at least two serious drawbacks to the Hartree-Fock model:

1. Molecular orbitals do not usually dissociate correctly, so that one cannot describe bond-breaking processes within this model.

2. Molecular orbitals have the full symmetry of the molecule and bear little resemblance to the expected shapes of bond orbitals and lone pair orbitals.[3]

Our objective here is to discuss an improved SCF method which is tractable and yet removes these serious deficiencies of MO theory. The emphasis will not be on getting 100% of the correlation energy. Rather the aim will be to obtain a generally useful orbital representation for describing molecular bonding and chemical reactions.

II. THE WAVEFUNCTIONS

A. Basic Approach

The Hartree-Fock (HF) wavefunction for (a closed shell) singlet state has the form

$$\mathcal{A}[\phi_1\alpha\phi_1\beta\phi_2\alpha\phi_2\beta\cdots\phi_n\alpha\phi_n\beta] \qquad (1)$$

with each orbital appearing twice (doubly occupied). This double occupation of the orbitals leads to some of the deficiencies of the HF procedure, and several approaches (SOGI,[4a] SO-SCF,[4b] and BRNO[4c]) have been proposed in which the pair

$$\phi_i\alpha\phi_i\beta$$

is replaced by

$$\phi_{ia}\alpha\phi_{ib}\beta$$

to yield the wavefunction

$$\mathcal{A}[\phi_{1a}\phi_{1b}\phi_{2a}\phi_{2b}\cdots\chi], \qquad (2)$$

where χ is allowed to be a general N-electron spinfunction and where χ and the orbitals ϕ_i are solved for self-consistently. This approach leads to the proper description of bond breaking[5] and leads directly to localized bonding and nonbonding orbitals (vide infra).

One reason for the simplicity of Hartree-Fock calculations is that the orbitals of (1) can be taken as orthogonal. Unfortunately this is not the case for wavefunctions of the form (2) (where χ is a general N-electron spinfunction). This lack of orthogonality leads to significant computational problems for large systems and greatly restricts the usefulness of such approaches. We would like to retain the conceptual usefulness of wavefunctions of the form (2) and yet simplify the calculations so that reasonably large molecules can be considered. Most of the basic restrictions and approaches to be used have been suggested elsewhere,[6,7] but are summarized here to clarify our later discussions:

(i) The spin function χ is taken to be

$$\chi_{VB} = [\alpha(1)\beta(2) - \beta(1)\alpha(2)][\alpha(3)\beta(4) - \beta(3)\alpha(4)]\cdots$$

where for a state of spin S the last 2S spins are α. This spin function is the one used in G1[8] and simple valence bond[9] wavefunctions. With restriction (1) the wavefunction (2) can be re-written as

$$\mathcal{A}[(\phi_{1a}\phi_{1b} + \phi_{1b}\phi_{1a})(\phi_{2a}\phi_{2b} + \phi_{2b}\phi_{2a})\cdots$$

$$(\phi_{na}\phi_{nb} + \phi_{nb}\phi_{na})\alpha\beta\alpha\beta\cdots\alpha\beta] \qquad (3)$$

where each term in parentheses is said to be singlet paired.

(ii) The various orbitals are required to be orthogonal to each other unless they are singlet paired, i.e.,

$$\langle \phi_{ia} | \phi_{ib} \rangle \neq 0$$

$$\langle \phi_i | \phi_j \rangle = 0 \qquad \text{otherwise.}$$

This restriction has often been used for wavefunctions and is known as the strong orthogonality[10] or separated pair[11,12] restriction.

(iii) The orbitals of (3) are solved for self-consistently.

The wavefunction (3) has the form of a simple valence bond (VB) function, the difference being that in (3) the orbitals are solved for self-consistently rather than taken as (hybridized) atomic orbitals as in VB. For this reason we refer to the wavefunction (3) as the generalized valence bond (GVB) wavefunction.

Wavefunction (3) is a special case of the strongly orthogonal geminal[12] wavefunction

$$\mathcal{A}[\Omega_1(1,2), \Omega_2(3,4) \cdots \chi_{VB}] \tag{4}$$

where each geminal Ω_i can be expanded in terms of natural orbitals.[13]

$$\Omega_i(1,2) = \sum_{j=1}^{P} C_{ji}\, \phi_{ji}(1)\phi_{ji}(2). \tag{5}$$

The ideas of representing electron pairs in this form were originally formulated by Hurley, Lennard-Jones and Pople[6] (HLJP), who discussed the strong orthogonality restriction as well as the representation of pair functions in both the natural orbital (5) and generalized valence bond (3) forms.

In terms of natural orbitals, each pair function of (3) has the form

$$\phi_{ia}(1)\phi_{ib}(2) + \phi_{ib}(1)\phi_{ia}(2) = C_{1i}\phi_{1i}(1)\phi_{1i}(2) + C_{2i}\phi_{2i}(1)\phi_{2i}(2)\,, \qquad (6)$$

that is, only two natural orbitals are used for each pair function.[14] Substituting (6) into (3) we find that the expansion of (3) in terms of those natural orbitals contains only terms of closed shell form. As discussed below this leads to great simplification in the calculations.

There are many cases in which we will want to keep some pairs doubly occupied rather than allowing them to be split. In such cases we take

$$C_{1i} = 1 \text{ and } C_{2i} = 0$$

in (6). In addition, for non singlet states of spin S we will usually take the last 2S orbitals to be unpaired and with the same spin.

B. The Equations

As has been shown by HLJP and Kutzelnigg,[7] the dependence of the energy in (3) upon the orbitals of pair i has the form

$$E = E_{(i)} + f_{1i}\langle\phi_{1i}|(2h_{eff} + J_{1i})|\phi_{1i}\rangle$$
$$+ f_{2i}\langle\phi_{2i}|(2h_{eff} + J_{2i})|\phi_{2i}\rangle + C_{1i}C_{2i}\langle\phi_{1i}|K_{2i}|\phi_{1i}\rangle \qquad (7)$$

where $E_{(i)}$ is independent of the orbitals in pair i,

$$h_{eff} = h + \sum_{j\neq 1i,2i} f_j(2J_j - K_j)$$

and

$f_k = 1$ for a double occupied orbital

$= \frac{1}{2}$ for an open-shell singly occupied orbital

$= C_k^2$ for a natural orbital of a split pair as in (6).

Here h_{eff} is analogous to the usual Hartree-Fock one-electron Hamiltonian except that it contains no terms due to either orbital of pair i. For a nonsinglet state of spin S there will be 2S orbitals corresponding to the unpaired spins; these orbitals are referred to as open-shell orbitals ($f_k = \frac{1}{2}$). Any number of the pairs can be double occupied ($f_k = 1$).

Separating from E_i the terms involving the other pairs, we obtain the general expansion

$$E = \sum_k f_k h_k + \sum_{k,\ell} (a_{k\ell} J_{k\ell} + b_{k\ell} K_{k\ell}) \tag{8}$$

which has the form appropriate for general HF and many types of MC-SCF wavefunctions. [In (8) $h_k \equiv \langle k|h|k\rangle$ and $J_{k\ell}$ and $K_{k\ell}$ are the normal Coulomb and exchange integrals.]

Using the variational principle, one obtains the self-consistent field equations[8, 15b]

$$\hat{\bar{H}}_k \phi_k = [\hat{H}_k - \sum_{j \neq k} |j\rangle\langle j|\hat{H}_j]\phi_k = \epsilon_k \phi_k \tag{9}$$

$$k = 1, 2, \cdots, M,$$

where $H_k = f_k h + \sum_\ell a_{k\ell} J_\ell + b_{k\ell k\ell}$ and M is the number of distinct orbitals. [J and K are the usual Coulomb and exchange operators from HF theory]. In general, there are fewer than M such equations to solve, since all doubly-occupied orbitals can be taken as eigenfunctions of the same closed-shell Hamiltonian.

In the homogeneous approach normally used in solving MC-SCF equations,[16-19] one explicitly constructs each $\overline{H}_k$ for a set of trial functions $\{\phi_j^0\}$ and solves (9) for the ϕ_k to use in the next iteration. We have found this approach to be unsatisfactory and instead use the method suggested in Ref. 15c. In this method each iteration in the SCF process consists of three distinct steps:

(1) The Hamiltonian matrices $\underset{\sim}{H}_k$ are constructed using the trial functions $\{\phi_j^0\}$ and trial CI coefficients $\{C_i^0\}$ and a new set of CI coefficients is obtained by solving the 2×2 matrix equations for each pair.

(2) Each Hamiltonian matrix $\underset{\sim}{H}_k$ is diagonalized according to the OCBSE[15a] procedure. In this approach the eigensolutions of $\underset{\sim}{H}_k$ are obtained in the space orthogonal to the vectors of shells k', where $k' \neq k$, thereby avoiding the necessity of using coupling operators in the SCF equations.

(3) Since this procedure does not permit mixing of occupied orbitals of shell k with occupied orbitals of other shells, we obtain this optimum mixing by using the set of old orbitals $\{\phi_i^0\}$ as a basis for the expansion of the new (unknown) orbitals $\{\phi_i\}$

$$\phi_i = \phi_i^0 + \sum_{v>i} \phi_v^0 \, \Delta_{vi} - \sum_{v<i} \phi_v^0 \, \Delta_{iv}$$

and optimize the mixing of occupied orbitals with each other by solving for the correction coefficients

$$\{\Delta_{vi},\ v > i,\ i = 1,\ M\}$$

as in Ref. 7. Since this procedure optimizes the mixing of natural orbitals, terms such as

$$C_{12}(\phi_{1i}\phi_{2i} + \phi_{2i}\phi_{1i})$$

need not appear in the expansion [Eq. (6)] of the GVB pair.

The above iterative procedure insures that when the SCF equations have converged, one has obtained the optimum set of orbitals. Although for step (2) the orbitals of shell k are restricted to be in a space orthogonal to the orbitals of other shells, this space changes from iteration to iteration as the occupied orbitals mix in virtual orbital components in step (2) and occupied orbital components in step (3). This differs from some previous strongly orthogonal geminal calculations[21,22,24] where each geminal was obtained in a partitioned subspace of the basis, but where the partition was imposed at the beginning of the calculation and not optimized.

C. Comparison with Other Methods

We emphasize that, with the exceptions of strongly orthogonal geminal calculations on small diatomic molecules[7,12,23] and of several multi-configuration SCF calculations,[16-19] previous calculations on wavefunctions of the form (3) have not optimized the orbitals within a given basis to a level comparable to the degree of convergence obtained in Hartree-Fock calculations.

The GVB method is related to the multi-configuration SCF approach except that the form of the GVB wavefunction is more restricted in order to lead to an orbital type wavefunction (3).

Several types of calculations have been carried out using strongly orthogonal geminals as in (4) including approximate treatments by McWeeny and Ohno[24] on the water molecule and Parks and Parr[11] on formaldehyde. Silver, Mehler, and Ruedenberg[12] obtained fully optimized SOG wavefunctions for Be, LiH, BH and NH using more than two NO's in each geminal, and Scarzafava[20] carried out similar calculations on H_2O. Ahrlichs and Kutzelnigg[7,23] also used a procedure similar to ours on Be and LiH.

Calculations by Franchini, et al.,[21] have employed the procedure of localizing the Hartree-Fock orbitals and expanding each geminal in a CI wavefunction as in (5) with a fixed partition of the basis set. In this scheme, the orbitals are not fully optimized since the space available to each geminal was arbitrarily determined before the calculation.

McWeeny and Klessinger[22,25] have carried out minimum basis self-consistent group calculations on many molecules by starting with a set of symmetrically orthogonalized hybridized atomic orbitals and carrying out a two by two CI calculation on each geminal. Since the energy was optimized as a function of only one hybridization parameter per atom, the resulting orbitals were not completely optimum. For several molecules this has resulted in very poor descriptions of the barriers to internal rotation.[22b] (e.g. ethane is calculated to have a barrier of 5.1 kcal with the eclipsed configuration lower).

Although several authors have discussed ways of relaxing orthogonality constraints,[27,28] the complications involved are excessive. Hinze[47] has developed an approach for general MC-SCF wavefunctions in which the mixings of occupied orbitals with each other is optimized through successive 2 x 2 rotations. This procedure leads to fully optimized orbitals. Hinze has applied this method to various states of LiH[47] and White, Dunning, Pitzer, and Matthews have applied Hinze's program to a series of calculations on various states of CF.[48]

Harrison and Allen[26] have used VB configurations with orbitals based on atomic HF calculations but do not solve for the optimum orbitals. Multi-configuration techniques for diatomic molecules using elliptic basis functions were discussed by Taylor and Harris.[29] VB-CI methods have also been used on LiH and BeH^+ by Miller et al.[30] and on He_2 potential curves by Klein[31] and Gupta and Matsen.[32]

III. TESTS OF STRONG ORTHOGONALITY AND "PERFECT PAIRING"

In order to test the validity of the restrictions involved in GVB calculations, we will compare the results of GVB and SOGI calculations for several systems. This forms a useful test of both the strong orthogonality and perfect pairing restrictions, since neither restriction is made in the SOGI method.

A. LiH and BH ($^1\Sigma^+$)

For a four-electron singlet system, we can write the GVB and SOGI wavefunctions as

$$\Psi_{GVB} = \mathcal{A}[\phi_{1a}\phi_{1b}\phi_{2a}\phi_{2b}\chi_1]$$

$$\Psi_{SOGI} = \mathcal{A}[\phi_{1a}\phi_{1b}\phi_{2a}\phi_{2b}(\cos\theta\chi_1 + \sin\theta\chi_2)]$$

where χ_1 and χ_2 are the two linearly independent spin functions

$$\chi_1 = \tfrac{1}{2}(\alpha\beta - \beta\alpha)(\alpha\beta - \beta\alpha)$$

$$\chi_2 = \frac{1}{\sqrt{3}}[2\alpha\alpha\beta\beta + 2\beta\beta\alpha\alpha - (\alpha\beta + \beta\alpha)(\alpha\beta + \beta\alpha)].$$

In GVB the pair $[\phi_{1a}, \phi_{1b}]$ is constrained to be orthogonal to pair $[\phi_{2a}, \phi_{2b}]$ and the second spin function χ_2 is not used.

SOGI calculations on the ground states of LiH[2,33] and BH[5] have shown that contributions from spin functions other than χ_1 are negligible. Thus comparing SOGI and GVB for these systems is primarily a test of the strong orthogonality restriction. From Table I we see that for LiH at R_e, E_{GVB} is 0.0296 h lower than E_{HF}

and only 0.0008 h higher than E_{SOGI}. Similar results were also obtained for BH at R_e where E_{GVB} was only 0.0018 h greater than E_{SOGI} while 0.045 h lower than E_{HF}. In comparing the GVB and SOGI orbitals of these systems (see Fig. 1 for BH), we find that the main effect involves orthogonality of the GVB valence orbital to the core orbitals, the GVB valence orbitals have a node in the core region. Otherwise the relative relationships between the valence orbitals are quite similar for these two methods. Thus we conclude that at least for these two systems the orbitals and energies are not greatly modified by the strong orthogonal restrictions.

We also carried out calculations in which the 1s orbitals of the LiH and BH were forced to be doubly occupied (but solved for self-consistently). Although in each case the energy is lowered about 0.012 h upon splitting the core orbitals, we find that this core splitting leads to a negligible modification in the valence orbitals. Thus, in the following calculations we will keep the 1s core orbitals paired [$f_k = 1$ in (10)], but we will solve for them self-consistently with the valence orbitals.

B. $H_2 + D \rightarrow H + HD$

A more significant test of the GVB approach is the description of the reaction

$$H_2 + D \rightarrow H + HD$$

where SOGI calculations have shown[4a] that the spin coupling changes from having singlet-coupled electron pair on the H_2 for the reactants to a singlet-coupled electron pair on the HD for the products. Thus

in the linear transition state with $R_{HH} = R_{HD}$, Ψ_{SOGI} contains equal contributions from the two spin couplings. GVB calculations at $R_{HH} = R_{HD} = 1.8$ bohr using Ladner's[4a] basis set yielded an energy 13 kcal/mole (0.021 a.u.) higher than E_{SOGI} (see Table II). This error in the GVB result is quite significant, being as large as for Hartree-Fock. (The calculated barrier height from the SOGI calculation was 16.9 kcal/mole). However, the GVB orbitals have shapes somewhat similar to those of the SOGI orbitals as shown in Fig. 3. The GVB wavefunction has the form

$$\mathcal{A}[(gg' + g'g)u\alpha\beta\alpha]$$

where all orbitals have the full $D_{\infty h}$ symmetry of the molecule (g or u). An alternative description of the $^2\Sigma_u^+$ state, $\mathcal{A}[(ab + ba)u\alpha\beta\alpha]$ with a and b symmetrically related by mirror plane reflections but solved for self-consistently yielded an even higher energy.

To determine whether one can improve upon the GVB results for H_3 without a great deal of effort, we used the three GVB orbitals as a basis set and carried out a SOGI calculation. This is equivalent to a three basis function, three electron CI calculation using all configurations. We find that this accounts for 69% of the error between GVB and SOGI, leading to a barrier 4 kcal greater than the SOGI barrier.

C. BH $^1\Pi$ and $^3\Pi$ States

Recent SOGI calculations[34] have shown that the lowest $^1\Pi$ and $^3\Pi$ states of BH also involve significant changes in spin-coupling as

the internuclear distance (R) is decreased from ∞ to R_e. Thus, this system serves as another good test case of the limitations of GVB. In the ^2P state of B, Ψ_{GVB} has the form[5]

$$\mathcal{A}\{[1s^2][sz, s\bar{z}]2p_x\,\alpha\beta\alpha\beta\alpha\}$$

where sz and $s\bar{z}$ have the form

$$sz = \phi_s + \lambda\phi_{pz}$$

$$s\bar{z} = \phi_s - \lambda\phi_{pz}$$

that is, these functions are sp-like hybridized orbitals polarized along the z axis.

In contrast to the $^1\Sigma$ state, where the 1s hydrogen orbital is singlet-coupled to the px orbital, the Π states arise from breaking up the nonbonding pair to form the BH bond:[34]

$$^3\Pi: \quad \psi_{GVB} = \mathcal{A}\{[1s^2][sz, h]\, s\bar{z}\ px\ \alpha\beta\alpha\beta\alpha\alpha\}$$

$$^1\Pi: \quad \psi_{GVB} = \mathcal{A}\{[1s^2][sz, h][s\bar{z},\ pz]\,\alpha\beta\alpha\beta\alpha\beta\}$$

Here we refer to the orbitals with symbols (sz, $s\bar{z}$, px, h) to denote their basic shapes, although each orbital is solved for self-consistently. From the results at R = 2.25 and R = 4.0 in Table II, it is seen that the GVB wavefunction is higher in energy than ψ_{SOGI} by amounts ranging from 0.0046 a.u. for the $^3\Pi$ state (R = 2.25) to 0.0198 a.u. for the $^1\Pi$ (R = 2.25).

The description of the $^1\Pi$ state is rather poor and so we examined the improvements to be obtained by solving for the CI wavefunction using the four GVB orbitals as the basis. At R = 2.25 a_0 this accounted for 56% of the error between GVB and SOGI but still led to an energy 0.0088 greater than E_{SOGI}. Another difficult case occurs in the $^2\Pi$ state of CH for large R. At R = ∞ the C atom is in the ^3P state and hence two valence orbitals are coupled antisymmetrically. Coupling the H orbital symmetrically to the carbon p-orbital is thus incorrect at large R. As a result the GVB wavefunction for CH at large R is 0.35 eV above the limit of $C(^3P) + H(^2S)$. However, Bobrowicz[49] has shown that starting with the GVB orbitals and carrying out a three-basis function CI (or SOGI) calculation leads to a proper description of the wavefunction at large R.

D. Summary

From reflections on these studies we have concluded that

(1) The GVB approach should lead to an adequate description of the ground state of most molecules that can be described in terms of one covalent VB structure,

(2) this method also should lead to an adequate description of bond breaking and bond formation when spin coupling changes are not important (thus, biradicals should be well described),

(3) however, the GVB approach may be of less quantitative use in describing reactions involving extensive spin coupling changes. In such cases a simple CI calculation using the GVB natural orbitals may be satisfactory.

Further implications for CI calculations will be discussed later.

IV. THE WATER MOLECULE

The optimum GVB orbitals of the ground state of H_2O lead to a description having two equivalent bonding pairs, two equivalent non-bonding pairs, and an oxygen 1s core pair:

$$\Psi_{GVB} = \mathcal{A}\{[1s_a,\ 1s_b][b_{1a},\ b_{1b}][b_{2a},\ b_{2b}][\ell_{1a},\ \ell_{1b}][\ell_{2a},\ \ell_{2b}]\chi\}$$

This description is not forced upon the system by any arbitrary symmetry requirements, but rather is obtained by solving for the optimum ten GVB orbitals. The orbitals for the equilibrium geometry of the H_2O molecule were obtained using a basis set[33] of contracted Gaussian functions including 3d oxygen polarization functions. We see from Table IV that the major improvement over the Hartree-Fock wavefunction is in the description of the bonding pairs, where an energy lowering of 13 kcal/mole for each bond is obtained.

In Fig. 2 we see that each orbital of a bonding pair (ϕ_{2a} and ϕ_{2b}) is localized on a different center. The ϕ_{2a} orbital, localized on the oxygen atom, has some s character but is mainly (81.9%) p-like (corresponding to sp 4.7 bonding). Similarly, the ϕ_{2b} orbital remains essentially a hydrogenic 1s orbital, delocalized onto the oxygen atom (indicating some ionic character in the bond).

The nonbonding pairs have 59% p-character ($sp^{1.46}$) and are bent back from the oxygen in the plane perpendicular to the molecular plane. Each pair consists of two orbitals (ϕ_{4a} and ϕ_{4b} in Fig. 2) oriented in the same direction but having different radial dependencies, i.e., one being more diffuse than the other. This description is not equivalent to the case where we require the lone-pair functions to have a_1 and b_1 symmetry (i.e., symmetric and antisymmetric with the molecular plane), which in fact (see Table III) leads to an energy only 0.0031 h (2 kcal/mole) higher.

The above results generally agree with previous GVB-like calculations on H_2O by other investigators. Klessinger[22a] has carried out a group function calculation on the OH bonds in H_2O where he obtained an energy lowering of each OH bond of 0.0142 h compared with our value of 0.0209 h. The uv form of Scarzafava's separated-pair wavefunction[20] and the group functions of Franchini, Moccia and Zandomeneghi[21] are roughly equivalent in sophistication to our GVB approach, but lead to slightly worse energies because their method does not achieve full optimization. Scarzafava[20] obtained full orbital optimization and his uv wavefunction is comparable in energy to ours; he also obtained more general separated pair and CI wavefunctions for H_2O. A recent strongly orthogonal geminal calculation by Shull and coworkers[36] demonstrated the transferability of geminals from H_2O to H_2O_2.

V. THE ETHANE MOLECULE

The ethane molecule is a good test case of the GVB approach since a highly restricted wavefunction might not lead to a proper description of the small (2.9 kcal/mole) rotational barrier.

For the ethane molecule, we solved for the GVB orbitals in the STO-4G minimum basis set of contracted Gaussian functions developed by Pople.[43] We obtain six equivalent C-H bond pairs, one of which is shown in Fig. 3 (orbitals ϕ_{2a} and ϕ_{2b}). In contrast to the delocalized molecular orbital, we see that one of the GVB orbitals is an essentially unchanged hydrogen 1s orbital and the other is a hybrid orbital (68.5% p-character, hence $sp^{2.17}$) on the C oriented toward the H. Each C-H bond is lowered 0.0157 h (10 kcal) relative to the HF description. The C-C bond

orbitals (orbitals ϕ_{1a} and ϕ_{1b} in Fig. 3) have a smaller energy lowering (0.0139 h or 9 kcal) and a higher overlap than the C-H bond orbitals (0.835 vs 0.826) but dissociate continuously into the p-orbitals of two methyl radicals as the groups are pulled apart.

We find that GVB leads to a rotational barrier of 3.1 kcal (with the staggered configuration lower) in good agreement with the HF results (3.3 kcpm) and with experiment (2.9 kcpm). This constrast with the barrier of -5.1 kcal (eclipsed from lower) found by Klessinger using partially optimized orbitals.

VI. THE OXYGEN MOLECULE

The failure to predict a triplet ground state for the O_2 molecule was one of the major difficulties of valence bond theory.[37] It is therefore of interest to examine O_2 in the GVB description, which is a synthesis of the MO and VB methods. The wavefunction for the $^3\Sigma_g^-$ state is

$$\psi_{GVB} = \mathcal{A}\{[\delta_A, \delta_B][\pi_{xu}^2][\pi_{yu}^2][\pi_{xg}\pi_{yg}\chi\}$$

(where the 1 and 2 orbitals have been taken to be doubly occupied and are not shown). Little improvement in energy (0.001 h) is obtained by allowing the π_u orbitals to split or to become asymmetric. Thus ψ_{GVB} differs from ψ_{HF} by the presence of two sigma orbitals [σ_A, σ_B] that are related to the $3\sigma_g$ and $3\sigma_u$ natural orbitals.

From Table V we see that the HF and GVB results both predict the correct qualitative relation of the $^3\Sigma_g^-$, $^1\Delta_g$, and $^1\Sigma_g^+$ states.[38] In using the GVB natural orbitals as a basis set for a small configuration interaction (CI) calculation effectively relaxes both

the strong orthogonality and the spin-coupling restrictions as well as including the correlation terms involving only valence-like orbitals (internal correlation). The importance of these terms has been emphasized in the theory of Silverstone and Sinanoglu[40] and by the first-order wavefunction calculations of Schaefer.[41]

The calculated dissociation energy from the GVB-CI calculation is in much better agreement with the experimental results and with the more extensive calculation by Schaefer.[41a] Calculations on other states using the natural orbitals from the ground state GVB wavefunction are also reported in Table V, where the results are in general agreement with experiment.[42]

VII. GENERAL CHARACTERISTICS OF THE GVB APPROACH TO MOLECULES

The previous discussions of H_2O, C_2H_6, and O_2 illustrated some specific aspects of the GVB method; in this section we will summarize some of the results obtained for other molecules. These will be discussed more fully in future publications.

The basis sets used are MBS (minimum basis set; Pople's STO-4G basis with standard molecular exponents)[43] and POL (the [4s2p] DZ set[35] augumented by one set of d-type uncontracted Gaussian functions on each of the B, C, N, O, and F atoms).

In Table VI we see that the two orbitals making up a sigma bond have high overlap: for C-H bonds it is 0.82-0.87 and for sigma bonds involving two first-row atoms, 0.85-0.93. Thus, at ————————|

the equilibrium distance, HF should yield a relatively good description since the energy gain in the GVB method is only 0.005-0.015 a.u. for each bond. However, pi bonds are not so well described by HF, as the GVB overlap is only 0.57-0.73 and the increase in bond energy in GVB is 0.03-0.045 a.u. (0.8-1.2 eV). Thus π bonds are much closer to the dissociated bond limit than is the case for sigma bonds.

The most drastic improvement can be noted in cases where there are two molecular orbitals--one occupied and one virtual--which are nearly degenerate. Such situations arise in biradicals such as singlet CH_2, the trimethylene biradical,[44] benzenes,[45] the C_2 molecule and cases where a bond is broken. In the last case, thw two nonbonding electrons are especially poorly described by a single $2\sigma_u$ orbital as in HF [The GVB orbitals have small overlap (0.33) and the pair splitting energy is 63 kcal]. This leads to a dissociation energy for C_2 of -22.1 kcal/mole in HF as compared with 72.7 for GVB and the experimental value of 144.

We conclude that the wavefunction leads to useful wavefunctions and remove many difficulties and inconsistencies of the Hartree-Fock method.

REFERENCES

1. One can transform the Hartree-Fock orbitals to a localized form, but the invariance of the energy under such transformations prevents a unique localization scheme.
2. R. B. Woodward and R. Hoffmann, The Conservation of Orbital Symmetry (Academic Press, New York, 1970).
3. A. D. Walsh, J. Chem. Soc., 1953, 2260.
4a. R.C. Ladner and W.A. Goddard III, J. Chem. Phys., 51, 1073 (1969).
4b. U. Kaldor and F. E. Harris, Phys. Rev., 183, 1 (1969).
4c. S. Hameed, S. S. Hui, J. I. Musher, and J. M. Schulman, J. Chem. Phys., 51, 502 (1969).
5. (a) R. J. Blint, W. A. Goddard III, R. C. Ladner, and W. E. Palke, Chem. Phys. Letters 5, 302 (1970); (b) R. J. Blint and W. A. Goddard III, J. Chem. Phys. 55, 0000 (1971); (c) W. A. Goddard III and R. C. Ladner, J.Amer.Chem.Soc., 93, 000 (1971).
6. A. C. Hurley, J. E. Lennard-Jones, and J. A. Pople, Proc. Roy. Soc. (London) A220, 446 (1953).
7. W. Kutzelnigg, J. Chem. Phys. 40, 3640 (1964).
8. W. A. Goddard III, Phys. Rev. 157, 73, 81 (1967).
9. (a) L. Pauling, J. Am. Chem. Soc. 53, 1367 (1931); L. Pauling, Proc. Natl. Acad. Sci. U.S. 14, 359 (1928); (b) J. C. Slater, Phys. Rev. 37, 481 (1931); ibid. 38, 1109 (1931).
10. T. Arai, J. Chem. Phys. 33, 95 (1960); P. O. Löwdin, ibid. 35, 78 (1961).
11. J. M. Parks and R. G. Parr, J. Chem. Phys. 28, 335 (1958); ibid. 32, 1567 (1960).
12. D. M. Silver, E. L. Mehler, and K. Ruedenberg, J. Chem. Phys. 52, 1174, 1181, 1206 (1970).
13. (a) P. O. Löwdin, Phys. Rev. 97, 1474 (1955); (b) P. O. Löwdin

and H. Shull, Phys. Rev. 101, 1730 (1956); (c) W. Kutzelnigg, Theoret. Chim. Acta 1, 327 (1963); (d) H. Shull, J. Chem. Phys. 30, 1405 (1959).

14. In Eq. (6) ϕ_{ia}, ϕ_{ib}, ϕ_{1i}, and ϕ_{2i} are all normalized so that $C_{1i}^2 + C_{2i}^2 = 1$.

15. (a) W. J. Hunt, T. H. Dunning Jr., and W. A. Goddard III, Chem. Phys. Letters 3, 606 (1969); (b) W. A. Goddard III, T. H. Dunning Jr., and W. J. Hunt, ibid. 4, 231 (1969); (c) W. J. Hunt, W. A. Goddard III, and T. H. Dunning Jr., ibid. 6, 147 (1970).

16. A. C. Wahl and G. Das, Advan. Quant. Chem. 5, 261 (1971).

17. E. Clementi and A. Veillard, J. Chem. Phys. 44, 3050 (1966).

18. J. Hinze and C.C. J. Roothaan, Progr. Theoret. Phys. (Kyoto) Suppl. 40, 37 (1967).

19. R. McWeeny, Trans. Faraday Soc. 2, 7 (1968).

20. E. Scarzafava, Ph.D. thesis, Indiana University, 1969.

21. P. F. Franchini, R. Moccia, and M. Zandomeneghi, Int. J. Quant. Chem. 4, 487 (1970).

22. (a) M. Klessinger, J. Chem. Phys. 43, S117 (1965); (b) ibid. 53, 225 (1970); (c) idem, Sym. Faraday Soc. 2, 73 (1968).

23. R. Ahrlichs and W. Kutzelnigg, J. Chem. Phys. 48, 1819 (1968).

24. R. McWeeny and K. A. Ohno, Proc. Roy. Soc. (London) A255, 367 (1960).

25. M. Klessinger and R. McWeeny, J. Chem. Phys. 42, 3343 (1965).

26. J. F. Harrison and L. C. Allen, J. Am. Chem. Soc. 91, 807 (1969).

27. V. A. Nicely and J. F. Harrison, J. Chem. Phys. 54, 4363 (1971).

28. D. M. Silver, J. Chem. Phys. 50, 5108 (1969).

29. H. S. Taylor and F. E. Harris, Mol. Phys. 6, 183 (1963).

30. J. Miller, R. H. Friedman, R. P. Hurst, and F. A. Matsen, J. Chem. Phys. 27, 1385 (1957).

31. D. J. Klein, J. Chem. Phys. 50, 5152 (1969).

32. B. K. Gupta and F. A. Matsen, J. Chem. Phys. 50, 3797 (1969).

33. C. Melius and W. A. Goddard III, J. Chem. Phys. 55, 0000 (1971).

34. R. J. Blint and W. A. Goddard III, to be published.

35. A (9s5p2d) and (4s) primitive set was contracted to a [4s, 3p, 1d] and [2s] set on the oxygen and hydrogens, respectively. (a) S. Huzinaga, J. Chem. Phys. 42, 1293 (1965); (b) T. H. Dunning, J. Chem. Phys. 53, 2823 (1970).

36. M. Levy, W. J. Stevens, H. Shull, and S. Hagstrom, J. Chem. Phys. 52, 5483 (1970).

37. See J. C. Slater, Quantum Theory of Molecules and Solids (McGraw-Hill Book Co., Inc., New York, 1963), Vol. 1, p. 121.

38. The [4s3p] contracted Gaussian basis described by Huzinaga and Dunning (Ref. 35) was used, augmented by d-type polarization functions on each center (z^2, xz, and yz only). The experimental value[39] of R_e = 1.209 Å was used.

39. G. Herzberg, Spectra of Diatomic Molecules (D. Van Nostrand-Reinhold Co., New York, 1950).

40. H. J. Silverstone and O. Sinanoglu, J. Chem. Phys. 46, 854 (1967).

41. (a) H. F. Schaefer III, J. Chem. Phys. 54, 2207 (1971); ibid. 55, 176 (1971).

42. S. Trajmar, W. Williams, and A. Kuppermann, J. Chem. Phys., in press.

43. W. J. Hehre, R. F. Stewart, and J. A. Pople, J. Chem. Phys. 51, 2657 (1969).

44. P. J. Hay, W. A. Goddard III, and W. J. Hunt, J. Amer. Chem. Soc., to be published.

45. R. Hoffmann, A. Imamura and W. J. Hehre, J. Amer. Chem. Soc., 90, 1498 (1968); D. L. Wilhite and J. L. Whitten, J. Amer. Chem. Soc., 93, 2858 (1971).

46. The results here were obtained in the STO-4G basis used for C_2H_6 (see Ref. 43).

47. J. Hinze, private communication.

48. W. White, T. H. Dunning Jr., R. M. Pitzer and W. Matthews, to be published.

49. F. Bobrowicz and W. A. Goddard III, to be published.

TABLE I. Comparison of HF GVB and SOGI calculations on ground states of LiH (R = 3.015 a_0) and BH (R = 2.336 a_0).

	Energy (Hartree)		D_e (eV)	Energy Lowering	
	R = R_e	R = ∞		Pair	$\Delta\varepsilon_i$ (Hartree)
LiH					
HF[a]	-7.98326	-7.93123	1.42	—	—
GVB[f]					
1-pair	-8.00054	-7.93123	1.89	bond	-0.01728
2-pair	-8.01289	-7.94336	1.89	bond	-0.01710
				core	-0.01249
SOGI[bf]	-8.01369	-7.94435	1.89	—	—
Exp[c]			2.52		
BH					
HF[a]	-25.12820	-25.01790	2.73	—	—
GVB[g]					
2-pair	-25.16542	-25.04735	3.21	bond	-0.01443
				lone	-0.02279
3-pair	-25.17769	-25.0599	3.21	bond	-0.01436
				lone	-0.02276
				core	-0.01236
SOGI[dg]	-25.18014	-25.06119	3.24	—	—
Exp[e]			3.56		

TABLE I. Continued

[a] Cade and Huo [J. Chem. Phys. 47, 614 (1967)] using a more extensive basis obtain E = -7.9873 and D_e = 1.49 for LiH and E = -25.13137 and D_e = 2.77 for BH.

[b] Palke and Goddard [J. Chem. Phys. 50, 4524(1969), using a more extensive basis obtain E = -8.0173 and D_e = 1.90.

[c] G. Herzberg, Spectra of Diatomic Molecules, (D. VanNostrand Co., Princeton, N.J., 1950); R. Velasco, Can. J. Phys. 35, 1204 (1957).

[d] Blint and Goddard (Ref. 5b).

[e] P. G. Wilkinson, Astrophys. J. 138, 614 (1967).

[f] Using a double zeta plus polarization (DZP) basis.

[g] Using the DZP basis from Ref. 5b.

[h] The energy lowering due to splitting the one pair.

TABLE II. Comparison of GVB and SOGI calculations for (a) the transition state of the $H_2 + D \rightleftharpoons H + HD$ reaction at $R_{12} = R_{23} = 1.8\ a_0$ and (b) the $^3\Pi$ and $^1\Pi$ states of BH.

	Energy (Hartree)		Barrier height (kcal/mole)
	$R_{12} = R_{23} = 1.8\ a_0$	$H_2 + D$	
HF	-1.5930	-1.6335	25
GVB			
$r\ell u^b$	-1.5936	-1.6517	36
$gg' u^b$	-1.6035	-1.6517	30
GVB-CI (3 BF)[c]	-1.6178	-1.6517	21
SOGI[d]	-1.6240	-1.6517	17
CI[e]	-1.6521	-1.6696	11

	Energy (Hartree)	
	$R = 2.25\ a_0$	$R = 4.0\ a_0$
BH $^3\Pi$		
HF	-25.11333	-25.01847
GVB	-25.12413	-25.03240
GVB-CI (4 BF)	-25.12800	-25.03742
SOGI[f]	-25.12874	-25.04170
BH $^1\Pi$		
HF	-25.03375	-25.02459
GVB	-25.04307	-25.03987
GVB-CI (4 BF)	-25.05400	-25.04964
SOGI[f]	-25.06285	-25.05242

TABLE II. Continued

[a] Energy of saddle point ($R_{12} = R_{23} = 1.8\ a_0$) relative to H + HD.

[b] $r\ell u$ and $gg'u$ refer to the two possible orbital configurations; see text for further discussion.

[c] Complete CI using the GVB orthogonal orbitals.

[d] Ladner and Goddard (Ref. 4a).

[e] I. Shavitt, R. M. Stevens, F. L. Minn and M. Karplus, J. Chem. Phys. 48, 2700 (1968).

[f] Blint and Goddard (Ref. 34).

TABLE III. Calculations on the ground state of the water molecule[a]

Method	Energy	Pair Information: Pair	Pair Information: $\Delta\Sigma$ Energy, Lowering
This work			
HF	-76.0377	—	—
GVB 4 pairs ($\sigma\pi$)	-76.0988	bond(2)	-0.0207
		lone-σ	-0.0086
		lone-π	-0.0118
GVB 4 pairs (lobes)	-76.1019	bond(2)	-0.0209
		lone(2)	-0.0115
GVB 5 pairs (lobes)	-76.1118	bond(2)	-0.0209
		lone(2)	-0.0114
		core(1)	-0.0100
Scarzafava (Ref. 20)			
HF	-76.038		
Separated pair (uv form) - 5 pairs	-76.1100		
Klessinger (Ref. 22c)			
HF	-75.6807		
Group function - 2 pairs	-75.7139		
Franchini, et al. (Ref. 21)			
HF	-76.0374		
Group function - 4 pairs	-76.0997		

TABLE III. Continued

Method	Energy	Pair Information: Pair	Pair Information: $\Delta\Sigma$
Other calculations			
HF[b]	-76.059		
HF[e]	-76.0630		
CI[c]	-76.1422		
CI[d]	-76.2205		

[a] The geometry is that used by Dunning (Ref. 35b).

[b] D. Neuman and J. W. Moskowitz, J. Chem. Phys. 49, 2056 (1968).

[c] R. P. Hosteny, R. R. Gilman, T. H. Dunning, A. Pipano and I. Shavitt, Chem. Phys. Letters 7, 325 (1970).

[d] C. Bender and H. F. Schaeffer, to be published.

[e] T. H. Dunning and R. N. Pitzer, to be published.

TABLE IV. Comparison of calculations on the ethane molecule.

	Energy (Hartree)		Barrier (kcal/mole)	Pair Information				
					Energy Lowering		Orbital Overlap	
	Staggered	Eclipsed		Pair	Staggered	Eclipsed	Staggered	Eclipsed
This work								
HF	-78.8608	-78.8555	+3.3					
GVB	-78.9691	-78.9641	+3.1	CC bond	-0.0139	-0.0139	0.835	0.836
				CH bond	-0.0157	-0.0158	0.826	0.826
Klessinger[b]								
HF	-78.9562	-78.9510	+3.3					
SCGF	-78.9641	-79.0188	-5.1					
Exper[c]			2.93					

[a] The geometry used was taken to be that used by R. M. Pitzer and W. N Lipscomb, J. Chem. Phys., 39, 1995 (1963).

[b] Ref. 22b.

[c] S. Weiss and G. Leroi, J. Chem. Phys., 48, 962 (1968).

TABLE V. Oxygen Molecule ($R = 2.282\ a_0$)

	$^3\Sigma_g^-$ state	
	E	D_e
HF	-149.6331	0.95
GVB (one pair)	-149.6595	1.68
GVB-CI	-149.7315	3.64
CI[a]	-149.7944	4.72
Exp[b]	—	5.21

State	Excitation Energies			
	HF	GVB	GVB-CI	Exp
$^3\Sigma_g^-$	—	—	—	—
$^1\Delta_g$	1.43	1.28	0.91	0.98
$^1\Sigma_g^+$	2.37	2.23	1.69	1.63
$^1\Sigma_u^-$	—	—	5.91	6.1[c]
$^3\Delta_u$	—	—	6.16	6.1[c]
$^3\Sigma_u^+$	—	—	6.31	6.1[c]

[a] H. F. Schaeffer III,

[b] Reference 39.

[c] Broad unresolved feature, Reference 42.

TABLE VI. Characteristics of GVB electron pairs in bonds

Pair Type	System-State	Basis	Pair Information		
			Pair	Overlap	Energy Lowering Relative to HF (Hartrees)
Sigma bond	CH $^2\Pi$	POL		0.8264	0.0173
	CH $^4\Sigma^-$	POL		0.8640	0.0104
	CH_4	POL		0.8342	0.0153
	C_2H_2 $^1\Sigma_g^+$	MBS	CH	0.8413	0.0138
			CC	0.9289	0.0045
	C_2H_4 $^1A_{1g}$	MBS	CH	0.8388	0.0142
			CC	0.8930	0.0078
	C_2H_6 $^1A_1$	MBS	CH	0.8259	0.0157
			CC	0.8354	0.0139
	BeO $^1\Sigma^+$	MBS		0.8618	0.0085
	BeO $^3\Pi$	MBS		0.9117	0.0046
	H_2O $^1A_1$	POL	OH	0.8247	0.0209
Pi bond	C_2H_2 $^1\Sigma_g^+$	MBS		0.6639	0.0329
	C_2H_4 $^1A_{1g}$	MBS		0.5782	0.0462
	CO $^1\Sigma^+$	MBS		0.7366	0.0308
	BeO $^1\Sigma^+$	MBS		0.6662	0.0313
Lone Pair	H_2O $^1A_1$	POL		0.8830	0.0115
	CH_2 $^1A_1$	POL		0.6827	0.0214
	C_2 $^1\Sigma_g^+$	MBS		0.3313	0.1013

FIGURE CAPTIONS

FIG. 1. Comparison of the SOGI and GVB orbitals for BH ($^1\Sigma^+$). ϕ_{2a} is one of the two symmetrically related nonbonding orbitals. ϕ_{3a} and ϕ_{3b} are the bonding orbitals.

FIG. 2. The GVB orbitals for the H_2O molecule. ϕ_{2a} and ϕ_{2b} represent the orbitals of one of the two equivalent lone pairs. ϕ_{4a} and ϕ_{4b} represent the orbitals of one of the two equivalent OH bonds.

FIG. 3. The GVB orbitals for the CC bond (ϕ_{1a} and ϕ_{1b}) and a CH bond (ϕ_{2a} and ϕ_{2b}) in ethane.

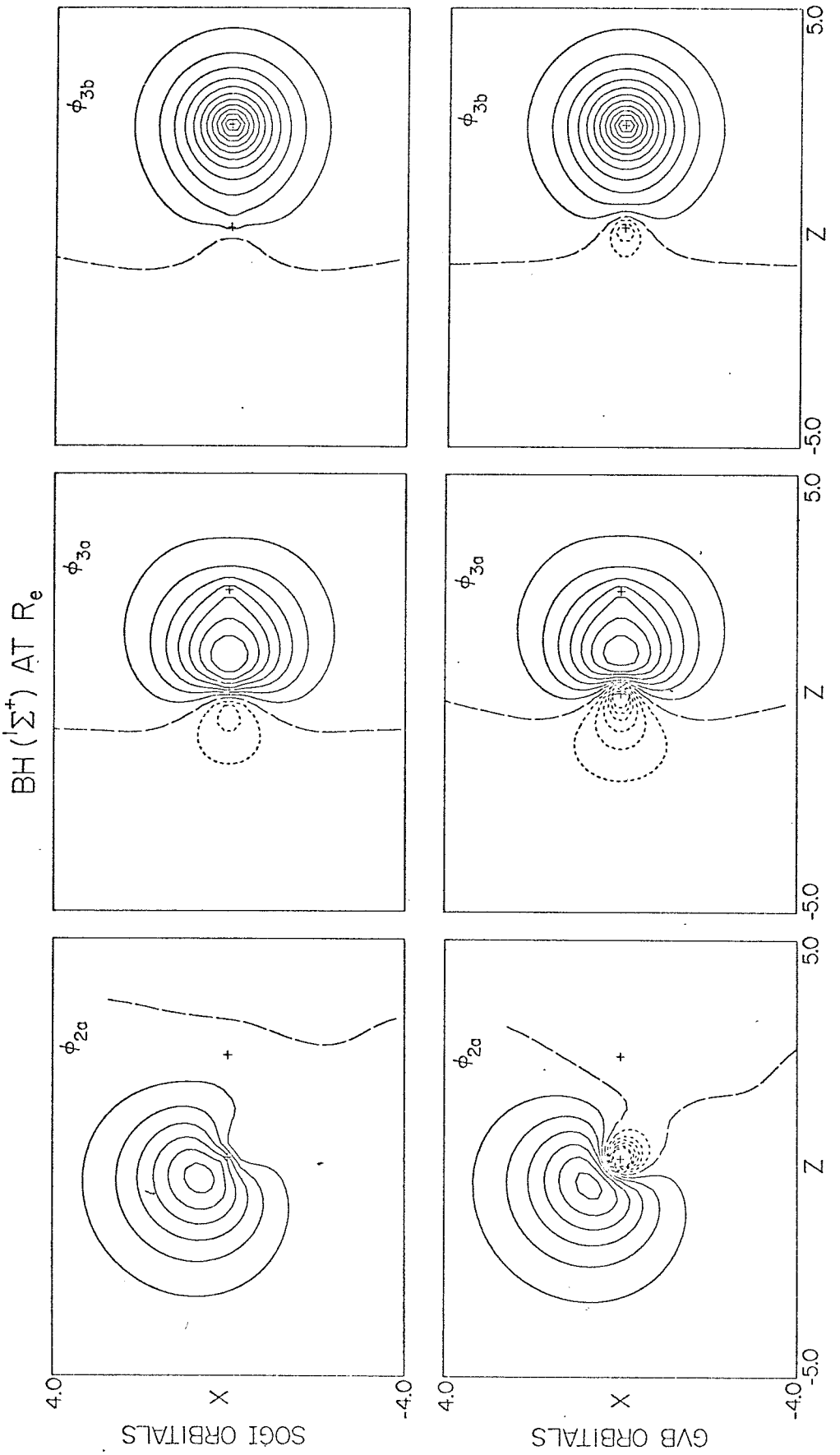
BH ($^1\Sigma^+$) AT R_e
SOGI ORBITALS
GVB ORBITALS
ϕ_{3b}
ϕ_{3a}
ϕ_{2a}
4.0
-4.0
5.0
-5.0
X
Z

FIG. 1

WATER MOLECULE

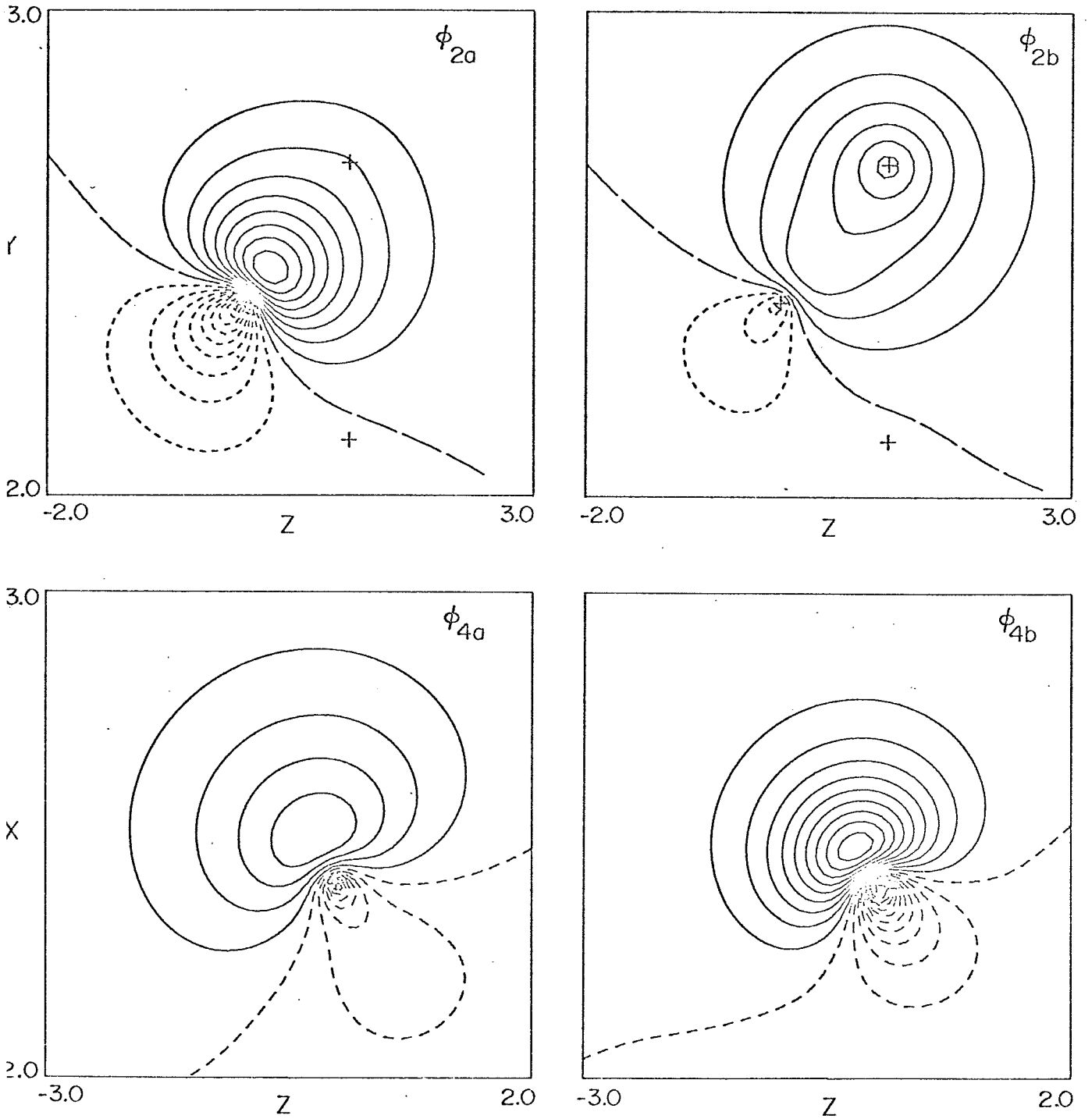

FIG. 2

ETHANE (STAGGERED)

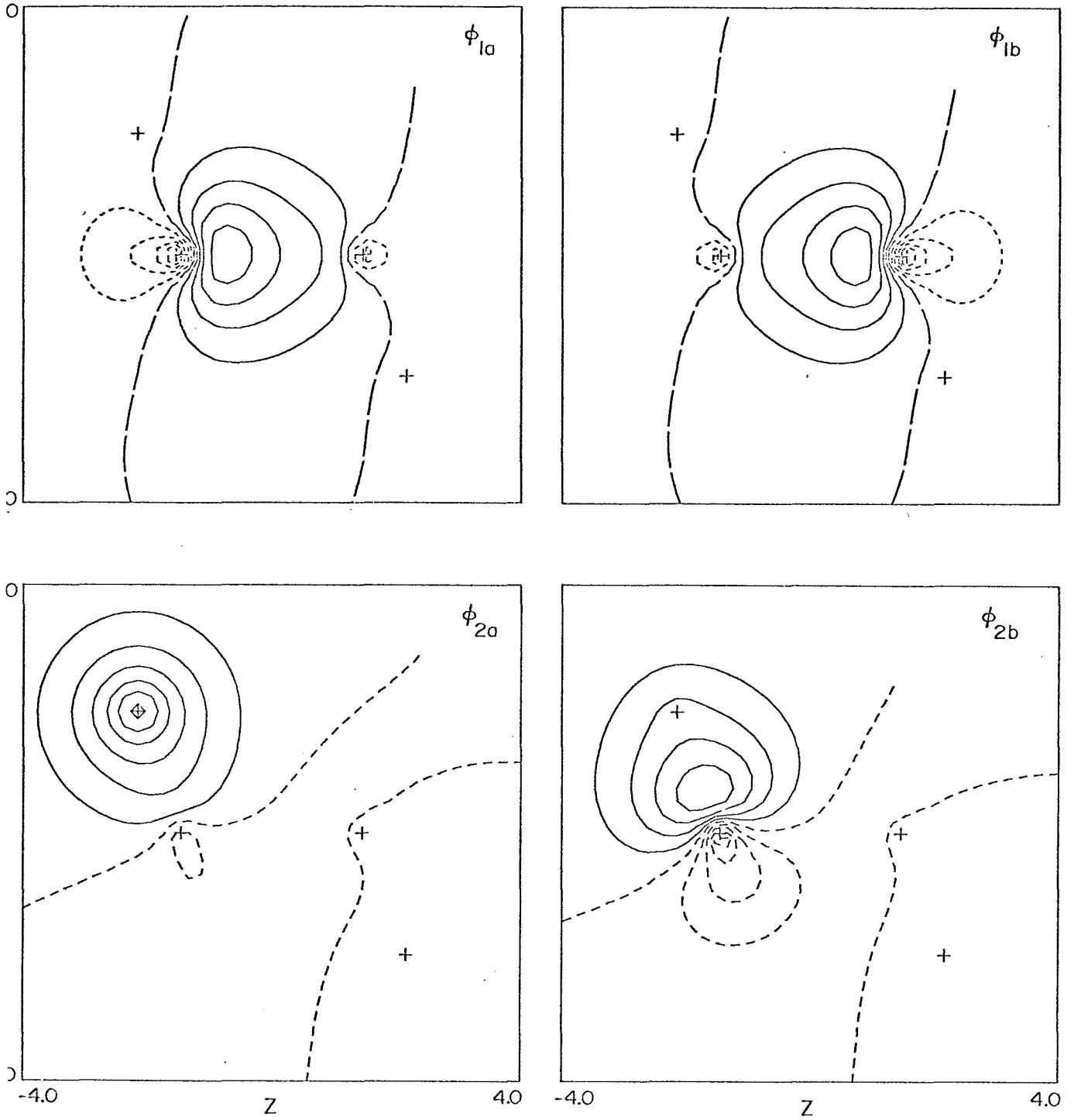

FIG. 3

II. AN ORBITAL INTERPRETATION OF SUPEREXCHANGE IN ANTIFERROMAGNETIC INSULATORS

INTRODUCTION

The study of magnetic properties of transition metal compounds has been of enormous value in understanding their electronic structure. Although many compounds exhibit "normal" paramagnetic behavior over a certain range of temperatures, antiferromagnetic materials become ordered at low temperatures with an S = 0 singlet ground state. The "superexchange" interaction refers to the weak coupling, usually no more than several hundred wavenumbers in magnitude, responsible for antiferromagnetism. There continues to be experimental and theoretical interest in the nature of this phenomenon, the most recent theoretical treatment having been given in the "kinetic exchange" model of Anderson[1] in 1963. In this investigation we have developed an easily interpretable model for superexchange on the basis of overlapping orbitals which is nearly equivalent to the Anderson model. In sections II and III the theory is developed for both models. In Section IV this model is tested on the linear Ni^{++} - F^{-} - Ni^{++} cluster occuring in antiferromatnetic $KNiF_3$.

Our calculations are ab-initio in nature, as contrasted with several recent semi-empirical estimates of exchange parameters.[2-4] Applications to other systems are discussed in section V.

THE "HEISENBERG" HAMILTONIAN

The interaction between two atoms each with spin S has often been represented in the form

$$H = -2J_{AB}\ \vec{S}_A \cdot \vec{S}_B \qquad (2\text{-}1)$$

Although first used by Heisenberg for two electrons,[5] the hamiltonian (2-1) was applied to many-electron systems by Dirac[6] and was also treated by Van Vleck.[7] Considering only the unpaired electrons on each atom we write the wavefunctions for each atom as

$$\psi_A = A\ a_1\alpha a_2\alpha \cdots a_n\alpha = A\ \Phi_A\ |S,\ S>_A \qquad (2\text{-}2)$$

$$\psi_B = A\ b_1\beta b_2\beta \cdots b_n\beta = A\ \Phi_B\ |S,-S>_B \qquad (2\text{-}3)$$

where $|S,\ S>$ and $|S,-S>$ represent the spin functions $|S,M_S>$ with spin S and spin projection M_S. Φ_A and Φ_B represent the spatial orbital product and S will be taken to be n/2. Since the two systems of spin S can be coupled into states with total spin S^1 ranging from 2S to 0, the many-electron function with spin S^1 can be written

$$\psi_{S^1} = A\ \Phi_A\ \Phi_B\ \chi_{S^1}$$

where

$$\chi_{S^1} = \sum_{M=-S}^{S} |S,\ M>_A\ |S_1\text{-}M>_B\ <SM\ S\text{-}M|S^1\ 0> \qquad (2\text{-}4)$$

$<SMS - S|S^1 0>$ are the vector coupling coefficients which produces the many-electron state of spin S^1. The energy expression then becomes

$$E(S^1) = \frac{< A\Phi_A \Phi_B \chi_{S^1} |H| A\Phi_A \Phi_B \chi_{S^1}>}{< A\Phi_A \Phi_B \chi_{S^1} | A\Phi_A \Phi_B \chi_{S^1} >} \qquad (2\text{-}5)$$

Alternatively, (2-4) can be written[8,9]

$$\psi_{S^1} = A\ \Phi_A \Phi_B [\omega_{ii}^{S^1}\ \chi_A\ \chi_B]$$
$$A[O_{ii}^{S^1}\ \Phi_A \Phi_B]\ \chi_A\ \chi_B \qquad (2\text{-}6)$$

where

$$\chi_A = \alpha\alpha\cdots\alpha$$

$$\chi_B = \beta\beta\cdots\beta$$

and $\omega_{ii}^{S^1}$ and $O_{ii}^{S^1}$ are spin and spatial projection operators, respectively, which insure that the many electron determinant function $\phi_A\phi_B$ $\chi_A\chi_B$ has total spin S^1. For example

$$O_{ii}^{S^1} = \sum_{\tau} U_{\tau}^{S^1}\ \hat{\tau} \qquad (2\text{-}7)$$

where τ are permutations of the 2n spatial orbitals and U_τ are numerical coefficients which depend on S^1.

Using (6) the energy can be written

$$E(S^1) = \frac{\langle \Phi_A\Phi_B | H | O_{ii}^{S^1} \Phi_A\Phi_B \rangle}{\langle \Phi_A\Phi_B | O_{ii}^{S^1} \Phi_A\Phi_B \rangle} = \frac{N}{D} \qquad (2\text{-}8)$$

For the case of one unpaired electron on each atom, we have the following:

$$S = 1: \; O_{11} = e - (12)$$

$$S = 0: \; O_{11} = e + (12)$$

and

$$E = \frac{\langle ab \,|H|\, ab \pm ba \rangle}{\langle ab \,|ab \pm ba \rangle}$$

where the + and - sign are associated with spin 0 and 1, respectively. If instead of using all (2n)! permutations in O_{ii}, one limits the sum in (8) to transpositions (ij); the projection operator becomes

$$O_{ii}^{S^1} \approx e + \sum_{\substack{i,j \\ i<j}} U_{ij}^{S^1} \; (ij) \qquad (2\text{-}9)$$

where (ij) permutes orbitals i and j.

The numerator in (8) then becomes

$$N = E_A + E_B + \sum_{i=1}^{n} \sum_{j=n+1}^{2n} U_{ij} \langle \Phi_A(1, \cdots, N) \, \Phi_B(N+1, \cdots 2N)$$

$$|H| \; (ij) \; \Phi_A \; (1, \cdots, N) \; \Phi_B \; (N+1, \cdots, 2N \rangle \qquad (2\text{-}10)$$

where all permutations among the orbitals of atom A have been included in the term E_A; and all permutations involving only orbitals of B, into E_B. The remaining term contains only permutations involving a transposition of orbitals between centers A and B. Similarly the denominator becomes

$$D = 1 + \sum_{i=1}^{n} \sum_{j=n+1}^{2n} U_{ij} < \Phi_A \Phi_B \,|\, (ij)\, \Phi_A \Phi_B > \qquad (2\text{-}11)$$

Writing N_{ij} and D_{ij} for the matrix elements accompanying U_{ij} we obtain

$$E(S^1) = \frac{E_A + E_B + \sum_{ij} U_{ij} N_{ij}}{1 + \sum_{ij} U_{ij} D_{ij}} \qquad (2\text{-}12)$$

$$\approx E_A + E_B + \sum_{ij} U_{ij} [N_{ij} - D_{ij}(E_A + E_B)]$$

$$= E_A + E_B + \sum_{ij} U_{ij} H_{ij}$$

where we have expanded the denominator and kept only terms of order U_{ij}.

Lowdin[10] has shown that for wavefunctions of the form (2) and (3)

$$U_{ij} = \frac{n - S^1(S^1 + 1)}{n^2} \qquad (2\text{-}13)$$

where n is the number of electrons on each atom. We note that

(a) U_{ij} is the same for all interatomic transpositions (ij) and

(b) U_{ij} depends only on the total spin state S^1.

This leads to the expression for the difference in energy between two spin states $S^1 = S_1$ and $S^1 = S_2$ as

$$E(S_2) - E(S_1) = - \frac{1}{n^2} [S_2(S_2 + 1) - S_1 (S_1 + 1)] \sum_{ij} H_{ij} \quad (2\text{-}14)$$

From the Heisenberg Hamiltonian (1) and using

$$\vec{S} = \vec{S}_A + \vec{S}_B$$

squaring both sides yields

$$S^1(S^1 + 1) = S (S + 1) + S(S + 1) + 2\vec{S}_A \cdot \vec{S}_B \quad (2\text{-}15)$$

$$E(S_2) - E(S_1) = - J_{AB} [S_2(S_2 + 1) - S_1(S_1 + 1)] \quad (2\text{-}16)$$

Equating (2-14) and (2-16) yields the quantum mechanical expression for the exchange parameter J_{AB}

$$J_{AB} = \frac{1}{n^2} \sum_{i,j} H_{ij} \quad (2\text{-}17)$$

The Heisenberg Hamiltonian is usually interpreted as requiring orthogonal orbitals. The above presentation shows that (2-1) is actually a result of retaining only inter-atomic transpositions in the energy

expression. For the case where all orbitals a_i are orthogonal to orbitals b_i then

$$D_{ij} = O$$

$$N_{ij} = \langle \phi_i(1)\, \phi_j(2) \mid \frac{1}{r_{12}} \mid \phi_i(2)\phi_j(1) \rangle$$

i.e., the H_{ij} in (17) are two-electron exchange integrals. As we shall see later, allowing non-orthogonal orbitals is crucial in our model for superexchange.

THEORIES OF SUPEREXCHANGE

In this section we will summarize the Anderson model of superexchange and discuss how the orbital model we propose is related to his model.

A. The Anderson Model

For the case of an antiferromagnetic solid consisting of 2N ions each with spin S let us imagine we have carried out the following calculations:

(a) Solve for the energy band solutions of the ferromagnetic (i.e., maximum spin) state. For ions each having n unpaired electrons the wavefunction has the form

$$\psi_F = A\,\Phi_1\chi_1\cdots\Phi_{2N}\chi_{2N} \qquad (3\text{-}1)$$

where for the I^{th} transition metal ion

$$\Phi_I = \phi_i^I\cdots\phi_n^I$$

$$\chi_I = \alpha\cdots\alpha$$

Here the one-electron orbitals ϕ_i^I will be symmetry functions transforming according to the full group of the lattice.

(b) Since ψ_F (and hence the energy) is invariant under unitary transformations of the orbitals we may perform a Wannier-like transformation to obtain orthogonal localized functions ϕ_j^I associated with site I (j = 1, $\cdots$, n).

(c) Using these ϕ_j^I in the Heisenberg Hamiltonian, we evaluate the exchange parameter between sites A and B. As shown in (2-17) and (2-18)

$$J_{AB} = \frac{1}{n^2} \sum_i \sum_j \langle \phi_i^A \phi_j^B | \phi_j^B \phi_i^A \rangle$$

which implies $J_{AB} > 0$ since exchange integrals $\langle ij \mid ji \rangle$ are positive. The effect of these terms, which lead to ferromagnetic coupling between pairs, is called potential exchange. It is this effect which gives rise to Hunds' rule in atoms and molecules, which states that of those configurations arising from the same set of orthogonal orbitals, the state of highest spin will have the lowest energy. (e.g., in He $(1s)^1 (2s)^1, {}^3S < {}^1S$ and in O_2 $(1\pi_{gx})^1 (1\pi_{gy})^1$ ${}^3\Sigma_g^- < {}^1\Delta_g$).

(d) Using these localized orthogonal orbitals ϕ_j^I as a basis, we introduce ionic configurations $\psi_{i \to j}$ corresponding to excitations from orbital i on center A to occupied orbital j on center β and vice versa:

$$\psi_{AF} = \psi_F + \sum_{i,j} C_{ij} [\psi_{i \to j} + \psi_{j \to i}] \qquad (3\text{-}2)$$

Using perturbation theory one obtains

$$E_{AF} = E_F - \frac{2 \langle \psi_F | H | \psi_{i \to j} \rangle^2}{\Delta E} = E_F - \frac{2 b_{ij}^2}{\Delta E} \qquad (3\text{-}3)$$

where

$$b_{ij} = \langle \psi_F | H | \psi_{i\to j} \rangle = \langle jj | ij \rangle + \langle j | h | i \rangle$$

$$\Delta E = [E(A^+) + E(B^-)] - E_F$$

Since configurations involving doubly occupied orbitals as in the ionic states $\psi_{i\to j}$ must necessarily have lower total spin than the fluoromagnetic state, these effects, referred to as kinetic exchange, will not contribute to the ferromagnetic state but will stabilize the antiferromagnetic state. In considering only potential exchange the exchange parameter J_{AB} was positive, but with kinetic exchange there are both positive and negative contributions to J_{AB}. If kinetic exchange dominates, J_{AB} will be negative.

$$J_{AB} = \frac{1}{n^2} \sum_{ij} \left[\langle ij | ji \rangle - \frac{b_{ij}^2}{\Delta E} \right] \qquad (3\text{-}4)$$

and according to (2-1) the ground state will be antiferromagnetic.

B. An Orbital Interpretation

An alternative interpretation of superexchange(also mentioned by Anderson within the unrestricted Hartree-Fock (UHF) framework) is to repeat the previous steps (a), (b), and (c) but argue as follows:

(d) Rather than requiring the orbitals ϕ_i^A and ϕ_j^B to be orthogonal localized functions, we allow the orbitals to be non-orthogonal. In UHF one would take $\psi_{AF} = \psi_{UHF} = A\,\phi_{1A}\alpha \cdots \phi_{nA}\alpha\ \phi_{1B}\beta \cdots \phi_{nB}\beta$ where the orbitals ϕ_{1A} need no longer be orthogonal to ϕ_{jB}.

In our approach we take

$$\psi_{AF} = \psi_{SOGI} = A\,\phi_{1A}\cdots\phi_{nA}\,\phi_{1B}\cdots\phi_{nB}\,\chi_{S^1}$$

where χ_{S^1} was defined in (4) so that ψ_{SOGI} has definite total spin S^1. Similarly in this case $<\phi_{iA}|\phi_{jB}>$ need not be zero, so that in (2-17) one obtains negative (i.e., AF) contributions to J_{AB}. It is this non-orthogonality between orbitals of different centers that is responsible for superexchange.

C. The Hydrogen Molecule as an Illustration

The interaction of two hydrogen 1s electrons gives rise to an energy splitting between the two $^1\Sigma_g^+$ and $^3\Sigma_u^+$ many-electron states with the ordering $^1\Sigma_g^+ < {}^3\Sigma_u^+$.

In the Anderson model the relative ordering of the "AF" singlet and "F" triplet states would be explained as follows: for the triplet the wavefunction is

$$\psi_F = A\,\phi_g\,\phi_u\,\alpha\alpha \qquad (3\text{-}5)$$

where ϕ_g and ϕ_n are orthogonal orbitals with the σ_g and σ_u symmetry, respectively, of the $D_{\infty h}$ point group. The energy is unchanged if we write

$$\psi_F = A\,\phi_a^{\circ}\,\phi_b^{\circ}\,\alpha\alpha \qquad (3\text{-}6)$$

where

$$\phi_a^{\circ} = \frac{1}{\sqrt{2}}\,(\phi_g + \phi_u)$$

$$\phi_b^\circ = \frac{1}{\sqrt{2}} (\phi_g - \phi_u)$$

ϕ_A° and ϕ_B° correspond to Wannier functions in that they are localized on the left and right hydrogens, respectively, but are still orthogonal. The energy is

$$E_F = \langle a^\circ | h | a^\circ \rangle + \langle b^\circ | h | b^\circ \rangle + J_{ab} - K_{ab} \qquad (3\text{-}7)$$

where

$$h = t + V_N$$

and J_{ij} and K_{ij} are the usual coulomb and exchange integrals.

One could also write a singlet wavefunction as

$$\psi_{AF} = A \phi_a^\circ \phi_b^\circ (\alpha\beta - \beta\alpha) \qquad (3\text{-}8)$$

[In UHF one would have

$$\psi_{AF} = A \phi_a^\circ \phi_b^\circ \alpha\beta$$

which has $M_S = 0$ but contains equal components of singlet and triplet character].

Since this wavefunction would have an energy

$$E_{AF} = \langle a^\circ | h | a^\circ \rangle + \langle b^\circ | h | b^\circ \rangle + J_{a^\circ b^\circ} + K_{a^\circ b^\circ} \qquad (3\text{-}9)$$

[in UHF the term $K_{a^\circ b^\circ}$ would not appear for E_{AF}], the triplet would be lower in energy by an amount $2K_{a^\circ b^\circ}$. The Anderson mechanism corresponds to the inclusion of ionic terms

$$\psi_{AF}' = C_1 \psi_{AF} + \frac{C_2}{\sqrt{2}} [A\phi_a^\circ \phi_a^\circ \alpha\beta + A\phi_b^\circ \phi_b^\circ \alpha\beta] \quad (2\text{-}28)$$

$$= C_1 \psi^\circ + C_2 \psi^1 \quad (3\text{-}10)$$

For large internuclear distances one can use perturbation theory to obtain

$$E_{AF}' = E_0 - \frac{H_{01}^2}{E_1 - E_0} \quad (3\text{-}11)$$

where the second term would be responsible for stabilizing the singlet state.

In our model we write

$$\psi_{AF} = A\phi_a \phi_b (\alpha\beta - \beta\alpha) \quad (3\text{-}12)$$

where we solve for the optimum orbitals ϕ_a and ϕ_b self-consistently. This ψ_{AF}, which we shall call the G1 wavefunction, has an energy

$$E_{AF} = [\langle a|h|a\rangle + \langle b|h|b\rangle + J_{ab} + K_{ab} + 2S_{ab}\langle b|h|a\rangle]/[1 + S_{ab}^2] \quad (3\text{-}13)$$

where $S_{ab} = \langle a|b\rangle$.

Similarly, from these orbitals one can construct a triplet wavefunction

$$\psi_F = A\phi_a \phi_b \alpha\alpha$$

with energy

$$E_F = [\langle a|h|a\rangle + \langle b|h|b\rangle + J_{ab} - K_{ab} - S_{ab}\langle a|h|b\rangle]/[1 - S_{ab}^2] \quad (3\text{-}14)$$

Thus

$$E_F - E_A = -2\,(K_{ab} + 2S_{ab}\langle a|h|b\rangle + S_{ab}^2\,[\langle a|h|a\rangle + \langle b|h|b\rangle + J_{ab}]) \qquad (3\text{-}15)$$

to order S_{ab}^2. As before we note that if a and b are orthogonal, $S_{ab} = 0$ and

$$E_F - E_A = -2K_{ab}$$

i.e., the triplet state will be lower. It is therefore the presence of the non-orthogonality that accounts for the binding in H_2. It is in this sense that we refer to superexchange as the formation of an extremely weak chemical bond.

As has been pointed out by Coulson and Fischer,[11] ψ_{AF} in (2-30) actually contains covalent and ionic parts. To show the correspondance to the Anderson model we write

$$\phi_g = \frac{1}{\sqrt{2+2S}}\,(\phi_a + \phi_b)$$

$$\phi_u = \frac{1}{\sqrt{2-2S}}\,(\phi_a - \phi_b)$$

and

$$\phi_a^{\circ} = \frac{1}{\sqrt{2}}\,(\phi_g + \phi_u)$$

$$\phi_b^{\circ} = \frac{1}{\sqrt{2}}\,(\phi_g + \phi_u)$$

as before. Then

$$\phi_a = \lambda_1 \phi_a^\circ + \lambda_2 \phi_b^\circ$$

$$\phi_b = \lambda_1 \phi_b^\circ + \lambda_2 \phi_a^\circ$$

and ψ_{AF} in (29a) can be written

$$\psi_{AF} = (\lambda_1^2 - \lambda_2^2) A[\phi_a^\circ \phi_b^\circ (\alpha\beta - \beta\alpha)] + \lambda_1\lambda_2 [A \phi_a^\circ \phi_a^\circ \alpha\beta + A \phi_b^\circ \phi_b^\circ \alpha\beta] \qquad (3\text{-}16)$$

Thus the G1 approach using non-orthogonal orbitals is seen to be equivalent to an approach where one uses orthogonal orbitals but allows "ionic" configurations in the wavefunction.

If we restrict the orbitals ϕ_a and ϕ_b to be purely atomic functions on each respective center, ψ_{G1} becomes the Heitler-London (HL) function. The HL function has been critized by Herring[12] who pointed out that at large distances the exchange term will dominate and eventually the triplet state will become the ground state. The G1 approach by implicitly including ionic terms, should be expected to give a singlet ground state.

CALCULATIONS ON THE Ni^{++} - F^- - Ni^{++} MODEL

In order to test the preceding models of the superexchange interaction, we have carried out several ab initio calculations on the Ni^{++} -F^- - Ni^{++} "molecule" to obtain theoretical estimates for the exchange parameter. In the antiferromagnet $KNiF_3$ (J = -45°K),[13] each Ni^{++} ion is octahedrally surrounded by six F^- ions with each F^- being shared between two such octahedra (Fig. 1).

A. Basis Sets and Geometry

All the electrons in the Ni-F-Ni system were treated rigorously by expanding the orbitals in a gaussian basis. For the Ni^{++} a basis of 11s, 5p, and 3d primitives optimized for Ni^{++} (^3F) and contracted to 3s, 2p and 2d functions as described by Roos et al.,[14] was used. An additional s and p_z function with exponents of 0.4 were used on each Ni^{++} [z is the direction of the NiFNi axis]. For the F^- we used a 7s3p basis optimized for F[15] atom and contracted to 3s and 2p functions was used. Counting p orbitals in each direction and the d orbitals of each symmetry (xx, yy, zz, xy, xz and yz) a total of 55 contracted gaussian functions were used in the SCF calculations. All integrals were evaluated rigorously for the three-center system with an assumed Ni-F distance of 3.78 bohr (= 2.00 Å) corresponding to the distance (2.009Å) in $KNiF_3$. To simulate the field of the remaining 10 nearest-neighbor F^- ions, point charges with Z = -1 were used with similar Ni-F spacings. We shall return later to the limitations of the point charge model.

SCF CALCULATIONS

Since Ni^{++} (d^8) in an octahedral field has a ground $^3A_{2g}$ state

$$^3A_{2g}: \; A\, d_{xy}^{\,2} d_{xz}^{\,2} d_{yz}^{\,2} d_{x^2-y^2}^{\,1} d_{z^2}^{\,1} \tag{4-1}$$

the NiFNi system the two (S = 1) states can couple to form S = 2, 1, and 0 states. In light of the known antiferromagnetic properties of $KNiF_3$ one would expect the singlet S = 0 state to be lowest with

$$\begin{aligned} E_2 - E_1 &= -4\, J_{AB} \\ E_1 - E_0 &= -2\, J_{AB} \end{aligned} \tag{4-2}$$

from the Heisenberg Hamiltonian (with $J_{AB} < 0$ for an antiferromagnet).

We adopted the following procedure in calculating the energies of the quintet, triplet and singlet states. A quintet wavefunction (S=2) of the form

$$\psi_2 = A\, \Phi^A_{core}\, \Phi^B_{core}\, \Phi^F\, \Phi^A_d\, \Phi^B_d \tag{4-3}$$

was obtained self-consistently where Φ^A_{core} and Φ^B_{core} represent the 9 doubly occupied orbitals containing the 18 core electrons of each Ni^{++},

$$\Phi^F = (1s_F)^2 (2s_F)^2 (2x_F)^2 (2y_F)^2 (2z_F)^2 \tag{4-4}$$

$$\Phi^A_d = (d^A_{xy})^2 (d^A_{xz})^2 (d^A_{yz})^2\, d^A_{x^2-y^2}\, d^A_{z^2}\, \alpha\alpha$$

and similarly for Φ_d^B. Of course, the self-consistent function ψ_2 will not have the idealized form indicated in (4-4) but the orbitals will become symmetry functions and extensive metal-fluorine mixing will occur.

C. Calculated Results for the Ni-F-Ni Model

Examining only the four unpaired electrons in the quintet state, one has for the SCF function

$$\psi_2 = A\,(d_{x^2-y^2})_g\,(d_{z^2})_g\,(d_{x^2-y^2})_u(d_{z^2})_u\,\chi_2 \qquad (4\text{-}5)$$

where

$$\chi_2 = \alpha\alpha\alpha\alpha$$

g and u specify whether the orbital is symmetric with respect to inversion about the F nucleus (the center of symmetry in the system). As discussed in section III, we can transform orbitals by adding and subtracting the g and u orbitals to obtain localized functions on either Ni site (A or B) without affecting the energy. Eq. (4-5) becomes

$$\psi_2 = A\,(d^\circ_{x^2-y^2})^A(d^\circ_{z^2})^A(d^\circ_{x^2-y^2})^B(d^\circ_{z^2})^B\,\chi_2 \qquad (4\text{-}6a)$$

$$= A\,\Phi^\circ\chi_2$$

Using these orbitals one can consider triplet and singlet functions of the form

$$\psi_1 = A\,\Phi^\circ\chi_1 \qquad (4\text{-}6b)$$

$$\psi_0 = A\,\Phi^\circ\,\chi_0 \qquad (4\text{-}6c)$$

$$\chi_1 = \tfrac{1}{2}\left[(\alpha\beta + \beta\alpha)\alpha\alpha - \alpha\alpha\,(\alpha\beta + \beta\alpha)\right]$$

$$\chi_0 = \frac{1}{2\sqrt{3}}\left[2\alpha\alpha\beta\beta + 2\beta\beta\alpha\alpha - (\alpha\beta + \beta\alpha)(\alpha\beta + \beta\alpha)\right]$$

Since all orbitals are orthogonal, were one to evaluate the relative energies of the three states, one would find $E_2 < E_1 < E_0$ (i.e., ferromagnetic ordering) as discussed in section III. As we noted, antiferromagnetism results from the fact that the orbitals in (4-6a) are not optimum for the states represented in (4-6b) and (4-6c).

The optimum orbitals within the space spanned by these 4 functions for the singlet and triplet states were obtained using the SOGI method, the results of which are given in Table I. We now find antiferromagnetic ordering with the spacing between the states almost exactly in agreement with a Heisenberg Hamiltonian. [i.e., $E_2 - E_1 = 2\,(E_1 - E_0)$]. This result is attributed to the overlap of $d_{z^2}^A$ and $d_{z^2}^B$ orbitals (for both the S = 1 and S = 0 states the overlap is 0.016)- which favors AF coupling. These orbitals would be expected to interact most strongly since they are both oriented along the NiFNi axis. Little change is noted in the $d_{x^2-y^2}$ orbitals which remain essentially orthogonal in all three states.

D. Discussion

The d_{z^2} orbitals, (shown in Fig. 2) although predominantly atomic-like in nature, contain significant amplitude on the F as well as on the other center. Much of this character is due to the requirement (arising from the Pauli principle) that the d_{z^2} orbitals be

orthogonal to the doubly-occupied fluorine p_z-like orbitals (Fig. 3). In fact, it is this orthogonality induced amplitude on other centers that is responsible for the large metal-metal interactions observed between otherwise widely separated paramagnetic ions. In effect, by forcing the metal orbitals out of the region occupied by the ligand orbitals, the ligand "diffracts" the metal electron on center A onto the other center B

$$d_{z^2}^{A} \rightarrow d_{z^2}^{A} + \lambda_1 p_z^{F} + \lambda_2 d_{z^2}^{B}$$

$$d_{z^2}^{B} \rightarrow d_{z^2}^{B} - \lambda_1 p_z^{F} + \lambda_2 d_{z^2}^{A}$$

enhancing the M-M interaction. In a later section the effect of the ligand orbitals will be discussed more fully.

To demonstrate the equivalence of the above approach to the "kinetic exchange" of the Anderson model, a configuration interaction calculation was performed using the orthogonal localized orbitals of (4-6a) as a basis. For each state (S = 1 and 0) the dominant configuration corresponded to (4-6a) with the appropriate spin function χ_1 and χ_0. As would be expected from the SOGI results, the only other configurations which were important were those corresponding to ionic excitations from one d_{z^2} orbital to the other (in effect, allowing the orbitals to become non-orthogonal). The CI results, also shown in Table I, are practically identical to the SOGI results.

The calculated exchange value, although of the correct sign (i.e., antiferromagnetic), is only ten percent of the experimental value (-45°K). Considering the extremely small effect and the lack of any semi-empirical parameters in the calculation, the agreement is nonetheless quite encouraging. It is interesting that ignoring the effects of the $x^2 - y^2$ orbitals results in a much larger (-56°K) antiferromagnetic coupling--indicating that the ferromagnetic effects of these orbitals are not negligible. Although a limited basis set was used (roughly two contracted gaussians for each valence orbital), the major defect in the model used is undoubtedly the point-charge approximation made for the surrounding ligands. Recent calculations, for example, on the NiF_6^{4-} cluster,[17] showed that in the point charge model, one obtained only 10 percent of the experimental $^3A_{2g} \rightarrow {}^3T_{2g}$ excitation energy, whereas an all-electron calculation gave relatively good agreement. In the point charge model, one has essentially five ion-like d wavefunctions, but in an all-electron calculation, the d orbitals have been orthogonalized to the fluorine orbitals. Orthogonality by making the orbitals less "smooth," raises the kinetic energy of these orbitals. As the e_g d_{z^2} and $d_{x^2-y^2}$ orbitals interact most strongly with the ligands, and since the $^3A \rightarrow {}^3T$ transition involves a $t_{2g} \rightarrow e_g$ excitation, one would expect lower values for the point charge model.

Similarly for superexchange we would expect a large J for metal orbitals which are less smooth since the dominant terms

involved quantities such as $S_{ij}\, t_{ij}$ and $-S_{ij}^{2}(t_{ii} + t_{jj})$ - both of which lead to negative (i.e., AF) contributions.

IMPORTANCE OF LIGAND ORBITALS IN SUPEREXCHANGE

It has long been recognized that the intervening ligands between metal ions are of critical importance in superexchange. In this section the importance of ligand-metal interaction will be discussed in terms of the non-orthogonal orbital model. This interpretation provides a simple viewpoint for analyzing the effect of geometry on superexchange.

A. Covalency and Linear Cation-Anion-Cation Superexchange

The preceding analysis has made clear that the phenomenon of superexchange is related to the non-orthogonality of the metal orbitals on metal A to those on metal B. As for the reason why the interaction is so large, it has already been implied that the ligand character of the predominantly -d- like orbital on A that serves to propagate the orbital to B. [Alternatively, in the language of the Anderson model, one can say that the ligand character of the orthogonalized metal orbitals serves to increase the exchange parameter b].

Since the terms in the energy expression which favor the antiferromagnetic state are proportional to the overlap, we examine the metal-metal orbital overlap in a series of these calculations:

(i) "Frozen" atomic Ni^{++} orbitals with no intervening F^- ion (Fig. 4).

(ii) "Frozen" atomic Ni^{++} and F^- functions with metal orbitals merely orthogonalized to the ligand orbitals.

(iii) The self-consistent orbitals discussed in Section IV (Fig. 2).

In Table II orthogonalization of "frozen" orbitals to the ligand orbitals has (ii) increased J_{AB} from essentially zero in the metal-metal calculation(i), to a value approximately 40 percent of that obtained in the self-consistent calculation. Similarly the orbital overlap has increased from 0 in (i) to .0013 in (ii) to .0164 in (iii) - indicating the correlation between overlap and superexchange.

Each SCF orbital can be decomposed into components:

$$\begin{aligned} \phi_a &= \lambda_0 d_{z^2}^A + \lambda_1 p_z^F - \lambda_2 s^F + \lambda_3 d_{z^2}^B \\ \phi_b &= \lambda_0 d_{z^2}^B + \lambda_1 p_z^F - \lambda_2 s^F + \lambda_3 d_{z^2}^A \end{aligned} \qquad (5\text{-}1)$$

where $\lambda_0 \gg \lambda_1, \lambda_2, \lambda_3$ and where each component represents all basis functions of that symmetry type on a given center. The total overlap $\langle \phi_a | \phi_b \rangle = S_{ab}$ becomes

$$S_{ab} = 2\lambda_0\lambda_3 - \lambda_1^2 - \lambda_2^2 + 2\lambda_0\lambda_1 \langle d_{z^2}^B \mid p_z^F \rangle + (\text{smaller terms})$$

$$= .0198 - .0086 + .0011 + .0047 + (-.0006)$$

$$= .0164$$

The dominant term comes from the delocalization of ϕ_a, localized mainly on metal A, onto metal B [$\lambda_0\lambda_3 \langle d_{z^2}^B \mid d_{z^2}^B \rangle$ in (5-1)]. This delocalization is made possible by the ligand orbitals, since the overlap in the metal-metal system was zero. Since the ligand

character λ_L of the metal orbital $\phi_n - \lambda_L \phi_L$ is essentially determined by orthogonality to the doubly occupied ligand orbital $\phi_L + \lambda_n \phi_n$, one expects that a more covalent bond (larger λ_n) would increase the metal metal overlap and consequently the magnitude of the exchange parameter J. Although such factors as bond lengths also are important, the well-known increase in the magnitude of J in the series $F^- < O^= < S^= < Se^=$ is consistent with a greater metal-ligand interaction.

B. Superexchange as a Function of Cation-Anion-Cation Angle

The importance of the local symmetry of the metal and ligand orbitals was recognized by Goodenough[18, 19] by Kanamori[20] and on the basis of a set of these empirical rules a wide variety of magnetic structures would be rationalized. As summarized by Anderson,[21] the Goodenough-Kanamori rules state that one would expect antiferromagnetic coupling when

(a) θ (the metal-ligand-metal angle) = 180° and two singly-occupied d_{z^2} orbitals can interact through the ligand p_σ orbital.

(b) θ = 180° and two singly-occupied d_π orbitals (xz or yz) interact through the ligand p_π orbital.

(c) θ = 90° and a d_π orbital on site A can interact with a d_σ orbital on site B through a ligand orbital which is p_π with respect to A and p_σ with respect to B.

Ferromagnetic coupling will occur when

(a) There is no ligand orbital which can have overlap with both metal orbitals(e.g., θ = 180° and a d_{z^2} orbital on A and d_{xy} on B).

In terms of GI orbitals we can write for $\theta = 180°$ (see Fig. 5).

$$\phi_A = c_1 d^A_{z^2} + c_2 z_F + c_3 d^B_{z^2}$$
$$\phi_B = c_1 d^B_{z^2} + c_2 z_F + c_3 d^A_{z^2} \qquad (5\text{-}1)$$

where $c_3 \ll c_1$ and all c's are taken to be positive [we will ignore s contributions to overlap, as they were small in Table II]. When orbital ϕ_A is orthogonalized to the fluorine orbitals, it acquires z_F character in (5-1). The only basis function on B with the correct symmetry to overlap with z_F is d_{z^2}. For $\theta > 0$, however, both d^B_{xz} and $d^B_{z^2}$ can overlap. [For $\theta > 0$, the metal B-ligand axes will define the z coordinate for d orbitals on center B]. Thus the GI orbitals become

$$\phi_A = c_1 d^A_{z^2} + c_2 z_F + c_3 (\cos\theta\, d^B_{z^2} - \sin\theta\, d^B_{xz})$$
$$\phi_B = c_1 d^B_{z^2} - c_2 (\cos\theta\, z_F + \sin\theta\, x_F) + c_3 (\cos\theta\, d^A_{z^2} + \sin\theta\, d^A_{xz}). \qquad (5\text{-}2)$$

Although the ligand field about A and B will fix the "large parts" of the orbitals to have prescribed symmetry (d_{z^2} in the above case), the symmetry introduced on the opposite center will be determined by the ligand character of the metal orbital. Thus at 90° the $d^A_{z^2}$ orbital will contain only d_{xz} character on the other center. Since in Ni^{++} ion, the d^B_{xz} orbital is already doubly occupied, there will be no increase in overlap between the singly occupied orbitals (d_{z^2} and $d_{x^2-y^2}$), and hence there will be weak ferromagnetic coupling between

the essentially orthogonal $d_{z^2}^A$ and $d_{z^2}^B$ orbitals.

Several clusters with approximate 90° Ni-O-Ni groups are known to have small ferromagnetic coupling between the Ni ions.[22-26] The first to be characterized was the $Ni_3(acac)_3$ trimer[23] where the three nickel ions are bridged by Ni-O-Ni linkages with bond angles of slightly less than 90°.[26] Nearest neighbor (nn) couplings are +26 cm^{-1} and the next nearest neighbor (nnn) interaction is weakly antiferromagnetic (-7 cm^{-1}).

In NiO crystals the interaction between next nearest neighbors, which are joined by a 180° Ni-O-Ni unit, is larger than the nearest neighbor 90° interaction (-85° compared with -50°) but both are antiferromagnetic.[13] This exception to the usual 90° interaction is fairly common when strong 180° interactions are present. Direct metal-metal overlap could also be important in such systems.

C. The Copper Acetate Dimer

Perhaps the most studied antiferromagnetic molecule has been the copper acetate dimer (J = -142 cm^{-1}).[27]

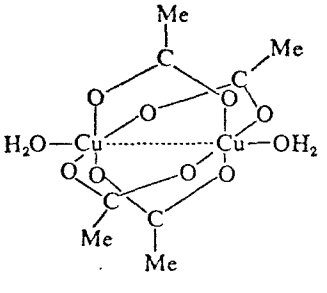

where each Cu(II) ion is surrounded by one of four oxygen atoms of the bridging $CH_3-C\begin{matrix}O-\\O\end{matrix}$ groups and two axial ligands are bonded to the copper ions.

It now appears firmly established[28-29] that the unpaired d orbital on each Cu occupies the $d_{x^2-y^2}$ "δ" orbital in accordance with the ideas of ligand field theory. If we consider the non-bonding p orbitals in the plane of each acetate molecule, there exist linear combinations of these orbitals with the same symmetry as the $d_{x^2-y^2}$ copper orbitals. Considering a single acetate ion the highest occupied molecular orbitals will have the general form

$$\phi_{a_1}: p_\sigma^L + p_\sigma^R$$

$$\phi_{b_2}: p_\sigma^L - p_\sigma^R$$

where p_σ represents the nonbonding σ-orbitals oriented more or less towards the Cu ion in the complex and L and R denote left and right oxygens. Antiferromagnetic coupling occurs because the overlap of the d orbitals has been increased through the interaction with the σ ligand orbitals. For the copper acetate dimer, our interpretation is quite similar to that of Dubicki and Martin.[30]

CONCLUSIONS

We have given a convenient interpretation of superexchange in terms of interacting non-orthogonal orbitals which have the correct spin symmetry. This interpretation is nearly equivalent to the kinetic exchange mechanism of Anderson who uses orthogonal Wannier function and the unrestricted Hartree-Fock method. In model calculations on the Ni-F-Ni system, which led to identical results in both methods, an exchange parameter J was obtained which was only 10 percent of the experimental value. This discrepancy is attributed to the model system itself rather than to any inherent difficulties in the theory.

Table 1. Energies of Ni^{++} - F-Ni^{++} in various spin states

	SOGI[a]	CI	EXP
E(S=2)	- .139825	- .139825	---
E(S=1)	- .139877	- .139881	---
E(S=0)	- .139909	- .139909	---
E(S=2)-E(S=1)	5.2×10^{-5}	5.6×10^{-5}	-4J
E(S=1)-E(S=0)	3.2×10^{-5}	2.8×10^{-5}	-2J
J	-4.0°K	-4.0°K	-45°K

[a] Energies relative to a fixed-core energy of -3098.597370 a.u.

Table II.

	J_{AB}(°K)	S_{AB}
Ni^{++} - Ni^{++} atomic orbitals	0	0
Ni^{++} - F^{-} - Ni^{++} orthogonalized atomic orbitals	-1.8	.0013
Ni^{++} - F^{-} - Ni^{++} SCF orbitals	-4.0	.0164
Ni^{++} -F^{-}- Ni^{++} SCF orbitals (ignoring $d_{x^2-y^2}$ orbitals)	-56.0	.0164
Exp	-45	

REFERENCES

1. P. W. Anderson, Solid State Physics 14, 99 (1963).
2. J. Hubbard, D. E. Rimmer, and F. R. A. Hopgood, Proc. Phys. Soc. (London). 88, 13 (1966).
3. D. E. Rimmer, J. Phys. C2, 329 (1969).
4. N. L. Huang and R. Orbach, Phys. Rev. 154, 487 (1967).
5. W. Heisenberg, Z. Physik. 38, 411 (1926); 49, 619 (1928).
6. P. A. M. Dirac, Proc. Roy. Soc. A123, 714 (1929).
7. J. H. Van Vleck, "Theory of Electric and Magnetic Susceptibilities," Chap. XI, Oxford Univ. Press, London and New York, 1934.
8. W. A. Goddard III, Phys. Rev. 157, 73 81 (1967).
9. R. C. Ladner and W. A. Goddard III, J. Chem. Phys. 51, 1073 (1969).
10. P. O. Löwdin, Phys. Rev. 97, 1474 (1955).
11. C. A. Coulsen and I. Fischer, Phil. Mag. 40, 336 (1949).
12. C. Herring, Magnetism, Vol IIB, (eds. G. T. Rado and H. Suhl) Academic Press, New York, 1966.
13. J. M. Smart, Magnetism, Vol III, (eds. G. T. Rado and H. Suhl) Academic Press, New York, 1963.
14. B. Roos, A. Veillard and G. Vinot, Theoret. Chim. Acta. 20 1 (1971).
15. D. R. Whitman and C. J. Hornback, J. Chem. Phys. 51, 398 (1969).

16. A. Okasaki and Y. Suemone, J. Phys. Soc. Jap. 16, 671 (1961).

17. T. F. Soules, J. W. Richardson and D. M. Vaught, Phys. Rev. B3, 2186 (1971).

18. J. B. Goodenough, Magnetism and the Chemical Bond, Wiley and Sons, New York, 1963.

19. J. B. Goodenough, Phys. Rev. 100, 564 (1955); J. B. Goodenough, Phys and Chem. Solids. 6, 287 (1958).

20. J. Kanamori, Phys. and Chem. Solids. 10, 87 (1959).

21. Reference 1, p. 200.

22. R. L. Martin in New Pathways in Inorganic Chemistry, (eds. E. A. V. Elisworth, A. G. Maddock and A. G. Sharpe) Cambridge Press, London, 1968.

23. A. P. Ginsberg, R. L. Martin and R. C. Sherwood, Chem. Comm. 856 (1967).

24. J. E. Andrew and A. B. Blake, Chem. Comm. 1174 (1967); J. E. Andrew and A. B. Blake, J. Chem. Soc., A. 1456 (1969).

25. J. A. Bertrand, A. P. Ginsberg, R. I. Kaplan, C. E. Kirkwood, R. L. Martin and R. C. Sherwood, Inorg. Chem. 10, 240 (1971).

26. G. J. Bullen, R. Mason and P. Pauling, Inorg. Chem. 4, 456 (1965).

27. E. Sinn, Coord. Chem. Rev. 5, 313 (1970) and references therein.

28. M. L. Tonnet, S. Yamada, I. G. Ross, Trans. Far. Soc. 60, 840 (1964).

29. G. F. Kokoszka, H. C. Allen Jr., and G. Gordon, J. Chem. Phys. 42, 3693 (1965).

30. L. Dubicki and R. L. Martin, Inorg. Chem. 5, 2203 (1966).

Figure Captions

Fig. 1. The structure of $KNiF_3$.

Fig. 2. (a) and (b) The SCF metal orbitals (d_{z^2}) for Ni^{++}-F^--Ni^{++}.

Fig. 3. The SCF fluorine orbital for Ni^{++}- F^--Ni^{++}.

Fig. 4. (a) and (b) The atomic metal orbitals (d_{z^2}) for Ni^{++} ion.

Fig. 5. The effect of geometry on the SCF orbitals--schematic drawing.

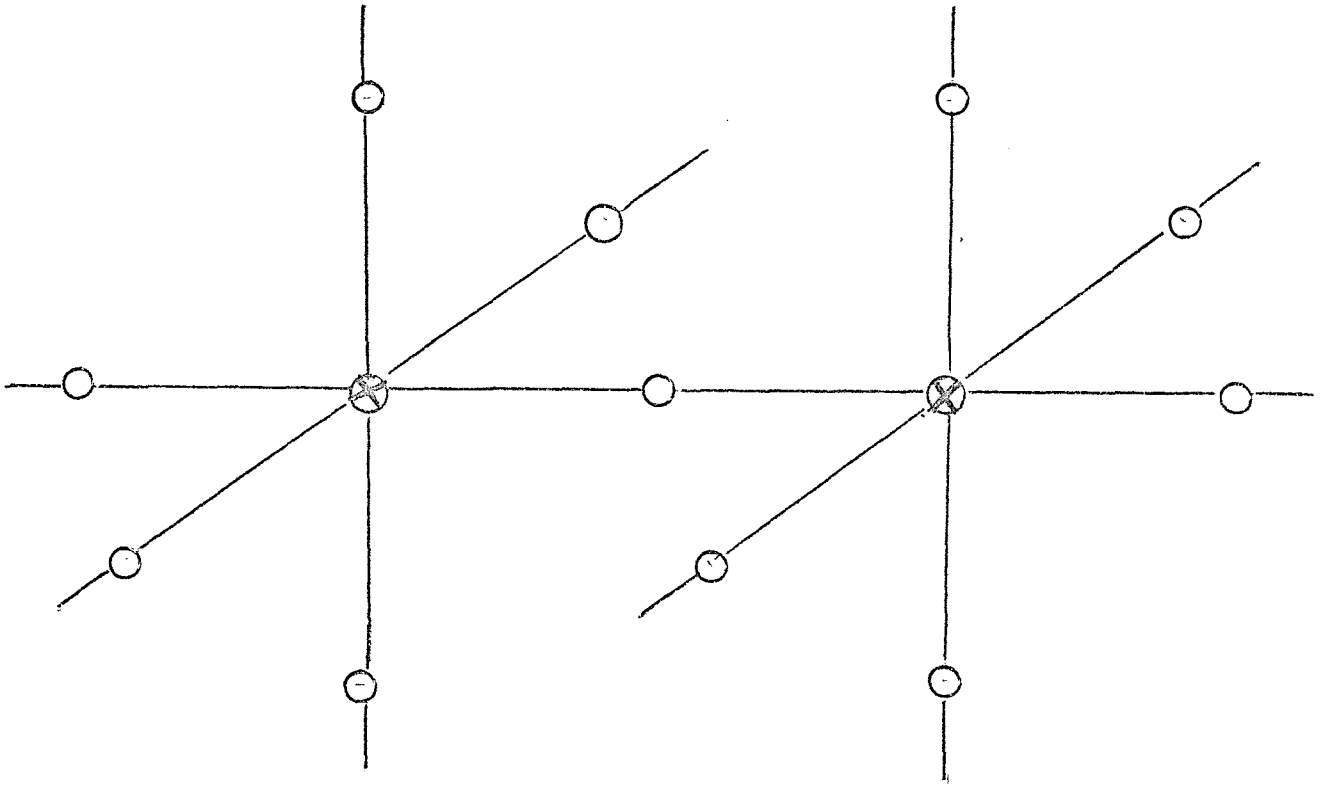

FIG. 1

○ F

⊗ Ni

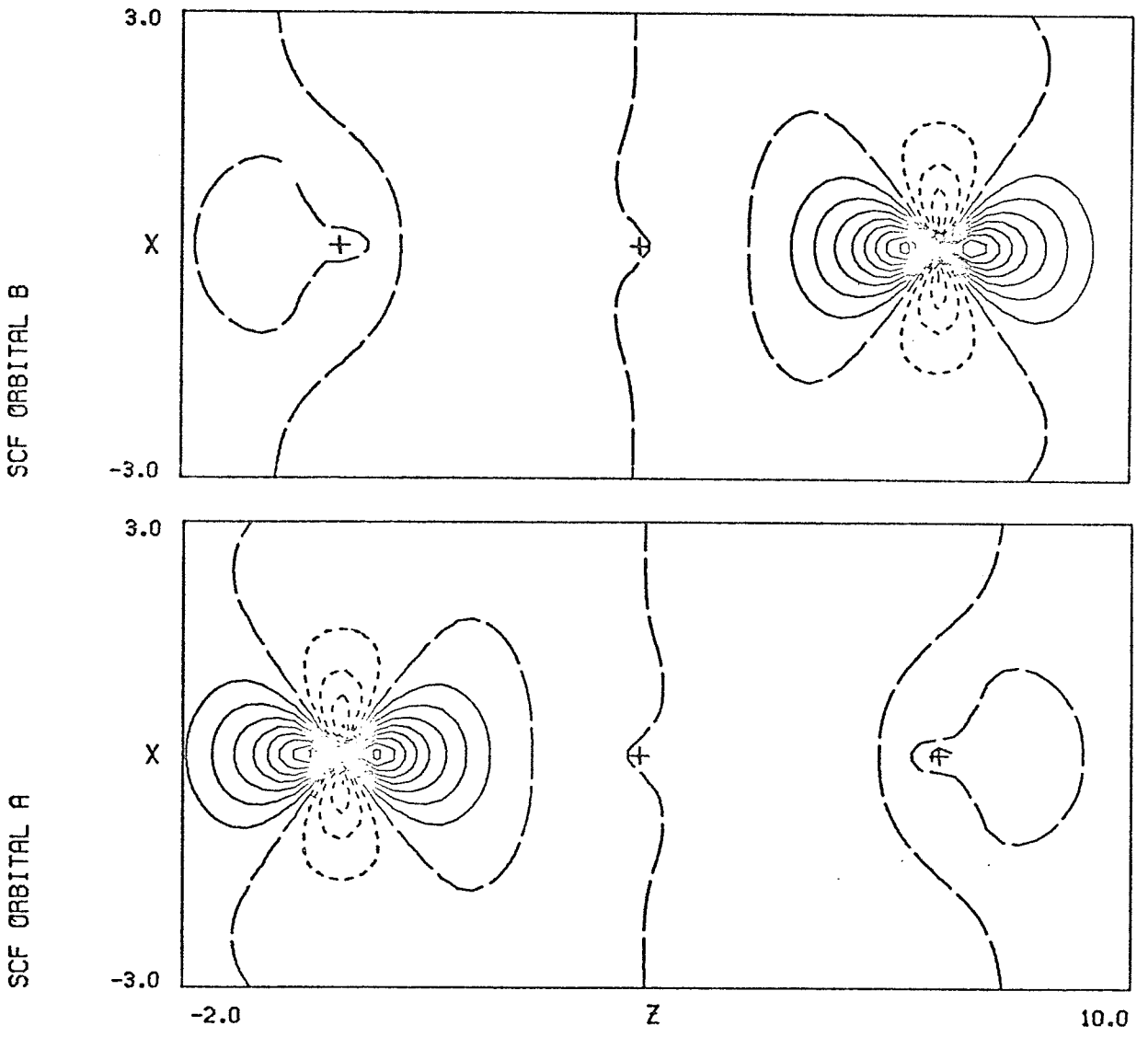

FIG. 2

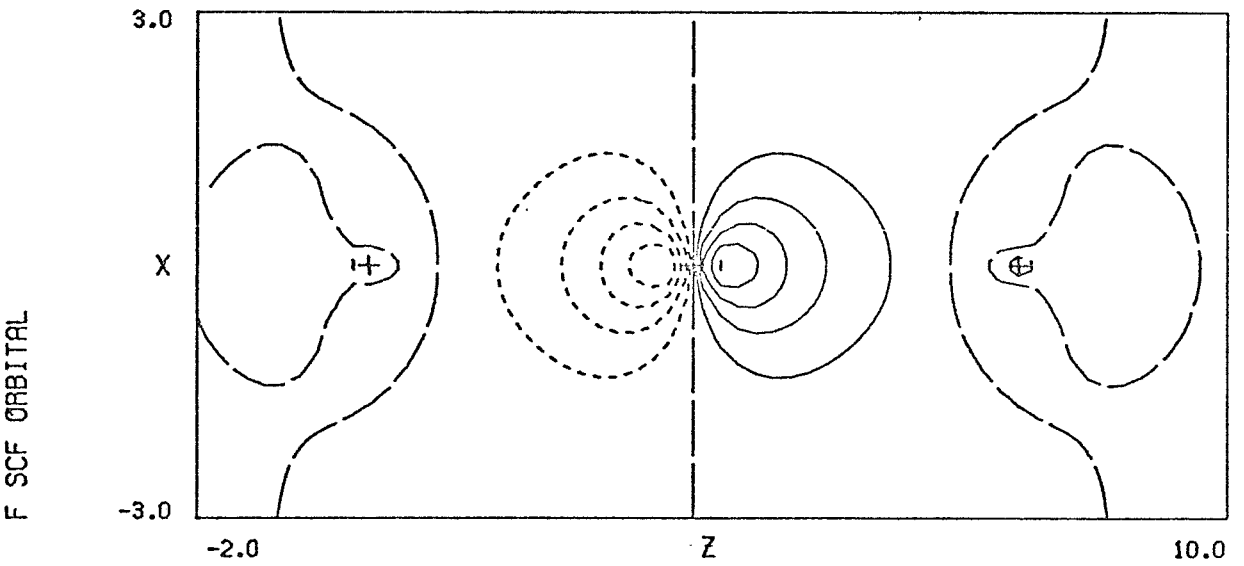

FIG. 3

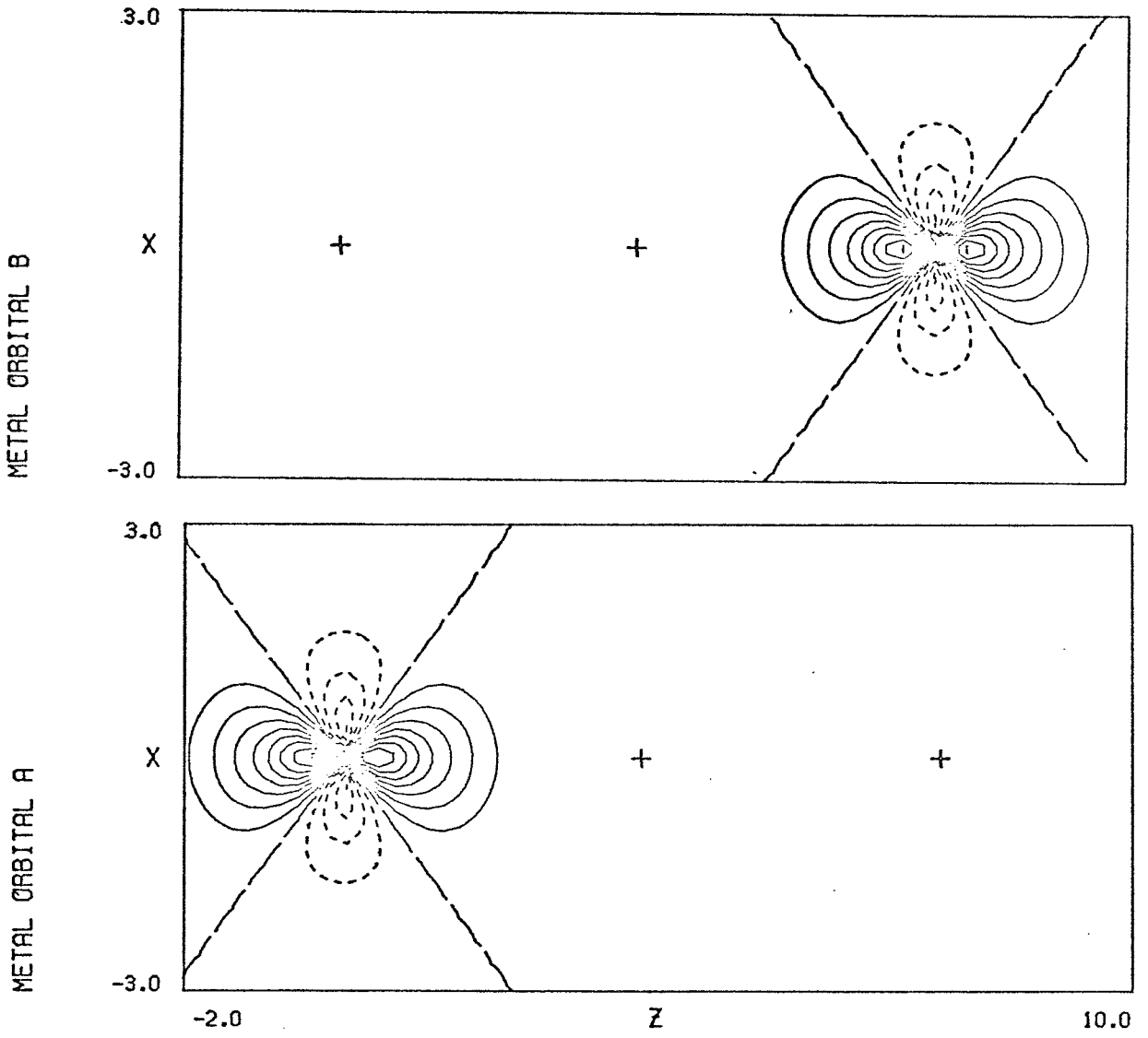

FIG. 4

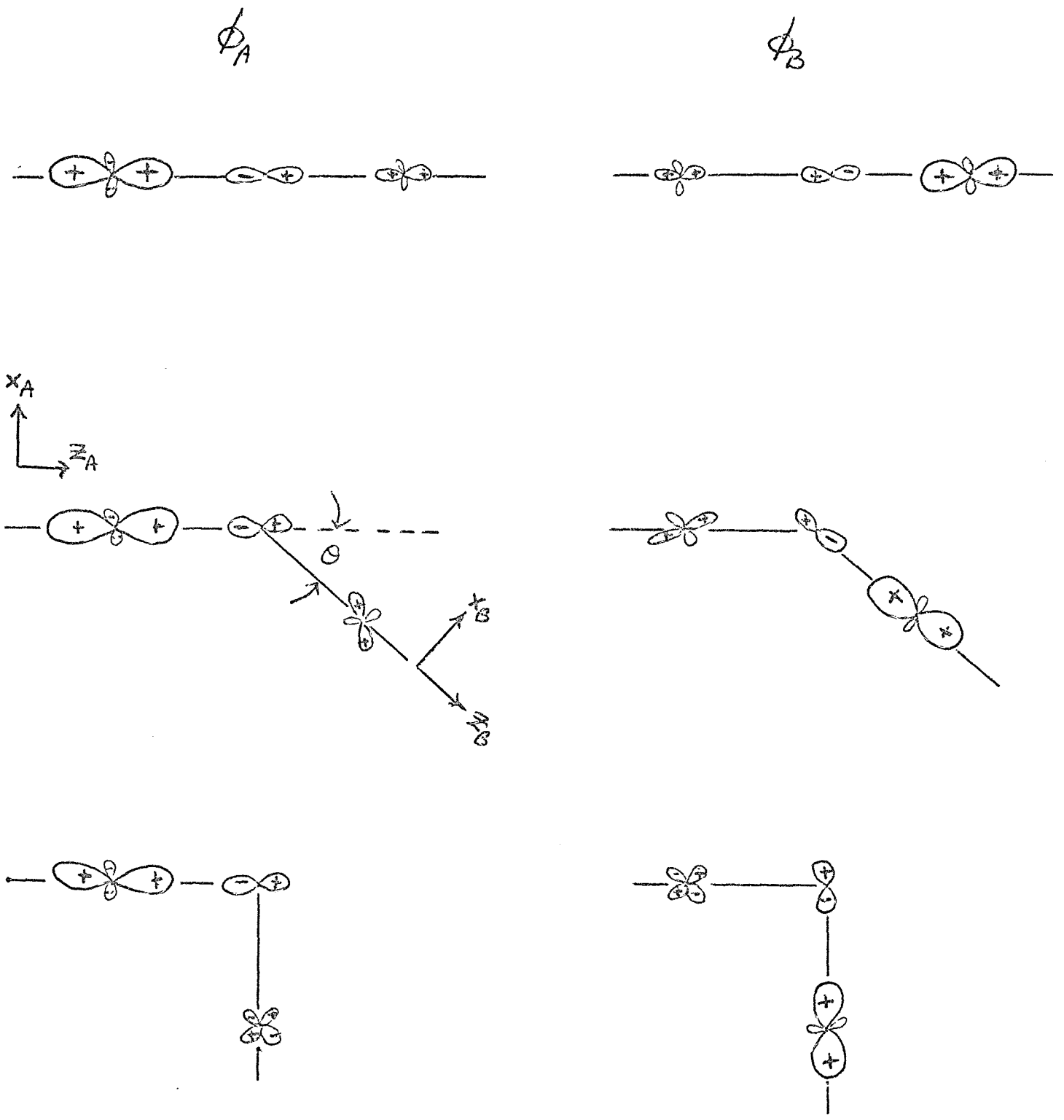
ϕ_A
ϕ_B
x_A
z_A
O
x_B
z_B

PROPOSITIONS

Abstracts of Propositions

I. A modern definition of resonance energy E_R is given and a scheme is proposed for computing E_R. Aromaticity is seen to arise from orbital orthogonality relations. The theory of resonance is extended to excited states of conjugated systems.

II. Multi-configuration SCF functions are suggested as a relatively simple means of obtaining accurate spin densities in atoms and molecules.

III. A simpler interpretation is suggested for intensity enhancement in simultaneous pair excitations in molecules and crystals.

IV. A consistent theory of metal-metal and organometallic bonding is developed using localized orbitals without artificial hybridization constraints.

V. An original composition for male chorus is presented.

PROPOSITION I

On Resonance and Aromaticity

The concept of resonance energy E_R originated in valence bond theory and referred to the extra binding energy in a molecule beyond that expected from a single valence bond structure. Although this approach led to the connection between aromaticity and the number of possible resonance structures, many nonaromatic molecules (e.g., cyclobutadiene, cyclo-octatetraene) can also be represented by equivalent resonance structures.[1]

In π-electron molecular orbital theory, E_R for a 2N π-electron system is defined[2]

$$E_R = \sum_{i=1}^{N} 2\epsilon_i - 2N\epsilon_0 \ ,$$

where the ϵ_i's are the MO eigenvalues and ϵ_0 is the eigenvalue for ethylene. This definition has proved quite useful in predicting molecular stabilities although it, too, has often (e.g., pentalene, heptalene) predicted large resonance energies for nonaromatic systems. With the advent of sophisticated semi-empirical MO schemes, more reliable estimates of E_R can now be made[3] although without much corresponding increase in our understanding of aromaticity.

The difficulty with the original valence bond approach will be indicated here and a practical scheme for determining E_R within this model will be set forth.

A. Resonance Energies in Ground States

For cyclic polyenes we shall define wavefunctions for the two dominant "resonance structures" A and B as

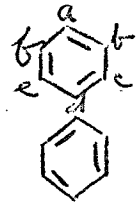

$$\psi_A = \mathcal{A}(ab+ba)(cd+dc)(ef+fe)\alpha\beta\alpha\beta\alpha\beta$$
$$\psi_B = \mathcal{A}(af+fa)(bc+cb)(de+ed)\alpha\beta\alpha\beta\alpha\beta\ , \qquad (2)$$

respectively. Using the GVB[4] or separated pair model,[5] one can solve self-consistently for the optimum wavefunctions of the forms (2). Ebbing and Poplanski,[5] using a separated pair model for benzene, found that the lowest solution had D_{3h} symmetry (corresponding closely to either one of ψ_A and ψ_B) instead of the D_{6h} symmetry of benzene. This suggests that an ab initio E_R can be defined as

$$E_R = E - E_I\ ,$$

where E is the lowest root λ of

$$\begin{bmatrix} H_{AA} & H_{AB} \\ H_{BA} & H_{BB} \end{bmatrix} \begin{bmatrix} C_A \\ C_B \end{bmatrix} = \lambda \begin{bmatrix} 1 & S_{AB} \\ S_{BA} & 1 \end{bmatrix} \begin{bmatrix} C_A \\ C_B \end{bmatrix} \ . \qquad (3)$$

In practice, even with some approximate potential for the σ-electrons, evaluation of the off-diagonal matrix elements is not trivial since the orbitals for ψ_I differ significantly from those of ψ_{II}. As shown in the Appendix, however, the corresponding orbital transformation vastly simplifies evaluation of these elements.

A common objection to VB theory has been that the number of possible resonance structures proliferates with increasing number of electrons. To this one can reply that

(a) the inclusion of "ionic" resonance structures

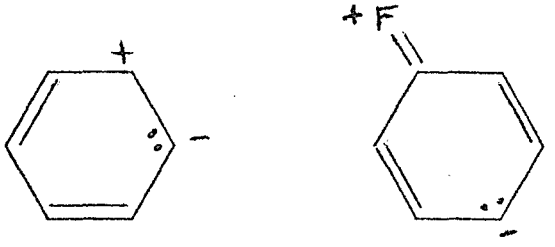

will be unnecessary since allowing the orbitals to delocalize and readjust self-consistently accounts for any necessary charge redistribution.

(b) only "true" covalent structures whose nearest neighbors are singlet coupled need be considered since preliminary self-consistent calculations show that the contributions from other structures (such as "Dewar" benzene) are negligible.[6] Thus, in calculating resonance energies one would

(a) solve for the optimum orbitals for the Kekule-like structures (symmetry considerations reduce the number of independent structures) using standard π-electron[3, 7, 8] or all-electron semi-empirical methods.

(b) form and diagonalize the $N \times N$ matrix to evaluate E_R.

Such a procedure would provide an estimate as to whether a given cyclic polyene would have typical aromatic chemistry. One would also like to know whether the cyclic polyene itself is very stable relative to the linear analogue. An alternative definition of E_R would then be

$$E'_R = (E_\ell - E_c) + E_R \ ,$$

where E_ℓ and E_c are the energies of the "localized bond" linear and cyclic systems, and E_R is the contribution from other resonance

structures as defined before. It could well turn out that for certain classes of compounds (e.g., C_nH_n), E_R is actually a monotonically decreasing function of ring size and that aromaticity is contained within E_ℓ. In other cases, such as the comparison between naphthalene and azulene, the extra valence bond structures of naphthalene would make E_R the dominant factor in the difference in aromaticities.

B. The Origin of Aromaticity

Considering resonance structures of the form A and B in (2), one can show[9, 10] that the wavefunction with the lowest energy will have the form

$$\psi_I - \psi_{II} \qquad \text{for } 4n \text{ systems}$$

$$\psi_I + \psi_{II} \qquad \text{for } 4n + 2 \text{ systems,}$$

i.e., the ground state of square cyclobutadiene would have $^1B_{2u}$ symmetry; and that of benzene, $^1A_{1g}$ symmetry. In noncyclic systems, the orbital phase continuity principle (OPCP)[10] can be applied to determine the sign. These approaches have not made it clear why a greater lowering can be expected for $4n + 2$ systems.

From Fig. 1, where we show the GVB orbitals for 4-, 6-, and 8-pi systems, we note that orthogonality considerations would predict a higher energy for $n = 4$ and 8. Since the orbitals of each pair must remain orthogonal to orbitals of other pairs, each pair has a nodal plane in square cyclobutadiene. In benzene no new nodes are needed to maintain orthogonality and thus the kinetic energy should decrease and greater delocalization can occur. In cyclooctatetraene,

a new node appears with resultant increase in kinetic energy and decreased delocalization. We conclude that in the VB framework, aromaticity is related to orthogonality constraints on the orbitals imposed by the Pauli principle. Using a localized MO scheme on several aromatic systems, England and Ruedenberg[11] recently concluded that "[aromaticity] arises from the fact that even the maximally localized π-orbitals are still more delocalized than the ethylene orbital" in qualitative agreement with the above analysis.

C. Resonance in Excited States

Although most discussions of resonance have been limited to ground state wavefunctions, some approaches have been developed that analyze excited states in terms of localized excitations. A recent analysis of ab initio configuration interaction calculations on butadiene by Dunning et al.[12] has been particularly revealing.

We will consider the excited states of benzene as resonating excitations. In Table I are listed the experimental assignments[13] of the observed bands in benzene as well as the results of a recent ab initio minimum basis configuration interaction calculation.[14] First, one notices that the two Kekule structures combine to give both the ground state ($^1A_{1g}$) and an excited singlet state ($^1B_{2u}$), which has the correct symmetry of the lowest excited singlet state of benzene. Assuming a splitting between these states of twice the resonance energy, one would estimate the $^1A_{1g} \rightarrow {}^1B_{2u}$ transition to be

$2 \times (36\ \text{kcal}) = 72\ \text{kcal} = 3.1\ \text{eV}$. However, one should really use the "vertical" resonance energy[15] that does not allow the molecule to relax to alternating bond lengths. Using an estimate[15] of 63 kcal, one predicts the transition to occur at $2 \times (63) = 126\ \text{kcal} = 5.5\ \text{eV}$ as compared with the observed bond at 4.9 eV.

In Fig. 2 we use the notation of N, T, and V, which is used to describe the ground state, $\pi \rightarrow \pi^*$ triplet and $\pi \rightarrow \pi^*$ singlet, respectively, of ethylene. We recall that the N $\rightarrow$T and N$\rightarrow$ V transitions occur at approximately 4.5 and 7.7 eV, respectively,[16] in ethylene. In addition, the V state, having much more ionic character than the other two, is not well described in a valence set of orbitals.[17]

In benzene, N$\rightarrow$V-like excitations (see Fig. 2) give rise to $^1B_{1u}$ and $^1E_{1u}$ states that agree with the experimental assignments for the second and third singlet bands--$^1B_{1u}$ (6.14 eV) and $^1E_{1u}$ (6.75 eV). It is not surprising that the resonance interaction would give excitation energies lower than 7.7 eV of ethylene. Whereas the minimum basis set CI calculations agreed quite well (within 0.4 eV) with the observed energy for the $^1B_{2u}$ state (see Table I), the predicted energies were 3.3 and 3.8 eV too high for the $^1B_{1u}$ and $^1E_{1u}$ states. This is exactly what one would expect if the latter two states resembled the V state of ethylene since the basis set would not be adequate for describing them. Thus, although all three states are described as single-excitation MO configurations, the preceding indicates that they are qualitatively different and that they might have different chemical properties.

A fourth singlet state ($^1E_{2g}$) at 8.18 eV has the appropriate energy and symmetry to arise from a double excitation NN→TT where the two resultant triplet excitations are recoupled into a singlet. This is not an altogether unrealistic assignment as TT states also give rise to triplet and quintet couplings, and the first calculated quintet occurs at 9.17 eV. Further support comes from the CI calculations that showed (a) a dramatic stabilization in the lowest $^1E_{2g}$ state upon including double excitations in the CI wavefunction (consistent with it being a NN → TT state) and (b) good agreement (8.62 vs 8.18 eV) between the predicted and observed energies (consistent with it being a valence state and not a V-like state).

The lowest predicted triplet (N→ T) VB states are $^3B_{1u}$ and $^3E_{1u}$ in agreement with the experimental assignments for the first triplet bands ($^3B_{1u}$ at 3.66 eV and $^3E_{1u}$ at 4.69 eV) as well as the CI energies (3.98 and 5.98 eV, respectively). Disparities of 1.5 and 2.9 eV in the CI energies for the next $^3E_{2g}$ and $^3B_{2u}$ states suggest these may have appreciable NN → TV character.

Examination of the VB structures for the lowest triplet states suggests possible stabilization distortion along an axis in the plane of the molecule, whereas one might expect alternate bond distortion in the "wrong" resonance state $^1B_{2u}$. Distortion in the $^3B_{1u}$ state is now well documented.[18, 19] Finally the fact that the $^1E_{2g}$ TT state can also be considered another way of writing Dewar benzene (see Fig. 2) implies that this state could be important in the valence isomerizations of benzene.

This is not to advocate that from a practical standpoint, VB techniques be devised for obtaining accurate values of excited state energies, for CI calculations in terms of orthogonal symmetry functions will no doubt prove to be the only realistic technique. Rather, one can gain possible insights into the nature of the states by a consideration of resonance structures.

APPENDIX

In evaluating matrix elements of the type

$$\langle \psi_A | H | \psi_B \rangle = \langle \mathcal{A}(ab+ba)(cd+dc)(ef+fe)\alpha\beta\alpha\beta\alpha\beta | H | \times \mathcal{A}(a'f'+f'a')(b'c'+c'b')(d'e'+e'd')\alpha\beta\alpha\beta\alpha\beta \rangle$$

one can rewrite each many-electron wavefunction in terms of orthogonal orbitals:

$$\psi_A = \mathcal{A}(g^2_{ab} - \lambda\mu^2_{ab})(g^2_{cd} - \lambda\mu^2_{cd})(g^2_{ef} - \mu^2_{ef})$$

and similarly for ψ_B. One then needs to evaluate matrix elements of the form

$$\langle \mathcal{A}\phi_1^2\phi_2^2\phi_3^2 | H | \mathcal{A}\phi_1'^2\phi_2'^2\phi_3'^2 \rangle \ ,$$

where the orbitals in each set $\{\phi_i\}$ and $\{\phi_i'\}$ are orthogonal, but orbitals of different sets are not orthogonal. Amos and Hall[20] have shown, however, that the sets may be transformed so that for each ϕ_i, ϕ_i is orthogonal to all ϕ_j' except one. Evaluation of the matrix element is then straightforward.

TABLE I. Excited States of Benzene

	State	Excitation Energy (eV)	
		Calc[a]	Obs[b]
	$^1A_{1g}$	0	0
	$^1B_{2u}$	5.26	4.89
1	$^1E_{2g}$	8.62	8.18
	$^1B_{1u}$	9.48	6.14
	$^1E_{1u}$	10.61	6.75
	$^1A_{1g}$	12.67	10.69
	$^1A_{1g}$	13.13	--
2	$^1E_{2g}$	13.78	8.36
3	$^1E_{2g}$	15.4	8.89
4	$^1E_{2g}$	--	10.36
	$^3B_{1u}$	3.98	3.66
	$^3E_{1u}$	5.39	4.69
	$^3E_{2g}$	7.48	5.96
	$^3B_{2u}$	8.61	5.76
	$^3B_{1u}$	11.34	--
	$^3E_{2g}$	--	8.36
	$^5A_{1g}$	9.17	--
	$^5E_{1u}$	11.25	

[a]Reference 14. [b]Reference 13.

REFERENCES

1. G. W. Wheland, J. Chem. Phys. 2, 474 (1934); Proc. Roy. Soc. (London) A164, 397 (1938).
2. A. Streitweiser, Jr., Molecular Orbital Theory for Organic Chemists (John Wiley and Sons, New York, 1961), p. 43.
3. M. J. S. Dewar and D. de Llano, J. Amer. Chem. Soc. 91, 789 (1971).
4. P. J. Hay, W. J. Hunt, and W. A. Goddard III, Chem. Phys. Letters, in press.
5. D. E. Ebbing and L. E. Poplanski, J. Chem. Phys. 45, 2657 (1966).
6. P. M. O'Keefe, unpublished results.
7. J. A. Pople, Trans. Faraday Soc. 49, 1375 (1953).
8. J. A. Pople, D. L. Beveridge, and P. A. Dobosh, J. Chem. Phys. 47, 2026 (1967).
9. J. J. C. Mulder and L. J. Oosterhoff, Chem. Comm. 1970, 305, 307.
10. W. A. Goddard III, J. Amer. Chem. Soc. 92, 7520 (1970).
11. W. England and K. Ruedenberg, Theoret. Chim. Acta 22, 196 (1971).
12. T. H. Dunning, R. Hosteny, and I. Shavitt, unpublished results.
13. D. R. Kearns, J. Chem. Phys. 36, 1608 (1962).
14. R. J. Buenker, J. L. Whitten , and J. D. Petke, J. Chem. Phys. 49, 2261 (1968).
15. Reference 1, p. 245.

16. P. G. Wilkinson and R. S. Mulliken, J. Chem. Phys. 23, 1895 (1955); R. S. Mulliken, ibid. 33, 1596 (1960).

17. T. H. Dunning, W. J. Hunt, and W. A. Goddard III, Chem. Phys. Letters 4, 147 (1970).

18. M. S. de Groot and J. H. van der Waals, Mol. Phys. 6, 545 (1963); 10, 91 (1965).

19. G. C. Nieman and D. S. Tinti, J. Chem. Phys. 46, 1432 (1967).

20. A. T. Amos and G. G. Hall, Proc. Roy. Soc. (London) A263, 483 (1961).

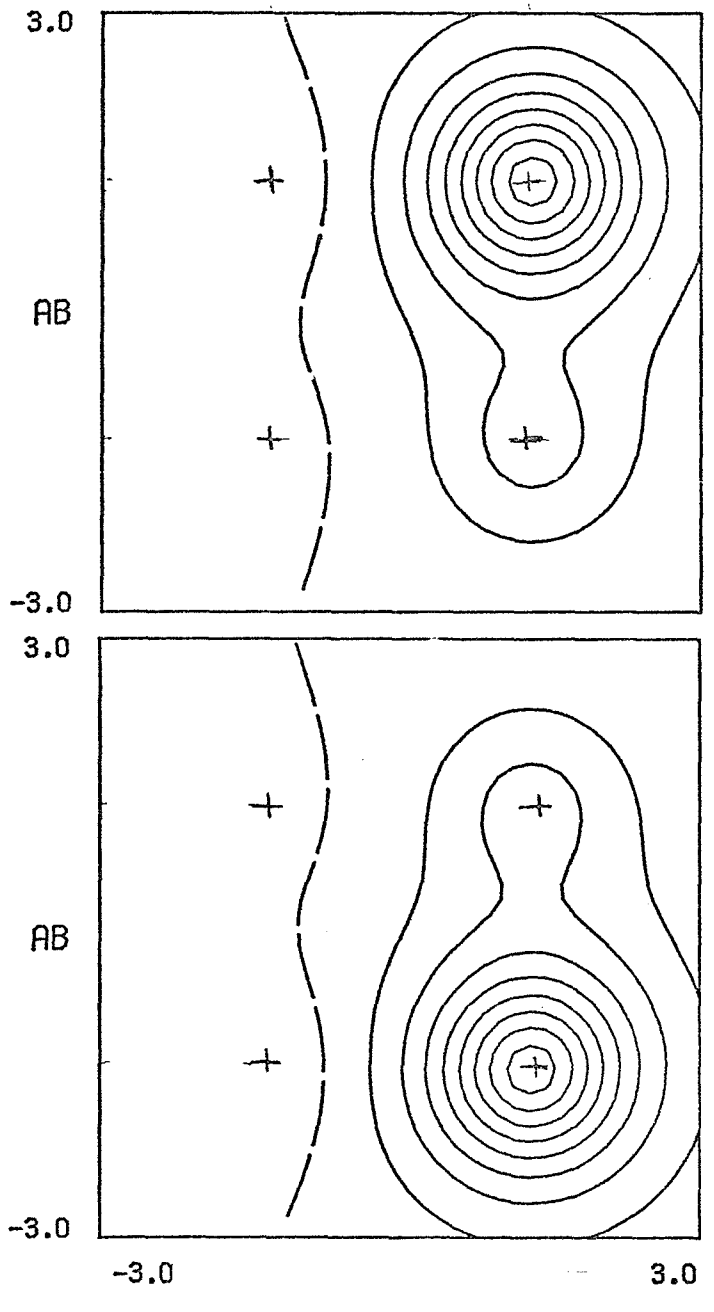

FIG. 1(a)

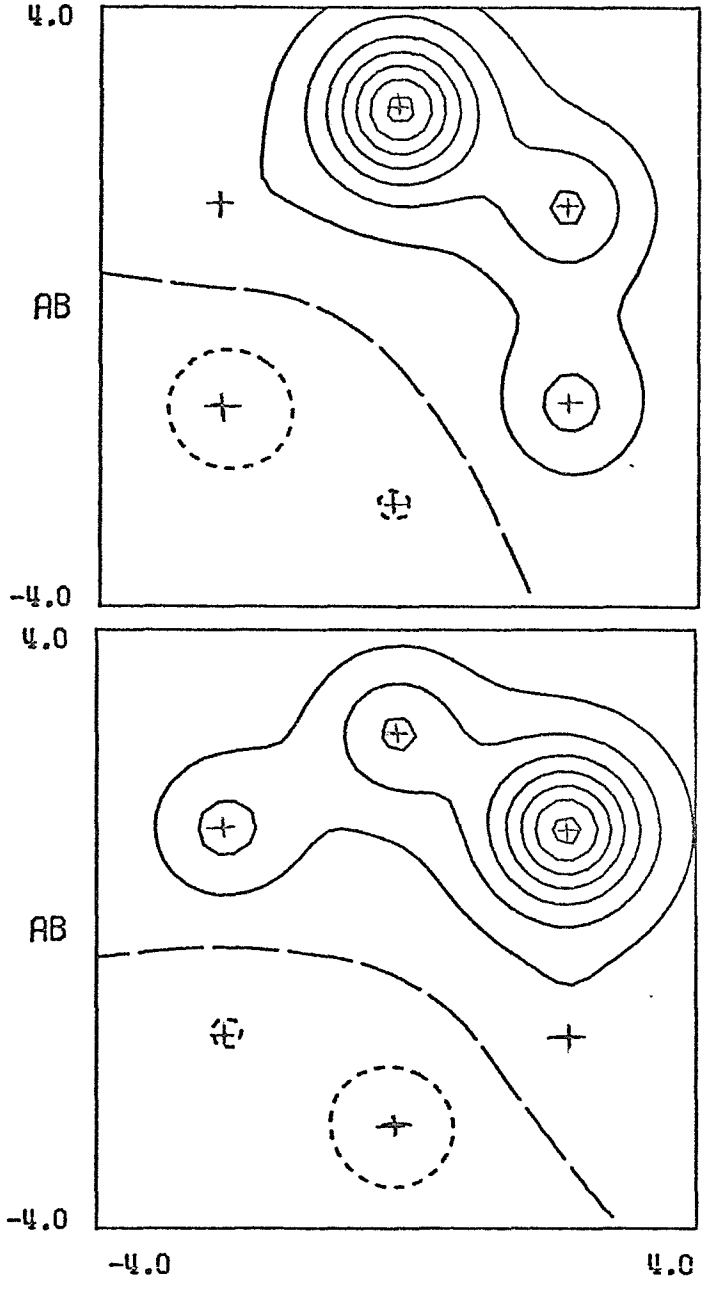

FIG. 1(b)

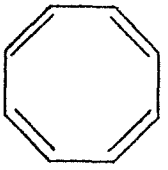

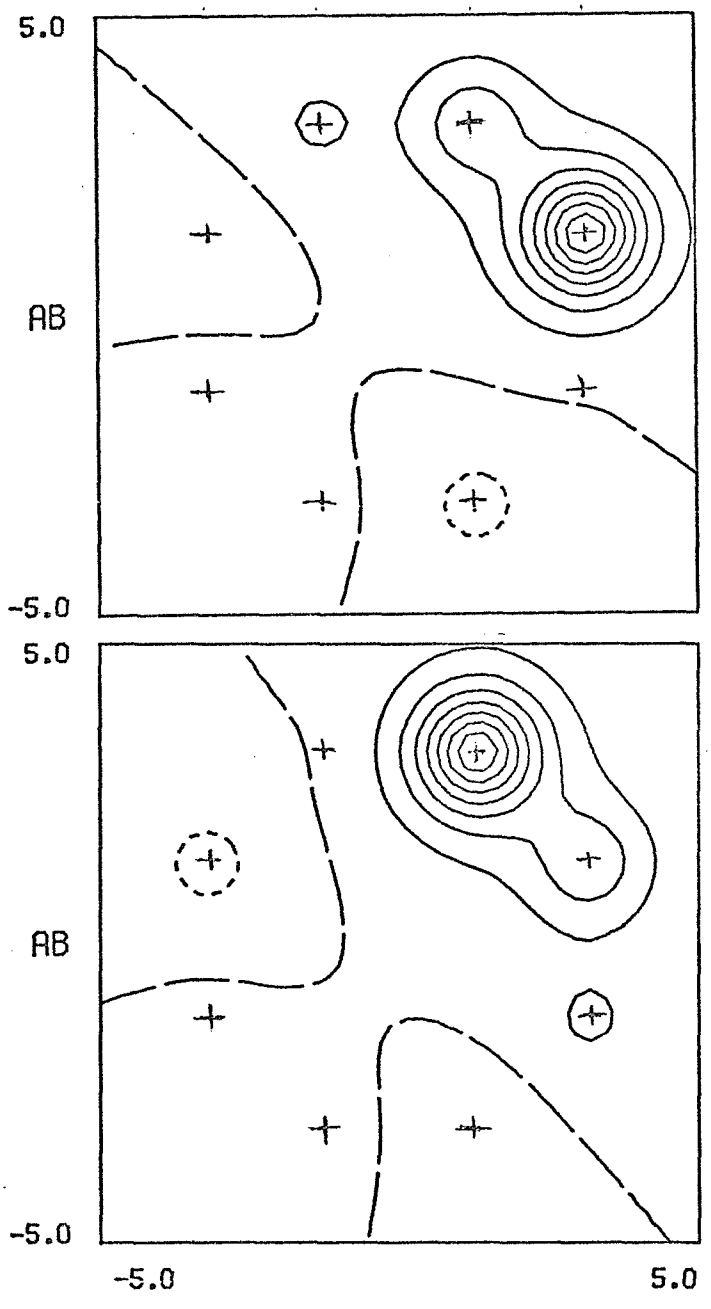

FIG. 1(c)

PROPOSITION II

On Spin Densities

The theoretical prediction of spin densities in atoms and molecules has proved to be one of the more frustrating exercises of molecular quantum mechanics. Even with highly sophisticated configuration interaction wavefunctions, the calculated value for Q(0) in nitrogen (^4S), for example, is 77% of the experimental value;[1] more typically, theoretical values often differ by 50% from experiment.[2-4]

Perhaps the most popular approach in the past has been the UHF function, which permits the spin orbitals to polarize but which is not an eigenfunction of S^2. UHF spin densities are usually within a factor of 2 of the experimental value but sometimes have the wrong sign.[5] Much better agreement with experiment has been obtained through the use of pair-correlation calculations[1] and many-body perturbation theory.[6, 7] These configuration interaction calculations have the disadvantage that the number of configurations (all single and double excitations away from the Hartree-Fock function) that must be included is still quite enormous.

Recently, the work of Ladner on Li[8] and Kaldor[9] on N has shown that SOGI or SOSCF functions give quite good agreement with experiment. These functions have the form of a simple orbital product but with general spin functions. For example, for Li

$$\psi^{\mathrm{SOGI}} = \mathcal{A}\phi_1\phi_2\phi_3[\cos\theta\, x_1 + \sin\theta\, x_2]$$

$$x_1 = \frac{1}{\sqrt{2}}(\alpha\beta - \beta\alpha)\alpha \qquad (1)$$

$$x_2 = \frac{1}{\sqrt{2}}[\alpha\alpha\alpha\beta - (\alpha\beta + \beta\alpha)] \ ,$$

where the ϕ_i and θ are all optimized. Since these techniques have become impractical for larger systems, it is proposed that multi-

configuration SCF wavefunctions be used to mimic the results of SOGI and SOSCF calculations in obtaining spin densities. Multi-configuration SCF functions Φ are usually defined as a linear combination of Slater determinants ψ_i, each comprised of orthogonal orbitals

$$[\Phi_{MCSCF} = C_0\psi_{HF} + \sum_i C_i\psi_i] .$$

The MCSCF equations are solved iteratively as in Hartree-Fock (where there is but one configuration of orthogonal orbitals) to obtain the optimum orbitals and configuration coefficients. The procedure is quite analogous to the optimization procedure in obtaining ψ^{SOGI} except that in MCSCF the fact that one is dealing with orthogonal orbitals greatly simplifies the equation.

For the case of Li with $\theta = 0$ (G1 coupling) in (1), it can be shown that the 2-configuration wavefunction

$$\psi = C_1 |\phi_{1s}^2 \phi_{2s}| + C_2 |\phi_{1s}'^2 \phi_{2s}| \qquad (2)$$

is equivalent to (1) provided $\langle \phi_{2s} | \phi_{1s} \rangle = \langle \phi_{2s} | \phi_{1s}' \rangle = 0$. Relaxing this orthogonality constraint would require the additional configurations

$$|\phi_{1s}^2 \phi_{1s}'| \quad \text{and} \quad |\phi_{1s}'^2 \phi_{1s}| .$$

Since allowing $\theta \neq 0$ permits contributions from the core orbitals, one would also add the configuration

$$|\phi_{1s}\phi_{1s}'\phi_{2s}x_2| .$$

In order to check the feasibility of the MCSCF approach, the following test calculation was performed on Li (^{2}S) [which admittedly is not an extremely sensitive test]:

(a) The best 2-configuration MCSCF function of the form (2) was obtained,

(b) A configuration interaction calculation within the 3-orbital space obtained from (a) was carried out, and

(c) Q(0) was calculated.

The hope behind this procedure was that the orbitals in the full MCSCF function would not differ significantly from the 2-configuration one and that the effects of other configurations could be handled in a perturbative way in the CI calculation. The results (Table I) gave good agreement with SOGI and experiment (although the SOGI used a different basis).

Spurred on by this success, we carried out a similar calculation on N with rather dismal results [Q(0) had the wrong spin]. Since difficulty was encountered in obtaining the second 2s orbital ϕ'_{2s} in the 4-configuration wavefunction

$$\Phi = \mathcal{A}[C_1\phi_{1s}^2 + C_2\phi_{1s}'^2][C_3\phi_{2s}^2 + C_4\phi_{2s}'^2]xyz\alpha\alpha\alpha ,$$

it would seem that the assumption that the full MCSCF orbitals differing little from the above orbitals was invalid. Probably the most important configurations to add would be

$$\mathcal{A}\phi_{1s}\phi'_{1s}\phi_{2s}\phi'_{2s}xyz\,\chi\,\alpha\alpha\alpha$$

with $$\chi = -\tfrac{1}{2}(\alpha\beta - \beta\alpha)(\alpha\beta - \beta\alpha) + \alpha\alpha\beta\beta + \beta\beta\alpha\alpha$$

$$\mathcal{A}\phi_{1s}^2\phi'_{1s}\phi_{2s}xyz(\alpha\beta - \beta\alpha)\alpha\alpha\alpha$$

and

$$\mathcal{A}\phi'^2_{1s}\phi_{1s}\phi_{2s}xyz\,(\alpha\beta - \beta\alpha)\alpha\alpha\alpha ,$$

which would allow for spin optimization and nonorthogonality effects between the valence and core s electrons.

This approach has the advantage over full CI techniques that normally one will be constructing only configurations within a space of N orthogonal orbitals where N is the number of electrons, and only a subset of these should be required.

References

1. O. R. Platas and H. F. Schaefer III, Phys. Rev. A 1, 33 (1971).
2. N. Bessis, H. Lefebvre-Brion and C. M. Moser, Phys. Rev. 124, 1124 (1961); ibid. 128, 213 (1962); ibid. 130, 1441 (1963).
3. W. A. Goddard III, Phys. Rev. 182, 48 (1969).
4. H. F. Schaefer III, R. A. Klemm, and F. E. Harris, Phys. Rev. 176, 49 (1968); H. F. Schaefer III and R. A. Klemm, Phys. Rev. 181, 137 (1969).
5. N. Bessis, H. Lefebvre-Brion, and C. M. Moser, Phys. Rev. 135, A588 (1964).
6. N. C. Dutta, C. Matsubara, R. T. Pu, and T. P. Das, Phys. Rev. 177, 33 (1969).
7. H. P. Kelly, Phys. Rev. 173, 142 (1968); ibid. 180, 55 (1969).
8. R. C. Ladner and W. A. Goddard III, J. Chem. Phys. 51, 1073 (1969).
9. U. Kaldor, Phys. Rev. A 1, 1586 (1970).

Table I

Q(0) in Li (^{2}S)

HF[a]	0.1660
UHF[b]	0.2248
SOGI[c]	0.2265
MCSCF[d]	0.2368
EXP[e]	0.2313

[a]C. C. J. Roothaan, L. Sachs, and A. W. Weiss, Rev. Mod. Phys. 32, 186 (1960).

[b]L. M. Sachs, Phys. Rev. 117, 1504 (1960).

[c]Reference 5.

[d]This work.

[e]P. Kusch and H. Taub, Phys. Rev. 75, 1477 (1949).

PROPOSITION III

On the Intensity Enhancement in Simultaneous Pair Excitations

The simultaneous electronic excitation of a pair of interacting systems by a single photon has been observed in several systems including Pr(III)-Pr(III) pairs in $PrCl_3$,[1] Ni(II)-Mn(II) pairs on perovskites,[2] and Fe(III)-Fe(III) pairs in the $[(HEDTA\ Fe)_2O]^{2-}$ dimer.[3] A particularly interesting example is the double excitations in O_2 pairs responsible for the blue color of liquid oxygen

$$^1\Delta_g\ ^1\Delta_g \leftarrow {}^3\Sigma_g^-\ {}^3\Sigma_g^- \qquad E = 2.0\ eV \qquad (1)$$

$$^1\Delta_g\ ^1\Sigma_g \leftarrow {}^3\Sigma_g^-\ {}^3\Sigma_g^- \qquad E = 2.6\ eV \qquad (2)$$

$$^1\Sigma_g^+\ {}^1\Sigma_g^+ \leftarrow {}^3\Sigma_g^-\ {}^3\Sigma_g^- \qquad E = 3.2\ eV\ . \qquad (3)$$

That simultaneous pair excitation was responsible for the liquid oxygen absorption spectra had been suggested by Ellis and Kneser[4] in 1933. These two-electron transitions have an intensity roughly equal to the spin- and parity-forbidden excitations[5]

$$^3\Sigma_g^-\ {}^1\Delta_g \leftarrow {}^3\Sigma_g^-\ {}^3\Sigma_g^- \qquad E = 1.0\ eV \qquad (4)$$

$$^3\Sigma_g^-\ {}^1\Sigma_g^+ \leftarrow {}^3\Sigma_g^-\ {}^3\Sigma_g^- \qquad E = 1.6\ eV \qquad (5)$$

in both the liquid and high-density gas phase. Emission corresponding to a double deexcitation of the metastable $^1\Delta_g$ and $^1\Sigma_g^+$ O_2 pairs has also been observed in the red chemiluminescence from the reaction

$$H_2O_2 + OCl^- \rightarrow O_2^* + H_2O + Cl^-\ .$$

Recently, Khan and Kasha[6] have studied the chemiluminescence bands

corresponding to the reverse processes of (1) and (2) at 6334 Å and 4780 Å, respectively.

Most theoretical treatments of oscillator strengths in simultaneous pair excitations[7-9] have accounted for the intensity in terms of "borrowing" intensity from other strongly allowed transitions. Although these approaches have provided some understanding of these phenomena, the need to include other excited state wavefunctions makes these methods less suitable for quantitative applications as well as less comprehensible from a qualitative standpoint.

The following discussion will demonstrate that one need consider only the two electronic states involved in each pair excitation without using "borrowed" states. This then permits a simple orbital interpretation of geometrical effects on the oscillator strength. Consider the simple hypothetical example of two atoms with ground-state configurations ψ_0 of $(ns)^2$. One could imagine an excited state ψ_1 arising from an $ns_A \rightarrow n's_A$ excitation on atom A and an $ns_B \rightarrow n''s_B$ excitation on atom B. The singlet → triplet single excitation is spin- and parity-forbidden for each atom but the double excitation (singlet → triplet)$_A$(singlet → triplet)$_B$ is formally allowed since the two triplet states can form a resultant singlet state.

There remains the question of why the one-electron dipole operator gives a finite oscillator strength for this two-electron excitation. The wavefunctions can be written

$$\psi_0 = \mathcal{A}\, s_A s_A s_B s_B\, \alpha\beta\alpha\beta \qquad (6)$$

$$\psi_1 = \mathcal{A}\, s_A s'_A s_B s''_B\, X \quad ,$$

where X is the spin function that represents a many-electron singlet state derived from two atomic triplet states:

$$X = \frac{1}{\sqrt{3}}[\alpha\alpha\beta\beta + \beta\beta\alpha\alpha - \tfrac{1}{2}(\alpha\beta + \beta\alpha)(\alpha\beta + \beta\alpha)] .$$

Evaluation of the dipole-matrix element yields

$$\langle \psi_0 | \underset{\sim}{r} | \psi_1 \rangle = 2[\langle S_A | \underset{\sim}{r} | S''_B \rangle \langle S_B | S'_A \rangle + \langle S_A | S''_B \rangle \langle S_B | \underset{\sim}{r} | S'_A \rangle] ,$$

where only the z-component (along the interatomic axis) will be non-zero. The transition becomes allowed because orbital S_A of atom A has a finite overlap with the excited orbital S''_B of atom B. [In the preceding one should really take $\psi_{g,u} = (1 \pm \hat{i})\psi_1$ to have a wavefunction of the correct symmetry--in which case only ψ_u will contribute.] On the $2[O_2]$ system, the Π_{gx} and Π_{gy} orbitals of molecule A should have a significant overlap with those of molecule B for intermolecular distances smaller than several angstroms.

Similarly, in the Fe(III) dimer, the origin of simultaneous pair excitations can be attributed to the nonorthogonality of the d orbitals of iron A with those of iron B. For the d^5 configuration, the low-lying states can be represented as [δ denotes $x^2 - y^2$]

$$^6A_{1g} = |xy\ xz\ yz\ z^2\ \delta|$$

$$^4T_{1g} = \frac{1}{\sqrt{2}} |(xy\bar{xy} - \delta\bar{\delta})xz\ yz\ z^2|$$

$$^4T_{2g} = \sqrt{\frac{3}{14}} |(z^2\bar{z^2} - xy\ x\bar{y})xzyz\ \delta| + \sqrt{\frac{2}{7}} |xy(x\bar{z}\ xz - y\bar{z}\ yz)z^2\ \delta| .$$

The single $^4T_{1g} \leftarrow {}^6A_{1g}$ and $^4T_{2g} \leftarrow {}^6A_{1g}$ transitions are forbidden but

the $^1B_2$ ($^4T_{1g_A} + {}^4T_{2g_B}$) $\leftarrow$ $^1A_1$ ($^6A_{1g} + {}^6A_{1g}$) is spin- and symmetry-allowed and would gain intensity by the overlap, for example, of the $d^A_{x^2-y^2}$ and d^B_{xy} orbitals appearing in the matrix element

$$\langle x^2 - y^2_A | z | xy_B \rangle \langle xy_A | x^2 - y^2_B \rangle$$

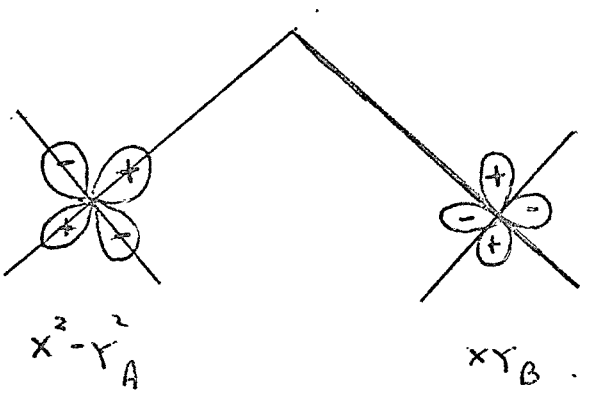

The intensity enhancement mechanism is very similar to the superexchange mechanism in that the metal-metal overlap is enhanced by the ligand orbitals. The much greater interaction expected with the highly polarizable O^{2-} ligand is consistent with the absence of simultaneous pair excitations with OH^- and OH_2 bridges.[3] The presence of such bands in the copper acetate[10] dimer, however, is somewhat puzzling in that the orbitals of copper A are orthogonal by symmetry to all but one orbital on copper B, and thus in D_{4h} symmetry no two-electron $\underset{\sim}{r}$ matrix elements arise. Slight distortions, however, could relax this symmetry restriction.

More detailed analysis of these systems with quantitative estimates of overlap and dipole matrix elements should be carried out to understand the relative intensities of these bands.

References

1. F. L. Varsanyi and G. H. Dieke, Phys. Rev. Letters 1, 442 (1961).
2. J. Ferguson, H. J. Guggenheim and Y. Tanabe, J. Chem. Phys. 45, 1134 (1966).
3. H. J. Schugar, G. R. Rossman, J. Thibeault, and H. B. Gray, Chem. Phys. Letters 6, 26 (1970).
4. J. W. Ellis and H. O. Kneser, Z. Physik 86, 583 (1933).
5. V. I. Dianov-Klokov, Opt. Spektrosk. 20, 954 (1966) [Opt. Spectry. 20, 530 (1966)], and references cited therein.
6. A. U. Khan and M. Kasha, J. Amer. Chem. Soc. 92, 3293 (1970).
7. D. L. Dexter, Phys. Rev. 126, 1962 (1962).
8. G. W. Robinson, J. Chem. Phys. 46, 572 (1967).
9. V. G. Krishna, J. Chem. Phys. 50, 792 (1969).
10. A. E. Hansen and C. J. Ballhausen, Trans. Faraday Soc. 61, 631 (1965).

PROPOSITION IV

On Metal-Metal Bonds

An increasing number of transition metal complexes involving metal-metal bonds have been reported in recent years.[1,2] Most treatments of the structure, bonding, and spectra of these compounds have used molecular orbital theory,[3] which has been quite successful in explaining the properties of monomeric transition metal complexes. An alternative description of polynuclear binding is suggested here--based partly on the ideas developed from the generalized valence bond[4] approach--which offers the following advantages:

(a) A consistent treatment of strong metal-metal bonds, weakly interacting metal-metal "superexchange" interactions, and "noninteracting" monomers can be given in the localized orbital model, while the MO method becomes appropriate only in the limit of short M-M distances and of strong M-M bonds.

(b) Just as a delocalized MO description of most saturated organic molecules becomes quite clumsy for all but the smallest systems, similarly treating polynuclear complexes in terms of delocalized functions often becomes much more unwieldy than an approach with discrete metal-metal and metal-ligand units.

Several treatments of localized descriptions of metal-metal binding have been given by Pauling,[5], Gillespie,[6] Kettle,[7-9] and others[10]--as will be discussed here--although usually the details as to the nature and hybridization of the bonding orbitals have not been given or else unrealistic assumptions were introduced.

A. The Metal-Ligand Bond, Hybridization and the Notion of the Expanded Valence Shell

The major difficulty with the usual valence bond approach to complexes concerned the "ionic"-"covalent" distinction needed to rationalize the high- and low-spin properties of complexes. The twin fallacies behind this problem lay with

(a) the insistence upon a "democratic" covalent bond with equal participation by the metal ϕ_M and the ligand ϕ_L orbitals; i.e., the requirement that the wavefunction for the bond be of the form

$$\Phi_{cov}(1, 2) = \left| \phi_M(1)\overline{\phi}_L(2) + \phi_L(1)\overline{\phi}_M(2) \right| \qquad (1)$$

and (b) the neglect of antibonding orbitals. Requirement (a) meant that for octahedral complexes one assumed $d^2\,sp^3$ hybridization for the bonding orbitals and thus needed to use 4d orbitals to hold the remaining d electrons. To avoid this predicament, we recognize two limiting forms for the wavefunctions for the metal-ligand bond:

(a) ψ_{cov}, as above, where the metal takes an "active" part in the binding. Such a bond is best typified by the metal carbonyls, where a relatively covalent metal-carbon bond is formed, although both electrons formally came from CO.

(b) ψ_{ionic} for both low-spin and high-spin spin cases where

$$\begin{aligned} \psi_{ion}(1, 2) &= \left| \sigma(1)\overline{\sigma}(2) \right| \\ \sigma &= N[\phi_{lig} + \lambda_s\phi_s + \lambda_p\phi_p + \lambda_d\phi_d] , \end{aligned} \qquad (2)$$

i.e., the metal has a "passive" role in the bonding ($\lambda_i \ll 1$) and the bond orbital is essentially localized on the ligand with small delocal-

ization onto the metal. Such bonding occurs, for example, in the aquo- and halide complexes. The relationship between the two may be seen by rewriting

$$\psi_{cov} = C_1\sigma_1\bar{\sigma}_1 + C_2\sigma_1^*\sigma_1^*$$
$$\sigma_1, \sigma_1^* = \phi_M \pm \phi_L \qquad (3)$$

and noting that if $C_2 \rightarrow 0$ and $\sigma_1 \rightarrow \sigma$, ψ_{cov} becomes ψ_{ion}. When there is a third orbital of the same symmetry as σ, we write

$$\psi_{ion}(1, 2, 3) = |\sigma(1)\bar{\sigma}(2)\phi_d(3)|$$

where ϕ_d is essentially a 3d orbital orthogonalized to σ. In ψ_{ion} [in (2)], the bonding orbital σ need not have any prescribed hybridization on the metal, while in ψ_{cov} [in (3)] rather strict conditions apply. In $Ni(H_2O)_6^{++}$, the O bonding orbitals might be essentially ligand-like with some d character and sp character on the metal. Six water molecules can make some use of one 4s and three 4p functions since the sp lobes are not fully occupied. A wide variety of complexes lying between these two extremes can all be treated consistently within this scheme.

Similar considerations apply to "expanded valence shell" compounds such as PCl_5 and SF_6 where the old VB argument of an orbital for each bond required sp^3d and sp^3d^2 hybridization, respectively. In light of the electronegativity differences involved in these "coordination compounds", a rather ionic bond would be expected, and consequently no fixed hybridization would be needed in the primarily halide-localized bonds. The nonexistence of NCl_5 could then be attributed mainly to N's higher electronegativity rather than its lack

of d functions, as the rather electronegative Sb does not form a pentahalide but does have the required d functions.

B. Metal Carbonyls

The success of valence bond theory in rationalizing the structure of metal carbonyls has been widely recognized and the point will not be belabored here. As pointed out earlier, with a bond between C and M^0 atoms of rather comparable electronegativities, the "active" participation of the M in binding is not surprising. Thus, few exceptions arise in the "rule of eighteen" [i.e., $Fe(CO)_5$ with dsp^3 hybridization; $Ni(CO)_4$, with sp^3 hybrids] and the exceptions are also understandable [e.g., $V(CO)_6$ with six ($d^2sp^3 + \phi_L$) bonds and an unpaired electron in the $(t_{2g})^5$ shell].

In $Fe_2(CO)_9$ (1) we presume the bridging CO groups to act as one-electron donors to each Fe:

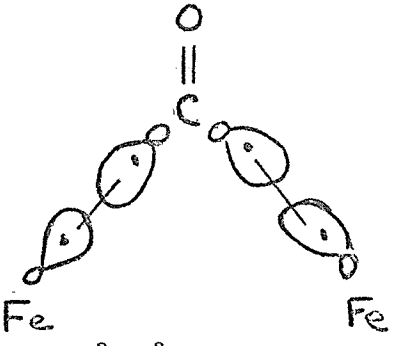

Assuming octahedral d^2sp^3 hybrids for each $Fe^0(d^8)$, the three CO's supply both electrons for the terminal bonds and the Fe use three electrons in the bridge bonds leaving a $(t_2)^5$ configuration. The unpaired electron may be taken to be oriented towards the other Fe with a consequent formation of a single Fe-Fe bond.

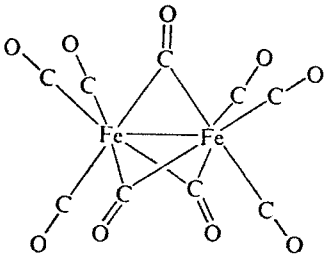

1

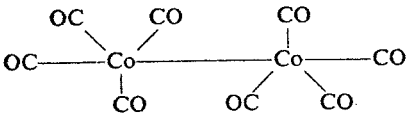

2

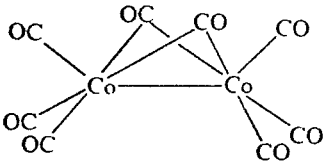

3

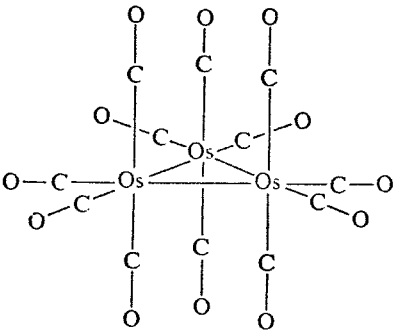

4

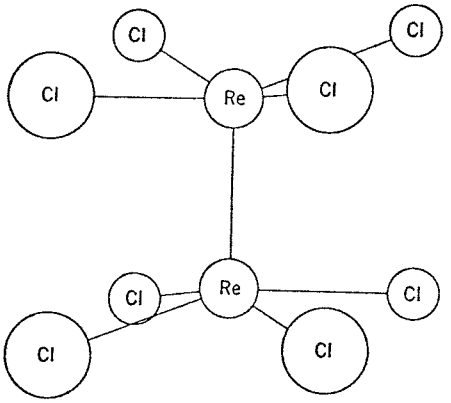

5

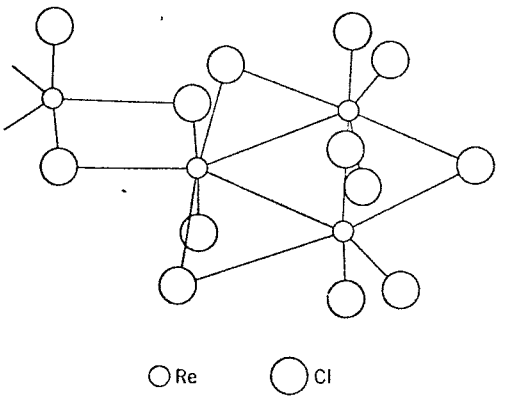

6

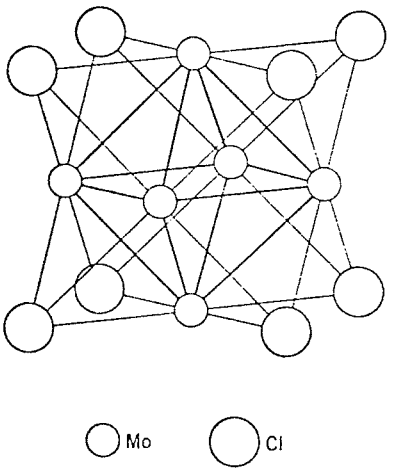

7

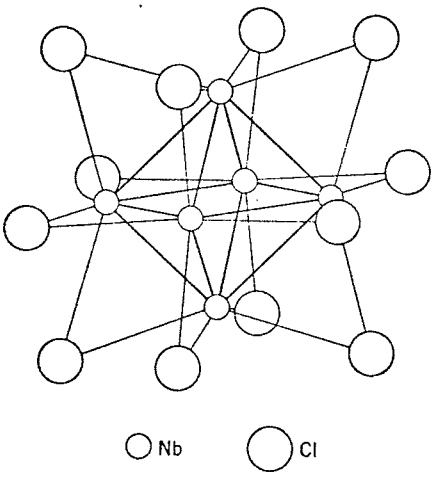

8

The $Co_2(CO)_8$ dimer exists in two forms (2) and (3), the first of which has a single Co-Co bond composed of two dsp^3 hybrids and each Co having a closed-shell d^8 configuration. The second (3) can be thought of as Fe_2CO_9 without the third bridge group and hence would have a "bent" d^2sp^3-d^2sp^3 Co-Co bond [rehybridization with other d orbitals would tend to make the bond less "bent"]. Similar arguments can be advanced to explain the bonding of other polymeric carbonyls in terms of simple metal-metal bonds. $Os_3(CO)_{12}$ (4), for example, consists of three $Os(CO)_4$ fragments bonded with Os-Os single bonds (d^2sp^3).

C. Polynuclear Halide Complexes

In the carbonyls, all bonds--metal-to-carbonyl and metal-to-metal--were relatively covalent. In the case of metal-metal bonds with halide ligands, one presumes the bonds to be essentially ionic and very little metal d, s, or p character to be involved in the M-X bonding. The basic assumption here will be that the ligands will have the dominant effect on the metal orbitals and will essentially control the role of metal-metal bonding.

To illustrate, we use the important d^4 system found in many Re(III), Mo(II), and Cr(II) compounds. The major effect of a square planar ligand field will be to produce the following ordering of the d levels:

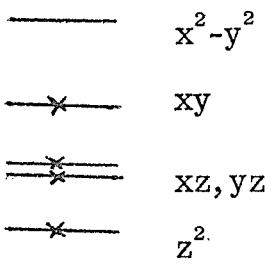

Thus the four lowest d orbitals can be used to form a total of four bonds depending on the environment. The various ways these four orbitals can be hybridized to form the strongest bonds with their neighbors nearly rivals the hybridizations found in carbon compounds. There are at least four important cases:

(a) One other metal atom. In the well-publicized $Re_2Cl_8^{=}$ (5) system, the two MX_4 planes are parallel and a quadruple bond results (second π-orbital not shown):

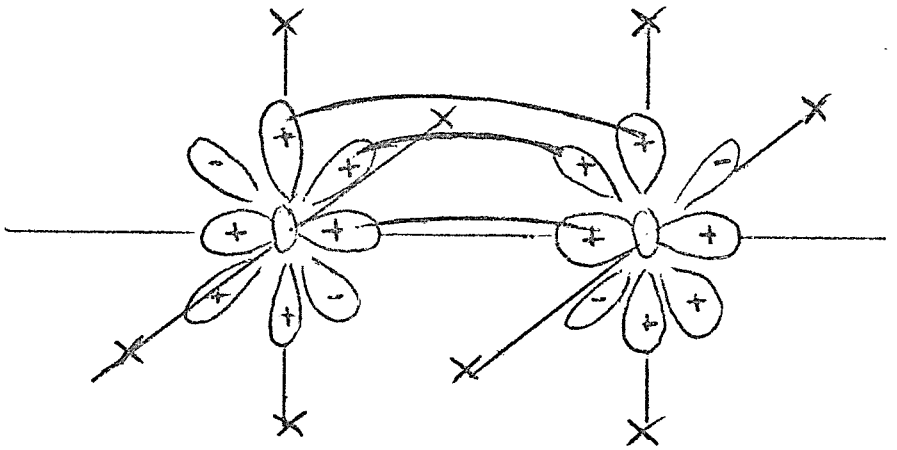

Other cases occur in $[Re(O_2CR)_4]^{++}$, $[Mo_2Cl_8]^{4-}$, $Mo_2(O_2CR)_4$, and $Cr_2(O_2CR)_4$.

(b) Two other metal atoms. In the case of Re_3Cl_9 (6), the two neighbors have the following orientation with respect to the MX_4 plane:

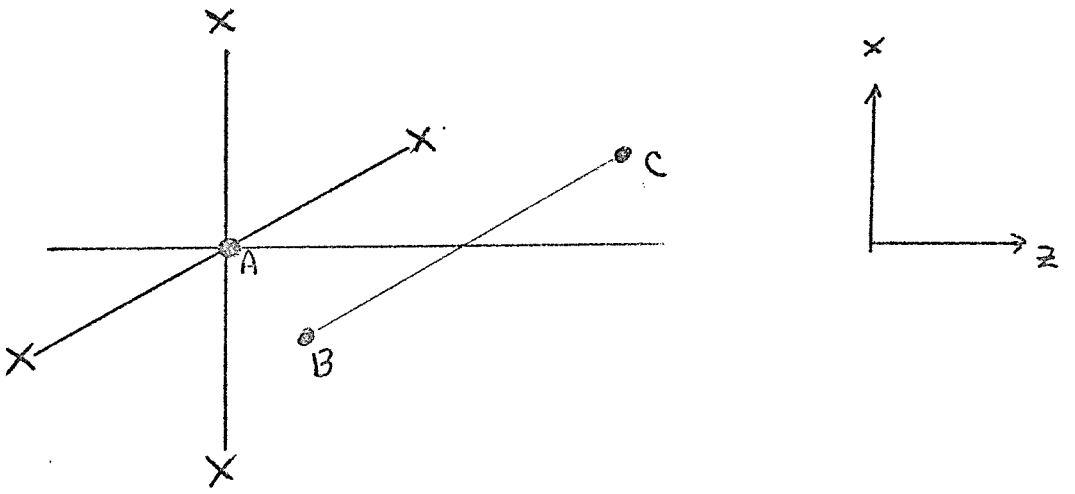

The z^2 and yz orbitals can be recombined to orient towards B and C, respectively, in the ABC plane. Similarly the xy and xz π-like orbitals can be rehybridized in the same directions, but in the π-plane. Thus Re_3Cl_9 should be diamagnetic with a σ- and π-bond between each metal atom. Other Cl^- ligands can coordinate to the metals but this does not affect the bonding.

(c) Four other metal atoms (i). In some cases the metal has four nearest-neighbor metal atoms in the following geometry:

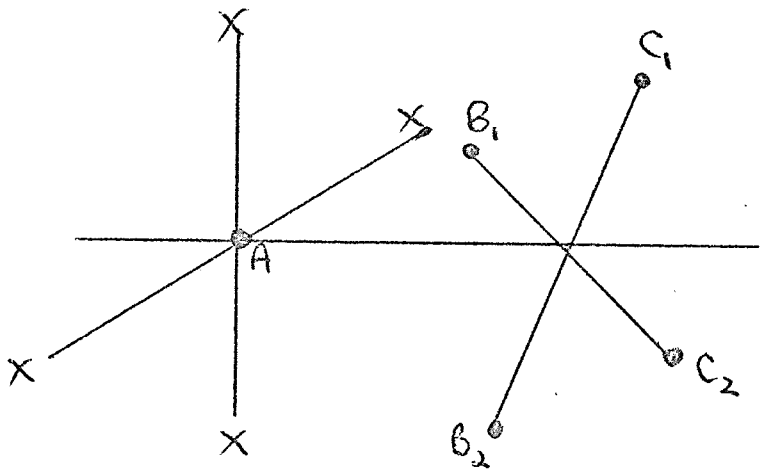

The σ- and π-bonds in (6), which had been oriented toward B, can be once more recombined to point at B_1 and B_2 (above) and similarly for C_1 and C_2. Thus in $Mo_6Cl_8^{4+}$ (7) still another hybridization has resulted

in four single metal-metal bonds from each Mo.

(d) Four other metal atoms (ii). Rotation of the metal atoms in (c) by 45° about the axis of symmetry would produce the following geometry

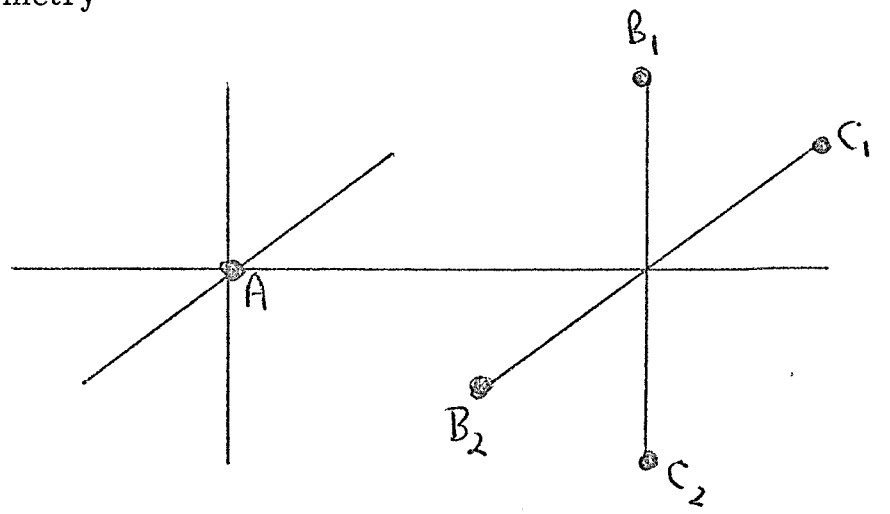

Leaving the hybridization unchanged from (c) now points the orbitals between the metals, and thus leads to 3-center 2-electron bonds reminiscent of the bonding in boron hydrides. In the $[Ta_6Cl_{12}]^{++}$ cluster (8) each Ta may be considered an electron-deficient atom forming 8 of these localized 3-center bonds. Kettle has also discussed some of these structures in terms of localized orbitals, but does not discuss very extensively the nature of the orbitals. In $[Ta_6Cl_{12}]^{++}$, he presumed Cl^- to be crucial in the 3-center bonds, a possibility we find remote. Our analysis has shown that these seemingly different species are actually different hybridizations of the same d^4 configuration.

Finally, two other interesting cases should be mentioned. The $Ru_2(O_2CR)_4^+$ system has 3 unpaired electrons and would be represented as having either the configuration[2] (the second π-bond is not shown):

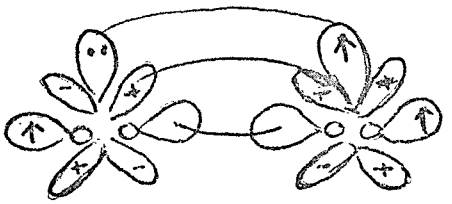

$$\sigma_1^2\pi_x^2\pi_y^2\delta^2\delta^{*1}\sigma_2^1\sigma_3^1$$

which involves d_z^2 - p_z hybridization or else the configuration

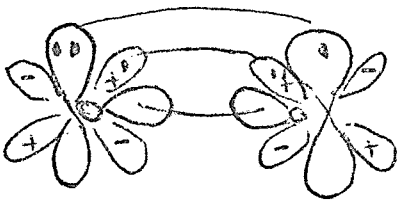

$$\sigma^2\pi_x^2\pi_y^2\pi_x^{*1}\pi_y^{*1}\delta^2\delta^{*1}$$

with a 3-electron δ-bond and two 3-electron π-bonds.

The series $M_2Cl_9^{3-}$ (M = Cr, Mo, W)[11] has weak antiferromagnetic coupling for Cr but rather strong M-M bonds for Mo and W (perhaps due to the greater spatial extent of their d orbitals) but with small magnetic moments. This is apparently a case of a spin coupling intermediate between $^4A + {}^4A$ and actual metal-metal bonds.

In conclusion, it appears that a consistent theory of metal-metal bonding can be developed using localized orbitals and that in quantitative form it should prove more useful than other approaches--statements such as "the classic conceptual simplicity of the two-center bond is virtually lost in the very procrustean attempt to retain it"[3] to the contrary!

References

1. M. C. Baird, Prog. Inorg. Chem. 9, 1 (1968).
2. F. A. Cotton, Accts. Chem. Res. 2, 240 (1969).
3. F. A. Cotton and T. E. Haas, Inorg. Chem. 3, 10 (1964).
4. This thesis.
5. L. Pauling, The Nature of the Chemical Bond (Cornell University Press, Ithaca, New York, 1960).
6. R. J. Gillespie, in Adv. Chem. Coordination Compounds, S. Kirschner, Ed. (Macmillan, New York, 1961), p. 34.
7. S. F. A. Kettle, Theo. Chim. Acta 3, 211, 282 (1965)
8. S. F. A. Kettle, Nature 209, 1021 (1966).
9. S. F. A. Kettle, J. Chem. Soc. A, 1013 (1966).
10. J. E. Fergusson, B. R. Penfold, M. Elder, and B. H. Robinson, J. Chem. Soc. 5500 (1965).
11. J. Lewis, R. S. Nyholm, and P. W. Smith, Chem. Soc. A 57 (1969).

PROPOSITION V

ORIGINAL SPECIES

1. The Ostrich
2. The Panther
3. The Fly - The Pigeon
4. The Turtle
5. The Abominable Snowman
6. The Guppy

Words by
Ogden Nash

Music © by
P. Jeffrey Hay

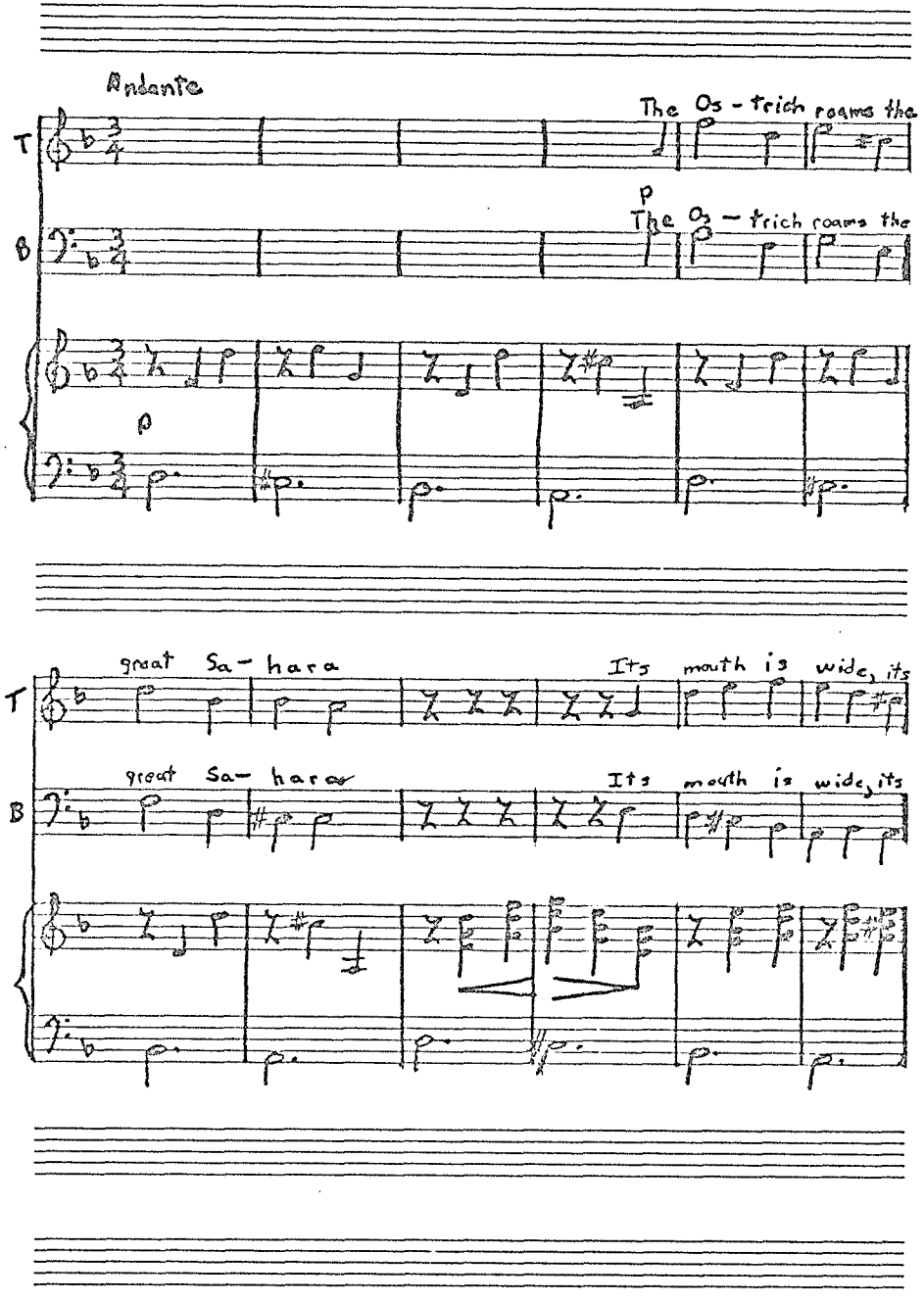
Andante
The Os - trich roams the
p
The Os - trich roams the
p
great Sa - hara
It's mouth is wide, its
great Sa - hara
It's mouth is wide, its

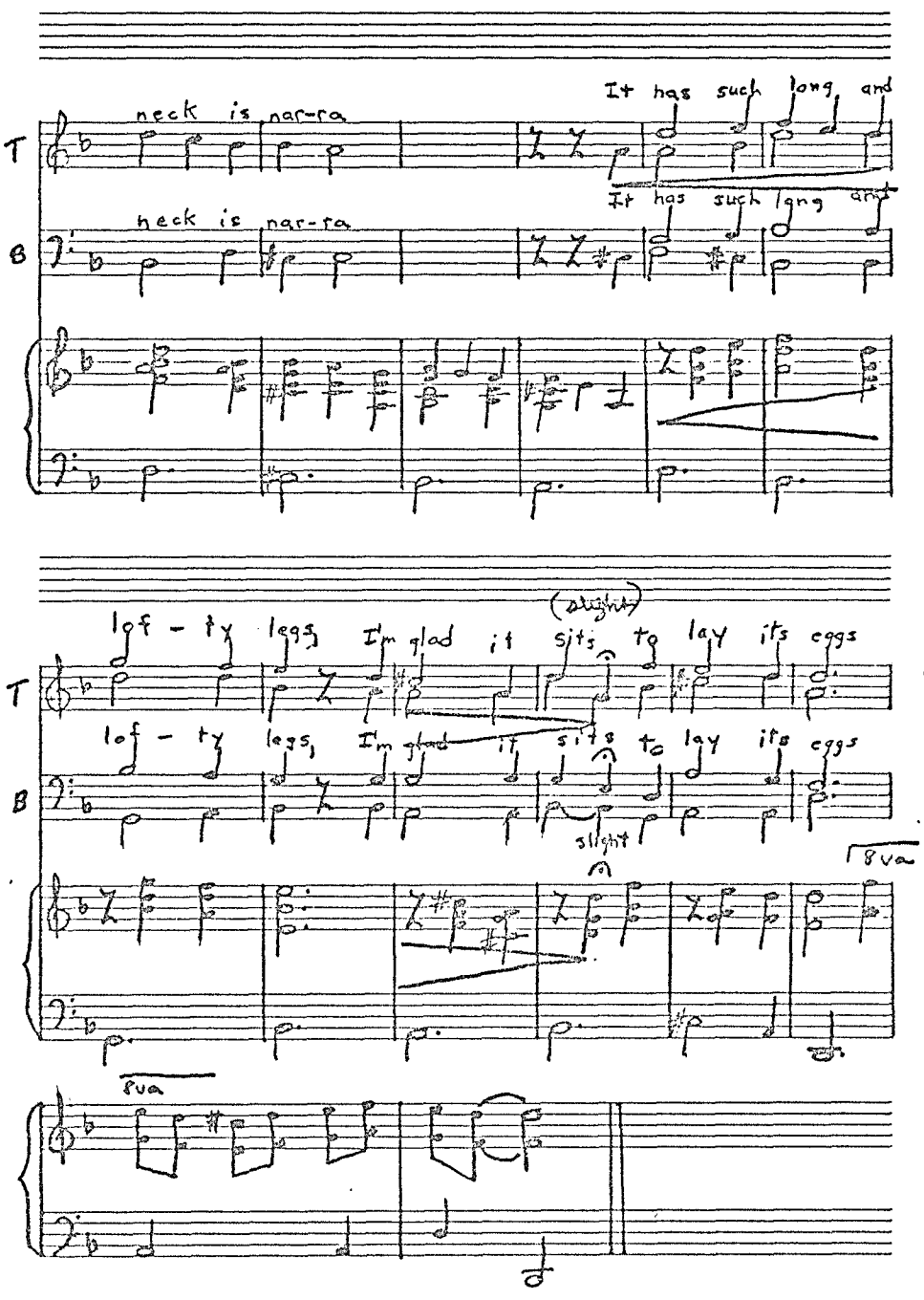
neck is nar-ra
It has such long and
neck is nar-ra
It has such long and
lof - ty legs, I'm glad it (slightly) sits to lay its eggs
lof - ty legs, I'm glad it sits to lay its eggs
slight
8va
8va

2. The Panther

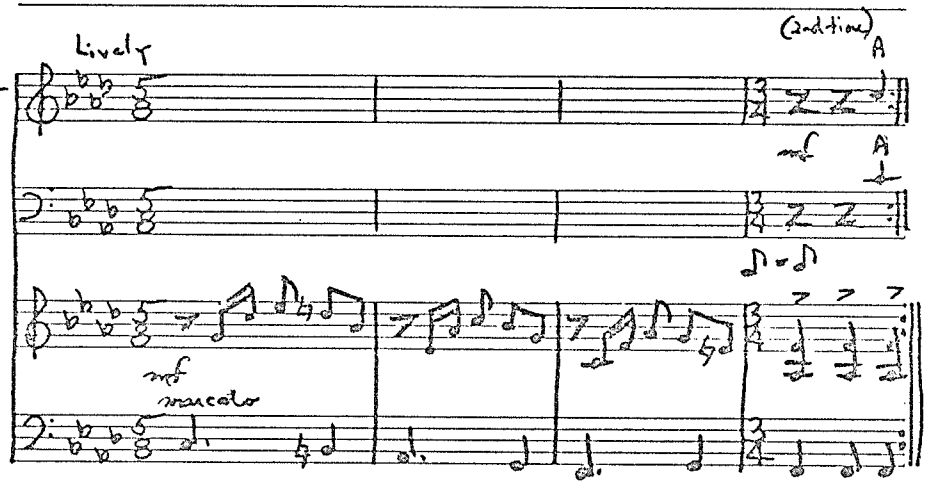

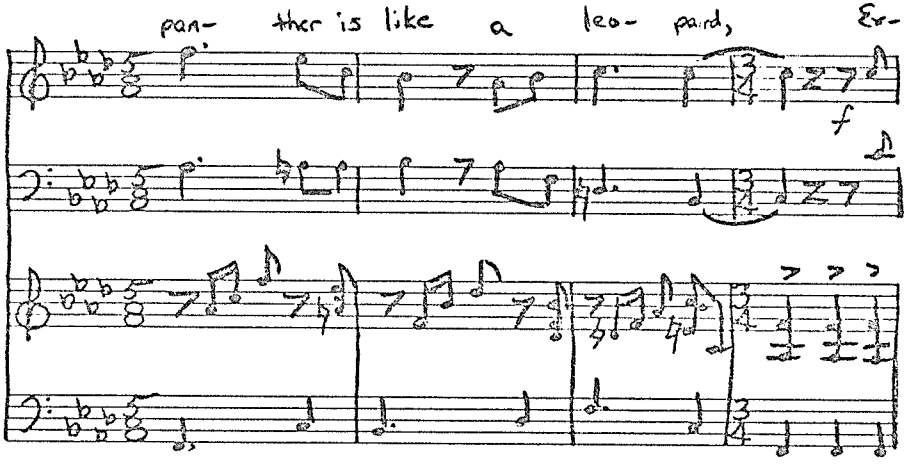

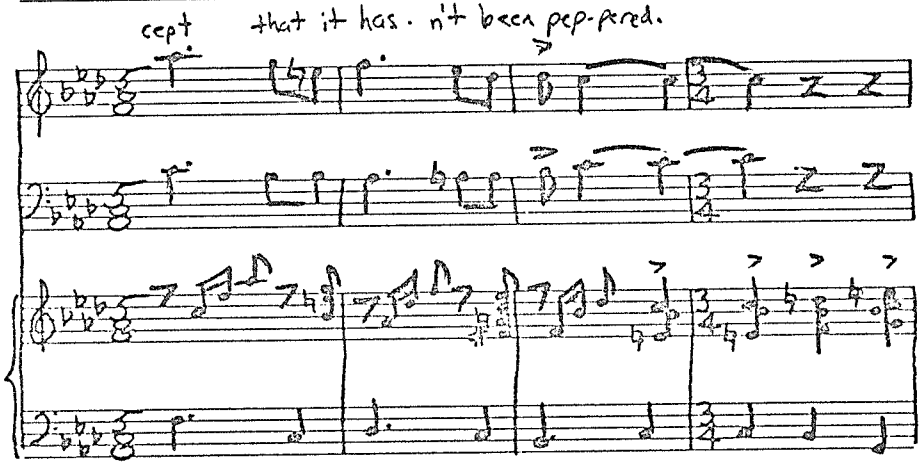

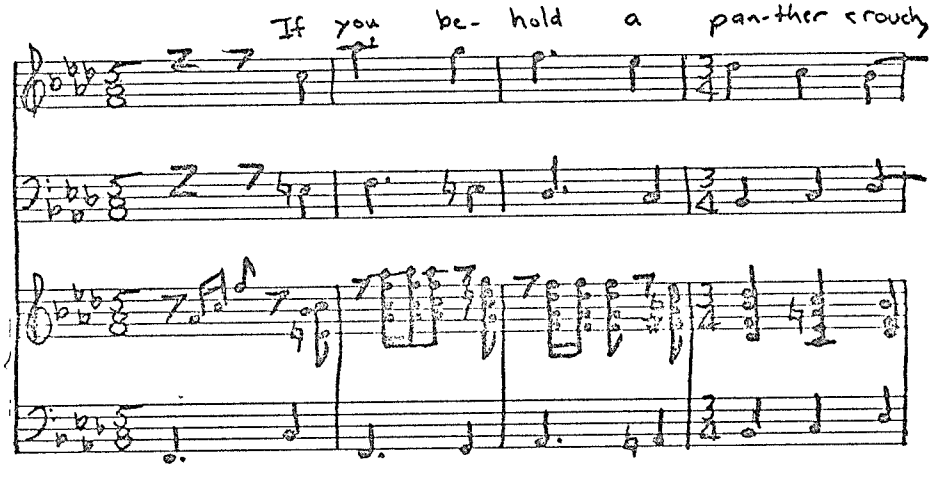

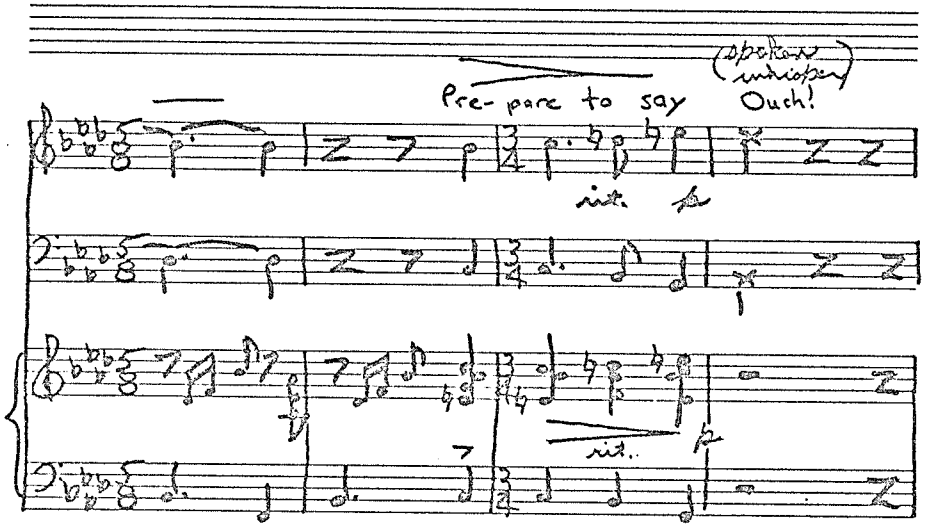
Pre- pare to say
(spoken whisper)
Ouch!
rit.
rit.

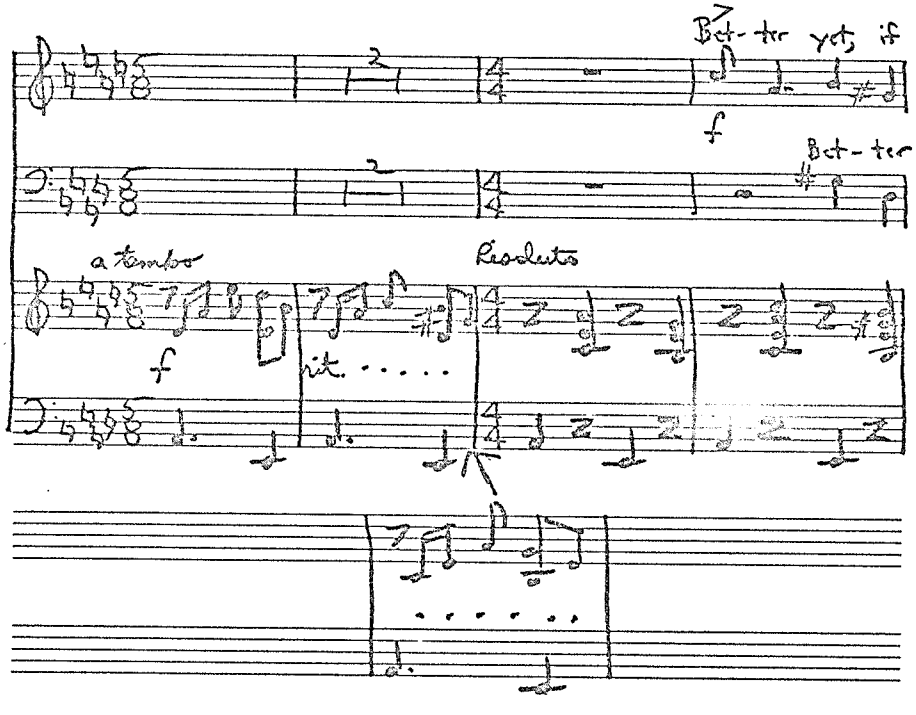
Bet- ter yet, if
f
Bet- ter
a tempo
Resoluto
f
rit.

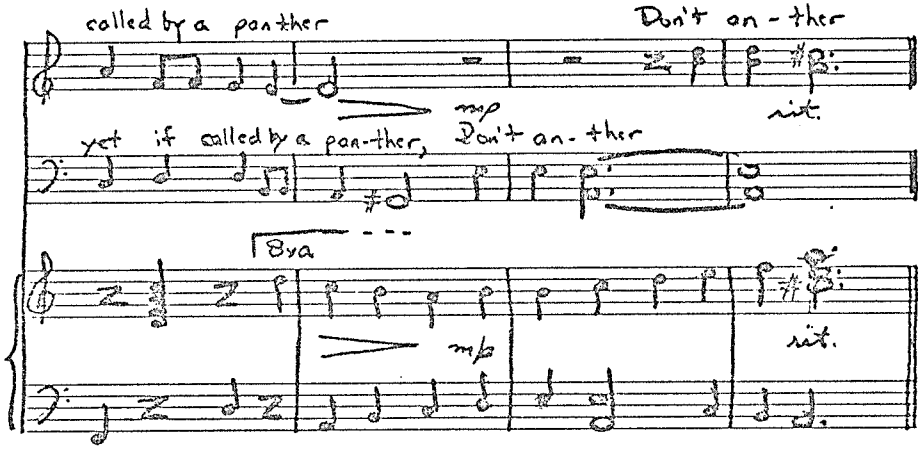
called by a pan-ther
Don't an- ther
mp
rit.
yet if called by a pan-ther,
Don't an- ther
8va
mp
rit.

3. The Fly / The Pigeon

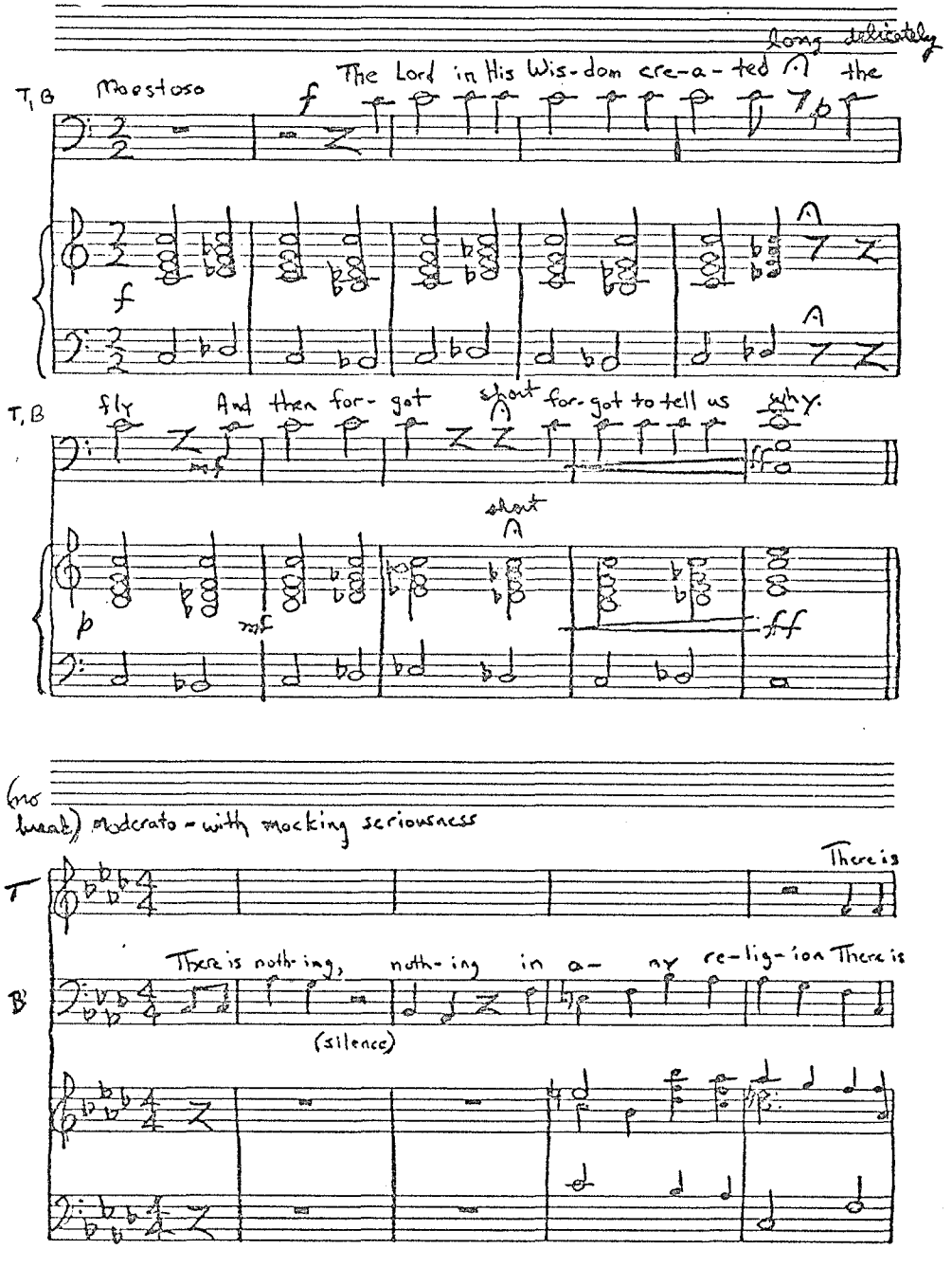

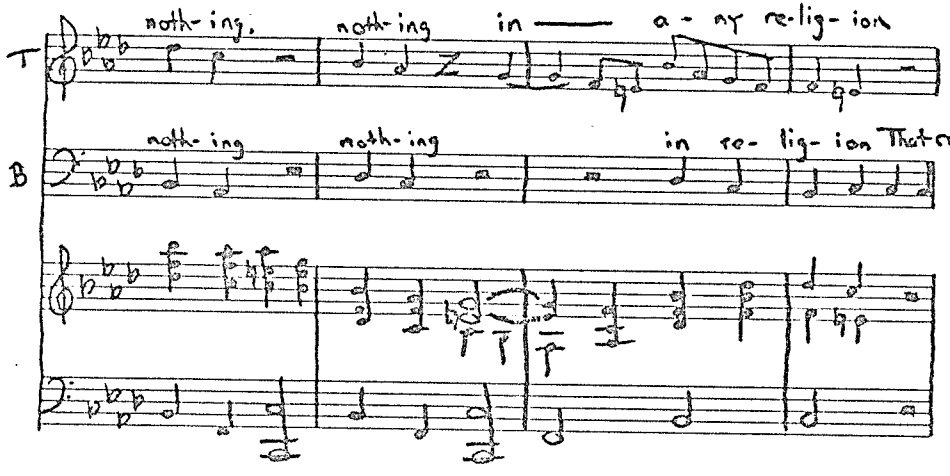
T
noth-ing. noth-ing in —— a-ny re-lig-ion
B
noth-ing noth-ing in re-lig-ion That com-

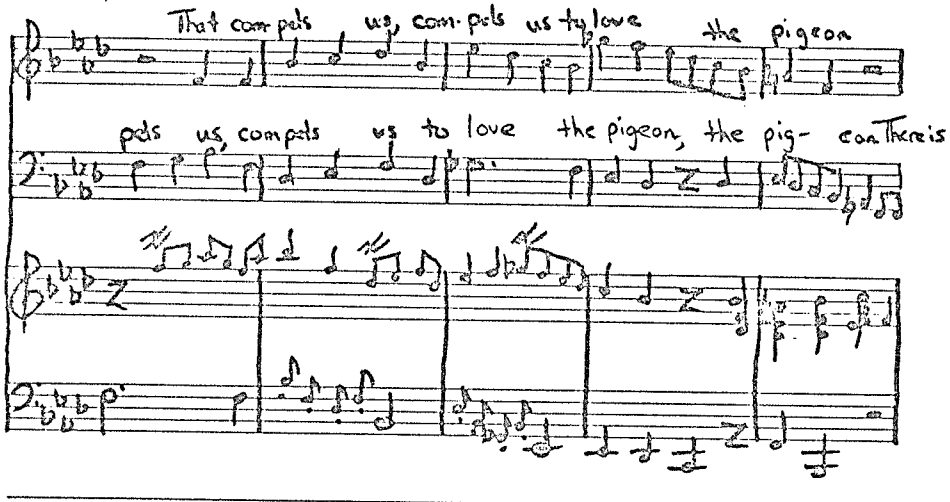
That com-pels us, com-pels us to love the pigeon
pels us, compels us to love the pigeon, the pig- con There is

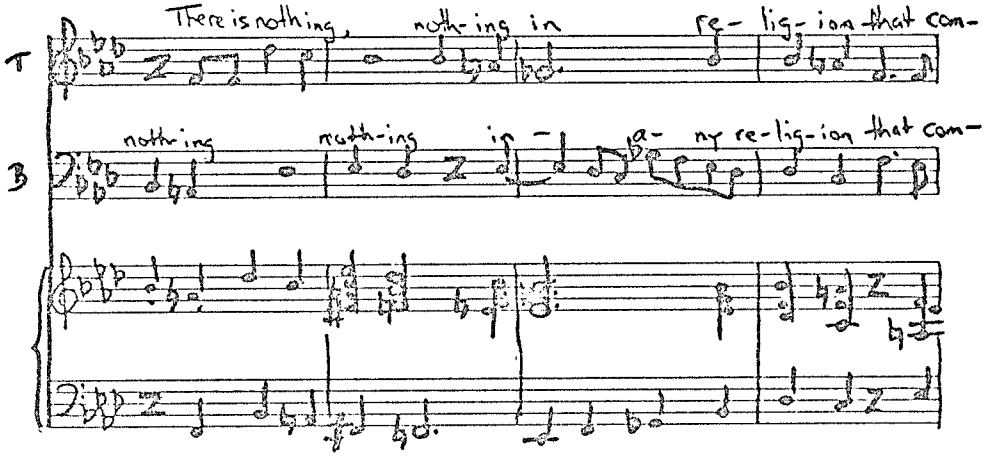
T
There is nothing, noth-ing in re- lig- ion that com-
B
noth-ing noth-ing in — a- ny re-lig-ion that com-

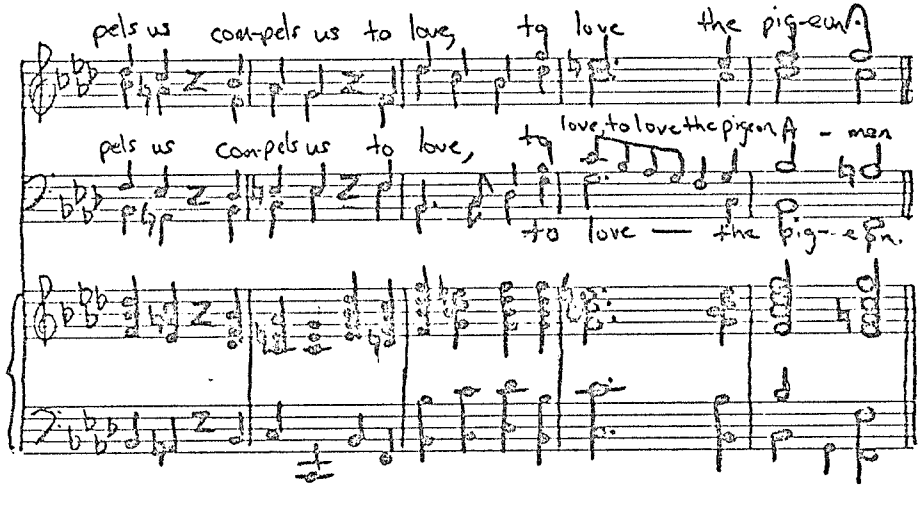
pels us com-pels us to love, to love the pig-eon
pels us compels us to love, to love, to love the pigeon A - men
to love — the pig- eon.

...rds by ...en Nash

4. The Turtle

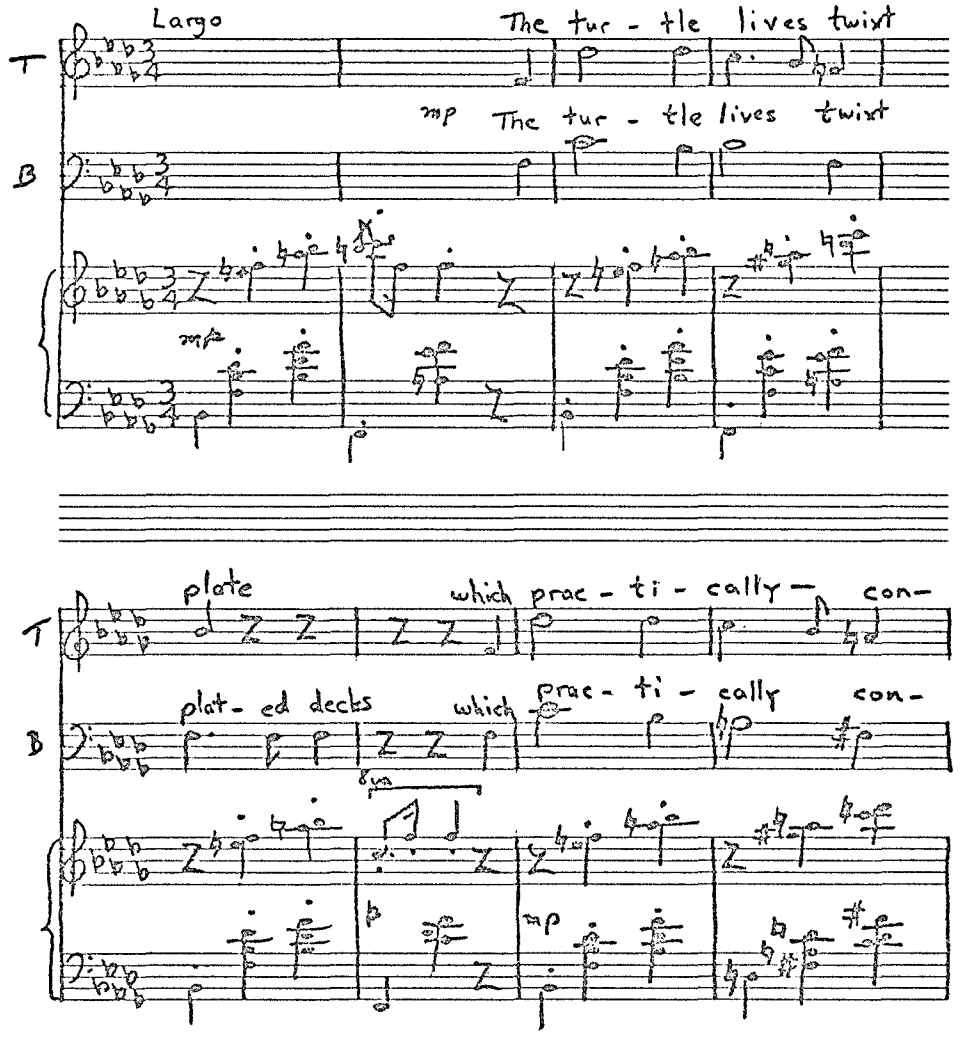

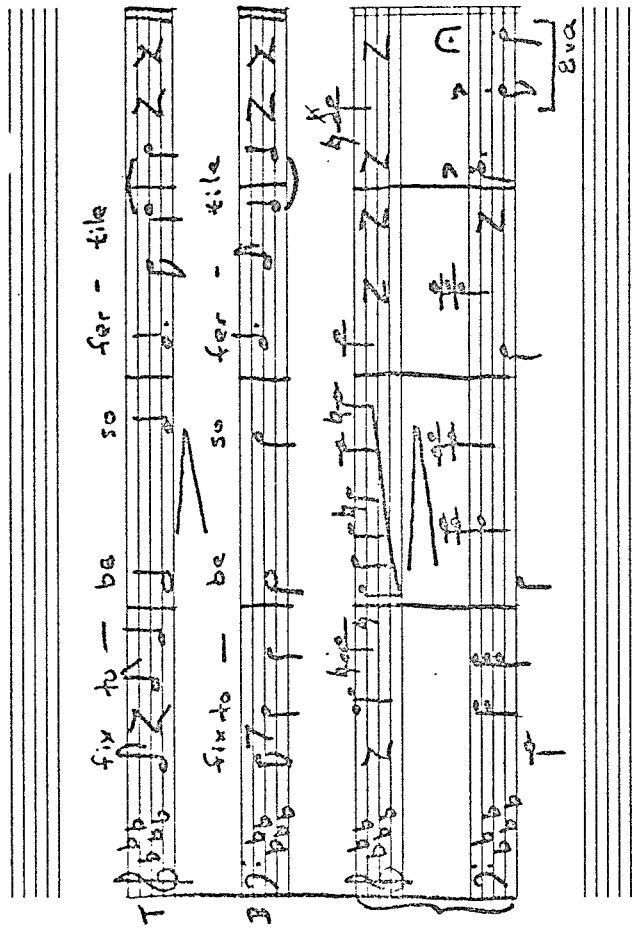
fix no — ba so fer - tile
fix no — be so fer - tile
8va

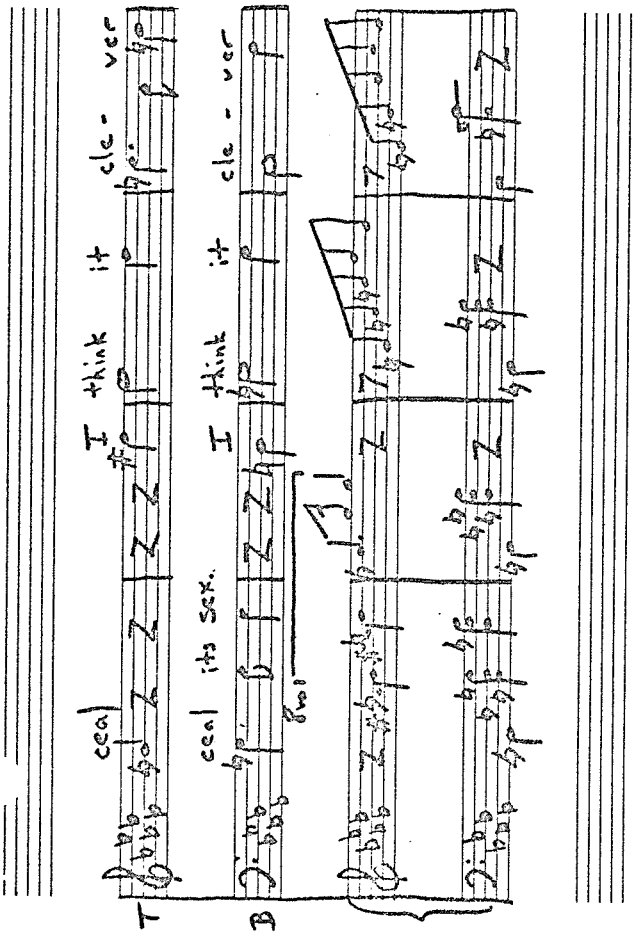
ceal I think it cle - ver
ceal its sex. I think it cle - ver
of the tur - tle In such a
of the tur - tle In such a

5. The Abominable Snowman

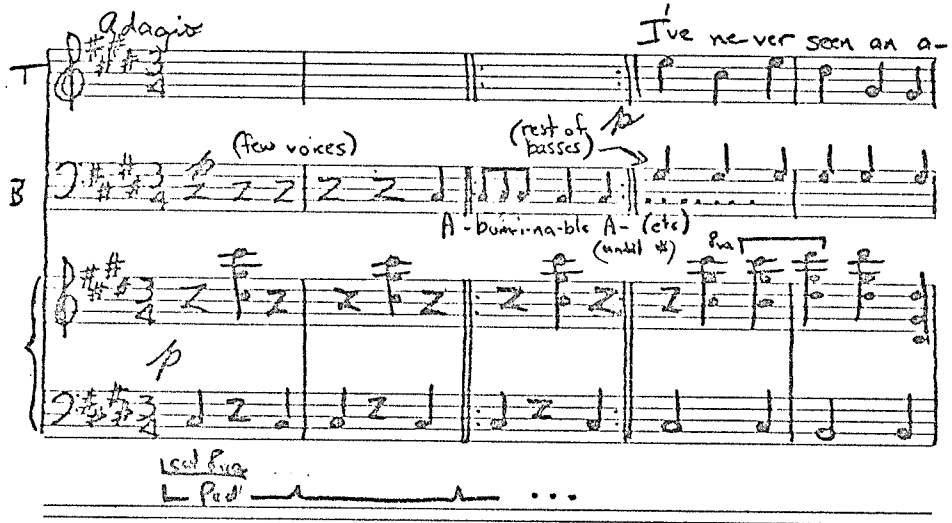

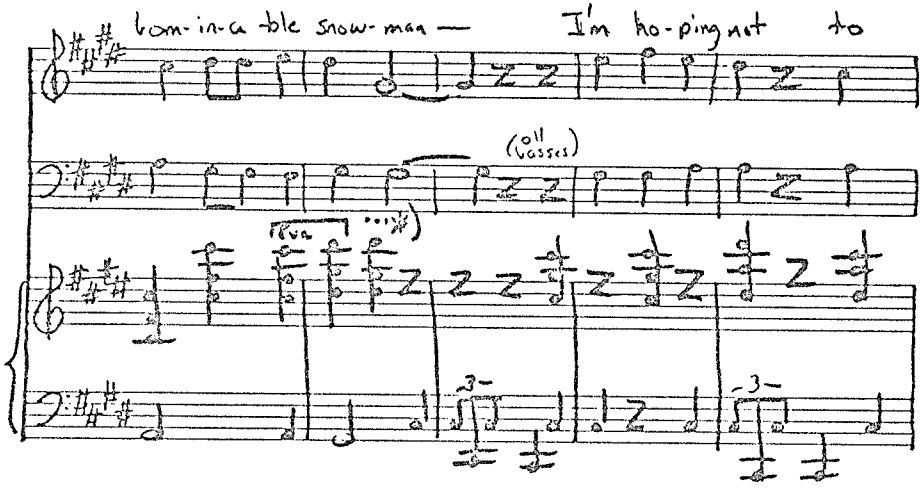

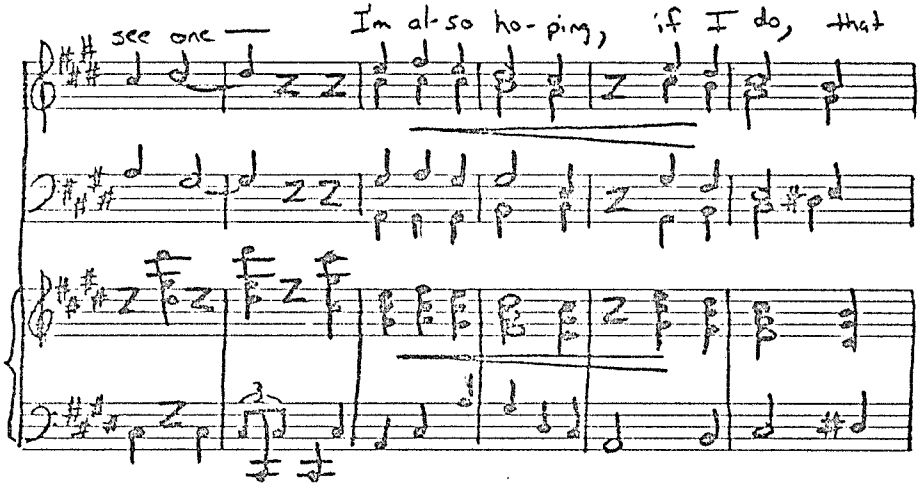

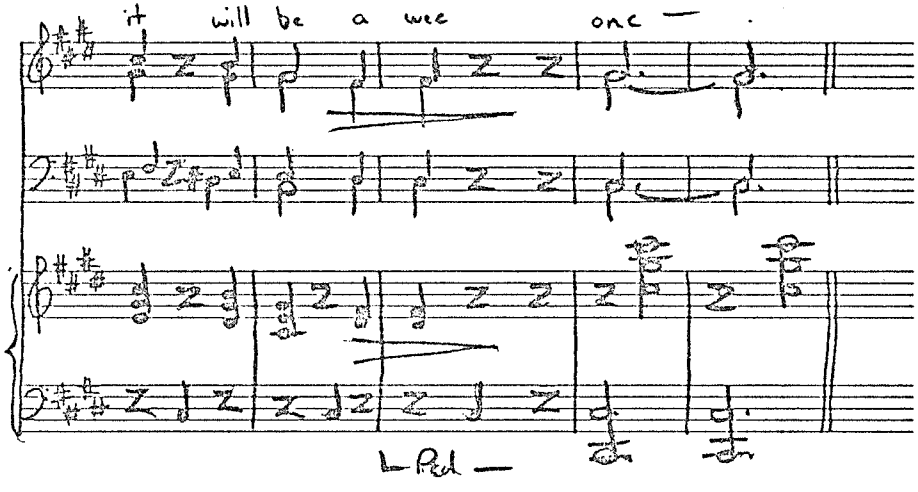

6. The Guppy

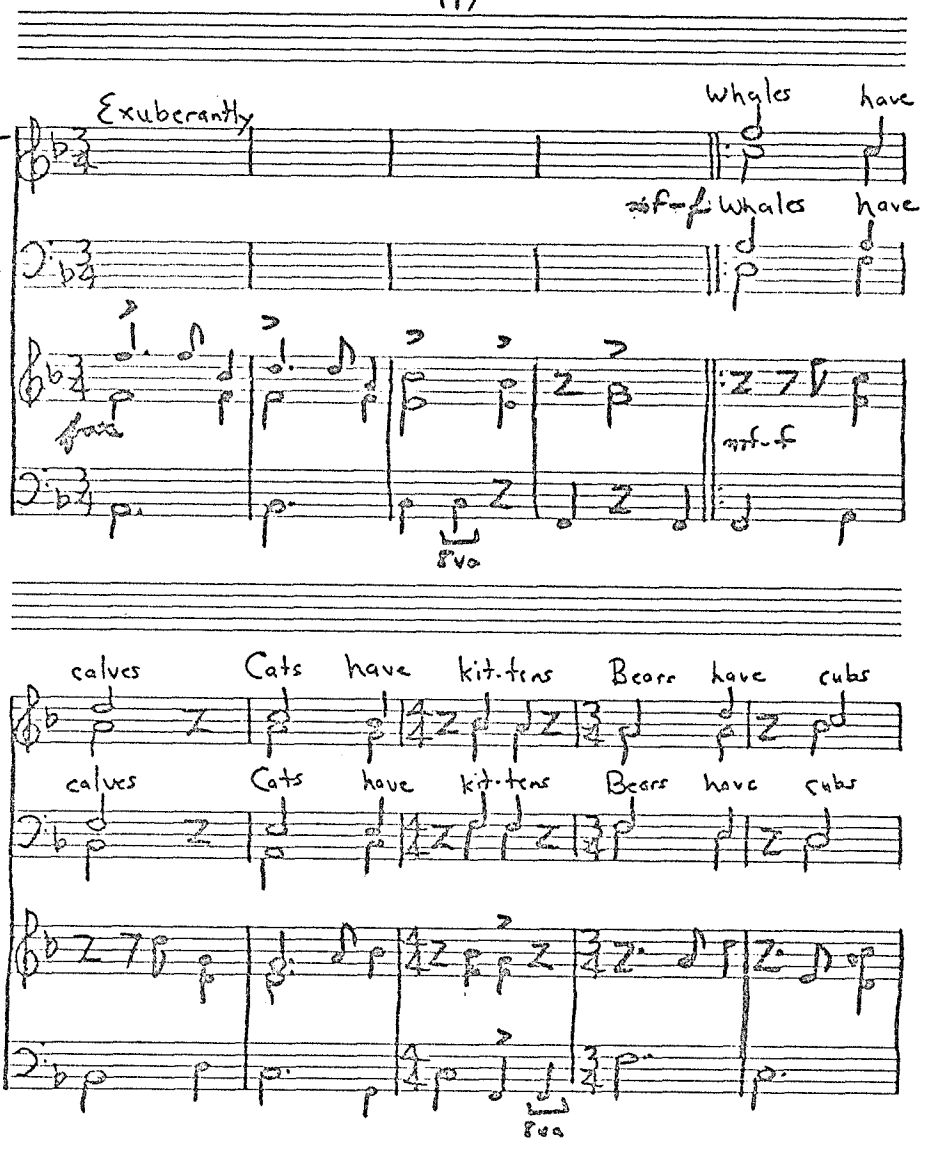
Exuberantly
Whales have
mf-f Whales have
T
B
fmf
mf-f
8va
calves Cats have kit-tens Bears have cubs
calves Cats have kit-tens Bears have cubs
8va

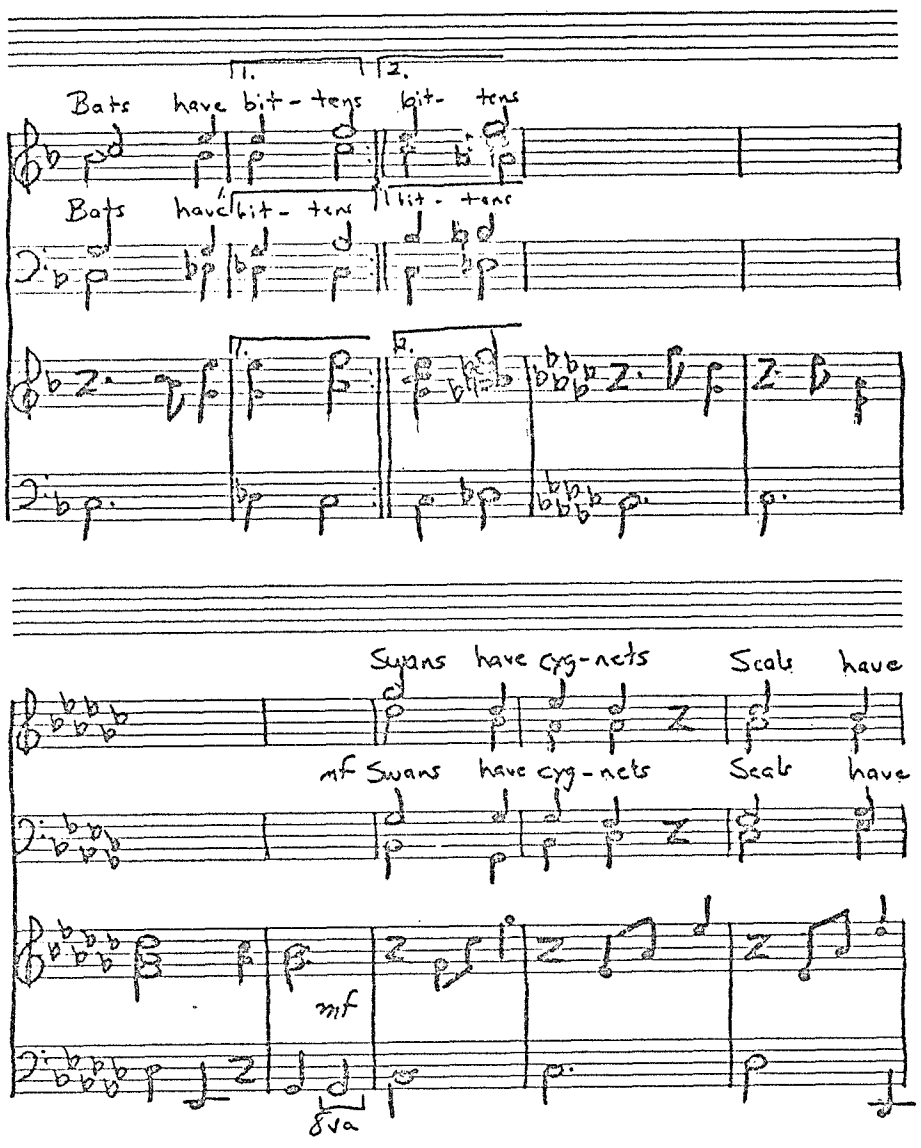
1. 2.
Bats have bit-tens bit- tens
Bats have bit- tens bit - tens
Swans have cyg-nets Seals have
mf Swans have cyg-nets Seals have
mf
8va

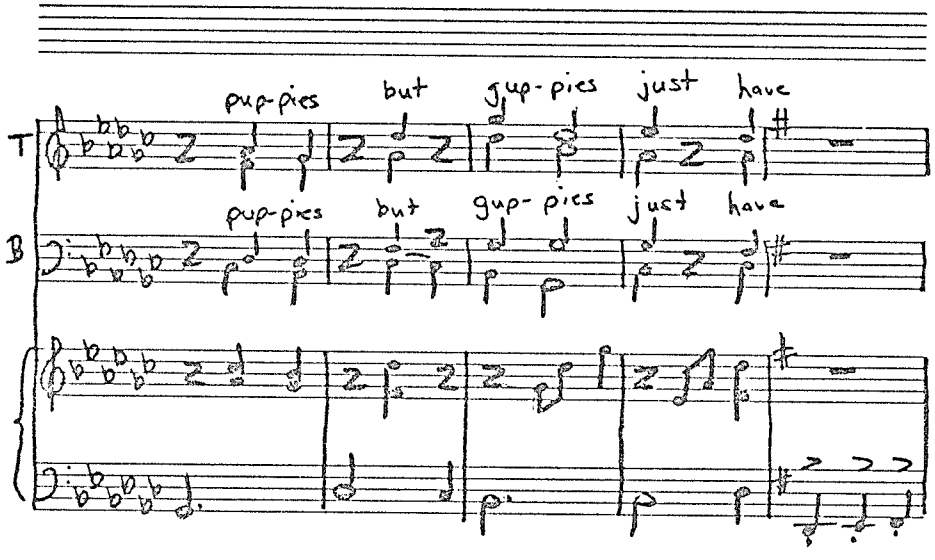
T
B
pup-pies but gup-pies just have
pup-pies but gup-pies just have

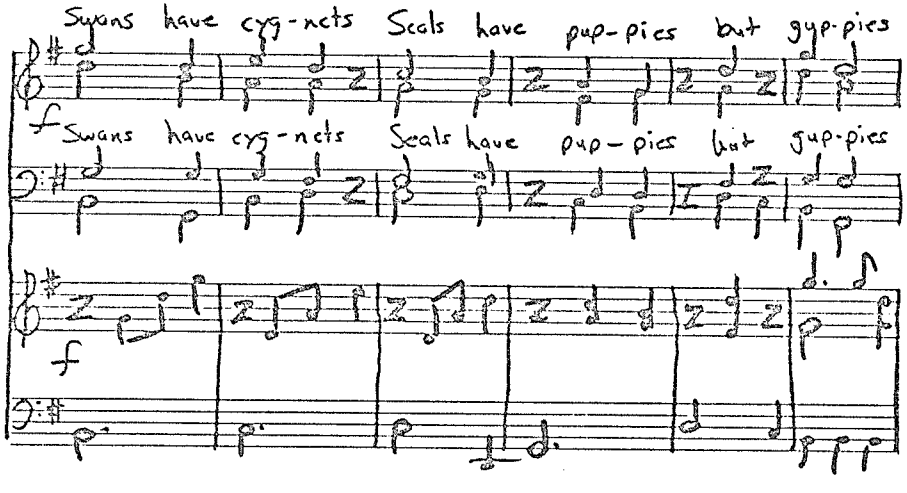
Swans have cyg-nets Seals have pup-pies but gup-pies
f
Swans have cyg-nets Seals have pup-pies but gup-pies
f

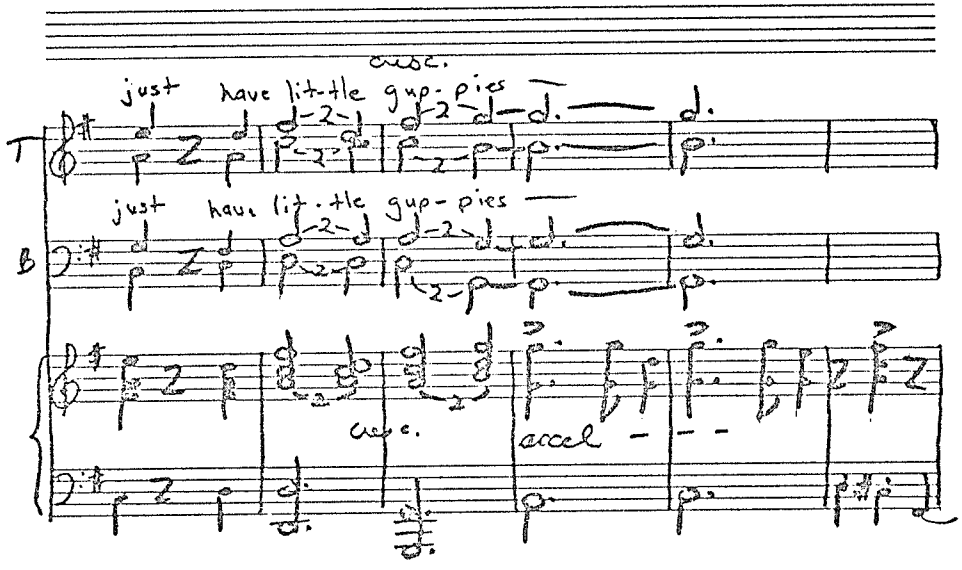
T
B
just have lit-tle gup-pies
just have lit-tle gup-pies
accel

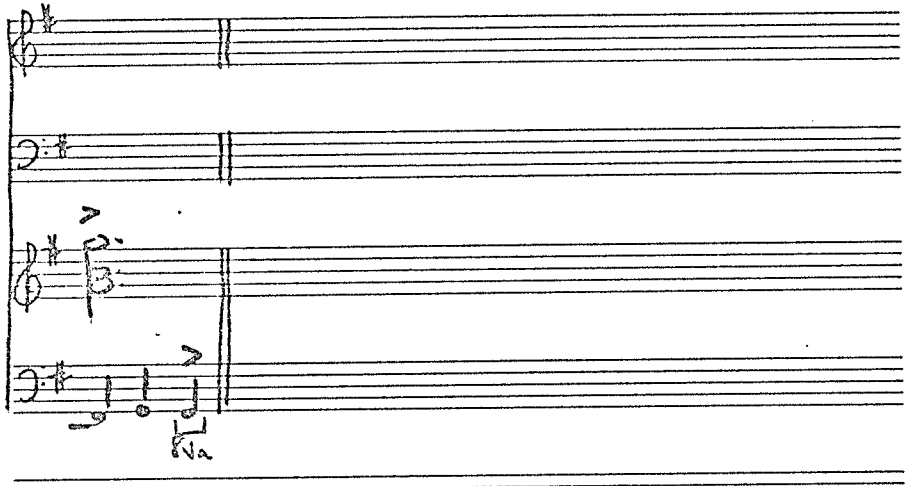
8va